VOLUME XLV

GEMS & GEMOLOGY

SUMMER 2009

Celebrating 75 Years of G&G

The Diamond Type System

Identifying Cu-Bearing Tourmaline

Andalusite

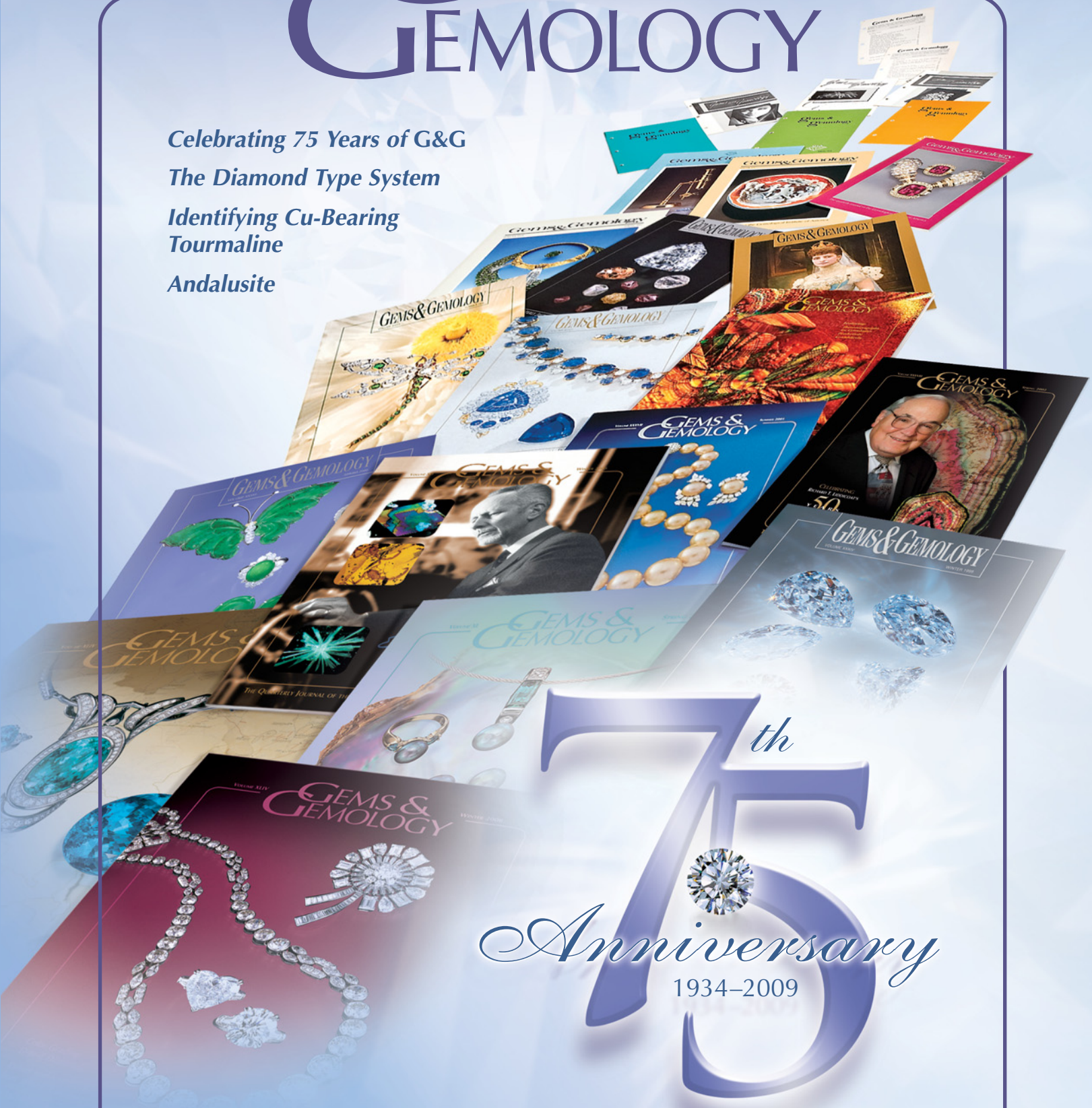

THE QUARTERLY JOURNAL OF THE GEMOLOGICAL INSTITUTE OF AMERICA

EXPERTISE THAT SPREADS CONFIDENCE. AROUND THE WORLD AND AROUND THE CLOCK.

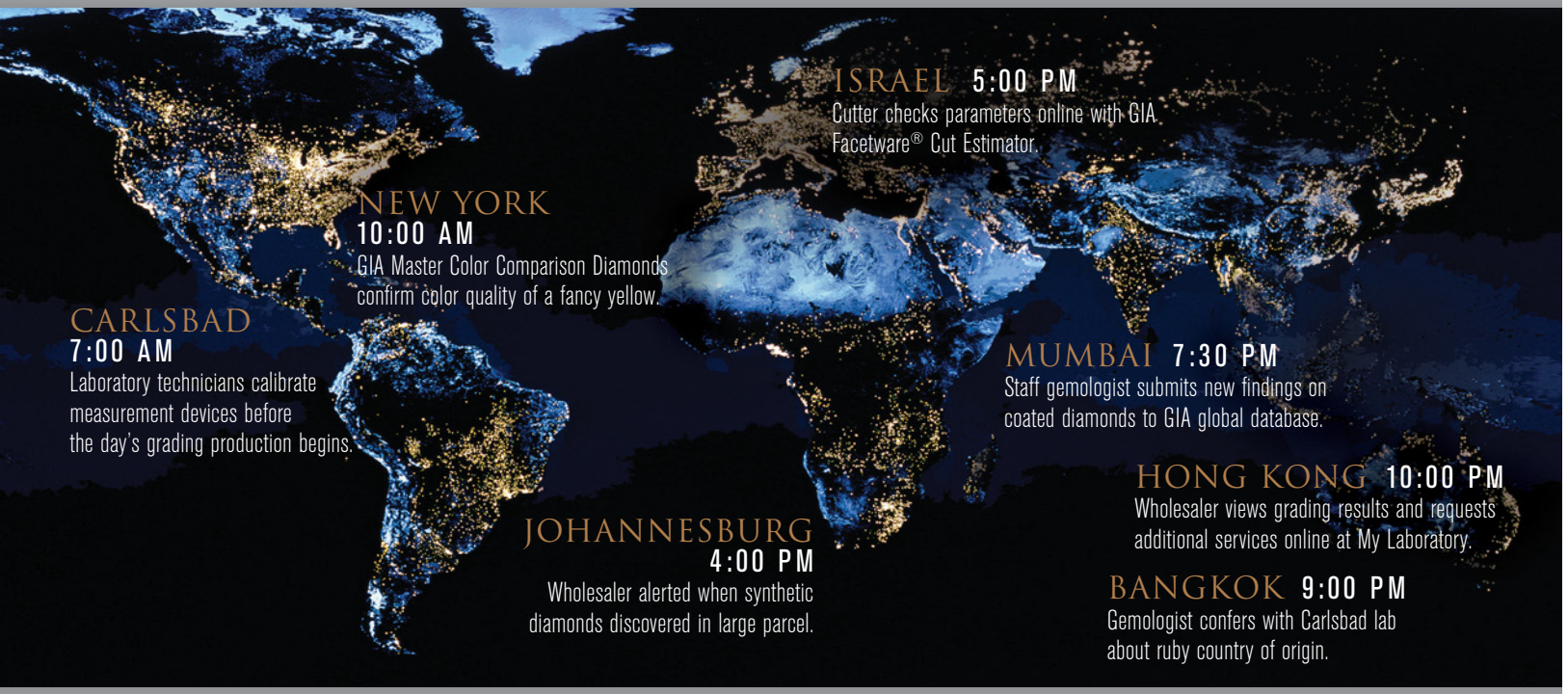

All across the planet, GIA labs and gemological reports are creating a common language for accurate, unbiased gemstone evaluation. From convenient locations in major gem centers. To frontline detection of emerging treatments and synthetics. To online services that include ordering, tracking, and report previews. GIA is pioneering the technology, tools and talent that not only ensure expert service, but also advance the public trust in gems and jewelry worldwide.

WWW.GIA.EDU

GIA
GEMOLOGICAL INSTITUTE OF AMERICA®

CARLSBAD NEW YORK LONDON ANTWERP FLORENCE GABORONE JOHANNESBURG
MOSCOW MUMBAI BANGKOK HONG KONG BEIJING TAIPEI SEOUL OSAKA TOKYO

GMSGG

Summer 2009 GEMS & GEMOLOGY Volume 45, No. 2

pg. 81

pg. 118

EDITORIAL

FEATURE ARTICLES

NOTES & NEW TECHNIQUES

RAPID COMMUNICATIONS

REGULAR FEATURES

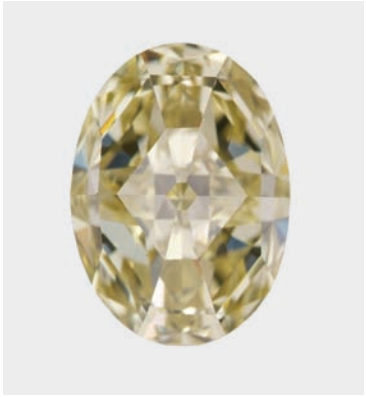

pg. 137

GEMS & GEMOLOGY

www.gia.edu/gemsandgemology

SUBSCRIPTIONS

Copies of the current issue may be purchased for **$19.00** in the U.S., **$22.00** elsewhere. Online subscriptions, and print subscriptions sent to addresses in the U.S., are $74.95 for one year (4 issues), $194.95 for three years (12 issues). Print subscriptions sent elsewhere are $85.00 for one year, $225.00 for three years. Combination print/online subscriptions are $99.95 in the U.S. and $110.00 elsewhere for one year, and $269.95 in the U.S. and $300.00 elsewhere for three years. Canadian subscribers should add GST. Discounts are available for group subscriptions, renewals, GIA alumni, and current GIA students.

To purchase subscriptions and single print issues, visit www.gia.edu/gemsandgemology or contact the Circulation Coordinator.

Electronic (PDF) versions of all articles and sections from Spring 1981 forward can be purchased at **gia.metapress.com** for $10 each. Full issue access can be purchased for $20.

To obtain a Japanese translation of *Gems & Gemology*, contact GIA Japan, Okachimachi Cy Bldg., 5-15-14 Ueno, Taitoku, Tokyo 110, Japan. Our Canadian goods and service registration number is 126142892RT.

DATABASE COVERAGE

Gems & Gemology's impact factor is 1.227 (ranking 11th out of the 26 journals in the Mineralogy category), according to Thomson Scientific's 2007 Journal Citation Reports (issued July 2008). *Gems & Gemology* is abstracted in Thompson Scientific products (*Current Contents: Physical, Chemical & Earth Sciences* and Science Citation Index—Expanded, including the Web of Knowledge) and other databases. For a complete list, see www.gia.edu/gemsandgemology.

MANUSCRIPT SUBMISSIONS

Gems & Gemology welcomes the submission of articles on all aspects of the field. Please see the Guidelines for Authors on our Website, or contact the Managing Editor. Letters on articles published in *Gems & Gemology* are also welcome.

Gems & Gemology is published quarterly by the Gemological Institute of America, a nonprofit educational organization for the gem and jewelry industry, The Robert Mouawad Campus, 5345 Armada Drive, Carlsbad, CA 92008.

Postmaster: Return undeliverable copies of *Gems & Gemology* to GIA, The Robert Mouawad Campus, 5345 Armada Drive, Carlsbad, CA 92008.

ABOUT THE COVER

Since its debut in January 1934, Gems & Gemology *has published groundbreaking research on diamonds, colored stones, and pearls. The lead article in this issue, by Stuart Overlin and Dona M. Dirlam, celebrates* G&G*'s 75th anniversary with a look back at the journal's history, which has coincided with the dramatic growth of gemology as a scientific field. The selection of* G&G *covers was photographed by Robert Weldon. Composite image designed by Karen Myers.*

Color separations for Gems & Gemology *are by Pacific Plus, Carlsbad, California. Printing is by Allen Press, Lawrence, Kansas.*

 ISSN 0016-626X

Gems & Gemology: The First 75 Years

I read with interest and more than a little nostalgia the lead article in this issue by Stuart Overlin and Dona Dirlam, which reviews *Gems & Gemology*'s first 75 years. As this manuscript wended its way through the review and revision process, it evolved into, in the words of British reviewer Alan Jobbins, "a history of the development of modern gemology."

Yet the journal is more than just words and pictures on paper. Behind every article, lab note, or gem news update is a great deal of hard work and often personal sacrifice. There is also a book's worth of anecdotes. Although I cannot speak for the full 75 years, I have been part of *G&G* for more than a third of that period, since 1980.

I already knew Dick Liddicoat and had a great deal of respect for his work as head of GIA and *G&G* when I first agreed to refurbish the journal. My respect only grew as we worked together to implement the journal's editorial philosophy: to promote the science of gemology for the protection of the jeweler, the gem dealer, and the public. When an author insisted on less stringent editing and less accountability, Mr. Liddicoat always reminded me that our first obligation was to the *reader*, and to the reader we had to be true. On one occasion, a disgruntled would-be author said what others have probably thought: that what I really needed was "a good punch in the nose." Mr. Liddicoat promptly called him, demanded an apology, and then banned him from having any further contact with me. I could not have asked for a better defender.

Actually, there are hundreds of authors who have been terrific to work with, who have shelved their personal and professional lives to deliver a solid article on an important topic. Keith Proctor moved to Santa Monica for weeks at a time to write his pegmatites of Minas Gerais series in the mid-1980s. And more than once we faxed page proofs across the Atlantic to Dr. Karl Schmetzer on Christmas Eve, so he could work on the article after his family had finished celebrating the holiday. Dona Dirlam wrote part of her 1992 "Gem Wealth of Tanzania" article sitting at my backyard patio table, while Bob Kammerling routinely spent evenings treating emeralds in his kitchen as he wrote and revised and then revised some more.

But perhaps my favorite author—yes, I do have a favorite—was Dr. Edward Gübelin. When I took over as managing editor in 1981, he found the new peer-review process far more demanding than any he had encountered previously. At one point, during a visit from a GIA colleague, he said he didn't think he could go through it again. Two hours later, though, as his guest was preparing to leave, Dr. Gübelin handed him a paper, asking: "Do you think Mrs. Keller would like this one?" To this day, I treasure the exquisite letters he sent and will always be grateful for his decision to endow the Dr. Edward J. Gübelin Most Valuable Article Award in perpetuity.

Equally important have been the members of the editorial review board. A few years ago, I received a letter from Dr. Connie Hurlbut, an original member of the board established in 1981. He had just closed his office at Harvard and no longer had access to his library. Perhaps he should resign from *G&G,* he suggested. He was, after all, turning 98 that year. Yet he was as sharp at 98 as when I first met him two decades earlier—and he continued to participate as a reviewer until his death just shy of his 100th birthday. Some reviewers have read manuscripts while in the field in Madagascar, Myanmar, and China. Others have done so from a hospital bed, or after a long day in the classroom or the laboratory. Some make a few key comments, while others—such as the legendary John Sinkankas—are willing to rewrite an entire paper to make it tighter, more accurate, and easier to read.

Many have also contributed to the "look" of the journal, in their efforts to get the right gem materials, line illustrations, or locality shots. For example, to create the Winter 1994 cover, John King and Tom Moses borrowed more than $17 million (at the time) in colored diamonds from several dealers and assembled the collection in a small room at GIA's New York Laboratory. Harold and Erica Van Pelt photographed the stones in a single session, expertly capturing their colors.

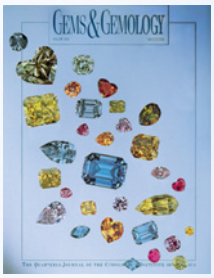

But these are only a few of the men and women who have contributed to *G&G* over the years. Others diligently prepared Lab Notes or Gem News International entries, or kindly provided samples for us to study and report on. Still others waded through the gemological literature to deliver the book reviews and abstracts that have kept our readers up to date, or provided photos that captured the essence of a new gem material, internal feature, or locality.

We at *Gems & Gemology* are proud to be part of this international effort to promote the science of gemology through reliable, well-vetted research. We are grateful to our contributors, grateful for the support we have had from GIA all these years, and grateful to you—our readers—for sharing our passion for gemology.

Alice S. Keller • Editor-in-Chief • akeller@gia.edu

CELEBRATING 75 YEARS OF *GEMS & GEMOLOGY*

Stuart Overlin and Dona M. Dirlam

Gems & Gemology, the professional quarterly of GIA, debuted in 1934. Appearing in the 306th issue, this article looks back at the first 75 years. By reviewing the journal's milestones, it also traces the history of modern gemology, as the articles, notes, and news updates in *G&G* represent a virtual encyclopedia of the developments that have influenced the science into the 21st century.

When the January 1934 premier issue of *Gems & Gemology* rolled off the presses, the world was in the throes of the Great Depression—daunting odds for any publication, let alone one devoted to an obscure field in its infancy. But one man's vision made all the difference.

Gems & Gemology (figure 1) was the brainchild of Robert M. Shipley, founder of the Gemological Institute of America. Shipley (figure 2) had once been a successful retail jeweler in Wichita, Kansas. After his business fell apart in 1927, he left America for Europe and, while living in Paris, completed gemology courses offered by Great Britain's National Association of Goldsmiths (NAG). He returned to the United States in 1929, settled in Los Angeles, and set out to professionalize America's gem and jewelry industry.

The enthusiastic response to his evening gem lectures at the University of Southern California led Shipley to incorporate GIA in Los Angeles in February 1931. The Institute aimed to safeguard the future of the gem and jewelry industry through education, instruments, and laboratory services. In 1934, Shipley created a sister organization, the American Gem Society (AGS), as a professional association of jewelers. GIA and AGS were headquartered under the same roof until their amicable parting 13 years later. (A more complete account of Robert Shipley and his founding of the two organizations appears in *G&G*'s Spring and Summer 1978 issues, as well as in William George Shuster's 2003 book, *Legacy of Leadership: A History of the Gemological Institute of America*.)

Shipley also saw another need: a periodical that would keep gemologists informed of developments and discoveries in the nascent field and keep them connected to GIA and AGS. He was no doubt influenced by *The Gemmologist*, the monthly journal begun by NAG in 1931 that was billed as a publication for "the jeweler, connoisseur, expert and manufacturer." Shipley started with a short-lived newsletter titled *Gemology: Bulletin of the Gemological Institute of America* in 1931. *Gems and Gemologists*, which followed in August 1933, was a prospectus for a future publication. If 2,000 initial subscriptions were sold, the cover announced, GIA would have the resources to create the periodical. In an editorial that acknowledged the influence of President Franklin Roosevelt's recently enacted New Deal, Shipley laid out the foundations of a grassroots

Authors' note: The original, smaller-format issues, from January 1934 through Winter 1980–1981, may be downloaded free of charge on the *G&G* website, www.gia.edu/gemsandgemology. To locate specific articles from past issues, please refer to the subject and author indexes also featured on the site.

See end of article for About the Authors and Acknowledgments.
GEMS & GEMOLOGY, Vol. 45, No. 2, pp. 80–95.

Figure 1. With the growth of gemology as a field of study over the past 75 years, Gems & Gemology *has provided the latest research on gem characteristics, sources, and technologies. Shown here is a selection of issues from the January 1934 premier through Spring 2009. Image by Karen Myers.*

"gemological movement" that would educate American jewelers and protect the gem-buying public. With features such as a history of the Pigott diamond, GIA news bulletins, a report on the World Jewelry Trade Congress, and a gem quiz, the lone issue of *Gems and Gemologists* succeeded in launching *Gems & Gemology*.

BIRTH OF THE JOURNAL

Gems & Gemology debuted with the January 1934 issue. The journal's aim was set forth on the cover, in what would now be called a mission statement:

> A bi-monthly periodical, without paid advertising, supported by subscriptions from Gemologists and other gem enthusiasts, aims to increase the gem merchant's knowledge and ability in order that he may protect more thoroughly his customers' best interests.

Intent on making the journal an independent, unbiased source of gemological research and information, Shipley established a policy of no advertising beyond GIA products and services.

From its first issue, *G&G* offered a broad mix of editorial content. Pages were devoted to profiles of famous diamonds such as the Jonker, Orloff, and Regent; tips on using the loupe and other basic gemological instruments; book reviews; and running segments such as a beginner's glossary and Henry Briggs's gemological encyclopedia, which ran from the premier issue to 1943. Throughout these early years, the journal sought to give jewelers and gemologists a common language with which they could communicate. Another staple was GIA and AGS news, as the journal sought to promote the gemological movement.

Gems & Gemology, along with every other aspect of the two organizations in the 1930s, was a family affair operated out of Shipley's Los Angeles

Figure 2. Former retail jeweler Robert M. Shipley (1887–1978) founded the Gemological Institute of America in 1931 and established its quarterly journal three years later. Shipley nurtured Gems & Gemology *until his retirement in 1952.*

Figure 3. Notable contributors during the journal's early decades included: (top row, left to right) Robert Shipley Jr., Sydney Ball, and Edward Wigglesworth; (middle row, left to right) Basil Anderson, Edward Gübelin, and George Switzer; and (bottom row, left to right) Robert Webster, G. Robert Crowningshield, Lester Benson Jr., and Eunice Miles.

apartment. His wife, Beatrice Bell Shipley, was the business administrator and an occasional contributor (under the pen name "B. W. Bell"). But the bulk of the writing initially fell on Shipley himself and Robert Jr. (figure 3), the elder of two sons from his first marriage and the Institute's resident scientist/inventor. The three Shipleys, involved as they were in every aspect of expanding GIA and AGS, still managed to produce the journal with the support of a small, thinly stretched staff. Then, as now, contributing authors were not paid for their articles. Yet Robert Shipley Sr., through his energy and force of personality, was able to draw on the talents of experts such as mining engineer Sydney Ball and Edward Wigglesworth, director of what is now the Museum of Science in Boston.

The fledgling journal's tight budget was reflected in its modest appearance. It began as a 5½ × 8½ in. publication, 32 pages per issue (though the page count was halved within two years). Each cover was simply the table of contents, and the pages contained little photography, all of it black-and-white. Subscriptions cost $3.50, an annual rate that would not increase for more than *40 years*, until the end of 1976. After two years as a bimonthly journal, *G&G* became a quarterly with the Spring 1936 issue.

An early milestone for the journal was GIA's 1941 hiring of Richard T. Liddicoat Jr. (figure 4; see also the Spring 2002 tribute), who had recently obtained his master's degree in mineralogy at the University of Michigan. Liddicoat's first byline in *G&G* was a Fall 1941 piece, written with Shipley Sr., titled "A solution to diamond grading problems" (see box A). Liddicoat would eventually lead the Institute and the journal to new heights.

WAR YEARS

Within a decade of *Gems & Gemology*'s birth, though, its very existence was threatened by the impact of World War II. GIA suffered a staggering drop in enrollments as millions of young men joined

the war effort. Among them were two of the journal's most important contributors. Robert Shipley Jr. was called up in 1941 by the Army Air Corps, which used his engineering talents to develop photo reconnaissance equipment. Liddicoat left for the Navy in 1942, serving as a meteorologist on aircraft carriers in the South Pacific.

Yet the journal continued to deliver original research, due in large part to a $50,000 endowment raised by AGS jewelers that made the Institute a nonprofit organization and kept it "from becoming a war casualty," as the February 1943 issue of *National Jeweler* put it. In addition to a diamond glossary that ran from 1941 through 1947, *G&G* issues from this period featured brief but influential articles. Leading the way were Wigglesworth in Boston and European authors Basil W. Anderson and Edward J. Gübelin. Until his death in 1945, Wigglesworth wrote on topics ranging from refractometer and polariscope use to specific gravity testing and synthetic emerald detection. Anderson, head of the Precious Stone Laboratory of the London Chamber of Commerce (which later merged with the Gemmological Association of Great Britain, now Gem-A), published a four-part series on the gemological applications of the handheld spectroscope.

Gübelin, a young Swiss gemologist, had recently begun his pioneering research on inclusions in gemstones. (For more on the career of Dr. Edward J. Gübelin, see the Winter 2005 cover story.) Among his dozen wartime articles for *G&G* were studies of the microscopic differences between Burmese and Thai rubies and Colombian and Russian emeralds (both in 1940), methods for determining a sapphire's geographic origin (1942–1943), and the identifying characteristics of various synthetics. To show the internal features of a gem, Gübelin made extensive use of photomicrography, a first for *G&G*.

Other highlights from the period were A. E. Alexander's pair of 1941 articles on distinguishing natural and cultured pearls and Shipley's first look at commercially available synthetic emeralds the following year. Gemological Digests, a series of industry news briefs from around the world, debuted in 1944 and became a regular column for the next two decades.

THE POSTWAR ERA

Having survived the war years, *Gems & Gemology* resumed its original 30-plus page count by 1947. Liddicoat had returned from military service the year before and, with the departure of Shipley Jr., was now Shipley Sr.'s heir apparent at GIA and as editor of the journal. Gübelin and Anderson remained leading authors, joined by George Switzer of the Smithsonian Institution and Robert Webster, Anderson's colleague from the Precious Stone Laboratory. The journal was further bolstered by the 1947 establishment of an editorial board, comprised of Anderson, Ball, Gübelin, Switzer, and William Foshag, also from the Smithsonian. With the appointment of the editorial board, the masthead no longer described *G&G* as a GIA "organ" but rather as the "official journal" of the Institute, implying a more academic perspective.

Notable articles from the early postwar years included Shipley's 1947 study of diamond fluorescence and William Barnes's four-part series that same year on X-ray diffraction to identify natural and cultured pearls. Shipley's final article for the journal was a 1949 piece that examined the business operations of De Beers.

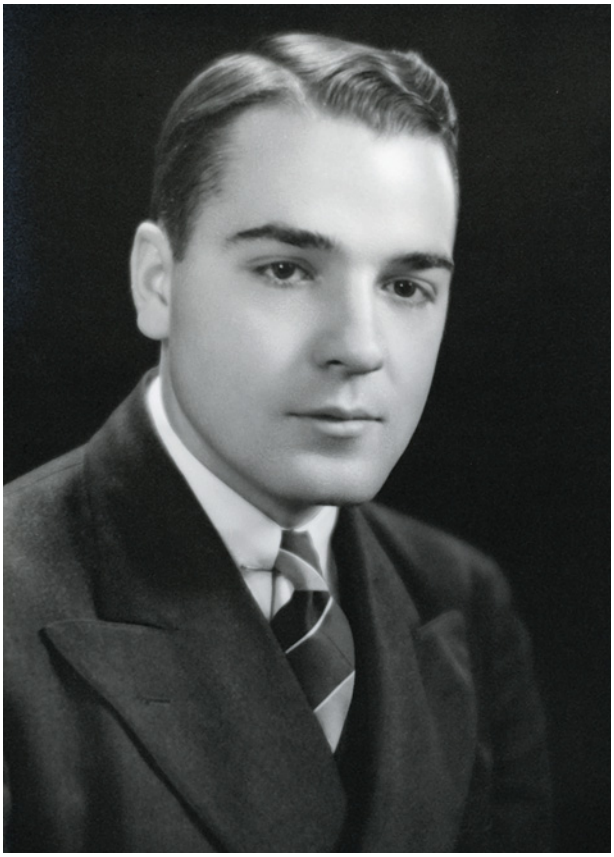

Figure 4. Richard T. Liddicoat Jr. (1918–2002) succeeded Shipley as GIA president and G&G *editor in 1952. Over the next 50 years, Liddicoat exerted an enduring influence on the journal. In addition to numerous feature articles and editorials, he penned GIA's West Coast lab highlights column from 1961 to 1980.*

BOX A: LANDMARK ARTICLES

Gems & Gemology has published some of the finest gemological research of the past 75 years. Members of the journal's editorial staff and several longtime contributors joined the authors in selecting 20 of the most noteworthy articles (or series) in *G&G*'s history, with apologies to the many others that deserve mention. This list includes particularly influential first reports, articles that cast new light on important topics, and studies that have been widely referenced and are considered authoritative years after publication.

Fall 1941: "A Solution to Diamond Grading Problems." Robert Shipley and Richard Liddicoat took on the monumental challenge of creating a system for consistent diamond color grading, at a time when none existed. It combined the Diamolite, a reliable natural daylight–equivalent lamp that provided a controlled viewing environment, with the Colorimeter, a device that compared a diamond's color against a fixed standard. This early color grading system was adopted by AGS and represented an important advancement in diamond grading methodology.


Edward J. Gübelin

Calcite in Burmese ruby.

1944–1945: The "Gemstones and the Spectroscope" series. In the 1940s, more than 70 years after the first observations of gemstones using the spectroscope, the instrument was still relegated to the background of gemological research. Based on his decade of experience with the spectroscope, Basil Anderson explored the capabilities of this simple tool and offered practical tips on using it that still apply today.

1945–1946: The "Inclusions as a Means of Identification" series. Edward Gübelin, the Swiss gemologist who pioneered the study of gemstone inclusions, set forth the fundamentals in this three-part series. The articles focused on the inclusion characteristics of the most common garnets, with numerous photomicrographs.

Winter 1957–1958: "Spectroscopic Recognition of Yellow Bombarded Diamonds." The advent of irradiated diamonds, in a range of colors, posed a difficult question for the industry in the mid-1950s: Was a diamond's color natural or the product of irradiation? After a study of more than 10,000 yellow diamonds with the spectroscope, G. Robert Crowningshield established the absorption line at 5920 Å (592 nm) as an identifying feature of irradiated yellow diamonds.

Winter 1962–1963 and Summer 1964: The "Coated Diamonds" series. As a wave of convincing diamond coatings entered the market in the 1950s, Eunice Miles undertook a two-year study. Miles's research culminated in these two *G&G* articles, where she presented her microscopic clues to detecting diamond coatings.

Summer 1971: "General Electric's Cuttable Synthetic Diamonds." When GE succeeded in producing cuttable-size synthetic diamonds, Crowningshield arranged to examine the first four faceted and several uncut specimens. This detailed study marked the first published report of their color, clarity, fluorescence, spectroscopic, and X-ray characteristics. Crowningshield concluded that the synthetics could be detected by their unusual inclusions, strong fluorescence, and prolonged phosphorescence. This was the first of several articles that *G&G* would publish as gem-quality synthetic diamonds transitioned from a research oddity to a commercial product.

1984–1985, 1988: The "Gem Pegmatites of Minas Gerais" series. For many years, the complex granitic pegmatites of Minas Gerais, Brazil, supplied most of the world's market for fine gem beryl, chrysoberyl, topaz, tourmaline, and kunzite. In this four-part series, Keith Proctor reviewed the occurrence of pegmatitic gems in the region, as well as related exploration and mining activities.

Winter 1985: "A Proposed New Classification of Gem-Quality Garnets." With the discovery of new types of garnets in the 1970s, the existing classification system for these gems had become inadequate. Carol Stockton and D. Vincent Manson devised a new system based on the chemical and spectroscopic analyses of more than 500 samples and proposed eight varieties of gem garnets, all of which could be identified with traditional gemological instruments.

Winter 1986: "The Gemological Properties of the Sumitomo Gem-Quality Synthetic Yellow Diamonds." In 1985, Sumitomo Electric Industries achieved the first commercial production of gem-quality synthetic diamonds, in the form of yellow crystals up to 2 ct. James Shigley et al. provided standard gemological methods for detecting these products. Similar articles followed over the next several years, as other manufacturers entered the marketplace with a broader product mix.

Fall 1987, Spring 1988, and Summer 1988: The "Update on Color in Gems" series. Emmanuel Fritsch and George Rossman's three-part series began with a summary of the factors that govern the perception of color, from the source of light to the human eye, and examined the role of dispersed metal ions in the coloration of gems such as ruby and emerald. The series went on to explore charge-transfer phenomena and color centers as the cause of color in blue sapphire, Maxixe beryl, and other gems. It concluded with colors that involve band theory and physical optics, such

as the play-of-color in opal and the blue sheen of moonstone feldspars.

Summer 1989: "The Characteristics and Identification of Filled Diamonds." In the late 1980s, the filling of surface-reaching cracks in diamonds with high-RI glass to enhance clarity became the most controversial diamond treatment up to that point. As the industry struggled to deal with the issue, John Koivula and coauthors described clear-cut methods to detect the filling. Their study also marked the beginning of *G&G*'s unprecedented reporting of treatments involving colorless diamonds, the mainstay of the industry.

Harold & Erica Van Pelt

Cu-bearing tourmalines from Paraíba, Brazil.

Fall 1990: "Gem-Quality Cuprian-Elbaite Tourmalines from São José da Batalha, Paraíba, Brazil." The introduction of exceptionally bright blue and green tourmalines from the Brazilian state of Paraíba in 1989 captivated the colored stone world. In one of the first reports on "Paraíba" tourmaline, Emmanuel Fritsch and coauthors described the gems and performed quantitative chemical analyses, which revealed that the striking colors were related to unusually high concentrations of copper. They also examined the role of heat treatment.

Spring 1991: "Age, Origin, and Emplacement of Diamonds: Scientific Advances in the Last Decade." Melissa Kirkley, John Gurney, and Alfred Levinson's definitive review was a key resource for understanding the formation of diamonds millions of years ago, as well as the mechanisms that brought them to the surface. The article resonated beyond the gemological community, becoming widely cited in the geological literature.

Summer 1991: "Fracture Filling of Emeralds: Opticon and Traditional 'Oils.'" The filling of surface-reaching fractures in emerald has long been a widespread practice, but as epoxy resins began to replace traditional fillers, the trade demanded to know more about these new substances. Robert Kammerling and coauthors examined the most widely used epoxy resin, Opticon, and found that it could be detected by established methods.

Winter 1994: "Color Grading of Colored Diamonds in the GIA Gem Trade Laboratory." During the 1980s, colored diamonds became more prevalent and far more popular than ever before. Amid this newfound appreciation for "fancies," John King and a team of colleagues presented the GIA Laboratory's updated system for color grading these diamonds, as well as the theory behind it.

Winter 1995 and Spring 1996: The "History of Diamond Sources in Africa" series. Since 1867, Africa has been the world's most important diamond source. A. J. A. (Bram) Janse chronicled the history of African diamond exploration and mining with this two-part series. South Africa was reviewed in part one, followed by East and West Africa in part two.

Fall 1996: "De Beers Natural versus Synthetic Diamond Verification Instruments." Christopher M. Welbourn and colleagues from the De Beers DTC Research Centre introduced a pair of instruments specially designed to distinguish synthetic diamonds: the DiamondSure and the DiamondView. The DiamondSure detects the presence of the 415 nm optical absorption line found in nearly all natural diamonds but not in synthetics. The DiamondView produces a fluorescence image from which the distinctive growth structures of natural and synthetic stones can be determined.

Fall 1998, Fall 2001, and Fall 2004: The "Diamond Cut" series. Of all the diamond quality factors, cut is the most difficult to evaluate objectively. Following a 15-year study that used computer modeling and observation testing, GIA researchers found that the *combination* of proportions is more important than any individual proportion value, and that attractive diamonds can be cut in a wider range of proportions than traditionally thought possible. The study resulted in the 2005 launch of GIA's diamond cut grading system for round brilliants.

Summer 2000: "Characteristics of Nuclei in Chinese Freshwater Cultured Pearls." In the late 1990s, the exceptional size and quality of some freshwater cultured pearls from China sparked debate over the growth process used, particularly claims that they were being beaded with reject cultured pearls. Based on the study of some 41,000 samples, Kenneth Scarratt, Thomas Moses, and Shigeru Akamatsu determined that these freshwater cultured pearls were being grown with mantle tissue only, using larger mussels and new tissue-insertion techniques, and that they could be identified with established X-radiographic methods.

Summer 2003: "Beryllium Diffusion of Ruby and Sapphire." The first major colored stone challenge of the 21st century was the heat treatment of corundum involving diffusion with beryllium. Stones artificially colored by the process were being sold undisclosed, which sent shockwaves through the colored stone market. John Emmett and coauthors tackled the issue with this 52-page article, the longest in the journal's history. Their study found that standard gemological testing could identify many of these goods, whereas quantitative chemical analysis by secondary ion mass spectrometry (SIMS) and LA-ICP-MS were required for the rest.

Figure 5. Early associate editors (top row, left to right) Virginia Hinton, Kay Swindler, and Jeanne Martin laid the foundations for (bottom row, left to right) Lawrence Copeland, Robert Gaal, and John Koivula during the late 1960s and 1970s. Koivula remains a major contributor to the journal.

When Shipley retired in 1952, Liddicoat assumed the reins of GIA and its quarterly. Like his predecessor, Liddicoat was an actively involved editor, and he continued to write extensively for *G&G*. But the day-to-day management of the journal was being handled by associate editors Virginia Hinton (1944–1946), Kay Swindler (1946–1953), and Jeanne Martin (1953–1966; see figure 5).

By the early 1950s, one of the greatest challenges facing the gem industry was the color alteration of diamonds through laboratory irradiation. Earlier *G&G* articles, in 1938 and 1949, reported on diamonds that had been colored green by exposure to radium. In a 1954 study, De Beers researchers J. F. H. Custers and H. B. Dyer identified irradiated blue diamonds by their absence of electrical conductivity. Yet there was still no means of detecting yellow irradiated diamonds, which were on the market and often sold without disclosure. That was when G. Robert Crowningshield, head of GIA's recently established New York laboratory, made one of gemology's most famous discoveries. Using a simple handheld spectroscope, Crowningshield spotted an absorption line at 5920 Å (592 nm) that was present in yellow diamonds artificially colored by irradiation. His Winter 1957–1958 "Spectroscopic recognition of yellow bombarded diamonds" was a breakthrough in identifying these treated stones.

Soon, more of Crowningshield's discoveries and observations would be featured in a regular lab column. The Winter 1958–1959 issue introduced the Highlights at the Gem Trade Lab section, featuring brief notes on interesting and unusual gems encountered at the GIA laboratories. Crowningshield was the New York correspondent, with GIA researcher Lester B. Benson Jr. reporting from Los Angeles. These entries were written for easy reading, with some as short as a single paragraph. The column continued for the next two decades and (in 1981) became the popular Lab Notes section, with Crowningshield as a contributing editor. (The lead article in the Fall 2003 issue took an in-depth look at Crowningshield's six-decade career.)

The postwar years also saw a new emphasis on photography, including *G&G*'s first foray into color. Between 1946 and 1951, the journal printed 38 full-page color plates that represented every major gem species, as well as lesser-known ornamental materials. Save for the color plates, though, the journal was still black-and-white. The covers became less austere with the Winter 1946 issue, which featured a bouquet of diamonds and emeralds from the Russian Crown Jewels. Black-and-white jewelry photos adorned the covers through 1966 (again, see figure 1).

THE SIXTIES AND SEVENTIES

The 1960s began on a somber note with the untimely death in 1961 of Lester Benson, whose Los Angeles lab column was carried on by Liddicoat. The *G&G* editor also produced two of the decade's most notable articles: 1962's "Developing the powers of observation in gem testing," and "Cultured-pearl farming and marketing" in 1967. Eunice Miles, the first female gemologist at the GIA laboratory, addressed one of the New York diamond industry's most pressing concerns with two articles on detecting coated diamonds (at the end of 1962 and in 1964). But with growing demand for GIA's new diamond grading services, gemological research assumed a lower priority at the Institute, and few other scientific studies would be conducted until the establishment of GIA Research in 1976.

As a result, the driving force behind *G&G* in the late 1960s and early 1970s was the lab highlights section. Roughly half of each issue was devoted to these accounts and photos of oddities, damaged stones, imitations, and outright frauds seen at the New York and Los Angeles labs. The section was also a record of gemological milestones, such as the introduction of the diamond imitation yttrium-aluminum garnet (YAG) at the end of 1964 and irradiated topaz in 1967. Another first was the 1967 identification of a previously unknown violet-blue zoisite, a material that would eventually become famous as *tanzanite* (figure 6). In 1970 and 1971, the lab highlights section noted the advent of laser drilling, a process used to bleach dark inclusions in a diamond to improve its apparent clarity. The section later described the first commercially available synthetic opal and synthetic alexandrite (1972) and the first specimen of gem-quality jeremejevite examined by lab staff members (1973).

In-depth reports on other critical developments appeared as *G&G* feature articles. In 1971, Crowningshield chronicled a major milestone in gem history with his description of the first cuttable-size synthetic diamonds, produced by General Electric. A 1974 article by Campbell Bridges offered a firsthand look at the green grossular garnet from Kenya that became known as *tsavorite*. Hiroshi Komatsu and Shigeru Akamatsu examined the differentiation of natural from treated black pearls in 1978, while two years later Robert Kane contributed a seminal study on graining in diamonds.

Through 1980, the journal was managed by a succession of distinguished associate editors (again, see figure 5), most notably Lawrence Copeland (1967–1971), Robert Gaal (1973–1977), and John I. Koivula (1978–1980). During this period, synthetic gem materials were being developed for laser applications in communications and other fields. These new materials invariably made their way into the gem market. In the 1970s, gemology attracted the interest of Kurt Nassau (figure 7), then a research scientist at Bell Laboratories. Nassau wrote several articles on synthetics (including a Winter 1979–1980 review of the decade's advances) and simulants (such as the new diamond imitation cubic zirconia in 1976), as well as treatment processes and the causes of color in gems (e.g., deep blue Maxixe-type beryl in 1973).

G&G's first all-color edition was the Spring 1977 special issue on the Hixon Collection of colored stones, which had been donated to the Natural History Museum of Los Angeles County between 1971 and 1977. A year later, the Summer 1978 Robert M. Shipley memorial issue was devoted to remembrances of the journal's founder and the early days of GIA and AGS.

Figure 6. In 1967, G&G *reported on a brilliant new violet-blue zoisite that came to be known as* tanzanite. *This photo, from the Summer 1992 cover shoot, shows a 98.4 g crystal and 24.30 ct faceted tanzanite. Courtesy of Michael Scott; photo by Harold & Erica Van Pelt.*

Figure 7. Among the most prolific contributors from recent decades are: (top row, left to right) Kurt Nassau, Robert Kane, and Emmanuel Fritsch; and (bottom row, left to right) John King, Alfred Levinson, James Shigley, and Karl Schmetzer. Shigley is also contributing editor of G&G *and editor of the* Gems & Gemology in Review *series; King is editor of the* Colored Diamonds *book in that series. Levinson was editor of the Gemological Abstracts section from 1997 to 2005.*

Figure 8. Editor-in-chief Alice Keller's transformation of G&G *began with the Spring 1981 issue. She was later joined by editor Brendan Laurs and managing editor Tom Overton, who bring geological, gemological, and legal expertise to the journal. Photo by Kevin Schumacher.*

A NEW ERA

In 1980, with GIA's 50th anniversary a year away, Liddicoat and the board of governors decided it was time to revitalize the Institute's flagship publication. Koivula, eager to return to his highly regarded gem inclusion research and photomicrography, stepped aside and Alice Keller (figure 8) was chosen to take over as managing editor. Unlike her predecessors, Keller was not a gemologist, but she had an extensive background in peer-reviewed medical and business journals. She immediately put a lasting imprint on *G&G*, beginning with the Spring 1981 issue, which was headlined by Gübelin's article on peridot from the Red Sea island of Zabargad and Nassau's update on cubic zirconia.

Keller's debut issue was a dramatic departure for the journal. It had a larger format (8½ × 11 in.) and twice the page count. But the most striking feature of the redesigned *G&G* was its emphasis on high-quality color photography, which finally did justice to the subtle nuances of gems and their eye-visible and microscopic features. With the next issue, Summer 1981, the renowned team of Harold and Erica Van Pelt (figure 9) began taking artistic cover shots and lead photos for feature articles. Over the years, Tino Hammid, Robert Weldon, Shane McClure, and Maha Tannous also contributed significantly, while Koivula's photomicrographs captured the internal world of gems (he shared some of his techniques in

Spring 2003's "Photomicrography for gemologists"). Complementing the photos were numerous color illustrations, including detailed maps and graphs.

But the changes were more than just cosmetic. Keller reestablished the journal's editorial review board, the backbone of any peer-reviewed journal, to evaluate manuscripts prior to publication. The new board included Nassau and Crowningshield, as well as Cornelius Hurlbut of Harvard University, George Rossman from the California Institute of Technology, Pete Dunn of the Smithsonian Institution, Anthony Kampf from the Natural History Museum of Los Angeles County, and venerable gem and mineral author John Sinkankas, among others from GIA and the gem trade. Meanwhile, Gem News (later Gem News International) was added as a forum for new sources, synthetics, and other breaking developments from around the world. The longstanding lab highlights section became Gem Trade Lab Notes (simply Lab Notes since Summer 2003) and grew more comprehensive under GIA Laboratory leaders Crowningshield, C. W. (Chuck) Fryer, Robert Kammerling, Thomas Moses, and Shane McClure (figure 10). The Gemological Abstracts section, which presented summaries of notable articles published elsewhere, expanded under the editorship of GIA library director Dona Dirlam and her successor, University of Calgary geochemist and diamond expert Alfred Levinson.

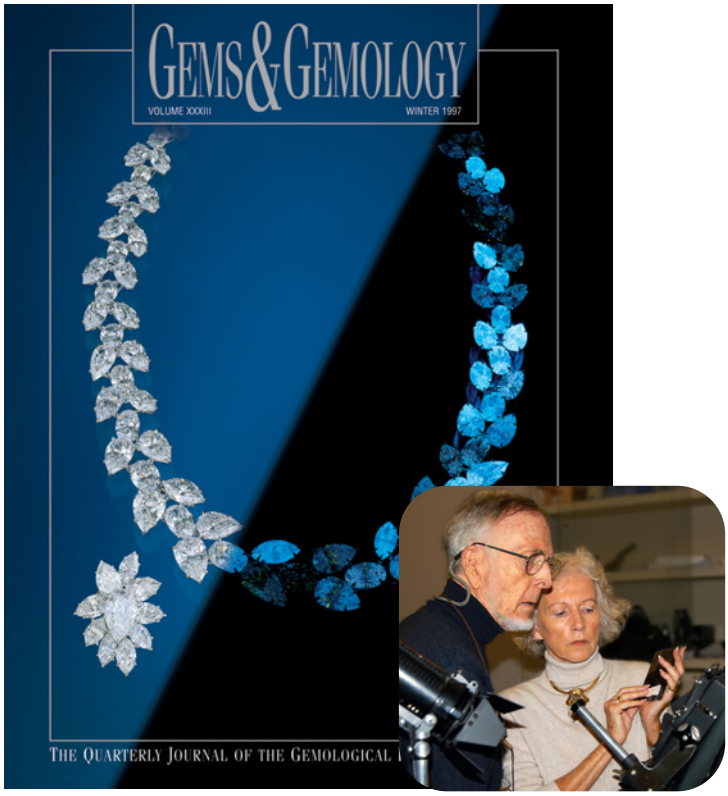

Figure 9. G&G*'s emphasis on attractive, informative color photography is evident in the Winter 1997 cover, which demonstrated the wide range of fluorescence shown by the fine diamonds in this Harry Winston suite. The composite image was taken by photographers Harold & Erica Van Pelt (inset, by Karen Myers), who have captured artistic cover shots for almost every issue since Summer 1981.*

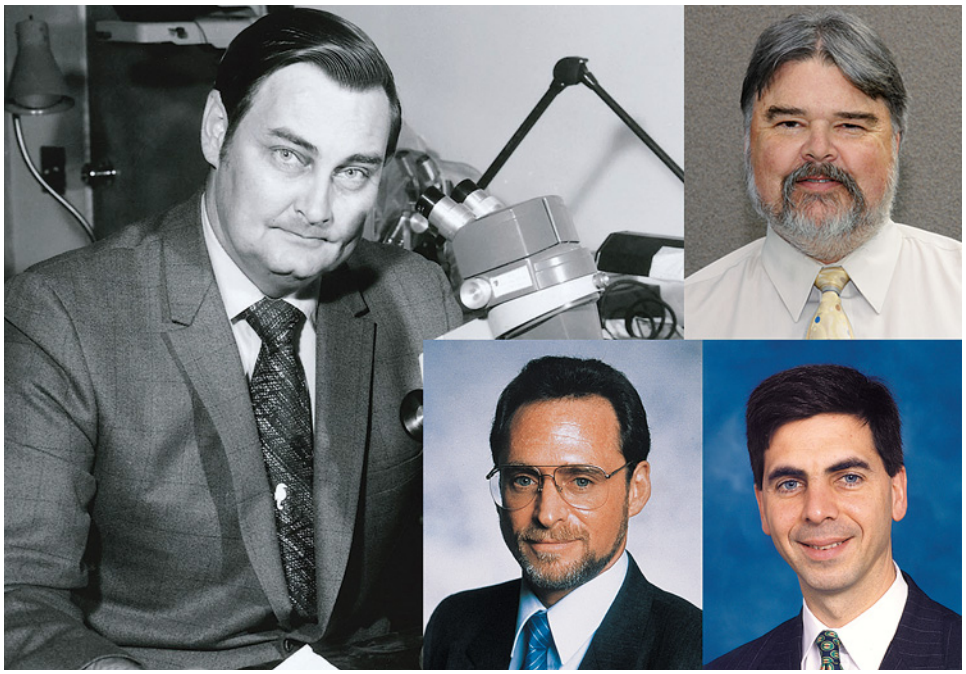

Figure 10. Since 1981, the Lab Notes section has grown under editors (clockwise from far left) C. W. (Chuck) Fryer, Shane McClure, Thomas Moses, and Robert Kammerling.

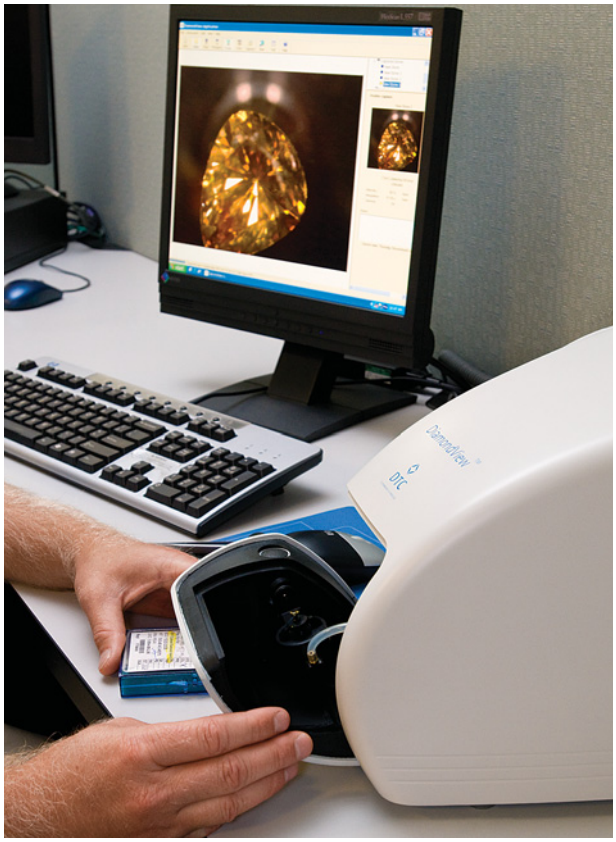

Figure 11. Shown here is a recent model of the DTC DiamondView, which was introduced to gemologists in a 1996 G&G *article by Chris Welbourn et al. It is one of many advanced technologies that have figured prominently in the journal since the 1980s. Photo by Kevin Schumacher.*

In 1982, *G&G* debuted a pair of perennial Spring issue features. The Most Valuable Article Award, voted on by readers and later renamed in honor of Gübelin, offers recognition and a monetary prize as an incentive for authors. The *G&G* Challenge, a multiple-choice quiz based on the previous year's articles, promotes continuing education in this rapidly developing field.

The Spring 1986 "China" issue, an unprecedented look at the country's gem resources, was the first of several special editions of the redesigned journal. Retrospectives of the 1980s and 1990s (Spring 1990 and Winter 2000) reviewed major developments for each decade in five key areas: gem sources (including a world map and table of important localities), synthetics, treatments, new technologies, and jewelry styles. In addition, the Fall 1999 and Fall 2006 issues were devoted to presentations by industry leaders and prominent researchers at GIA's third and fourth International Gemological Symposiums.

The Impact of Technology. The changes in *G&G* coincided with a virtual revolution in gemology. Technological advances in the 1980s began to foster more precise, sophisticated forms of gem synthesis, resulting in an influx of high-quality synthetic rubies, sapphires, and emeralds. Although GE had produced the first jewelry-quality synthetic diamonds for experimental purposes years earlier, Sumitomo was the first to make such material commercially available—initially for industrial use. During this decade, *G&G* covered the Ramaura and Lechleitner synthetic rubies, among others, as well as the Sumitomo and De Beers gem-quality synthetic diamonds. At the same time, experimentation in other fields, such as high-pressure physics and materials science, brought a new generation of enhanced gems to the fore. The traditional gauges and scopes—and even electron microprobe analysis and UV-visible absorption spectroscopy, techniques first applied in the 1970s—were not always sufficient to characterize these materials. Out of this necessity came new tools for gemological discovery.

Many of these new identification technologies involved spectroscopic methods, which measure the absorption or emission of electromagnetic radiation to determine a gem material's composition and characteristics. Several advanced forms of spectroscopy were introduced to gemologists through the pages of *Gems & Gemology* during the 1980s, most notably infrared, energy-dispersive X-ray fluorescence, and Raman. The decade also saw further development of the electron microprobe as a useful tool in measuring the chemical composition of gem materials. The increasingly technical nature of the submitted manuscripts led Keller to add the position of technical editor to the journal's staff in 1985. Carol M. Stockton, a well-published GIA researcher, held the post for more than 20 years and continues to support *G&G* as consulting editor.

In the 1990s and 2000s, advances in diamond synthesis and challenging new treatments would forever change the way gemologists looked at diamonds, rubies, and sapphires. Following on the broader application of Raman analysis for gem identification, laser ablation–inductively coupled plasma–mass spectrometry (LA-ICP-MS)—also adapted from other research disciplines—emerged as an important technique for quantitative chemical analysis of gem materials. However, not all of gemology's new methods were borrowed from other fields: A 1996 article presented two instruments developed by De Beers

researchers specifically for detecting synthetic diamonds. One of them, the DiamondView, produces a luminescence image revealing the growth structure of the diamond being tested, thereby indicating its natural or synthetic origin (figure 11).

Gem Sources. During the 1980s, reviews and updates on classic colored stone localities—Colombia, Burma (Myanmar), Sri Lanka, Pakistan, Kashmir, Afghanistan, and Thailand—prevailed in the pages of *G&G*. To this day, Keith Proctor's four-part "Gem pegmatites of Minas Gerais" series, which appeared between 1984 and 1988, serves as a comprehensive overview of the major occurrences in this gem-rich Brazilian state. But this decade and the next also saw increased exploration and the emergence of new localities. Soon after the discovery of unusually vivid green and blue copper-bearing tourmalines at a mine in northeastern Brazil, Emmanuel Fritsch headed a 1990 report on these new "Paraíba" tourmalines. The following year, Robert Kane led a report on rubies and fancy sapphires from Vietnam, and in 1992, Dirlam et al. surveyed the colored stone wealth of Tanzania.

Adolph Peretti and coauthors provided the authoritative article on the new rubies from Mong Hsu, Myanmar, in 1995. Richard Hughes et al.'s 2000 report on their visit to Myanmar's jadeite mines marked the first time foreign gemologists had been allowed into this historic locality in more than 30 years. Kenneth Scarratt led a 2000 study of the nuclei in Chinese freshwater cultured pearls, laying to rest unfounded claims about how these exceptionally large, attractive goods were being cultivated, with an update the following year by Akamatsu et al. on the processes used (figure 12). A 2003 article by Brendan Laurs and colleagues marked the first scientific description of the new gem mineral pezzottaite.

Important new diamond sources came onto the scene during the 1980s and 1990s, and groundbreaking articles soon followed. Among these were the seminal 1991 article by Melissa Kirkley et al. on the age and origin of diamonds, and the two 1995–1996 articles by A. J. A. (Bram) Janse on diamond sources in Africa. The discovery and mining of Australia's Argyle diamond deposit, the world's largest by volume, was the focus of a 2001 article by James Shigley and coauthors, and a year later Bruce Kjarsgaard and Alfred Levinson reported on the emerging Canadian diamond deposits and their potential impact on the industry.

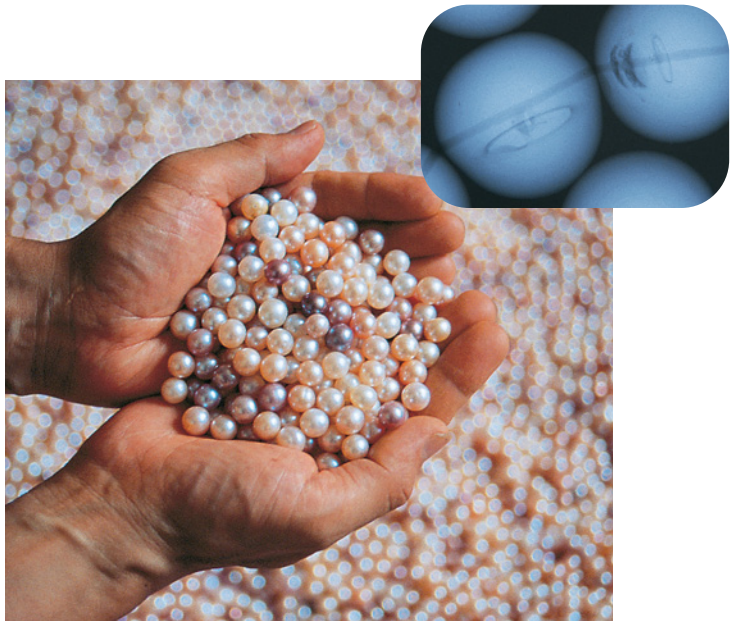

Figure 12. In the past decade, the journal has examined Chinese freshwater cultured pearls and the cultivation process that has resulted in dramatically larger, higher-quality goods, such as those shown in this photo by Shigeru Akamatsu. The inset shows an X-radiograph of these cultured pearls, where the oval shapes mark the original tissue implant; courtesy of Kenneth Scarratt and Thomas Moses.

Colored Stone Identification. Along with examining the geographic sources of colored stones, *G&G* delved further than ever into gem characterization and identification. Responding to the discovery of several new garnet types, Stockton and D. Vincent Manson proposed a more precise garnet classification system in 1985. The following year, Crowningshield, Fryer, and Hurlbut presented their method for separating natural and synthetic amethyst using a simple polariscope, addressing a problem that had plagued the colored stone industry for years. Technology developed for the defense and other industries led to the proliferation of new synthetic rubies and sapphires, which posed a challenge for gemologists around the world. To keep pace, Kane and other researchers examined the new Chatham, Lechleitner, and Ramaura synthetic corundum products, while Karl Schmetzer focused on state-of-the-art synthetic beryls being grown in Russia, China, and elsewhere.

The rise of new and ever more sophisticated treatments likewise demanded attention in the pages of *G&G*. One of the biggest challenges to the colored stone industry during the 1980s was the emergence of diffusion treatment, in which light-colored sapphires were heated with titanium oxide to impart a thin surface-related blue coloration. In

Figure 13. In 2002, the industry learned that beryllium diffusion was being used to significantly alter the color of corundum, changing pink stones (such as those on the left of this photo by Sriurai Scarratt) to pink-orange after treatment (right). This was dramatically illustrated by Shane McClure's inset photo of a 0.51 ct pink sapphire that had been cut in half, with the portion on the right undergoing Be diffusion.

1990, Kane et al. addressed the identification of these treated sapphires, the first of three *G&G* articles on a process that would change the face of the ruby and sapphire industry in the 21st century. When the corundum trade was rocked by the emergence of "deep" diffusion with beryllium in 2002 (figure 13), John Emmett et al.'s comprehensive 2003 article laid out the mechanics of the treatment and clues to its identification. One year later, SSEF's Michael Krzemnicki and Henry Hänni helped describe a new detection method for Be diffusion, laser-induced breakdown spectroscopy (LIBS).

During the 1990s especially, the emerald trade was hit by numerous scandals over undisclosed clarity enhancement. Although common for decades, the oiling of emeralds was not well understood by consumers, and the use of new and different fracture-filling substances challenged trade and public acceptance of the treatment. Concerns about the stability of these new filling materials led to a 1991 article by Kammerling et al. that examined their effectiveness. In 1999, a series of articles presented detection criteria for different emerald fillers and GIA's policy for grading them. GIA's emerald research project culminated in a 2007 article analyzing the durability of various emerald fillers (figure 14).

Diamond Treatments. For most of the journal's existence, colored stone treatments and synthetics were the hot-button topics. While articles were published on diamond grading, simulants such as CZ, and occasionally coating and irradiation treatments, the diamond industry remained relatively untouched by problems that had long plagued colored stones. That ended in 1987, with the discovery that surface-reaching cracks in diamonds were being filled with a lead-based glass to improve their apparent clarity. Unlike irradiation, an issue limited to colored diamonds, glass filling directly affected colorless diamonds. Koivula et al. responded with a 1989 article on the identifying characteristics of these goods, while Kammerling and colleagues delivered a 1994 follow-up (figure 15).

In 1999, the industry was again shaken by the emergence of a new treatment for colorless diamonds—one that permanently removed brown coloration from type IIa stones yet left little gemological evidence. Lazare Kaplan International subsidiary Pegasus Overseas Ltd., the distributor of the treated diamonds, announced that GE had developed the process and that hundreds of these goods had passed through gem laboratories undetected. *G&G* responded with a series of investigations, beginning with Thomas Moses et al.'s Fall 1999 "Observations on GE-processed diamonds: A photographic record," which revealed characteristic internal features of these diamonds and confirmed the use of a high-pressure, high-temperature (HPHT) treatment

Figure 14. Mary Johnson's 2007 article on emerald fillers investigated their durability over time and under common conditions of wear and cleaning. The fissures in this 0.74 ct emerald filled with Araldite 6010 (left) partially emptied out after 30 minutes of ultrasonic cleaning (right).

Figure 15. The late 1980s saw the introduction of a new treatment that used lead-based glass to fill surface-reaching cracks in diamonds to improve their apparent clarity. The left and center photos show a 0.20 ct diamond before and after filling. G&G *articles noted identifying features of these treated diamonds, such as the "flash effect" seen on the right (magnified 29×). Photomicrographs by Shane F. McClure.*

method. Subsequent issues provided additional important clues, first by Karl Schmetzer and then by De Beers researchers David Fisher and Raymond Spits. In 2000, Christopher Smith and coauthors offered an in-depth gemological and spectroscopic analysis of diamonds before and after HPHT processing (figure 16).

Diamond Synthetics and Imitations. Although GE had created gem-quality synthetic diamonds on a small scale in the early 1970s, technical barriers and high production costs kept them in the experimental stage for more than a decade. Starting with Sumitomo in 1985, as noted earlier, a number of manufacturers began to achieve commercial production of gem-quality synthetic diamonds for industrial purposes, a development with serious implications for the jewelry industry. Several articles on the characterization and identification of synthetic diamonds appeared in the journal into the 21st century (figure 17), most of them spearheaded by GIA research director James Shigley.

While these early synthetic diamonds were created by the same basic method—heating carbon with a metal flux at high temperatures and high pressure inside a large press—the technique of chemical vapor deposition (CVD) emerged in the 2000s. The CVD synthetics had very different gemological and spectroscopic characteristics, requiring a new round of intensive research. Landmark articles on CVD synthetic diamonds, led by GIA's Wuyi Wang and De Beers researchers Philip Martineau et al., would follow in the pages of *G&G*.

Even diamond simulants saw advances in technology, with the introduction of synthetic moissanite as a jewelry material in the 1990s. A 1997 article by Nassau and coauthors showed how to identify this new imitation, which could not be detected by the thermal conductivity probes then in wide use.

Diamond Cut and Diamond Grading. GIA had begun grading diamonds in the 1950s, but by the 1980s it was clear that refinements to the system were necessary. One of the earliest concerns was the need for a cut grade. Thus began a 15-year research project, which culminated in a series of *G&G* articles that laid out the basis for the Institute's cut-grading system for round brilliant diamonds, launched in 2005. Color grading saw advances as well, for both fancy-color and colorless stones. In 1994, John King and a

Figure 16. High-pressure, high-temperature (HPHT) treatment removed the brown coloration from this 0.97 ct type IIa diamond (courtesy of the Gübelin Gem Lab).

Figure 17. As gem-quality synthetic diamonds began to enter the market, G&G *provided the tools to identify them. These yellow, blue, and pink synthetic diamonds from Chatham Created Gems were featured in 2004. Photo by Harold & Erica Van Pelt.*

team of coauthors presented the GIA Laboratory's updated system for color grading fancy-color diamonds; this was followed over the next several years by companion articles on grading blues, pinks, and yellows. In 2008, King spearheaded a comprehensive article outlining the development of GIA's color grading system for D-to-Z diamonds.

Scientific and Industry Reviews. Not all *G&G* articles are based on original research—many of the journal's most important contributions have been reviews of developments in the field. Emmanuel Fritsch and George Rossman's three-part "Color in gems" series in 1987 and 1988 remains a seminal reference on the topic two decades later. In 1988, nuclear engineer Charles E. Ashbaugh III provided a comprehensive review of the physics and methods of gemstone irradiation. William Boyajian, then GIA's president, wrote the 1988 classic "An economic review of the past decade in diamonds," which set the stage for similar in-depth analyses of the state of the diamond trade. Menahem Sevdermish et al. profiled the rise of India's diamond cutting industry in 1998, and Russell Shor contributed 2005's update on the state of the global diamond industry. In 2007, Janse took on the monumental task of compiling global rough diamond production statistics since 1870. That same year, Shor analyzed the economics of the cultured pearl industry.

Jewelry History and Fashion. Along with its more scientific studies, *Gems & Gemology* also published scholarly articles on jewelry history and fashion. Looking back to the turn of the 20th century, jewelry historian Elise Misiorowski examined Art Nouveau and Edwardian jewelry (figure 18) in 1986 and 1993. J. Mark Ebert's 1983 article captured the creative spirit of the Art Deco period of the 1920s and 1930s, as did Sally Thomas's 1987 article covering jewelry from the 1940s to the 1960s. In 1985, Dirlam and coauthors reviewed pearl fashion from antiquity through modern times. The importance of gemstone durability in jewelry design and manufacturing was featured in Deborah Martin's 1987 article and accompanying chart.

TWENTY-FIRST CENTURY DEVELOPMENTS

Having stepped down as GIA president in 1983, Liddicoat remained chairman and *G&G* editor-in-chief until his death in 2002. After his passing, Alice Keller was named editor-in-chief. Geologist Brendan Laurs, the journal's senior editor since 1997 and a widely published expert on global gem sources, became editor. Attorney and copyright specialist Tom Overton has been managing editor since 2002 (again, see figure 8).

Meanwhile, a number of *G&G* products have supplemented the quarterly issues. Illustrated wall charts, a more regular feature under longtime art director Karen Myers, provide easy reference and have become popular educational and sales tools. These include a world map of gem localities and charts of commercially available gem treatments, synthetic diamonds, and beryllium-diffused corundum. Another valuable resource has been the cumulative indexes, which help users access the subjects and authors that have appeared in the journal since 1981. Printed every five years from 1990 to 2005, the index has been updated online each year since 2005. That same year, the journal launched the *Gems & Gemology in Review* book series, each volume a collection of *G&G* articles and news briefs on a particular topic. Edited by James Shigley, the series to date includes *Synthetic Diamonds* (2005), *Colored Diamonds* (2006), and *Treated Diamonds* (2008).

In the late 1990s, *G&G* began delivering content electronically on the GIA website, and updates from the journal became a regular feature in the *GIA Insider*, the Institute's free electronic newsletter. Today, articles and issues—from the most recent back to 1981—can be downloaded at gia.metapress.com (with all earlier issues and a data depository available for free along with the indexes at www.gia.edu/gandg). What started as a small publication for American jewelers has become a professional journal reaching a worldwide audience of jewelers, gemologists, educators, and researchers. *G&G* is delivered to more than 100 countries, with a Japanese version provided by GIA Japan.

Since 1981, *G&G* has received 31 honors for editorial excellence and print quality, including 12 Gold Circle Awards for best peer-reviewed journal from the American Society of Association Executives and five Gold Ink Awards, the nation's most respected print competition. In 2004, *Gems & Gemology* was accepted into the database of the Institute for Scientific Information (now the Thomson Reuters database), the world's most prestigious resource for indexing and referencing academic journals. To date, *G&G* is the only gemological journal to achieve this recognition.

Figure 18. Elise Misiorowski's 1993 "Jewels of the Edwardians" is one of several jewelry history articles published in G&G. *The cover of that issue, I. Snowman's circa-1910 portrait of Queen Alexandra, consort of King Edward VII, captured the essence of the era in the fabulous jewels she wore. Painting courtesy of A. Kenneth Snowman.*

SUMMARY

Just as print production has shifted from film photography and linotype machines to digital photography and desktop publishing, the field of gemology has witnessed changes that were unimaginable 75 years ago. Once, gemologists used only a few basic tests and techniques (refractive index, specific gravity, fluorescence, prism spectroscope, and microscopic examination). Today, they rely on a multitude of sophisticated instruments and specially trained technicians. *Gems & Gemology* has introduced its readers to these new methods, educated them on how to use and interpret the results, and helped them determine when the identification of a gem material requires more advanced testing. Throughout, the journal has remained committed to its original purpose, set forth in the first issue's editorial: providing "accurate and up-to-date information concerning gem-stones."

In the process, *G&G* has become a powerful forum for up-to-date technical information, derived from global research efforts, that has been rigorously reviewed and insightfully illustrated. As long as there are new gem localities and gem features to explore, new treatment processes and synthetic materials to address, and technological innovations to embrace, the role of *Gems & Gemology* will remain crucial.

ABOUT THE AUTHORS
Mr. Overlin (soverlin@gia.edu) is associate editor of Gems & Gemology. *Ms. Dirlam (ddirlam@gia.edu) is director of GIA's Richard T. Liddicoat Gemological Library and Information Center in Carlsbad, California.*

ACKNOWLEDGMENTS
The authors thank the staff of GIA's Richard T. Liddicoat Gemological Library and Information Center for their help with archival information and images, particularly Caroline Nelms, Kevin Schumacher, Judy Colbert, and Robert Weldon. The subject and author indexes of G&G*'s first 35 years, prepared by Dr. Richard V. Dietrich and the late Dr. Alfred A. Levinson, were immensely valuable.*

THE "TYPE" CLASSIFICATION SYSTEM OF DIAMONDS AND ITS IMPORTANCE IN GEMOLOGY

Christopher M. Breeding and James E. Shigley

Diamond "type" is a concept that is frequently mentioned in the gemological literature, but its relevance to the practicing gemologist is rarely discussed. Diamonds are broadly divided into two types (I and II) based on the presence or absence of nitrogen impurities, and further subdivided according to the arrangement of nitrogen atoms (isolated or aggregated) and the occurrence of boron impurities. Diamond type is directly related to color and the lattice defects that are modified by treatments to change color. Knowledge of type allows gemologists to better evaluate if a diamond might be treated or synthetic, and whether it should be sent to a laboratory for testing. Scientists determine type using expensive FTIR instruments, but many simple gemological tools (e.g., a microscope, spectroscope, UV lamp) can give strong indications of diamond type.

Gemologists have dedicated much time and attention to separating natural from synthetic diamonds, and natural-color from treated-color diamonds. Initially, these determinations were based on systematic observations made using standard gemological tools such as a microscope, desk-model (or handheld) spectroscope, and ultraviolet (UV) lamps. While these tools remain valuable to the trained gemologist, recent advances in synthetic diamond growth, as well as irradiation and high-pressure, high-temperature (HPHT) treatment techniques, have rendered them less definitive in identifying synthetic and color-treated diamonds. Thus, most gemological laboratories now use more-sophisticated scientific techniques such as absorption and photoluminescence spectroscopy to detect treatments and synthetics.

These developments in gem diamond identification have introduced many scientific terms and concepts into the gemological literature. One of the most important of these concepts is diamond "type." The diamond type classification system is widely used in diamond research, because it provides a convenient way to categorize diamonds based on their chemical and physical properties. Understanding this system is critical to evaluating the relationships between diamond growth, color (e.g., figure 1), and response to laboratory treatments. With the increasing availability of treated and synthetic diamonds in the marketplace, gemologists will benefit from a more complete understanding of diamond type and of the value this information holds for diamond identification.

Considerable scientific work has been done on this topic, although citing every reference is beyond the scope of this article (see, e.g., Robertson et al., 1934, 1936; and Kaiser and Bond, 1959). Brief gemological discussions of diamond types appeared in Shigley et al. (1986), Fritsch and Scarratt (1992), and Smith et al. (2000), and more-detailed descriptions were given in Wilks and Wilks (1991) and Collins (2001). Nevertheless, repeated inquiries received at GIA indicate that many practicing gemologists do not have a clear understanding of the basics of diamond type. This article offers a readily accessible, gemology-specific guide to diamond type and related

See end of article for About the Authors and Acknowledgments.
GEMS & GEMOLOGY, Vol. 45, No. 2, pp. 96–111.

Figure 1. Gem diamonds such as these are prime examples of their respective diamond types (from left): 0.47 ct type Ia pink, 0.38 ct type Ia "cape" yellow, 1.04 ct type IIa colorless, 0.56 ct type IIb blue, and 1.01 ct type Ib "canary" yellow. All the colored diamonds are part of the Aurora Butterfly of Peace collection. Composite photo by Robert Weldon and Kevin Schumacher.

trace-element impurities, including how impurities are measured, why type is important, and how type can be determined using simple gemological tools. With this foundation, it then explains the application of diamond type concepts to the detection of diamond color treatments and synthetic diamonds.

BACKGROUND

Having grouped diamonds in the past on the basis of their color, fluorescence, visible absorption spectra, and other properties, scientists eventually sought to organize these groupings into a formal classification system. Robertson et al. (1934, 1936) were the first to do so, dividing "colorless" diamonds into two categories on the basis of differences in their transparency to both UV (10 nm to ~400 nm) and infrared (IR; ~700 nm to 1000 µm) wavelengths. The larger group consisted of *type I* diamonds, which were opaque to UV radiation below ~300 nm and absorbed strongly in parts of the IR region (specifically the range 7000–20000 nm). The smaller group was composed of *type II* diamonds, which transmitted UV wavelengths and displayed little or no anomalous birefringence when viewed between crossed polarizers. Robertson and his colleagues thus concluded that type II diamonds were nearly "perfect" in terms of their crystal structure. Two decades later, Sutherland et al. (1954) suggested that the "less perfect" character of type I diamonds resulted from carbon atoms in the diamond structure being in an "abnormal state" and from the presence of "chemical impurities." Their assertions proved correct when it was later determined that the differences between diamonds in these two categories were due to the presence (type I) and apparent absence (type II) of nitrogen in the diamond structure (Kaiser and Bond, 1959).

Other researchers began to note systematic relationships between the optical properties of diamonds. UV fluorescence reactions were correlated with diamond color and absorption bands seen with the prism spectroscope (Nayar, 1941a,b; Anderson, 1943a,b,c, 1962, 1963; Mitchell, 1964). Color, transparency, and luminescence properties of more than 300 diamonds were also documented by the famous scientist, Sir C. V. Raman (1944). This pioneering work on diamond color and luminescence was expanded by studies of the different IR absorption spectra produced by type I and type II diamonds (see Sutherland and Willis, 1945; Blackwell and Sutherland, 1949). These studies became the foundation for today's use of IR spectroscopy to determine diamond type.

Kaiser and Bond (1959) were the first to correlate certain characteristics (i.e., yellow coloration, blue fluorescence, and a particular IR absorption spectrum) with the presence of nitrogen impurities in type I diamonds. Other studies confirmed their findings (Anderson, 1961; Lightowlers and Dean, 1964). Shortly thereafter, Dyer et al. (1965) used IR spectroscopy to distinguish between diamonds with aggregated (type Ia) and isolated (type Ib) nitrogen atoms. The vast majority (>95%) of natural diamonds turned out to be type Ia, and only a rare few were found to be type Ib (Davies, 1977). Some of those rare type Ib diamonds showed extraordinary yellow color and corresponded to those termed *canary* in the gem trade (Anderson, 1962; Collins, 1980). Custers (1952, 1954) found that type II diamonds also occur very rarely in nature and proposed splitting them into two groups, IIa and IIb.

The latter diamonds were blue (sometimes grayish blue, gray, or brown) and exhibited electrical conductivity (Custers, 1955; Anderson, 1960, 1962). Further work demonstrated that boron was the impurity that gave rise to the unique properties of type IIb diamonds (Wentorf and Bovenkirk, 1962; Chrenko, 1973).

HOW ARE DIAMOND TYPES CLASSIFIED AND WHY ARE THEY IMPORTANT IN GEMOLOGY?

Pure diamond is made of only one element: carbon. The atoms are arranged in a regular repeating pattern (the diamond lattice) that is unique among gems. However, atoms of elements such as nitrogen (N) and boron can replace some of the carbon atoms in the lattice. While other impurities can also be incorporated, the diamond type classification system divides diamonds into categories based solely on the presence or absence of certain nitrogen and boron impurities and the ways in which they are arranged in the lattice (figure 2).

Diamond Type Classification. The foundation of the type classification system is the presence or absence of nitrogen, the most common impurity in diamond. Type I diamonds are defined as containing sufficient N to be measurable by IR absorption spectroscopy, whereas type II diamonds do not contain enough N to be detected by the IR spectrometer. These general categories are then subdivided based on the nature of the impurities that are present.

As noted above, type I diamonds are divided into type Ia and type Ib. Both subgroups contain nitrogen, but the nitrogen atoms in each are arranged differently (again, see figure 2). In type Ib diamonds, single nitrogen atoms that have replaced carbon atoms in the lattice are isolated from one another; that is, they generally do not occur in adjacent lattice positions. These N impurities are called by several names in the scientific literature, including *isolated N*, *single substitutional N*, and *C centers*. In contrast, type Ia diamonds contain N atoms that are in close proximity to one another in one of two spectroscopically detectable configurations. The most common configuration for type Ia diamonds

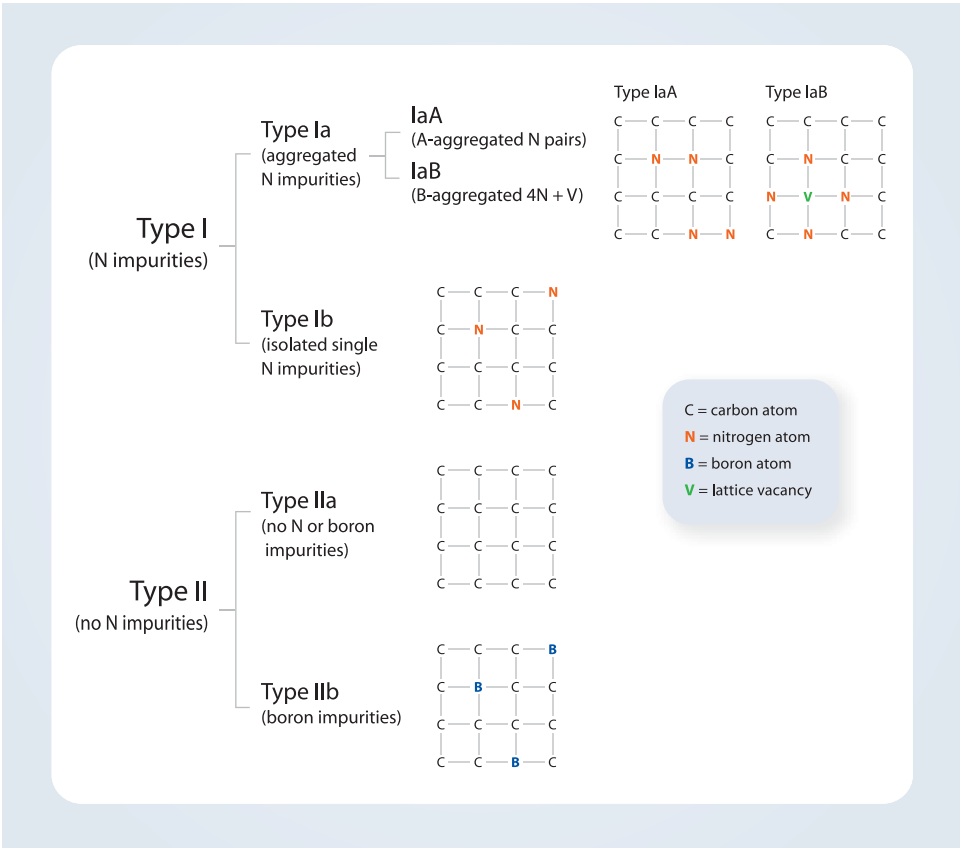

Figure 2. Diamond type classification is based on the presence or absence of nitrogen and boron impurities and their configurations in the diamond lattice. These schematic diagrams illustrate the manner in which N and boron atoms replace C atoms in the diamond lattice. The diagrams are simplified two-dimensional representations of the tetrahedrally bonded C atoms (four bonds per C atom) that form the three-dimensional diamond crystal structure. Type Ia diamonds contain aggregated N impurities—including A-aggregates (IaA), which consist of pairs of N atoms, and B-aggregates (IaB), which are made up of four N atoms around a vacancy (V). Type Ib diamonds have isolated N atoms. Type IIa stones contain no measurable impurities, and type IIb diamonds have boron impurities.

Figure 3. Color is strongly influenced by the impurities/defects in the diamond lattice. Consequently, diamond type plays an important role in the potential colors of natural, synthetic, and treated stones. Although much experience is necessary to even attempt an assessment of diamond type using color observations, these images show some of the representative colors for each category. Photos by various GIA staff.

involves two N atoms adjacent to each other in the lattice. Although these two atoms occupy neighboring sites, each pair is isolated from other N atoms in the lattice. These N impurities are commonly referred to as *A aggregates* (or *A centers*), and the diamonds that contain them are termed *type IaA*. The other configuration involves four N atoms that symmetrically surround a vacancy. (A vacancy is a lattice site normally occupied by a carbon atom that is not occupied by any atom.) This complex grouping is formed when two A centers combine. These N impurity groupings are called *B aggregates* (or *B centers*), and the associated diamonds are *type IaB*. Other arrangements of N atoms (see box A) do occur, but they are not included in the diamond type classification system (Collins, 1982, 2001).

Type II diamonds are divided into types IIa and IIb (again, see figure 2). Type IIa diamonds contain no easily measurable N or boron impurities. Natural type IIb diamonds likewise contain no IR-measurable N impurities. Instead, type IIb diamonds contain boron impurities that are thought to be isolated single atoms that replace carbon in the diamond lattice. Characteristic properties of type IIb diamonds, such as electrical conductivity, are a direct result of the boron impurities.

What Can a Gemologist Learn from Diamond Type? In many cases, the geologic conditions to which natural diamonds have been exposed during their extended period in the earth and the conditions imposed in a laboratory during treatment or synthetic growth are quite different, yet the resulting structural lattice defects can yield natural, treated, and synthetic diamonds with very similar colors. (See box A for information about non–type related defects that also influence color.) Diamond impurities control the nature of the lattice defects that occur naturally and their evolution during lab growth or treatment. Therefore, a diamond's type reflects its history, whether in nature or in the laboratory, or both—and an adequate understanding of diamond type is critical for identification purposes. Since the detection of many modern treatments and synthetics requires the facilities of a well-equipped gemological laboratory, it is important to know when to send a diamond for advanced testing. With a better understanding of how diamond type relates to natural color, treated color, and synthetic growth processes, a gemologist should be able to make that decision more easily.

Relationship of Type to Diamond Color and Treatments. Natural diamonds often show colors that correlate to their diamond type (figure 3). For example, type Ia colorless, brown, pink, and violet diamonds are unlikely to have been color-treated, whereas treated-color type Ia yellow, orange, red, blue, and green stones are relatively common.

BOX A: SUMMARY OF COLOR-PRODUCING DIAMOND DEFECTS NOT RELATED TO DIAMOND TYPE

Several lattice defects contribute to the color of diamond even though they are not involved in the assignment of diamond type. Most of these features selectively absorb light in the visible range of the electromagnetic spectrum to produce color, and they can be seen with a gemological spectroscope or a UV-Vis-NIR absorption spectrometer. These defects are commonly mentioned in the scientific and gemological literature. A brief description of each is given below (from Clark et al., 1979; Collins, 1982, 2001; Zaitsev, 2001; and GIA staff observations).

N3 (415 nm): This defect consists of three nitrogen atoms surrounding a vacancy. In addition to contributing to yellow color in "cape" diamonds, it can also produce blue luminescence in response to long-wave UV radiation.

N2 (478 nm): This broad absorption is associated with N3 and is part of the well-known "cape" spectrum in many yellow diamonds. It is also related to nitrogen impurities.

480 nm: This broad band is a defect of unknown origin that commonly produces yellow or orange color in type Ia diamonds. Strong yellow fluorescence is typical of diamonds colored by this mechanism.

H4 (496 nm): This defect consists of four nitrogen atoms separated by two vacancies. It is created when a vacancy migrates through the diamond lattice and combines with a B-aggregated nitrogen impurity. H4 produces yellow color in diamond.

H3 (503.2 nm): This is an uncharged defect consisting of two nitrogen atoms separated by a vacancy [i.e., $(N\text{-}V\text{-}N)^0$]. H3 absorption alone creates yellow color, while the defect can also produce green luminescence in response to illumination.

3H (503.5 nm): This defect is thought to be related to an interstitial carbon atom in the diamond lattice. It is created by radiation damage and often occurs with the GR1. On rare occasions, 3H absorbs strongly enough to enhance the green color caused by GR1 absorption.

550 nm: This broad band is poorly understood and thought to be associated with plastic deformation of the diamond lattice. This is the most common defect that produces pink-to-red color in natural diamonds, but it is also common in brown stones.

NV^0 (575 nm): This defect consists of a nitrogen atom adjacent to a vacancy; it is in a neutral charge state. In combination with the 637 nm defect, the NV^0 center produces pink color in most treated pink diamonds as well as in a few natural pink stones.

595 nm: This band is a nitrogen-related defect of uncertain structure. It is commonly associated with laboratory irradiation and annealing of diamond to produce green, yellow, or pink colors, but it is also present as a weak feature in many natural-color green or yellow diamonds.

NV^- (637 nm): This defect consists of a nitrogen atom adjacent to a vacancy. This defect is in a negative charge state. In combination with the 575 nm defect, the NV^- center produces pink color in most treated pink diamonds as well as a few natural stones.

GR1 (741 nm): This defect is a single, uncharged vacancy in the diamond lattice. It is common in most natural and artificially irradiated type Ia and IIa blue or green diamonds. Although outside the visible spectral range (~400–700 nm), strong absorption by GR1 produces related bands at the red end of the spectrum that result in green or blue color.

H2 (986 nm): This is a negatively charged defect that consists of two nitrogen atoms separated by a vacancy [i.e., $(N\text{-}V\text{-}N)^-$]. It is closely related to H3 and is commonly cited as evidence for HPHT treatment in type Ia diamonds. Occasionally, H2 (and related broad band absorptions) can be so intense that the combination of H3 and H2 produces a strong green bodycolor.

Natural type Ib diamonds are almost always brown, yellow, or orange, whereas their artificially irradiated and annealed counterparts are usually pink to red. HPHT treatment can produce yellow in an off-color type Ib diamond. HPHT processes may enhance type IIa brownish diamonds to appear colorless or pink, and may produce blue in some type IIb diamonds. However, HPHT treatment cannot alter a type Ia diamond to colorless (except rare pure IaB), so if a gemologist determines that a colorless diamond is type Ia, it is usually not necessary to send it to a gemological laboratory for further testing (the few colorless syn-

thetic diamonds currently on the market are type IIa).

Most permanent (i.e., not related to surface coatings) diamond treatments add, change, or remove color by reorganizing defects in the diamond lattice. Diamond type may determine whether or not the necessary color-causing defects can be produced or destroyed during the treatment process to achieve the desired result. Irradiation is routinely performed on all types of diamonds to produce green or blue colors, so type is not very useful in that case. However, if irradiation is followed by heating to temperatures of 800–1000°C to produce a yellow or pink color, then the diamond type of the starting material is critical. Type I diamonds will often change to intense yellow, orange, pink, or red with irradiation followed by annealing, whereas type II diamonds rarely develop intense colors in these hues due to the lack of impurities (primarily N) needed to create complex, color-producing defects. Therefore, it is useful for a gemologist to understand that type II diamonds are not likely to have been subjected to treatments involving irradiation followed by annealing.

The detection of HPHT treatment requires an even better knowledge of diamond type (Fisher and Spits, 2000; Smith et al., 2000). In most cases, HPHT treatment will only decolorize a type IIa diamond (see figure 4). The HPHT conditions cause changes in the brown, deformed regions in these stones, allowing them to become colorless to near-colorless. Occasionally, HPHT treatment can change type II diamonds to pink or blue. When a type I brown stone is subjected to similar treatment conditions, the presence of N impurities causes it to change to various shades of yellow (again, see figure 4). Thus, a

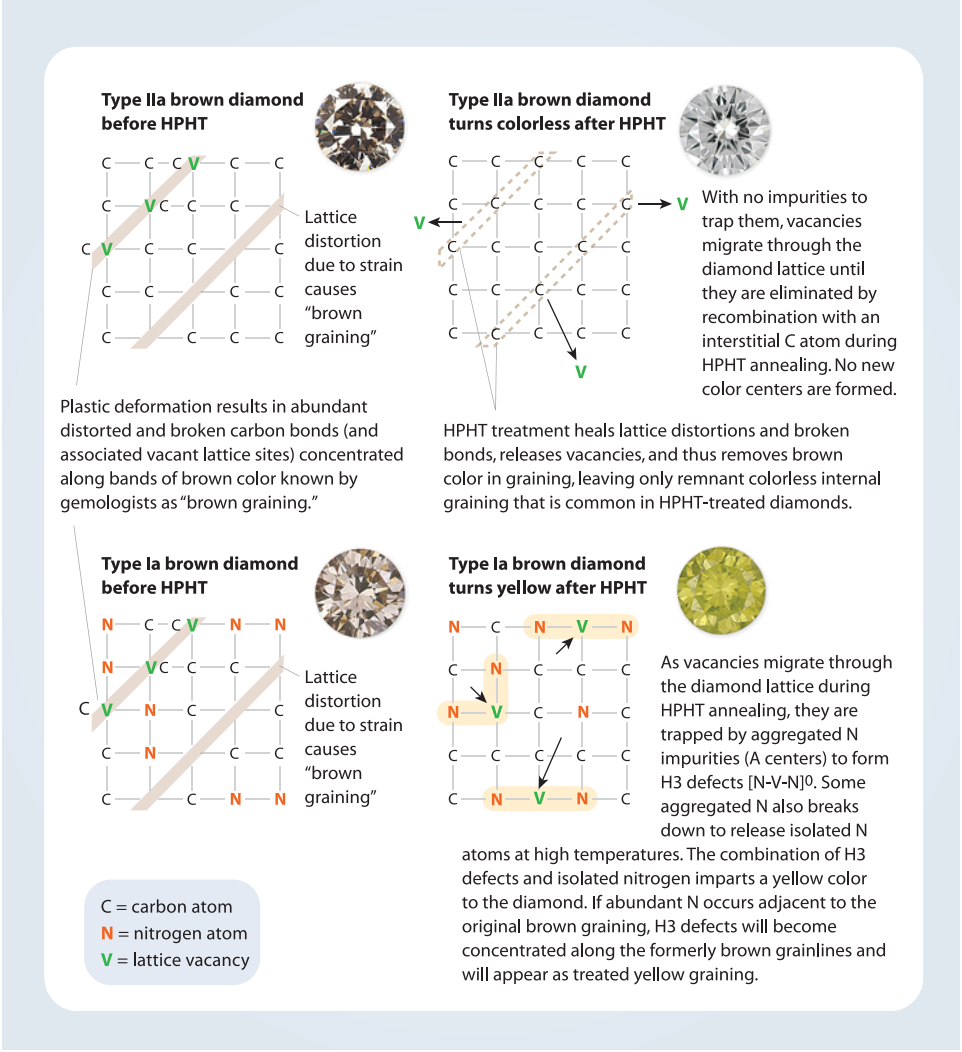

Figure 4. The effects of HPHT treatment are strongly dependent on the diamond type of the starting material. Type IIa brown diamonds can be decolorized because the brown color associated with plastic deformation is sensitive to the effect of high temperatures and pressures; usually, no new color centers are formed due to the absence of significant N impurities. Conversely, type Ia brown diamonds contain abundant aggregated N impurities that trap vacancies during treatment to create complex H3 defects and also break down aggregates to release isolated nitrogen; both of these processes contribute to the newly formed yellow bodycolor.

gemologist working with colorless diamonds can quickly determine which ones should be sent to a gemological laboratory simply by checking to see if they are type II or not. Recently, a combination of HPHT treatment and irradiation with low-pressure annealing has been used to create more intense pink, red, or orange hues in both type Ia and IIa diamonds (Wang et al., 2005).

Relationship of Type to Synthetic Diamonds. Over the last several years, the production of HPHT-grown synthetic diamonds has increased dramatically, and chemical vapor deposition (CVD) synthetic diamonds have started to enter the gem market (Wang et al., 2007). Therefore, gemologists are under even greater pressure to identify these laboratory-grown products. Diamond type can provide a few clues in this regard. HPHT-grown synthetic diamonds are almost all type Ib, a type that is rare in natural diamonds. Those few natural diamonds that are type Ib usually contain abundant inclusions of natural minerals and exhibit colorful strain patterns (discussed below). In contrast, type Ib HPHT-grown synthetic diamonds contain only metallic flux inclusions (when any inclusions at all are present), and they typically show a very weak strain pattern or none at all (Shigley et al., 2004). CVD synthetic diamonds are most commonly type IIa and are typically near-colorless or light brown. These synthetics can usually be distinguished from their natural- and treated-color counterparts by the absence of cross-hatched "tatami" strain patterns (see also below). Occasionally, both HPHT and CVD growth techniques will produce attractive blue type IIb synthetic diamonds. The absence of "tatami" strain, combined with the presence of electrical conductivity, can be used to identify these synthetics.

Most synthetic (type Ib) diamonds currently in the market have intense yellow to orange colors. Because they respond to treatment in essentially the same way that natural type Ib diamonds do, the colors of treated-color natural and synthetic diamonds may be very similar. With the recent advances in CVD synthetic diamond growth techniques, colorless type IIa diamonds must also be considered as possibly synthetic.

Is There a Link Between Diamond Type and Geographic Origin? In some cases, certain diamond types have become associated with specific geographic occurrences. However, we rarely know the geographic origin of a cut diamond, and this cannot be reliably determined from diamond type. Nonetheless, this topic deserves brief mention because of the historical importance associated with several well-known diamond-producing localities.

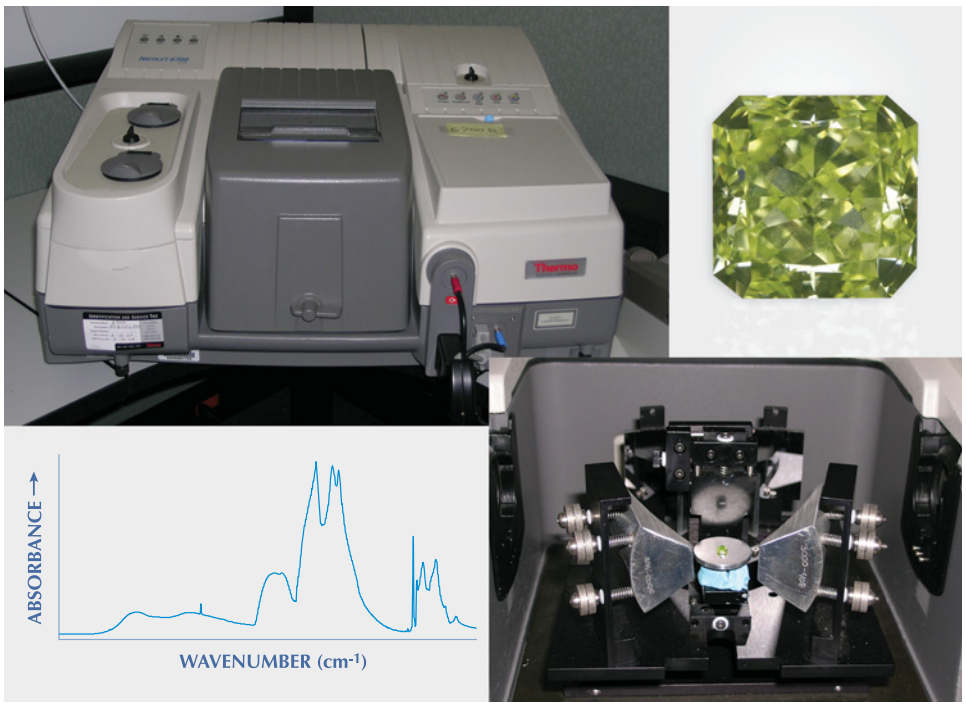

Figure 5. GIA uses an FTIR spectrometer such as this Thermo Nicolet 6700 (top left; 1 cm^{-1} resolution, KBr beam splitter, mid-IR range) to determine diamond type. A faceted diamond like the one shown here (top right) is placed table-down on a specially designed beam condenser stage to focus the IR beam through the girdle of the stone (bottom right). The result is an absorption spectrum from which diamond type can be determined (bottom left). Photos by C. M. Breeding and Robison McMurtry.

Type Ia stones occur in all major diamond deposits, but they are perhaps best known from the mines of South Africa. As a result, yellow type Ia diamonds are often termed "cape" diamonds (King et al., 2005). Pink type Ia diamonds are typically a product of the Argyle mine in Australia (King et al., 2002). Type Ib diamonds can occur in all major deposits, but they are well known from mines in India, Brazil, and South Africa (King et al., 2005). Type IIa diamonds likewise occur in all deposits, but the Golconda region of India has historically been known as one important source. Many type IIa pink diamonds are thought to originate from Brazil, Africa, and India (King et al., 2002). Type IIb diamonds are less widely distributed; most come from India and the Cullinan (formerly Premier) mine in South Africa (King et al., 1998).

HOW DO SCIENTISTS DETERMINE DIAMOND TYPE?

To determine a diamond's type, scientists must be able to detect and measure the impurities involved. The most common method is Fourier-transform infrared spectroscopy (FTIR, as illustrated in figure 5; Clark et al., 1979). Several other techniques, such as EPR/ESR (electron paramagnetic resonance/electron spin resonance spectroscopy) and SIMS (secondary ion mass spectrometry) chemical analysis, offer some ability to measure impurities in diamond. However, these techniques are complicated, destructive, expensive, and limited in the amount of information they provide about the configuration of specific nitrogen and boron impurities. By contrast, FTIR analysis is nondestructive and relatively inexpensive (for a spectrometer), and it provides a tremendous amount of information about diamond lattice impurities.

In simple terms, FTIR analysis involves sending a beam of infrared radiation through a diamond and measuring how much of it is absorbed (and at what wavelengths). Interactions between nitrogen and boron impurity configurations and the surrounding carbon atoms cause distinctive features in the IR region of the electromagnetic spectrum; that is, each kind of type-related N and boron impurity causes a specific and unique absorption band or bands. The diamond lattice itself also produces characteristic absorption features, so that FTIR spectroscopy can both identify a sample as diamond and reveal the types and amounts of impurities present.

To discuss the detection of impurities using FTIR, we must first describe the details of a diamond's FTIR spectrum (figure 6). Whereas nanometers (nm) are often given as units of wavelength in the UV and visible range of the electromagnetic spectrum, the IR range is usually described in terms of wavenumbers (cm^{-1}; to convert between units: 10^7 / [wavelength in nm] = [wavenumber in cm^{-1}]). Diamonds show important absorption features in the mid-IR range (~4000–400 cm^{-1}). For diamond, this range is divided into three zones—known as the one-, two-, and three-phonon regions—based on how the chemical bonds between carbon atoms (and any impurities) within the diamond lattice vibrate when exposed to IR energy (Zaitsev, 2001). Figure 6 shows these regions for both type I and type II diamonds.

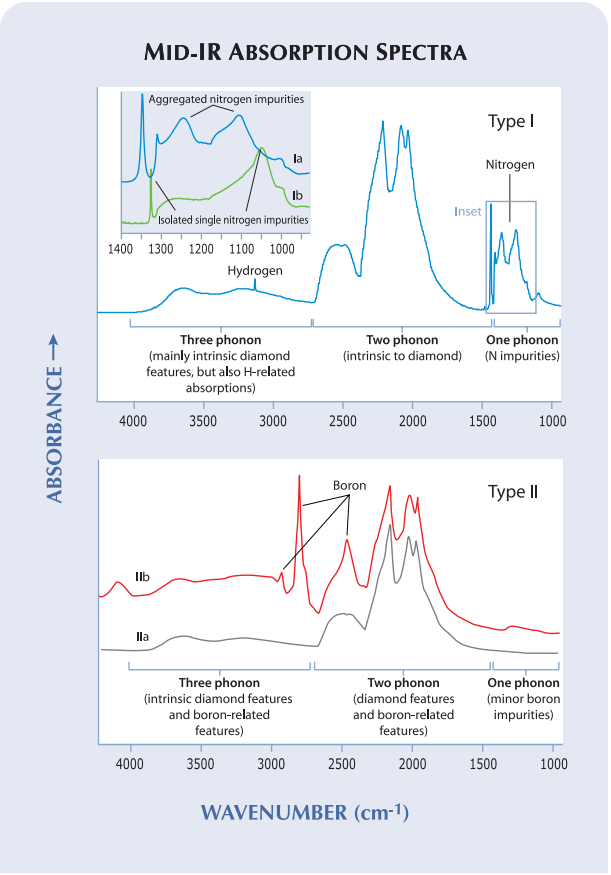

Figure 6. An FTIR absorption spectrum of diamond consists of one-, two-, and three-phonon regions where absorptions related to nitrogen and boron impurities can be identified to determine diamond type. Type I features (top) occur mostly in the one-phonon region, whereas type IIb boron-related absorptions occur more prominently in the two- and three-phonon regions (bottom). The expanded spectrum of the one-phonon region (top, inset) illustrates the differences between aggregated (type Ia) and isolated (type Ib) N impurities.

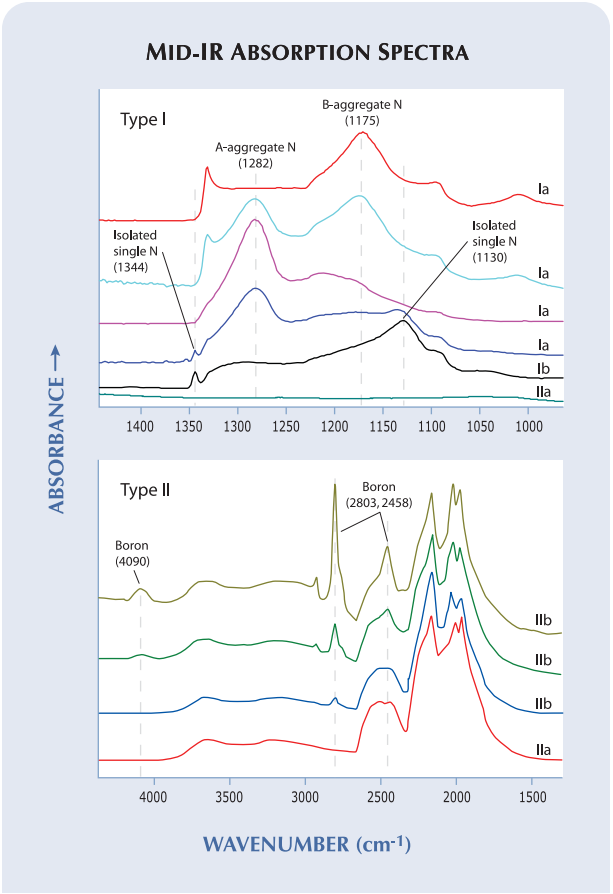

Figure 7. Nitrogen and boron impurities in diamond occur in varying abundances. FTIR spectra not only can identify the impurities present, but they also can establish the configuration in which N atoms occur in the diamond lattice (isolated or aggregated; top). Several boron-related absorptions become visible with increasing concentration (bottom).

The one-phonon region (~1332 to ~400 cm^{-1}) is where type I–related N impurities produce characteristic absorptions. Equally important is the fact that type II diamonds show few features in this region.

The two-phonon (2665 to ~1332 cm^{-1}) and three-phonon (~4000 to 2665 cm^{-1}) regions contain features that are intrinsic to diamond; that is, they occur in all diamond types. These features are caused by vibration of carbon-carbon bonds of the diamond lattice when exposed to infrared energy (e.g., Zaitsev, 2001, and references therein). These two regions are also the part of the IR spectrum where boron impurities can be detected most easily. While the features caused by boron impurities are usually weak in the one-phonon region, relatively sharp and stronger absorption peaks are present at ~2458 cm^{-1} in the two-phonon region, and at ~2930 and ~2803 cm^{-1} in the three-phonon region; these result from electronic effects of boron on the diamond lattice. In some type I diamonds, other impurities that do not affect type determination (e.g., hydrogen) can also display features in the three-phonon region.

The one-phonon region for type I diamonds illustrates the distinctive spectral features resulting from different configurations of N impurities in type Ia and Ib stones (see expanded area in figure 6 and figure 7, top). Figure 7 shows a series of FTIR spectra that reveal the progression of N impurities from isolated, single N (detected at 1344 and ~1130 cm^{-1}) to A-aggregated N (detected at ~1282 cm^{-1}) to B-aggregated N (detected at ~1175 cm^{-1}). Variable concentrations of A and B aggregates along with single substitutional N create a continuum of peak intensities in this region (an idea first proposed by Custers, 1952). It should be emphasized that the classification system is based on gradational transitions between types, so there are actually few "pure" examples of diamond type. Box B discusses several factors that commonly result in "mixed-type" IR spectra.

In addition to indicating the presence and arrangement of nitrogen and boron impurities that are used to determine type, FTIR analysis can provide information about the concentration of the impurities. Both type I and type II diamonds may show a range of impurity concentrations, which often have important effects on their optical properties. The intensity of an absorption peak in a diamond's FTIR spectrum is related to two factors: the concentration of the impurity causing the peak, and the thickness of the diamond through which the beam of IR radiation passes. When the thickness (i.e., path length) can be directly measured, the intensity of the FTIR spectral peak can be calculated to produce an "absorption coefficient," which eliminates the thickness factor, leaving only the intensity related to the impurity concentration. The peak height can then be compared to the peak heights in diamonds of known concentration to calculate the amount of impurity present (see references below for calculation equations). However, the fact that most gem diamonds are faceted makes accurate measurement of the path length difficult, if not impossible (again, see box B).

Fortunately, it is widely accepted that the absorption coefficient of diamond in most parts of the two- and three-phonon regions is constant. At 2000 cm^{-1}, for example, the absorption coefficient is 12.3 cm^{-1} (Tang et al., 2005). Thus, IR absorbance at

BOX B: WHY ARE MIXED-TYPE DIAMONDS COMMON?

Most diamonds contain characteristic features of more than one diamond type, and many factors contribute to the prevalence of mixed-type diamond spectra. The first factor is the process of nitrogen aggregation. When diamonds crystallize, all N impurities are thought to occur as single atoms in the lattice (Collins et al., 2005). As the diamonds reside at high temperatures and pressures at great depths in the earth for very long periods of time, the N atoms move around in the lattice and aggregate into groups. When two N atoms combine, an A-aggregate forms, and when two A-aggregates combine (with a vacancy between them), a B-aggregate forms. This tendency for nitrogen aggregation helps explain the rarity of type Ib versus type Ia natural diamonds.

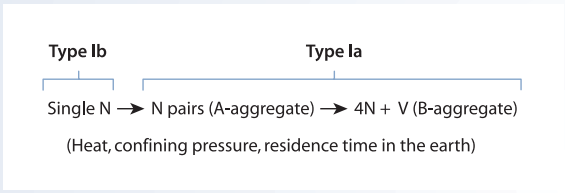

This progression of N impurity aggregation goes nearly to completion for some natural diamonds (Collins et al., 2005), which results in almost "pure" type IaB, but in many cases multiple configurations of nitrogen impurities coexist in a single crystal due to incomplete aggregation (Hainschwang et al., 2006).

Another factor causing mixed-type spectra is that most type I diamonds contain zones with different amounts or configurations of nitrogen in the same crystal (e.g., Breeding, 2005; Chadwick, 2008). This fact, combined with the way in which IR spectra are collected from a faceted diamond, makes it nearly impossible to avoid mixed-type spectra. To obtain a spectrum, the technician must orient the diamond so that the IR beam can pass through it to a detector on the opposite side. Faceted diamonds force light to bounce around inside and not pass directly through, making the task of recording FTIR spectra difficult. Typically, diamonds are placed table-down on a specially designed stage in the FTIR instrument (again, see figure 5) to allow the beam to pass through opposite sides of the girdle region, where minimum internal reflection should occur. Absorption occurs across the entire distance (or path length) through which the IR beam passes. Thus, if any variations in N impurities occur in a diamond along this path, they are automatically added together to produce a mixed-type IR spectrum.

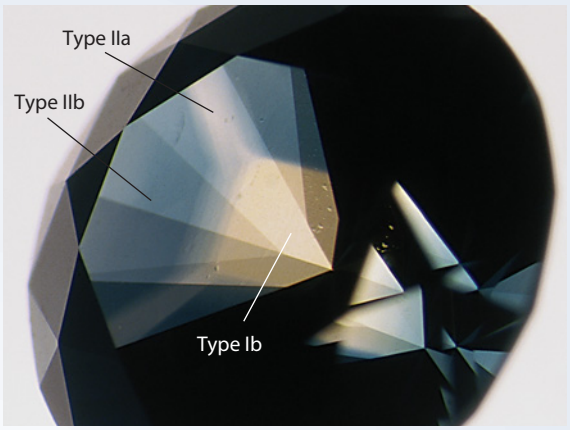

Figure B-1. This HPHT-grown synthetic diamond, seen immersed in water, shows growth zones with different diamond types. The yellow zone is type Ib, the colorless zones are type IIa, and the blue zones are type IIb. Only synthetic diamonds commonly show mixtures of nitrogen and boron impurities in the same crystal. Photo from Shigley et al. (2004); magnified 20×.

The mixture of diamond types is not unique to natural diamonds. Most (HPHT) synthetic diamonds grow as type Ib. If they are subjected to high temperatures, either during or after laboratory growth, the N atoms tend to aggregate to produce type Ia synthetics with remnant concentrations of isolated N atoms. Similarly, if boron is introduced into the growth chamber (N is also present because it is difficult to exclude from the growth environment), a mixed-type diamond is formed. When visible color zones occur, such as in some mixed-type (Ib + IIa + IIb) synthetic diamonds such as that seen in figure B-1 (Shigley et al., 2004), distinguishing between zones of different type can be done on the basis of color. This is because different impurities produce different colors and are well known to be enriched in particular diamond growth sectors (Welbourn et al., 1996).

2000 cm^{-1} is proportional to the thickness of the sample, allowing any IR spectrum to be normalized to remove the effects of variation in thickness or path length (i.e., it does not matter how much the light bounces around inside the diamond; figure 8). After normalization, the intrinsic two- and three-phonon region diamond peaks are removed by subtracting a pure type IIa spectrum from the unknown

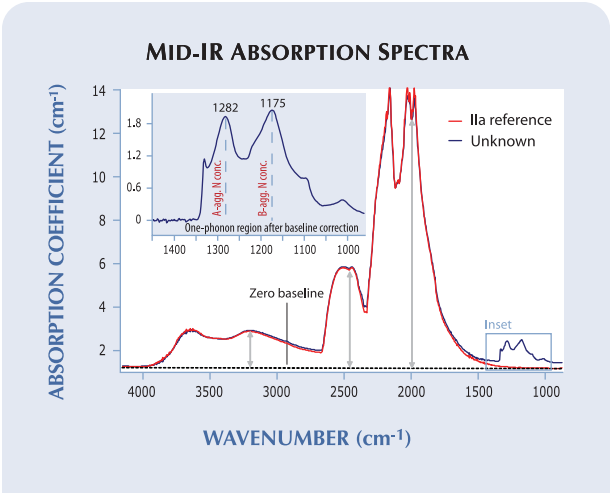

Figure 8. The concentration of N impurities in a diamond can be determined from the FTIR absorption spectrum. The concentration of each form of nitrogen is calculated from its absorption coefficient at a specific wavelength. The spectrum of a "pure" type IIa diamond is subtracted to eliminate the absorption coefficients in the diamond-intrinsic region (i.e., those related only to carbon). When several forms of nitrogen are present in the sample—here, A and B aggregates—a deconvolution of the bands is necessary because they overlap.

diamond spectrum, leaving a baseline-referenced spectrum showing only those absorption peaks caused by impurities. These peak intensities can be measured and impurity concentrations calculated from them using equations derived from diamonds with known impurity concentrations (Kiflawi et al., 1994; Boyd et al., 1994, 1995). The end result is a measurement of the absolute concentration of impurities of various configurations in a diamond. Most of the nitrogen impurity concentrations reported in the literature are calculated in this way.

HOW CAN A GEMOLOGIST INFER DIAMOND TYPE?

Unlike scientists in universities and gemological laboratories, most gemologists do not have expensive analytical instruments available to them for everyday use. Fortunately, some common gemological tools can provide insights into the impurities present in a diamond and, correspondingly, its type.

Absorption Spectrum: Desk-model/Handheld Spectroscope. The spectroscope has long been used to detect color treatments in diamond (Crowningshield, 1957), but it also provides some information about diamond type. It can be especially useful for identifying most type I diamonds. Type II (as well as some pure type IaA and Ib) diamonds rarely show absorption lines in the spectroscope. The presence of a 415 nm line (N3 defect; see box A) and its accompanying "cape" lines at 435, 452, 465, and 478 nm indicate that a diamond is type Ia (figure 9A) because, in order for these lines to appear, the diamond must contain aggregated nitrogen impurities. For similar reasons, the presence of a line at ~503 nm (H3 defect; again, see box A) is also a good indication that a diamond is type I. Very strong general absorption up to ~450 nm may suggest the presence of abundant isolated, single N in type Ib diamonds, but plastic deformation in some other types of diamonds can produce a similar absorption pattern.

Inclusions and Strain Patterns: Gemological Microscope. While most diamonds contain crystals that were trapped during growth, a few inclusions are considered characteristic of certain diamond types (see Crowningshield, 1994). Type Ib natural diamonds commonly contain clusters of small needle-like inclusions that are usually associated with yellow color zoning and rarely occur in other diamond types (GIA staff observations; figure 9B). Fine-grained, patterned clouds that form cross-like shapes are common in type Ia diamonds that contain high concentrations of hydrogen impurities (known as "asteriated" diamonds; see Wang and Mayerson, 2002; Rondeau et al., 2004, and references therein). Synthetic type Ib diamonds often show distinctive color zoning or metallic flux inclusions under magnification (Shigley et al., 2004).

Strain-free diamond is optically isotropic, meaning that it appears dark in all directions between crossed polarizers. However, almost all natural diamonds exhibit some degree of lattice distortion formed during crystallization or caused by post-growth plastic deformation. As a result, a variety of strain patterns and interference colors can be seen with crossed polarizers in a gemological microscope. One pattern of cross-hatched lines, known as "tatami" strain, is considered characteristic of type II natural and treated-color diamonds (Smith et al., 2000; figure 9C). The tatami pattern has also been observed in some pure type IaB and type Ib diamonds with very low nitrogen concentration (Chalain, 2003; GIA staff observations). To our knowledge, this pattern has never been observed in synthetic diamonds of any type.

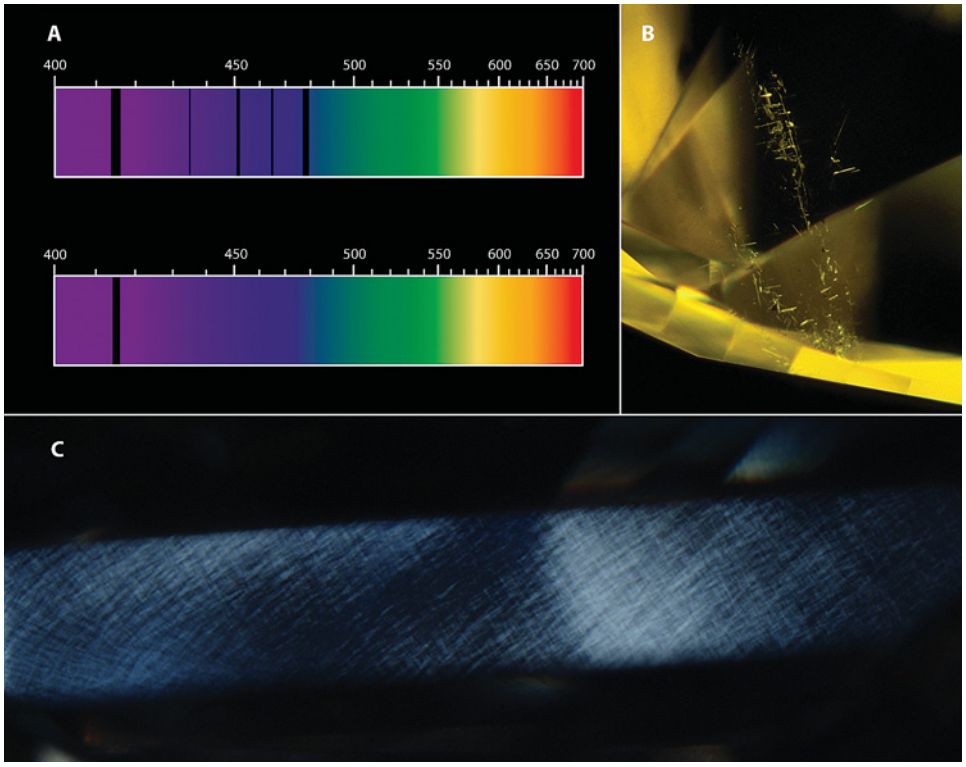

Figure 9. Several common gemological tests can be used to infer diamond type in natural diamonds. (A) Type Ia diamonds often show only a 415 nm line with or without additional "cape" lines in a desk-model or handheld spectroscope. (B) Type Ib diamonds often contain characteristic arrays of needle-like inclusions (magnified 50×). (C) Natural type II diamonds almost always show a cross-hatched "tatami" strain pattern between crossed polarizers in a microscope (magnified 40×). Photomicrographs by Wuyi Wang.

Electrical Conductivity: Conductometer/Ohmmeter. Another property that is easily tested is electrical conductivity. In the 1960s, GIA produced a tool for this purpose called a gemological conductometer. This device is no longer manufactured, but a sensitive ohm-meter can adequately determine if a diamond is electrically conductive (ohmmeters measure resistivity, which inversely correlates with conductivity). Boron impurities in the diamond lattice cause both natural and synthetic type IIb diamonds to be electrically conductive (Collins, 1982; King et al., 1998). No other diamond type shows this property. Occasionally, type IIb diamonds will also emit flashes or sparks of blue light (known as electroluminescence; Gumlich et al., 1998) when tested with a conductometer in a dark room.

Short-wave UV Transparency: Various Commercial/Custom-Made Testers. As mentioned earlier, type II diamonds were originally distinguished from type I using the property of short-wave UV transparency. A simple, easily constructed gemological testing device consists of a short-wave (~254 nm) UV lamp that emits light upward through an opening, above which a diamond can be positioned (figure 10). A material with a strong fluorescence reaction to short-wave UV radiation, such as scheelite, is placed above the diamond. If the diamond transmits short-wave UV radiation, the material will fluoresce. If the diamond absorbs short-wave UV radiation, it will not. This simple test is very effective at separating type I and II diamonds, because N impurities strongly absorb light in the UV range of the spectrum (~225–320 nm in figure 10). Very rare type I diamonds with only B-aggregated N impurities (i.e., pure type IaB diamonds) also sometimes transmit short-wave UV radiation (Chalain, 2003). Commercial diamond screening devices based on ultraviolet transparency are also available (Chalain et al., 2000).

UV-Visible Absorption/Luminescence: DiamondSure/DiamondView. Although not inexpensive, two gemological instruments that are useful for evaluating diamond type are the DiamondSure and DiamondView. They were designed and built by the De Beers Diamond Trading Co. (DTC) for the purpose of separating natural from synthetic diamonds (see Welbourn et al., 1996, for detailed descriptions). When tested with the DiamondSure, colorless type II and type IaB diamonds will be reported as such and referred for more testing. All other diamonds are given a "Pass" response. The DiamondView provides ultra short-wave UV fluorescence images of diamonds that may reveal distinctive growth sector

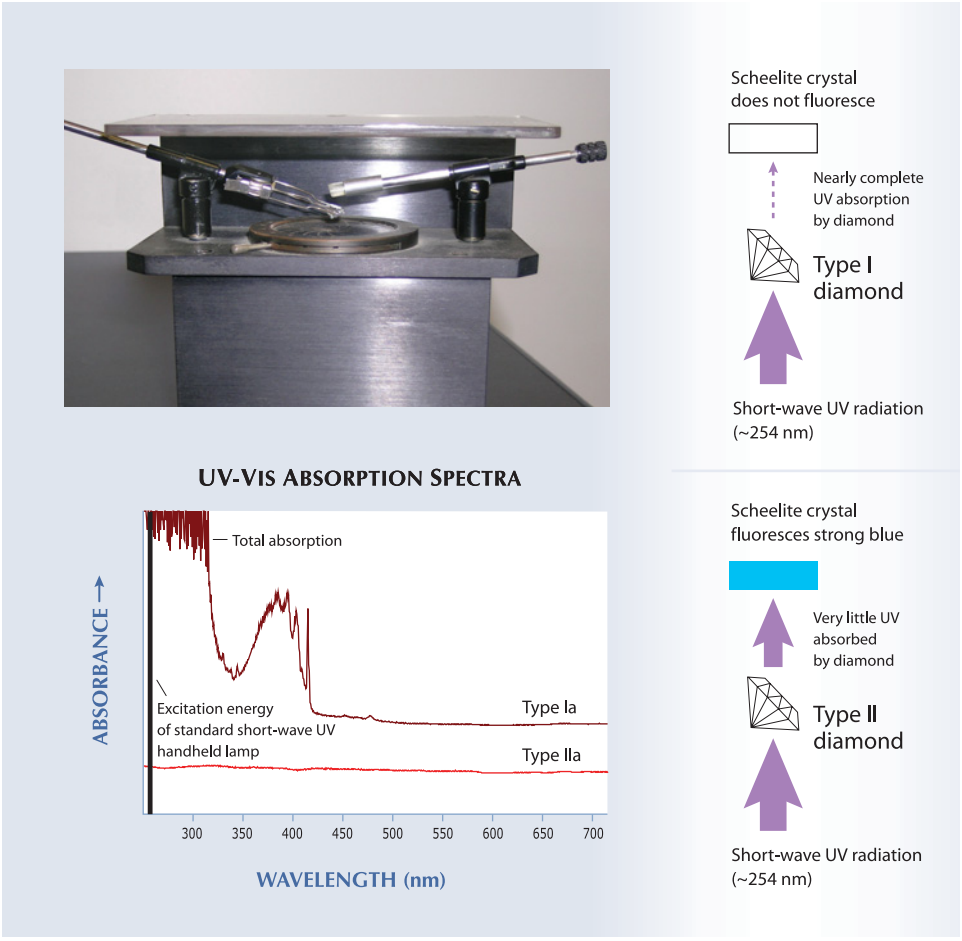

Figure 10. Short-wave UV transparency is a good test for the separation of type II from type I diamonds. This tester consists of a short-wave UV lamp that passes through a slit into the diamond, above which a crystal of scheelite (or other fluorescent material) is positioned (top left). Type I diamonds absorb short-wave UV radiation (~254 nm), but type II diamonds allow such wavelengths to pass through (see spectrum at bottom left). As a result, the scheelite crystal fluoresces blue only when a type II diamond is tested. Note that eye and/or skin exposure to short-wave UV radiation is dangerous and should be avoided. Safety glasses should always be worn. Photo by C. M. Breeding.

arrangements characteristic of synthetic diamonds. Several natural diamond types also show characteristic fluorescence patterns in the DiamondView (GIA staff observations; figure 11). Type Ia diamonds usually show blue fluorescence with irregular natural growth patterns. Natural type Ib diamonds often show an array of green luminescence lines on a background of orange fluorescence, whereas their synthetic counterparts often show greenish yellow and blue fluorescent growth zones in cross-like patterns (Shigley et al., 2004). Type IIa and IIb diamonds usually show a network of criss-crossing features that are thought to be due to dislocations in the diamond lattice. In addition, type IIb diamonds nearly always show blue or red phosphorescence in the DiamondView. Blue phosphorescence alone should not be used as evidence for diamond origin, because boron impurities in type II HPHT-grown synthetic diamonds will also produce blue phosphorescence.

Indirect Visual Evidence: Color, Fluorescence, Rough Diamond Morphology. Color can provide a hint about diamond type, but much experience is required to see the slight differences that might correlate with type. A representative range of colors for natural, treated-color, and synthetic diamonds of all four types is shown in figure 3. "Canary" yellow and orange colors are very common in type Ib diamonds, whereas lighter "straw" yellow-colored "cape" diamonds are usually type Ia. Very pale pink natural-color diamonds are often type IIa, whereas more saturated natural pink colors are often type Ia. Blue and gray diamonds are usually type IIb.

Fluorescence reactions observed using a handheld gemological UV lamp can also provide a clue to diamond type. Many type Ia diamonds exhibit blue fluorescence due to nitrogen impurities. Type Ib diamonds often are inert or fluoresce weak orange to both long- and short-wave UV radiation (Hainschwang et al., 2006). Usually synthetic type Ib diamonds display uneven fluorescence patterns that help in their identification (see Shigley et al., 2004). Type IIb diamonds are often inert to long-wave UV and show weak blue fluorescence to

short-wave UV, in addition to occasional blue or red phosphorescence (King et al., 1998). Unlike the DiamondView, gemological UV lamps emit lower-energy UV radiation and the phosphorescence of type IIb diamonds is not always visible.

A few aspects of rough diamond shape and surface texture are strongly indicative of type as well. For example, sorters have recognized that, unlike type I stones, type II diamond crystals typically occur in irregular or flattened shapes and do not exhibit crystallographic faces (Wilks and Wilks, 1991). Sunagawa (2001) suggested that this is due to the latter experiencing greater degrees of fracturing and breakage in their ascent to the earth's surface during eruptions of kimberlitic or lamproitic magmas, whereas type I diamonds tend to retain their original crystal morphology during magma transport.

Multiple Tests are Optimal When Investigating Diamond Type. Each of the properties and gemological tools mentioned above provides some indication of diamond type without the use of an FTIR spectrometer. They are most powerful, however, when used in combination. For example, type II diamonds can easily be distinguished from type I on the basis of short-wave UV transparency and strain patterns. Types IIa and IIb can easily be separated on the basis of electrical conductivity. The largest group of natural diamonds, type I, is a bit harder to subdivide, but with practice it is still usually possible. Type Ia diamonds commonly show 415 nm or "cape" lines in the spectroscope, whereas type Ib diamonds often show strong general absorption from <400 to ~450 nm. The presence of needle-like inclusions in type Ib diamond helps reinforce the diamond type evaluation. Table 1 provides a summary of the technical and gemological information discussed in this article for representative natural diamonds of each type. Shigley et al. (2004) provide an excellent reference chart for HPHT-grown synthetic diamonds, and Wang et al. (2007) gives information for CVD synthetics.

CONCLUSIONS

Recent advances in diamond growth and treatment have led to a greater dependence on sophisticated analytical instrumentation to distinguish natural from synthetic and natural-color from treated-color diamonds. However, we have shown that many of the standard tools used by gemologists in the trade

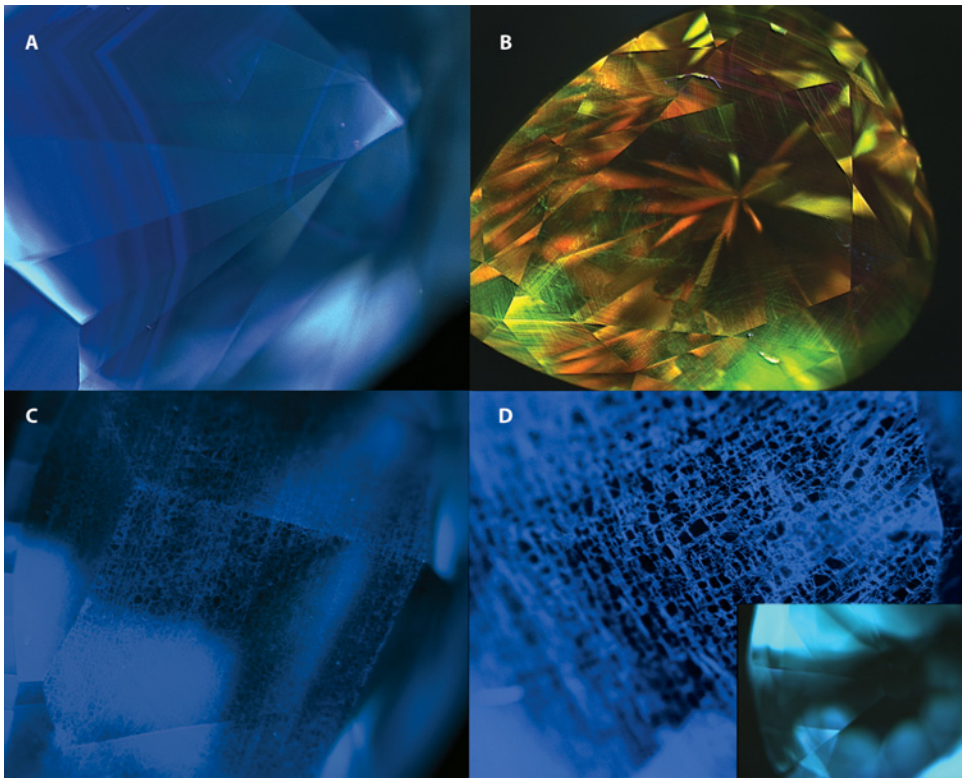

Figure 11. Natural diamonds of each type show distinctive fluorescence colors and patterns when examined with the DTC DiamondView ultra-short-wave UV unit. Type Ia diamonds commonly show blue fluorescence with straight-to-wavy growth patterns (A), whereas type Ib diamonds often fluoresce orange with green lines caused by the H3 defect (B). Both type IIa and IIb diamonds usually show blue-fluorescent web-like dislocation networks (C, D). Type IIb diamonds almost always show distinctive phosphorescence (either blue or red) in the DiamondView (inset). Photos by C. M. Breeding and Andy Shen.

TABLE 1. Characteristics of natural diamonds according to diamond type.

Type	Impurity	Most common colors	FTIR indicators	Inclusions	UV fluorescence		Helpful gemological clues
					Long-wave	Short-wave	
Ia	Nitrogen (aggregated)	Colorless, brown, yellow, pink, orange, green, violet	Aggregated N (1282, 1175 cm^{-1})	Common; all sorts	Inert, blue, yellow, orange	Inert, blue, yellow, orange	415 nm or "cape" spectrum; opaque to short-wave UV
Ib	Nitrogen (isolated)	Yellow, orange, brown	Isolated single N (1344, 1130 cm^{-1})	Common; clouds, needles	Inert to weak orange	Inert to weak orange	Strong general absorption up to 450 nm; distinctive needle-like inclusions
IIa	None	Colorless, brown, pink, green	No detectable impurities	Rare; crystals	Inert, blue, or orange	Inert, blue, or orange	Cross-hatched "tatami" strain pattern; transparent to short-wave UV
IIb	Boron	Blue, gray	Boron (2803, 2458 cm^{-1})	Rare; crystals	Inert to weak blue	Inert to weak blue or yellow	Cross-hatched "tatami" strain pattern; transparent to short-wave UV; electrically conductive; blue or red phosphorescence

are effective for identifying characteristic combinations of diamond properties, which help infer diamond type and possibly identify treatments and synthetics.

For example, simple observations such as a cross-hatched strain pattern in a colorless diamond that is transparent to short-wave UV radiation indicate that the stone is likely type IIa and should be sent to a laboratory to be tested for HPHT treatment. Similarly, a blue diamond exhibiting electrical conductivity is type IIb and also needs lab testing. If the type IIb blue diamond shows no strain pattern when viewed with cross-polarized light and magnification, then it might be a synthetic. And a strongly colored yellow diamond that does not produce "cape" lines in the spectroscope may be type Ib. If no color zoning characteristic of synthetic origin is present and needles similar to those shown in figure 9B are observed, it is probably a natural type Ib diamond. These are just a few situations where gemological tests can provide clues to diamond type and its possible implications for identification.

Information about type helps gemologists assess the possibility that a diamond is treated or synthetic and, conversely, provides some measure of confidence that it is natural and naturally colored. With the constantly evolving world of treatments and synthetics, however, we strongly encourage gemologists to exercise caution and send their diamonds to a gemological laboratory for testing if there is any doubt.

ABOUT THE AUTHORS
Dr. Breeding is research scientist, and Dr. Shigley is distinguished research fellow, at the GIA Laboratory in Carlsbad, California.

ACKNOWLEDGMENTS
The authors thank Dr. Wuyi Wang, Shane McClure, Dr. Andy Shen, Matt Hall, and Tom Moses of the GIA Laboratory for providing helpful suggestions in the revision of the manuscript.

REFERENCES

Anderson B.W. (1943a) Absorption and luminescence in diamond I. *The Gemmologist*, Vol. 12, No. 138, pp. 21–22.
——— (1943b) Absorption and luminescence in diamond II. *The Gemmologist*, Vol. 12, No. 139, pp. 25–27.
——— (1943c) Absorption and luminescence in diamond III. *The Gemmologist*, Vol. 12, No. 141, pp. 33–35.
——— (1960) Luminescence of a large pink diamond. *Journal of Gemmology*, Vol. 7, No. 6, pp. 216–220.
——— (1961) Some notes on an important discovery: Nitrogen in diamond. *The Gemmologist*, Vol. 30, No. 225, pp. 21–22.
——— (1962) Lines and line systems in the fluorescence spectra of diamonds. *Journal of Gemmology*, Vol. 8, No. 5, pp. 193–202.
——— (1963) The classification of diamonds on the basis of their absorption and emission of light. *Journal of Gemmology*, Vol. 9, No. 2, pp. 44–54.
Boyd S.R., Kiflawi I., Woods G.S. (1994) The relationship between infrared absorption and the A defect concentration in diamond. *Philosophical Magazine B*, Vol. 69, No. 6, pp. 1149–1153.
——— (1995) Infrared absorption by the B nitrogen aggregation in diamond. *Philosophical Magazine B*, Vol. 72, No. 3, pp. 351–361.
Blackwell D.E., Sutherland G.B.B.M. (1949) The vibrational spectrum of diamond. *Journal de Chimie Physique et de Physico-*

Chimie Biologique, Vol. 46, No. 1, pp. 9–15.
Breeding C.M. (2005) Lab Notes: Light blue diamond, with type IIb and IIa zones. *G&G*, Vol. 41, No. 2, pp. 167–168.
Chadwick K.M. (2008) Lab Notes: Fancy dark brown-yellow zoned type IIa/IIb diamond. *G&G*, Vol. 44, No. 4, pp. 364–365.
Chalain J.-P. (2003) A type IaB diamond showing a "tatami" strain pattern. *G&G*, Vol. 39, No. 1, pp. 59–60.
Chalain J.-P., Fritsch E., Hänni H.A. (2000) Identification of GE POL diamonds: A second step. *Journal of Gemmology*, Vol. 27, No. 2, pp. 73–78.
Chrenko R.M. (1973) Boron, the dominant acceptor in semiconducting diamond. *Physical Review B*, Vol. 7, No. 10, pp. 4560–4567.
Clark C.D., Mitchell E.W.J., Parsons B.J. (1979) Colour centres and optical properties. In J.E. Field, Ed., *The Properties of Diamond*, Academic Press, London, pp. 23–77.
Collins A.T. (1980) Spectroscopic investigation of a canary yellow diamond. *Journal of Gemmology*, Vol. 17, No. 4, pp. 213–222.
——— (1982) Colour centres in diamond. *Journal of Gemmology*, Vol. 18, No. 1, pp. 37–75.
——— (2001) The colour of diamond and how it may be changed. *Journal of Gemmology*, Vol. 27, No. 6, pp. 341–359.
Collins A.T., Connor A., Ly C., Shareef A., Spear P.M. (2005) High-temperature annealing of optical centers in type-I diamond. *Journal of Applied Physics*, Vol. 97, No. 8, pp. 083517-1 to 083517-10.
Crowningshield G.R. (1957) Spectroscopic recognition of yellow bombarded diamonds and bibliography of diamond treatment. *G&G*, Vol. 9, No. 4, pp. 99–104, 117.
Crowningshield G.R. (1994) Gem Trade Lab Notes: Characteristic inclusions in fancy-color diamonds. *G&G*, Vol. 30, No. 1, pp. 41–42.
Custers J.F.H. (1952) Unusual phosphorescence of a diamond. *Physica*, Vol. 18, No. 8/9, pp. 489–493.
——— (1954) Letter to the Editor: Type IIb diamonds. *Physica*, Vol. 20, No. 4, pp. 183–184.
——— (1955) Semiconductivity of a type IIb diamond. *Nature*, Vol. 176, No. 4473, pp. 173–174.
Davies G. (1977) The optical properties of diamond. In P.L. Walker Jr. and P.A. Thrower, Eds., *Chemistry and Physics of Carbon*, Vol. 13, Marcel Dekker Inc., New York, pp. 1–143.
Dyer H.B., Raal F.A., Du Preez L., Loubser J.H.N. (1965) Optical absorption features associated with paramagnetic nitrogen in diamond. *Philosophical Magazine*, Vol. 11, No. 8, pp. 763–774.
Fisher D., Spits R.A. (2000) Spectroscopic evidence of GE POL HPHT-treated natural type IIa diamonds. *G&G*, Vol. 36, No. 1, pp. 42–49.
Fritsch E., Scarratt K. (1992) Natural-color nonconductive gray-to-blue diamonds. *G&G*, Vol. 28, No. 1, pp. 35–42.
Gumlich H.E., Zeinert A., Mauch R. (1998) Electroluminescence. In D.R. Vij, Ed., *Luminescence of Solids*, Plenum Press, New York, pp. 221–270.
Hainschwang T., Notari F., Fritsch E., Massi L. (2006) Natural, untreated diamonds showing the A, B and C infrared absorptions ("ABC diamonds"), and the H2 absorption. *Diamond and Related Materials*, Vol. 15, No. 10, pp. 1555–1564.
Kaiser W., Bond W.L. (1959) Nitrogen, a major impurity in common type I diamond. *Physical Review*, Vol. 115, No. 4, pp. 857–863.
Kiflawi I., Mayer A.E., Spear P.M., Van Wyk J.A., Woods G.S. (1994) Infrared absorption by the single nitrogen and A defect centres in diamond. *Philosophical Magazine B*, Vol. 69, No. 6, pp. 1141–1147.
King J.M., Moses T.M., Shigley J.E., Welbourn C.M., Lawson S.C., Cooper M. (1998) Characterizing natural-color type IIb blue diamonds. *G&G*, Vol. 34, No. 4, pp. 246–268.
King J.M., Shigley J.E., Gelb T.H., Guhin S.S., Hall M., Wang W. (2005) Characterization and grading of natural-color yellow diamonds. *G&G*, Vol. 41, No. 2, pp. 88–115.
King J.M., Shigley J.E., Guhin S.S., Gelb T.H., Hall M. (2002) Characterization and grading of natural-color pink diamonds. *G&G*, Vol. 38, No. 2, pp. 128–147.
Lightowlers E.C., Dean P.J. (1964) Measurement of nitrogen concentrations in diamond by photon activation analysis and optical absorption. *Diamond Research*, pp. 21–25.
Mitchell E.W.J. (1964) Optical properties of diamond. *Diamond Research*, pp. 13–16.
Nayar P.G.N. (1941a) Luminescence, absorption and scattering of light in diamonds: Part I. Fluorescence. *Proceedings of the Indian Academy of Science*, Series A, Vol. 13, pp. 483–497.
——— (1941b) Luminescence, absorption and scattering of light in diamonds: Part III. Absorption. *Proceedings of the Indian Academy of Science*, Series A, Vol. 14, pp. 1–17.
Raman C.V. (1944) The nature and origin of the luminescence of diamond. *Proceedings of the Indian Academy of Science*, Series A, Vol. 19, pp. 199–215.
Robertson R., Fox J.J., Martin A.E. (1934) Two types of diamond. *Philosophical Transactions of the Royal Society A*, Vol. 232, No. 1, pp. 463–535.
——— (1936) Further work on two types of diamond. *Proceedings of the Royal Society A*, Vol. 157, No. 892, pp. 579–593.
Rondeau B., Fritsch E., Guiraud M., Chalain J-P., Notari F. (2004) Three historical "asteriated" hydrogen-rich diamonds: Growth history and sector-dependent impurity incorporation. *Diamond and Related Materials*, Vol. 13, No. 9, pp. 1658–1673.
Shigley J.E., Breeding C.M., Shen A.H. (2004) An updated chart on the characteristics of HPHT-grown synthetic diamonds. *G&G*, Vol. 40, No. 4, pp. 303–313.
Shigley J.E., Fritsch E., Stockton C.M., Koivula J.I., Fryer C.W., Kane R.E. (1986) The gemological properties of the Sumitomo gem-quality synthetic yellow diamonds. *G&G*, Vol. 22, No. 4, pp. 192–208.
Smith C.P., Bosshart G., Ponahlo J., Hammer V.M.F., Klapper H., Schmetzer K. (2000) GE POL diamonds: Before and after. *G&G*, Vol. 36, No. 3, pp. 192–215.
Sutherland G.B.B.M., Willis H.A. (1945) Some new peculiarities in the infra-red spectrum of diamond. *Transactions of the Faraday Society*, Vol. 41, No. 1, pp. 289–293.
Sutherland G.B.B.M., Blackwell D.E., Simeral W.G. (1954) The problem of two types of diamond. *Nature*, Vol. 174, No. 4437, pp. 901–904.
Sunagawa I. (2001) A discussion on the origin of irregular shapes of type II diamonds. *Journal of Gemmology*, Vol. 27, No. 7, pp. 417–425.
Tang C.J., Neves A.J., Carmo M.C. (2005) On the two-phonon absorption of CVD diamond films. *Diamond and Related Materials*, Vol. 14, No. 11/12, pp. 1943–1949.
Wang W., Mayerson W. (2002) Symmetrical clouds in diamond: The hydrogen connection. *Journal of Gemmology*, Vol. 28, No. 3, pp. 143–152.
Wang W., Smith C.P., Hall M.S., Breeding C.M., Moses T.M. (2005) Treated-color pink-to-red diamonds from Lucent Diamonds Inc. *G&G*, Vol. 41, No. 1, pp. 6–19.
Wang W., Hall M.S., Moe K.S., Tower J., Moses T.M. (2007) Latest-generation CVD-grown synthetic diamonds from Apollo Diamond Inc. *G&G*, Vol. 43, No. 4, pp. 294–312.
Welbourn C.M., Cooper M., Spear P.M. (1996) De Beers natural versus synthetic diamond verification instruments. *G&G*, Vol. 32, No. 3, pp. 156–169.
Wentorf R.H. Jr., Bovenkirk H.P. (1962) Preparation of semiconducting diamond. *Journal of Chemical Physics*, Vol. 36, No. 8, pp. 1987–1990.
Wilks E., Wilks J. (1991) *Properties and Applications of Diamond*. Butterworth-Heinemann Ltd., Oxford, UK.
Zaitsev A.M. (2001) *Optical Properties of Diamond: A Data Handbook*. Springer-Verlag, Berlin.

SPECTRAL DIFFERENTIATION BETWEEN COPPER AND IRON COLORANTS IN GEM TOURMALINES

Paul B. Merkel and Christopher M. Breeding

The authors used Vis-NIR spectral measurements combined with LA-ICP-MS data to investigate the usefulness of absorption spectra for differentiating between copper and iron as sources of greenish blue coloration in gem tourmaline. While both Cu^{2+} and Fe^{2+} produce absorption bands with maxima near 700 nm, Cu^{2+} also has a strong band with a maximum near 900–925 nm, where absorption due to Fe^{2+} is typically at a minimum. In addition, Vis-NIR spectroscopy successfully identified Cu in pink/purple and violet stones that could be candidates for heat treatment. For the blue, green, and violet Cu-bearing tourmalines of pale-to-moderate color intensity in this study, weight percent of CuO could be estimated from the absorbance at 900 nm. This relatively inexpensive identification method may prove to be a valuable screening tool for Cu-bearing tourmaline.

The availability of copper-bearing tourmaline from Mozambique (Abduriyim and Kitawaki, 2005; Laurs et al., 2008) has intensified the gemological interest that was first generated after discovery of cuprian tourmaline in Brazil's "Paraíba" State (Fritsch et al., 1990; Abduriyim et al., 2006, and references therein) and later in Nigeria (Smith et al., 2001; Abduriyim et al., 2006, and references therein). In 2007, the Laboratory Manual Harmonization Committee proposed that blue ("electric" blue, "neon" blue, violet-blue), bluish green to greenish blue, or green elbaite tourmaline of moderate-to-high saturation colored by traces of Cu and Mn be called "Paraíba" tourmaline, regardless of geographic origin.

Analytical procedures used to quantify Cu content include laser ablation–inductively coupled plasma–mass spectroscopy (LA-ICP-MS), electron-microprobe analysis, and energy-dispersive X-ray fluorescence (EDXRF; Fritsch et al., 1990; Abduriyim et al., 2006; Laurs et al., 2008). However, a simpler, less expensive supplementary procedure for evaluating Cu content is desirable in instances where cost or convenience is important. The visible–near infrared (Vis-NIR) spectroscopic instrumentation described in this article is easy to use, portable, and costs as little as $3,500. It can perform a measurement in one minute or less, on a rough or polished gem sample of any size.

Both iron as Fe^{2+} (Faye et al., 1968; Mattson and Rossman, 1987) and copper as Cu^{2+} (Fritsch et al., 1990; Laurs et al., 2008) can impart greenish blue coloration to gem tourmaline. The required absorption near 700 nm is associated with metal ions in distorted octahedral environments (Burns, 1993). Thus, whether coloration is due to Fe and/or Cu cannot reliably be distinguished by looking at a

See end of article for About the Authors and Acknowledgments.
GEMS & GEMOLOGY, Vol. 45, No. 2, pp. 112–119.

Figure 1. These 26 faceted and preformed tourmalines (weights listed in table 1) were analyzed for this study. Left to right, top row: B1–B8; second row from top: G1–G8; second row from bottom: P1–P5; bottom row: P6, P7, V1, V2, and Y1. Photo by P. Merkel.

sample. In this study, we analyzed 26 gem tourmalines by Vis-NIR spectroscopy and LA-ICP-MS, and compared the two sets of data to investigate the potential for spectral differentiation between Cu and Fe as chromophores. An additional objective of this study was to determine whether the absorption near 900 nm could be used to estimate Cu content in tourmaline colored by this element.

MATERIALS AND METHODS

We studied 26 faceted and preformed tourmalines (figure 1). They are designated in table 1 according to the predominant color observed: blue and greenish blue (B), green and bluish green (G), pink (P), violet (V), and greenish yellow (Y). Most of the Cu-bearing tourmalines were from Mozambique, but we also included samples from Brazil and Nigeria. Most of the non-Cu-bearing tourmalines were from Afghanistan, Brazil, Mozambique, and Namibia. One "chrome" uvite, from Tanzania, was also included for comparison. The greenish yellow sample was added because Mozambique tourmalines of very similar color and with no spectral evidence of Cu^{2+} are being sold as copper-bearing (e.g., on eBay); it was included to illustrate that not all greenish yellow tourmalines from Mozambique derive their blue color component in the spectrum (i.e., absorption at 700 nm) from Cu^{2+}.

For each sample, we determined specific gravity hydrostatically and measured refractive indices using a standard gemological refractometer. Vis-NIR spectra were collected with two different spectrometers. We analyzed most of the larger samples using a Perkin-Elmer Lambda 950 spectrometer equipped with a 150 mm integrating reflectance sphere, in the range 350–1150 nm. The gem was held (~5° from normal) in the jaws of center-mount sampling module PELA-9038, and the beam was directed through the table and reflected back off the pavilion facets. Smaller samples (<1 cm) could not be reliably measured with this configuration, because they did not completely intercept the beam. They were instead measured using a StellarNet EPP2000-CXR CCD array spectrometer with an SL1 tungsten-krypton light source and a R400-7-VisNIR bifurcated fiber-optic reflectance probe, in the range 400–900 nm. These smaller gems were usually placed table-down on a white reflective standard. The small tip of the fiber-optic probe, providing both the analyzing beam and the collection of transmitted light, was placed near the culet and aimed toward the table. The beam reflected off the white standard back through the table to the probe. Intensity measurements with and without the gem in place allowed absorbance to be determined.

For both techniques, the approximate path of the analyzing beam consisted essentially of a dual traverse between the table and the culet. Both spectrometers provided absorbance vs. wavelength directly (uncorrected for path length). Spectral maxima of gems measured on both spectrometers were identical, and absorbance values were within ~10%. Some polarized absorption spectra were obtained using the Lambda 950 spectrometer in the transmission mode together with a calcite polarizer.

Trace- and major-element analyses of all samples were obtained at the GIA Laboratory in Carlsbad

TABLE 1. Properties and absorption data for the 26 tourmaline samples in this study.

Sample no.	Description	Locality	RI[a]	SG	MnO (wt.%)[b]	FeO (wt.%)[b]	CuO (wt.%)[b]	A/L (cm^{-1}) at 525 nm (Mn^{2+})	A/L (cm^{-1}) at 700 nm (Cu^{2+}, Fe^{2+})	A/L (cm^{-1}) at 900 nm (Cu^{2+})	Estimated path length, L (cm)
B1	0.80 ct greenish blue	Brazil	1.619–1.641	3.09	**3.028**	0.028	**1.862**	0.249	3.029	2.686	0.70
B2	4.02 ct greenish blue	Namibia	1.620–1.639	3.09	**1.454**	**2.972**	bdl	0.239	1.562	0.265	1.30
B3	1.44 ct greenish blue	Nigeria	1.619–1.638	3.06	**0.204**	bdl	**0.291**	0.113	1.440	2.307	0.75
B4	8.93 ct greenish blue	Afghanistan[c]	1.619–1.639	3.06	**0.331**	**0.126**	bdl	0.101	0.484	0.078	1.50
B5	5.67 ct blue	Brazil	1.620–1.639	3.08	**0.508**	**0.278**	bdl	0.119	1.477	0.255	1.30
B6	14.50 ct greenish blue	Mozambique	1.621–1.637	3.04	0.018	bdl	**0.076**	0.021	0.308	0.475	1.70
B7	7.50 ct greenish blue	Afghanistan	1.62–1.63	3.05	**0.264**	**0.571**	0.001	0.048	0.594	0.047	1.65
B8	36.33 ct greenish blue	Mozambique	1.62–1.64	3.05	0.016	bdl	0.025	0.020	0.182	0.286	2.80
G1	3.29 ct bluish green	Mozambique	1.620–1.640	3.09	**3.365**	0.018	**0.177**	0.051	0.717	1.087	1.15
G2	2.42 ct bluish green	Brazil	1.620–1.640	3.09	**0.978**	**1.706**	0.001	0.073	1.880	0.051	1.00
G3	8.81 ct green	Africa	1.622–1.642	3.09	**5.572**	**0.112**	**0.136**	0.106	0.669	0.775	1.60
G4	32.30 ct bluish green	Afghanistan	1.620–1.638	3.07	**1.272**	**1.012**	bdl	0.109	0.525	0.058	2.00
G5	14.21 ct green	Mozambique	1.620–1.639	3.07	**0.443**	**0.557**	bdl	0.107	0.423	0.061	2.05
G6	7.24 ct yellow-green	Mozambique	1.624–1.640	3.07	**0.714**	**1.134**	0.006	0.181	0.557	0.081	1.55
G7	46.16 ct bluish green	Mozambique	1.620–1.639	3.06	**0.258**	0.015	0.039	0.037	0.272	0.407	2.80
G8	1.64 ct green	Tanzania[d]	1.618–1.639	3.08	0.011	bdl	bdl	0.682	0.393	0.043	0.90
P1	6.68 ct pink	Brazil	1.620–1.639	3.05	**1.219**	**0.081**	bdl	0.612	0.135	0.207	1.30
P2	8.87 ct pink	Nigeria	1.620–1.640	3.06	**0.876**	bdl	0.002	0.933	0.284	0.491	1.50
P3	2.84 ct purple	Mozambique	1.620–1.640	3.05	**1.206**	bdl	**0.173**	1.038	0.622	1.314	1.05
P4	11.50 ct pink	Mozambique	1.620–1.639	3.04	**0.289**	bdl	0.042	0.488	0.282	0.398	1.70
P5	50.07 ct pink	Mozambique	1.62–1.64	3.06	**0.408**	0.038	0.028	0.346	0.321	0.398	2.20
P6	13.55 ct pinkish purple	Mozambique	1.620–1.640	3.06	**1.415**	bdl	**0.070**	0.336	0.309	0.470	1.90
P7	29.02 ct purplish pink	Mozambique	1.619–1.639	3.05	**2.234**	0.007	0.045	0.400	0.350	0.469	2.60
V1	5.05 ct violet	Mozambique	1.62–1.64	3.07	**2.402**	bdl	**0.478**	1.325	1.783	1.508	1.20
V2	14.28 ct violet	Mozambique	1.62–1.63	3.06	**1.056**	bdl	**0.209**	0.628	0.853	1.013	1.50
Y1	10.51 ct greenish yellow	Mozambique	1.625–1.640	3.07	**0.394**	**0.108**	bdl	0.272	0.330	0.082	1.80

[a] RI values of preforms were measured to the hundredths.
[b] Average of two LA-ICP-MS analyses; bold type indicates gems with moderate-to-high levels (>0.05 wt.% oxides) of Mn, Fe, and Cu. Abbreviation: bdl = below detection limit.
[c] Likely but uncertain origin.
[d] Uvite, containing ~7.80 wt.% Mg, 2:1 Ca:Na, 0.21 wt.% V, and 0.01 wt.% Cr.

using a Thermo X Series II ICP-MS with a New Wave UP-213 laser ablation sampling system. We analyzed two random locations on the girdle of each gem, and processed the data using boron as an internal standard.

To investigate the effects of heating on the Vis-NIR spectra of Cu-bearing tourmalines, we measured the absorption spectra of 10 additional preforms (2–12 g; spectrally indicated to contain Cu) that were initially various shades of violet or brownish violet both before and after heating for one hour at ~600°C (and for three samples, after being heated again to ~700°C for one hour). Although heating for one hour at 550°C is usually sufficient to fully remove the pink color component, traces of Mn^{3+} absorption have remained in some stones under this condition. The intention in this study was to investigate whether somewhat

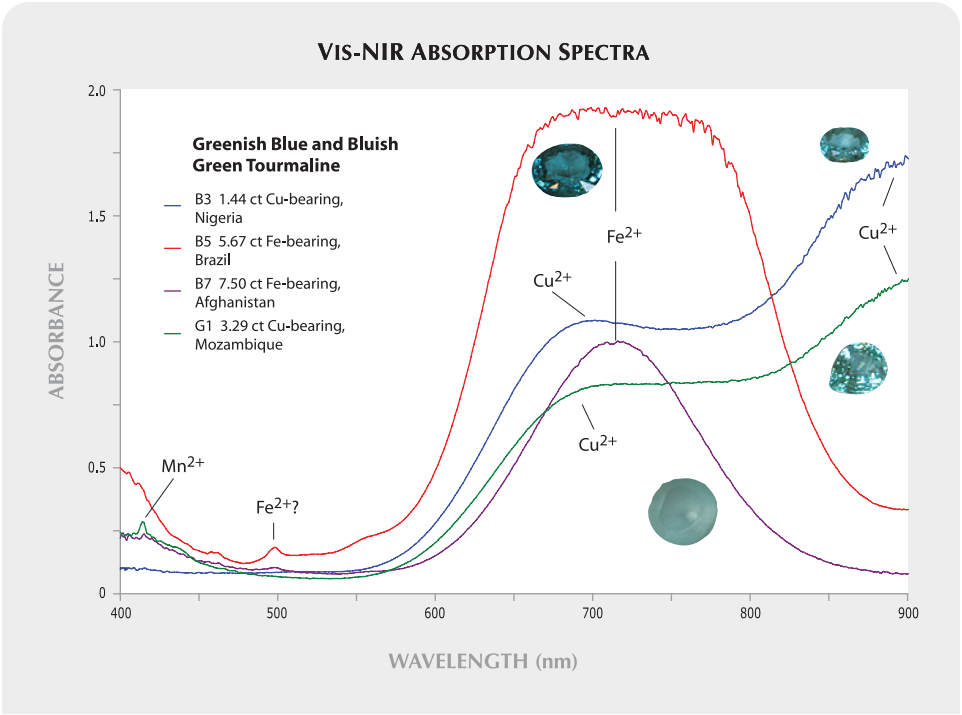

Figure 2. Vis-NIR absorption spectra (collected with the EPP2000 spectrometer) are shown for selected greenish blue (B3, B5, and B7) and bluish green (G1) tourmalines colored by Fe^{2+} or Cu^{2+}.

higher temperatures would alter the Cu^{2+} absorption. We placed the samples in a Pyrex beaker containing alumina powder, and then raised and lowered the temperature at a rate of about 50°C/hour to minimize thermal shock.

RESULTS AND DISCUSSION

Chemical and spectral data for the 26 tourmalines are compiled in table 1. The RI, SG, and absorbance values (per centimeter of path length; A/L) at 525, 700, and 900 nm are given along with the average concentrations of MnO, FeO, and CuO determined by LA-ICP-MS. (MnO data are included because Mn^{3+} can produce a red-magenta color component and Mn^{2+} can produce a yellow component in tourmaline.) Most samples have significant levels of either Cu or Fe, but not both. Data are also included for one green tourmaline that is colored primarily by vanadium (sample G8). As determined from an analysis of the LA-ICP-MS data (see *G&G* Data Depository at www.gia.edu/gandg), most of the tourmalines were identified as elbaite, whereas B4, G6, and Y1 were found to be liddicoatite, and G8 to be uvite.

Vis-NIR Spectroscopy. As illustrated by the spectra in figures 2 and 3, both Cu^{2+}- and Fe^{2+}-bearing samples have absorption maxima in the vicinity of 700 nm. It is this component of the absorption by traces of Fe^{2+} or Cu^{2+} that produces greenish blue color in gem tourmaline (Faye et al., 1968; Smith, 1978; Mattson and Rossman, 1987; Rossman et al., 1991). Due to the similarity of the ~700 nm bands produced by the two metal ions, color induced by Cu^{2+} and Fe^{2+} cannot reliably be distinguished either visually or by visible-range absorption spectra. However, as further illustrated by the Vis-NIR absorption spectra in figures 2 and 3, the samples containing substantial Cu^{2+} (see table 1) have an additional absorption peak in the neighborhood of 900 nm, similar to what has been observed in earlier studies (see figure 5 in Bank et al., 1990; figure 14 in Fritsch et al., 1990; and Laurs et al., 2008). Additionally, as also seen in prior investigations (Faye et al., 1968; Mattson and Rossman, 1987), Fe^{2+} has an absorption *minimum* near 900 nm (along with additional absorption in the region of ~1000–1200 nm).

Other common chromophores such as Mn^{2+}, Mn^{3+}, Fe^{3+}, and charge-transfer transitions also do not appear to produce strong absorptions in the vicinity of 900 nm (Mattson and Rossman, 1987; Reinitz and Rossman, 1988). Thus, absorption near 900 nm provides a potentially useful property to distinguish coloration by Cu and Fe and to estimate copper content. The spectral comparisons in figures 3 and 4 illustrate that the 900 nm absorption also can be used to assess the presence of significant Cu^{2+} in tourmalines of other hues, such as green and vio-

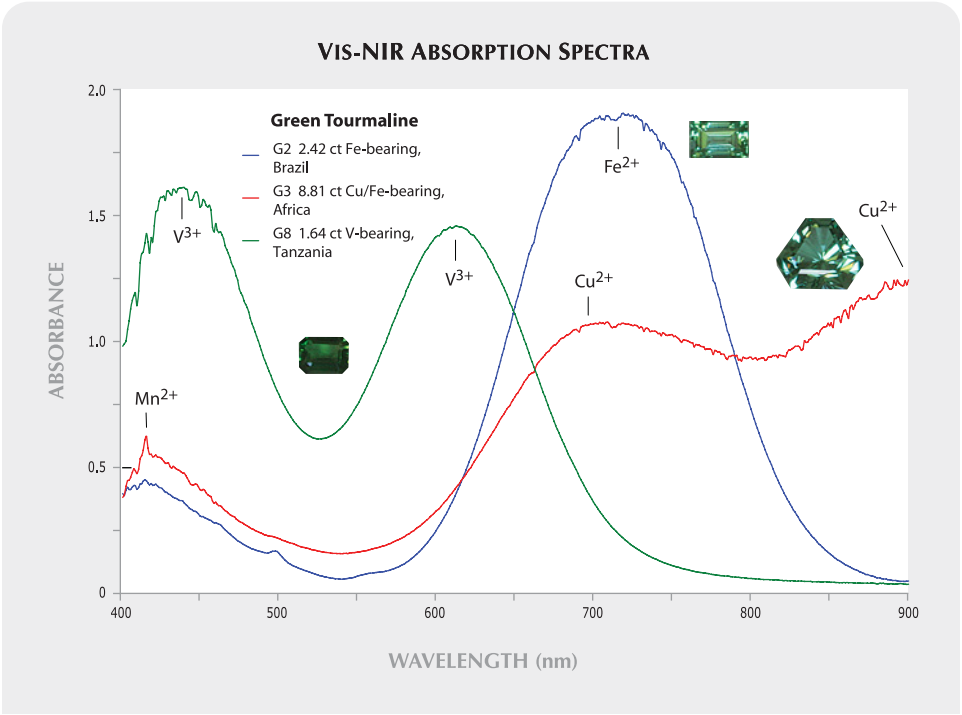

Figure 3. These Vis-NIR absorption spectra (collected with the EPP2000 spectrometer) are from green tourmalines colored primarily by Cu^{2+} (G3), Fe^{2+} (G2, G3), or V^{3+} (G8).

let, which contain additional colorants. The green coloration of G2 and G3 in figure 3 may arise in part from Mn^{2+} contributions to blue absorption (which includes the narrow band at ~415 nm; Rossman and Mattson, 1986) combined with the red absorption by Fe^{2+} and/or Cu^{2+} near 700 nm. Substantial Mn^{3+} absorption at ~510–530 nm contributes to the color of the pink and violet samples in figure 4. The spectrum of V^{3+}-colored green uvite sample G8 (see footnote d in table 1 and Schmetzer et al., 2007) is also included in figure 3 for comparison.

Without exception, the samples in our study with moderate-to-strong absorption features near 900 nm had substantial levels of Cu. In contrast, those with substantial absorbance near 700 nm and low absorbance near 900 nm had significant levels of Fe and minimal Cu (again, see table 1). Absorption spectra of all the samples of this study, as well as complete LA-ICP-MS data, are available in the *G&G* Data Depository.

Blue, greenish blue, and green tourmalines with substantial absorbance at 900 nm but greater absorbance at 700 nm may be colored by a combination of Fe^{2+} and Cu^{2+}, because for gems colored by Cu^{2+} alone (e.g., G1 and B3 in figure 2) there is usually *greater* absorbance at 900 nm than at 700 nm. G3 was the only sample examined that had moderate levels of both iron (0.112 wt.% FeO) and copper (0.136 wt.% CuO); as with the other Cu-bearing gems, the strong absorption near 900 nm shows the presence of copper (figure 3). The relative absorbances at 700 and 900 nm suggest that most of the absorption near 700 nm in G3 is also due to copper. The lack of absorption near 520 nm and the sharp band near 415 nm implies that the Mn in G3 is in the form of Mn^{2+}. This African gem was reportedly from Namibia, but it could be of Nigerian origin; to our knowledge, Cu has not been reported in Namibian tourmaline.

The absorbance features near 900 nm for P5 and P6 in figure 4 are consistent with their Cu contents. The absorbance value for P5 is substantial despite its low Cu content due to the relatively long analyzing path length for this large gem. This result and similar behavior for B8, G7, and P7 illustrate that CuO levels as low as ~0.03 wt.% can readily be detected spectrally in large stones. In contrast, the behavior in figure 4 of P1, which contains some Fe but no Cu, exemplifies a situation where caution must be exercised in spectrally assessing the presence of Cu. Relatively weak absorptions near 700 and 900 nm in pink or red tourmaline such as P1 may be related to Mn^{3+} rather than Cu^{2+}. A low-intensity Mn^{3+} band has been observed previously near 700 nm (Manning, 1973; Reinitz and Rossman, 1988), and a weak Mn^{3+} band has also been reported in the region of ~900–1025 nm in thin-layer synthetic elbaite with

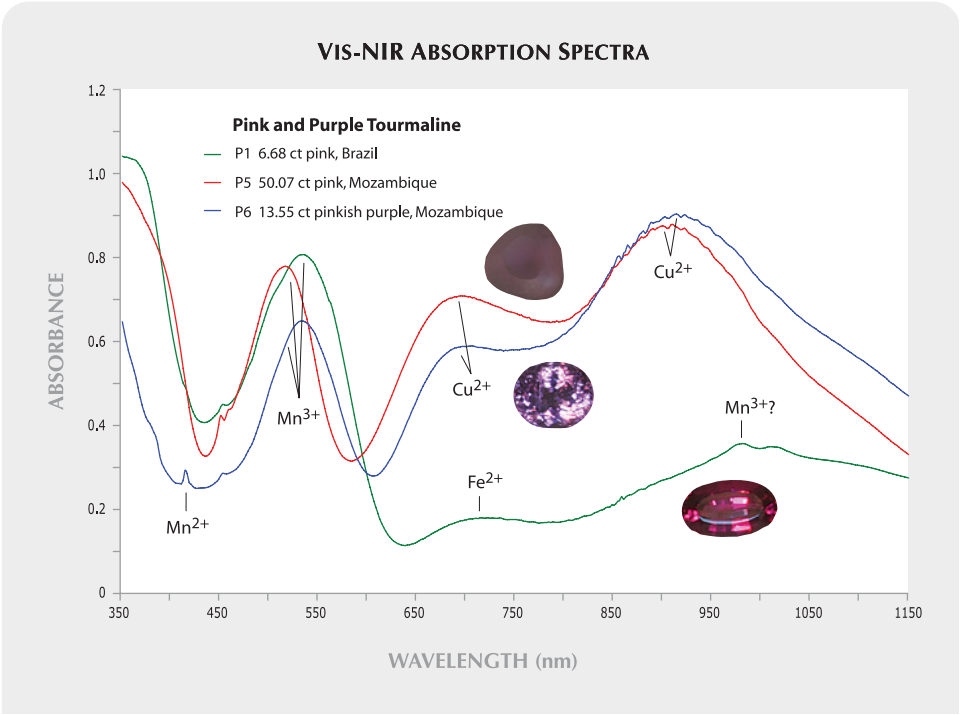

Figure 4. Vis-NIR absorption spectra (collected by the Lambda 950 spectrometer) are shown for pink (P1 and P5) and pinkish purple (P6) tourmalines from Brazil and Mozambique. Samples P5 and P6 contain substantial amounts of Cu.

Mn as the only colorant (see figure 7 in Taran et al., 1993). Fe^{2+} probably contributes to the absorptions near 700 and 1050 nm (Faye et al., 1968; Mattson and Rossman, 1987) in P1, but the weak absorption near 900 nm may be due to Mn^{3+}. The small bumps at ~970 and 1000 nm are due to OH vibrational overtones (Rossman et al., 1991).

Estimation of Cu^{2+} Abundance. The above examples illustrate the use of spectroscopy for qualitative assessment of the presence of Cu. However, spectral measurements can also provide quantitative *estimates* of Cu levels. Figure 5 illustrates that for most of the Cu-bearing tourmalines studied, there is a reasonably linear relationship between the absorbance at 900 nm divided by the path length in centimeters (A_{900}/L) and the copper content (wt.% CuO).

The ±50% error bars for the A_{900}/L values in figure 5 represent the estimated uncertainty due to several factors. The first factor is the variation in the extinction coefficient (a measure of the absorbing strength of a colorant) of Cu^{2+} with crystallographic direction. Polarized absorption measurements have shown that the extinction coefficient of Cu^{2+} near 900 nm is reduced by about three-fold for the extraordinary ray (i.e., $E \parallel c$) relative to the ordinary ray ($E \perp c$; Rossman et al., 1991). There is also a slight shift in the absorption maximum between the ordinary and extraordinary rays. Therefore, the precise absorbance at 900 nm that is produced by a given concentration of Cu^{2+} will be somewhat

Figure 5. In this diagram, the absorbance at 900 nm divided by path length in centimeters (A_{900}/L) is plotted against Cu content. Data are shown only for tourmaline samples with low-to-moderate absorbance (≤1.7), since they were least affected by surface reflections. The A_{900}/L values include error bars for a ±50% estimated uncertainty.

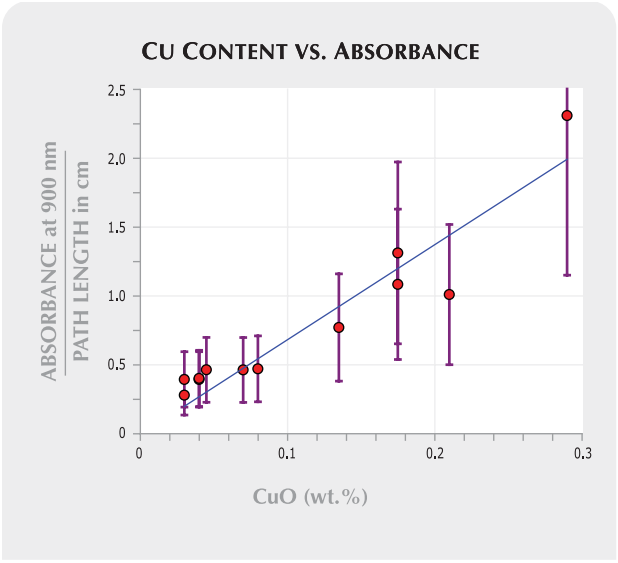

Figure 6. The blue-to-green color of tourmaline may be caused by absorption mainly due to copper (e.g., the three stones on the left, 3.86–11.69 ct) or to iron (the three on the right, 2.86–6.89 ct). Such material may be spectrally differentiated to identify whether it should be classed as Paraíba-type tourmaline. Courtesy of the Gladnick Collection and Palagems.com; photo by Robert Weldon.

dependent on the arbitrary orientation of the axes of the gem relative to the direction of the analyzing beam. Second, there is some uncertainty as to the exact path length traveled by the beam in these measurements, due to the complex geometry of the cut gemstones and the potential effects of inclusions. Third, the absorbance at 900 nm reflects the average bulk concentration of Cu^{2+}, while LA-ICP-MS is a spot analysis and only measures the surface composition. Last, the recorded absorbances are influenced by surface reflections, which may be particularly significant for darker gems. The straight-line fit of the data in figure 5 excludes the highest-absorbance (>1.7) Cu-bearing tourmalines, for which surface reflections greatly limit the maximum absorbances measurable by the techniques of this study. The correlation represented by the line in figure 5 is remarkably good (r^2 = 0.88) considering the sources of variability. The slope of 6.86/cm translates to a CuO content of ~0.15 wt.% per unit of absorbance/cm at 900 nm.

Estimation of Fe^{2+} Abundance. Estimating Fe^{2+} content from absorbance near 700 or 1100 nm is more problematic. Cu^{2+} absorption can interfere near 700 nm, and absorptions due to OH stretching vibrational overtones can begin to interfere at wavelengths >950 nm (i.e., sample P1 in figure 4; see also the *G&G* Data Depository). Like that of Cu^{2+}, the Fe^{2+} absorption depends on orientation. However, the major additional sources of uncertainty in the estimation of iron content are the presence of Fe^{3+} and the nonlinear relationship between iron concentration and Fe^{2+} absorbance (Smith, 1978; Mattson and Rossman, 1987).

Effects of Heat Treatment on Vis-NIR Spectra. Heat treatment is commonly applied to Cu-bearing tourmaline to create or enhance blue/green coloration (Fritsch et al., 1990; Abduriyim et al., 2006; Laurs et al., 2008). While our heating experiments on 10 violet or brownish violet samples removed some absorption features (particularly the Mn^{3+} band near 520 nm) to produce blue or green hues, none of the heated samples showed significant changes in the positions or intensities of the Cu^{2+} absorption bands at ~700 and ~900 nm. Therefore, Vis-NIR spectroscopy can be used to evaluate the Cu^{2+} content of tourmaline samples that have been heat treated.

CONCLUSIONS

Spectral measurements can provide information on the causes of color in gemstones, whereas chemical analyses only indicate which elements are present. In this study, Vis-NIR spectroscopy coupled with LA-ICP-MS analyses demonstrated that absorption spectra can be useful in assessing the contribution of Cu^{2+} to the greenish blue color component in gem tourmaline. Both Fe^{2+} and Cu^{2+} produce absorption bands with maxima near 700 nm, but only Cu^{2+} has a strong maximum near ~900 nm, where the absorption due to Fe^{2+} is typically at a minimum. All the samples in our study with a moderate-high absorption feature near 900 nm contained substantial Cu. In contrast, samples with a substantial absorption

band near 700 nm, but low absorbance near 900 nm, had significant levels of Fe and little or no Cu. Spectral analysis cannot replace more quantitative procedures such as LA-ICP-MS or even EDXRF. Based on this study, however, absorption measurements in the region of 900–925 nm appear to be a relatively quick and simple means for assessing the presence of Cu in gem tourmaline, the key criterion for designation of a stone as "Paraíba" or "Paraíba-type" (e.g., figure 6). Furthermore, in blue, green, and violet gems of pale-to-moderate color intensity, it was possible to estimate wt.% CuO within ~50% accuracy. Spectral measurements may also aid in selecting off-color Cu-bearing tourmalines that are suitable candidates for heat treatment.

We have shown that simple CCD array spectrometers with fiber-optic reflectance probes offer a relatively portable and inexpensive method to screen rough or faceted gem tourmalines (even small samples) for Cu. Most common Vis-NIR spectrometers in gemological laboratories are not well suited to measure Cu^{2+} concentrations because they are configured to measure transmittance of light through a sample, and therefore are useful for performing reasonably quantitative measurements only on parallel-polished slabs or on faceted gemstones with fairly large parallel facets. Nevertheless, fiber-optic probe attachments or small integrating sphere accessories may be compatible with some more-traditional spectrometers.

ABOUT THE AUTHORS

Dr. Merkel (pmerkel@rochester.rr.com) is a senior scientist in the Department of Chemistry and the Center for Photo-induced Charge Transfer at the University of Rochester, New York. Dr. Breeding is a research scientist at the GIA Laboratory in Carlsbad, California.

ACKNOWLEDGMENTS

The authors thank Dr. George Rossman (California Institute of Technology, Pasadena) for helpful comments and suggestions, and Kim Rockwell (former staff gemologist, GIA Laboratory, Carlsbad) for assistance in collecting gemological data.

REFERENCES

Abduriyim A., Kitawaki H. (2005) Gem News International: Cu- and Mn-bearing tourmaline: More production from Mozambique. *G&G*, Vol. 41, No. 4, pp. 360–361.

Abduriyim A., Kitawaki H., Furuya M., Schwarz D. (2006) Paraíba-type copper-bearing tourmaline from Brazil, Nigeria, and Mozambique: Chemical fingerprinting by LA-ICP-MS. *G&G*, Vol. 42, No. 1, pp. 4–21.

Bank H., Henn U., Bank F.H., v. Platen H., Hofmeister W. (1990) Leuchtendblaue Cu-führende Turmaline aus Paraíba, Brasilien. *Zeitschrift der Deutschen Gemmologischen Gesellschaft*, Vol. 39, No. 1, pp. 3–11.

Burns R.G. (1993) *Mineralogical Applications of Crystal Field Theory*, 2nd ed. Cambridge University Press, Cambridge, UK.

Faye G.H., Manning P.G., Nickel E.H. (1968) The polarized optical absorption spectra of tourmaline, cordierite, chloritoid and vivianite: Ferrous-ferric electronic interaction as a source of pleochroism. *American Mineralogist*, Vol. 53, pp. 1174–1201.

Fritsch E., Shigley J.E., Rossman G.R., Mercer M.E., Muhlmeister S.M., Moon M. (1990) Gem-quality cuprian-elbaite tourmalines from São José da Batalha, Paraíba, Brazil. *G&G*, Vol. 26, No. 3, pp. 189–205.

Laurs B.M., Zwaan J.C., Breeding C.M., Simmons W.B., Beaton D., Rijsdijk K.F., Befi R., Falster A.U. (2008) Copper-bearing (Paraíba-type) tourmaline from Mozambique. *G&G*, Vol. 44, No. 1, pp. 4–30.

Manning P.G. (1973) The effect of second-nearest-neighbor interaction on Mn^{3+} absorption in pink and black tourmalines. *Canadian Mineralogist*, Vol. 11, pp. 971–977.

Mattson S.M., Rossman G.R. (1987) Fe^{2+}-Fe^{3+} interactions in tourmaline. *Physics and Chemistry of Minerals*, Vol. 14, pp. 163–171.

Reinitz I.M., Rossman G.R. (1988) Role of natural irradiation in tourmaline coloration. *American Mineralogist*, Vol. 73, pp. 822–825.

Rossman G.R., Mattson S.M. (1986) Yellow, Mn-rich elbaite with Mn-Ti intervalence charge transfer. *American Mineralogist*, Vol. 71, pp. 599–602.

Rossman G.R., Fritsch E., Shigley J.E. (1991) Origin of color in cuprian elbaite from São José da Batalha, Paraíba, Brazil. *American Mineralogist*, Vol. 76, pp. 1479–1484.

Schmetzer K., Bernhardt H.-J., Dunaigre C., Krzemnicki M.S. (2007) Vanadium-bearing gem-quality tourmalines from Madagascar. *Journal of Gemmology*, Vol. 30, pp. 413–433.

Smith G. (1978) Evidence for absorption by exchange-coupled Fe^{2+}-Fe^{3+} pairs in the near infrared spectra of minerals. *Physics and Chemistry of Minerals*, Vol. 3, pp. 375–383.

Smith C.P., Bosshart G., Schwarz D. (2001) Gem News International: Nigeria as a new source of copper-manganese-bearing tourmaline. *G&G*, Vol. 37, No. 3, pp. 239–240.

Taran M.N., Lebedev A.S., Platonov A.N. (1993) Optical absorption spectroscopy of synthetic tourmalines. *Physics and Chemistry of Minerals*, Vol. 20, pp. 209–220.

GEM-QUALITY ANDALUSITE FROM BRAZIL

Shyamala Fernandes and Gagan Choudhary

Widely known as a rock-forming mineral, andalusite is not frequently encountered as a gem material. This article documents the gemological and spectroscopic properties of numerous rough and cut samples of gem-quality andalusite from Brazil. The color varied from yellowish green and green to brownish pink (including bicolored green and brownish pink), and some were faceted with the pleochroic colors attractively oriented. Transparent samples of the chiastolite variety of andalusite were particularly interesting. All the samples displayed a complex growth pattern, with the various inclusions oriented along the growth directions. Heat treatment produced subtle changes in color, if any, but fracture filling with resin resulted in obvious improvements in apparent clarity.

The name *andalusite* is derived from the Andalusia region of southern Spain, where the mineral was first discovered (Dana and Ford, 1992). Gem-quality material is known from Brazil (Espírito Santo and Minas Gerais States), Sri Lanka, the United States, Madagascar, Russia (Siberia), Myanmar (O'Donoghue, 2006), and China (Liu, 2006). Andalusite varieties include highly pleochroic brownish pink/green (e.g., figure 1), Mn-rich bright green ("viridine"), and chiastolite. The last is typically opaque and features a dark cross-shaped pattern formed by carbonaceous inclusions (Webster, 1994; O'Donoghue, 2006).

This article reports the properties recorded from an ~1 kg parcel of medium-quality andalusite that was purchased from a gem merchant in Jaipur, India, who deals in rough from Brazil. The exact source of the andalusite in Brazil was, unfortunately, not available. Additional photos to accompany this article are available in the *G&G* Data Depository (www.gia.edu/gandg).

MATERIALS AND METHODS

From the parcel of rough, we randomly selected about 150 specimens for examination that ranged from ~0.4 to 3 g. We studied 15 samples in detail for their crystallographic features, surface markings, cleavage directions, and pleochroism with respect to crystallographic orientation. These samples exhibited a variety of colors: green, yellowish green to brownish green, brownish pink, and distinctly bicolored green/pink. In addition, we selected six samples of the pinkish brown to brownish pink variety chiastolite, which displayed distinct (sometimes partial) cross-shaped arrangements of dark inclusions. About 20% of the 150 specimens were chiastolite, and they ranged in diaphaneity from transparent to opaque.

We selected 72 of the 150 specimens, of moderate commercial quality, for fashioning on the basis of their coloration, clarity, and projected yield. Of these, 18 were faceted (figure 2) and the other 54 were left preformed. The preformed stones were categorized into three color groups: green (17 specimens), brownish pink (14), and strongly pleochroic pinkish brown/yellowish green (23). On an additional seven specimens (figure 3), we polished the largest parallel surfaces so we could obtain RI readings and examine their internal features.

Standard gemological tests—including color observations, SG measurements, fluorescence reactions, and visible-range spectroscopy—were performed on all samples. RI and optic sign were measured only on

See end of article for About the Authors and Acknowledgments.
GEMS & GEMOLOGY, Vol. 45, No. 2, pp. 120–129.

Figure 1. Brazil is a source of rare gem-quality andalusite, as shown by this exceptional 17.96 ct stone. Due to its strong dichroism, both pleochroic colors are distinctly visible. Courtesy of Palagems.com, Fallbrook, California; photo by Robert Weldon.

the seven polished slices and the 18 faceted samples. To determine the variations in refractive index with respect to crystallographic axis, we polished the prism faces [(110), ($1\bar{1}0$), ($1\bar{1}0$), ($\bar{1}10$)], one of the corners [representing (100) or (010)], and the pinacoidal face (001) of one prismatic crystal. RI was measured with a GemLED refractometer. We obtained hydrostatic SG values using a Mettler Toledo CB 1503 electronic balance. Fluorescence was tested using standard long-wave (366 nm) and short-wave (254 nm) UV bulbs. Absorption spectra were observed using a desk-model GIA Prism 1000 spectroscope. We examined internal features with both a binocular gemological microscope and a horizontal microscope with immersion, using fiber-optic and other forms of lighting (including darkfield and brightfield).

Qualitative energy-dispersive X-ray fluorescence (EDXRF) chemical analyses of 31 green and brownish pink preforms, the seven polished slices, and the 18 faceted samples were performed with a PANalytical Minipal 2 instrument using two different conditions. Elements with lower atomic number (e.g., Al and Si) were measured at 4 kV tube voltage and 0.850 mA tube current with no filter; transition and heavier elements were analyzed at 25 kV and 0.025 mA using an Al filter.

Infrared spectra of 31 preforms (green and brownish pink), 15 crystals (4–15 mm thick), seven polished slices, and five faceted samples that had undergone fracture-filling processes were recorded in the 6000–400 cm^{-1} range at a standard resolution of 4 cm^{-1}; 50 scans per sample were recorded with a Nicolet Avatar 360 Fourier-transform infrared (FTIR) spectrometer at room temperature in transmission mode. We collected multiple spectra to find the orientation of best transmission (depending on the thickness and transparency of the samples), considering the pleochroic colors and crystallographic axes.

Raman analysis was performed on five rough samples and two polished slices in two directions—along the c-axis and along the a- or b-axis—in the 2000–100 cm^{-1} range using a Renishaw InVia Raman confocal microspectrometer with 514 nm Ar-ion laser excitation, an exposure time of 10 seconds per scan, and 10 scans per sample.

We selected 24 rough samples for heat-treatment

Figure 2. Eighteen andalusite samples (0.15–0.58 ct) were faceted to display the range of color. Photo by G. Choudhary.

Figure 3. Seven andalusite specimens (0.81–3.87 ct) were polished as slices for inclusion studies and RI readings. Photo by G. Choudhary.

Figure 4. A few of the specimens in the rough parcel of andalusite displayed characteristic crystal forms with prism faces terminated by pyramids. The crystal shown here weighs 1 g. Photo by G. Choudhary.

experiments; the original colors were brownish pink (8 samples), green (5), bicolored (3), and brownish pink with a green component at their corners (8). We heated the stones in a muffle furnace with digital temperature controls. Six stones were heated at 350°C and eight at 550°C for 8 hours, while 10 samples were heated at 800°C for 2½ hours and then at 550°C for 5½ hours. In addition, five of the faceted samples with eye-visible surface-reaching fissures were selected for fracture filling. We used a colorless epoxy resin on three samples and Johnson & Johnson baby oil (also colorless) on two samples, at pressures of 40 to 50 psi for 48 hours. The samples were photo-documented before the experiments, and the colors and inclusions were compared before and after the treatments.

RESULTS AND DISCUSSION

Crystal Morphology and Visual Observations. The majority of the rough consisted of broken crystals with frosted surfaces. Approximately 10% of them were terminated by pinacoids or pyramids (figure 4) and exhibited four-sided prisms, often with the rectangular- or rhomb-shaped cross section associated with the orthorhombic crystal system (Webster, 1994). Most of these crystals had only one termination and were broken at the other end.

More than 80% of the rough displayed pronounced etching, consistent with their frosted surfaces. This was evident on 12 of the 15 crystals selected for crystallographic study. The etching pattern varied from irregular to square or rectangular in shape (figure 5, left). Many of the samples also exhibited striations on the prism faces, parallel to the c-axis. One of the crystals displayed two sets of striations on the same face (figure 5, right). One set was oriented along the c-axis, while the other consisted of lateral striations; such patterns indicate twinning or various stages of overgrowth where two sectors/crystals have grown in different directions. Some crystals clearly displayed a smaller attached twinned crystal oriented along or inclined toward the c-axis of the main crystal. In addition, step-like planes indicating cleavage (again, see figure 5, left) were present on the surfaces of all the samples studied; only one cleavage plane was seen in most samples, but in some cases two directions were visible. Both directions were oriented parallel to the prism faces, as reported previously (Phillips and Griffen, 1986).

About 20% of the pinkish brown/brownish pink samples contained black inclusions that formed partial or complete chiastolite cross patterns. Most of these samples revealed black material in the core when viewed along the c-axis, while a few had a green central core with black outlines and arms. The six specimens selected for study included three with dark cores (figure 6) and three with green cores (e.g., figure 7, left). The cores varied from transparent to opaque and from almost square (figure 6, center) to

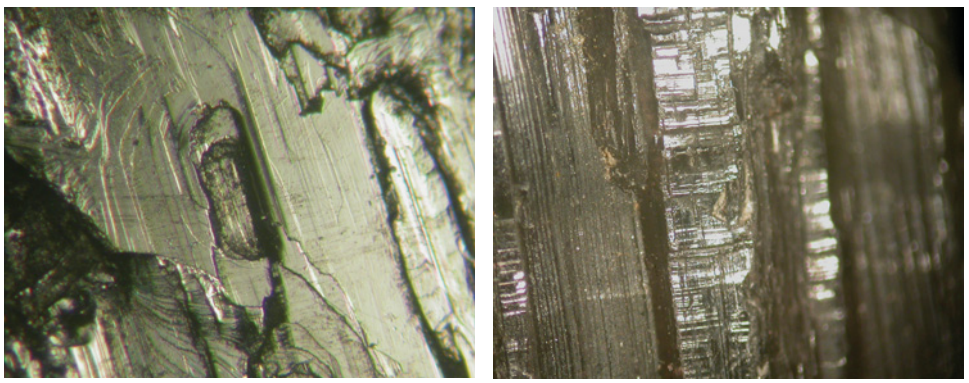

Figure 5. Many of the andalusite samples displayed strong etching that varied from irregular to square or rectangular (left). Also common were striations on the prism faces (right). The two-directional striations indicate the presence of twinning or various stages of overgrowth. Photomicrographs by G. Choudhary; magnified 60× (left) and 45× (right).

rectangular (figure 6, left and right). The green cores were distinctly pleochroic: When the plane of the core was perpendicular to the viewing angle, it appeared green (again, see figure 7, left); as the host was tilted slightly, the core appeared brownish pink/red (figure 7, right) while the rest of the sample remained unchanged. A similar effect was visible when these crystals were viewed through prism faces.

The color-zoned or bicolored green-and-pink samples (figures 8 and 9, left) somewhat resembled "watermelon" tourmaline.

Orientation of Crystal for Best Cut. Overall, the parcel of rough was better suited for beads and cabochons than for faceted stones. Among the major considerations in the cutting process were the abundance of inclusions, bodycolor, and orientation of the pleochroism to achieve the best table-up color. The brownish pink crystals had about the same color after cutting (i.e., their strong pleochroism was not visible face-up), so the rough was oriented simply for best yield. For the green stones, an attempt was made to orient the green color to the table; however, crystals that also exhibited a strong pink pleochroic color displayed a pinkish hue at the corners of the finished stones. Bicolored stones were specifically cut to display the color zoning in a table-up position. Crystals with long tube-like inclusions needed to be oriented in such a way that these inclusions were perpendicular to the table facet, to make them less visible. Although the rough sizes ranged from ~0.4 to 3 g, the resulting stones weighed only 0.15–0.58 ct after faceting. The overall yield from rough to the finished product was approximately 20%.

Gemological Properties. The gemological properties of the samples are described below and summarized in table 1.

Figure 6. The chiastolite samples, here ranging from 3 to 6.5 mm thick, displayed a characteristic black cross pattern at the basal pinacoid with a square-to-rectangular core. The unusual transparency of these chiastolites made them particularly interesting. Photo by G. Choudhary.

Pleochroism. All but the brownish pink samples displayed strong, eye-visible pleochroism that ranged from weak to strong. Along the c-axis, the samples appeared brownish pink; perpendicular to the c-axis, they appeared yellowish or brownish green. Depending on their orientation and their main bodycolor, the cut stones appeared brownish pink to yellowish green; both colors were often visible in the same sample when viewed table-up (again, see figures 1 and 2). The bicolored samples also displayed strong pleochroism. In one sample, rotating the polarizer 90° turned the brownish pink area almost colorless while the green portion became brighter yellowish green (see figure 9).

Refractive Index. We recorded a range of RI values—n_α=1.637–1.649 and n_γ =1.646–1.654—with a negative optic sign; birefringence varied from 0.008 to 0.010. These values are consistent with those reported previously for andalusite (Webster, 1994; Phillips and Griffen, 1986). RI and birefringence increase with

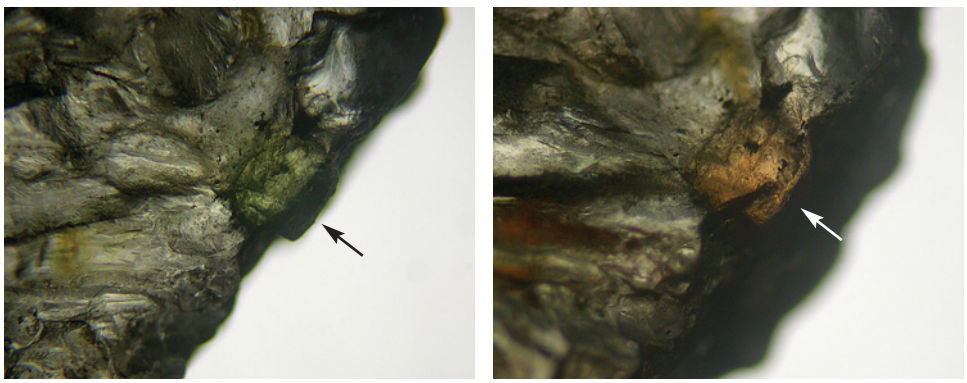

Figure 7. A small percentage of the brownish pink to pinkish brown andalusite contained a green core with a black outline and arms. When the plane of the core was perpendicular to the viewer, it appeared green (left). As the sample was tilted slightly, it appeared brownish pink (right), with no change in the rest of the stone. Photomicrographs by G. Choudhary; magnified 15×.

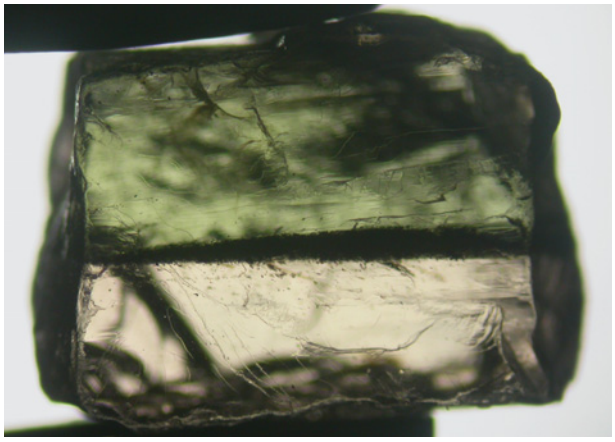

Figure 8. Many bicolored samples of andalusite appeared to display various growth stages, with their colors separated by a sharp plane marked by brown granular inclusions. Photomicrograph by G. Choudhary; magnified 25×.

the increasing percentage of Mn (as in the viridine variety) to as high as 1.690 with birefringence of about 0.025 (Phillips and Griffen, 1986), although not in our specimens. Measurements of the oriented sample revealed that the pinacoidal face (001), or α-ray direction, gave the lowest RIs and birefringence (0.008), while the polished corner (100) or (010) gave the highest values (with maximum birefringence of 0.009), indicating that it represented the b-axis or γ-ray direction. Such variations were reported previously by Kerr (1959) and Phillips and Griffen (1986).

Specific Gravity. The samples had SG values in the 3.11–3.16 range. Webster (1994) listed SG values of 3.15–3.17, while Phillips and Griffen (1986) reported 3.13–3.16. The SG values of our samples are similar, though a few specimens had slightly lower values (probably due to fractures and surface-reaching inclusions).

TABLE 1. Properties of the Brazilian andalusite specimens studied for this report.

Property	Description
Color range	Green, yellowish green to brownish green, brownish pink, bicolored green/pink, and pinkish brown (chiastolite)
Pleochroism	Brownish pink (parallel to the c-axis) Yellowish or brownish green (perpendicular to the c-axis)
Diaphaneity	Transparent to opaque
Refractive index	n_α = 1.637–1.649 n_γ = 1.646–1.654
Birefringence	0.008-0.010
Optic sign	Biaxial negative
Specific gravity	3.11–3.16
UV fluorescence	
Long-wave	Inert
Short-wave	Moderate to strong yellowish green
Visible-range absorption spectrum	Diffuse band at ~455 (weak to strong) in some samples
Microscopic features	Two types of curved inclusions, minute films/discs, numerous mineral inclusions, "fingerprints," pinpoints, twinning/growth patterns, cross patterns in chiastolite varieties
EDXRF analysis	Presence of Al, Si, Fe, Ca, and Cr (two specimens had Zn and Cu, probably due to contamination from the polishing wheels); no Mn detected in any samples
FTIR analysis	Complete absorption up to 2100 cm^{-1}; peaks at ~3687, 3652, and 3624 cm^{-1}; twin peaks at ~3520 and 3460 cm^{-1}; shoulders at ~3280 and 3095 cm^{-1}
Raman analysis	Several sharp peaks at ~1063, 917, 550, 463, 356, 325, and 290 cm^{-1}; smaller peaks at ~1120, 850, and 717 cm^{-1}

Fluorescence. The samples were inert to long-wave UV radiation but fluoresced yellowish green to short-wave UV; the intensity varied from moderate to strong. Webster (1994) and O'Donoghue (2006)

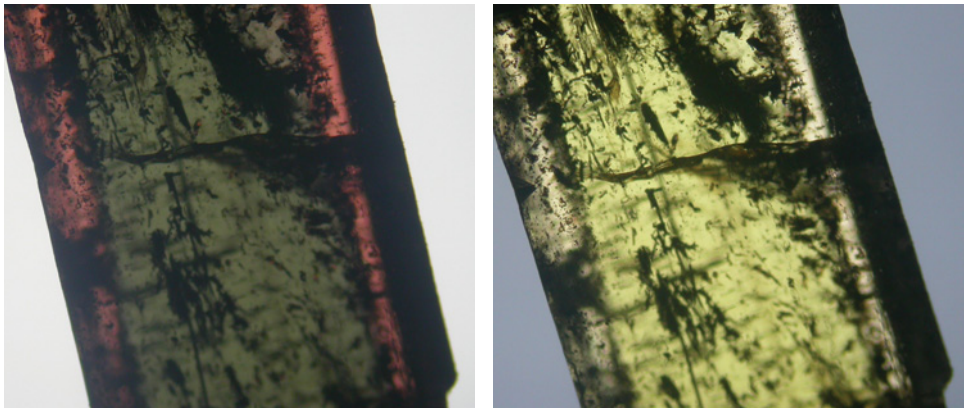

Figure 9. Many of the andalusite samples exhibited color zoning in green and brownish pink (left), a combination reminiscent of bicolored tourmalines. When the polarizer was rotated 90°, the brownish pink area turned almost colorless, while the green portion became brighter yellowish green (right). Photomicrographs by G. Choudhary; magnified 25×.

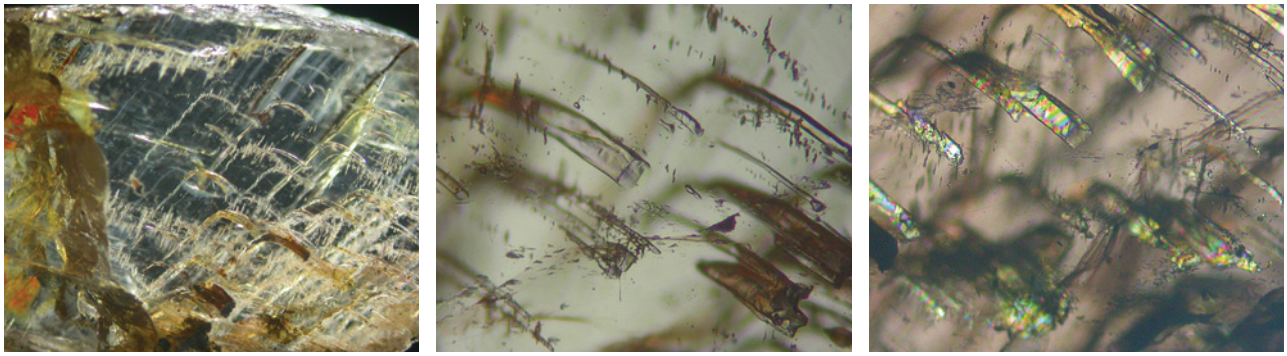

Figure 10. Type 1 curved inclusions are colorless and transparent, often with fine fringes (left and center). They appear birefringent between crossed polarizers, indicating their mineral nature (right). Note the stained surface and angle of curvature of these tubes, which are bent almost 90°. Photomicrographs by G. Choudhary; magnified 40× (left), 80× (center, brightfield illumination), and 70× (right, crossed polarizers).

reported similar fluorescence reactions for andalusite from Brazil.

Absorption Spectrum. With a desk-model spectroscope, a number of samples displayed a weak-to-strong diffuse band in the blue region at ~455 nm. When viewed along the c-axis, the absorption appeared weaker than in the perpendicular direction. Some samples did not exhibit any absorption.

Microscopic Features. The samples displayed a wide range of internal patterns, such as curved features, mineral inclusions, and various twinning/growth patterns.

Curved Inclusion Features. Many samples contained numerous curvilinear inclusions, of which two different varieties were defined: Type 1 inclusions occurred in the pleochroic brownish pink/green stones, while type 2 were present in some chiastolitic samples.

The type 1 curved inclusions were colorless and transparent, and had associated fine fringe-like films oriented perpendicular to their length (figure 10, left), giving the impression of icicles on branches. The cross sections of the inclusions appeared rectangular (figure 10, center), and between crossed polarizers they were birefringent (figure 10, right), indicating their mineral nature. Gübelin and Koivula (2008) reported sillimanite fibers in andalusite from Santa Teresa in Minas Gerais, Brazil. The possibility of these inclusions being sillimanite cannot be ruled out, since their appearance seems consistent with the orthorhombic crystal form. Many of these inclusions also had a coating of some brownish epigenetic material where they reached the surface (again, see figure 10, left). EDXRF analysis of polished slices with these surface-reaching inclusions revealed the presence of Cu and Zn, which were absent from those without such surface-reaching inclusions. The Cu and Zn may have originated from the polishing wheels used, which contained these elements.

The type 2 curved inclusions appeared to be growth tubes filled with a brown or black material. Some samples displayed these tubes in parallel bundles oriented in various directions (figure 11, left). Each direction terminated at a sharp plane. In one specimen, these planes created a rectangular/square profile. They also appeared to run across the stone (similar to a twin plane) in different directions. At higher magnification, the tubes appeared to contain

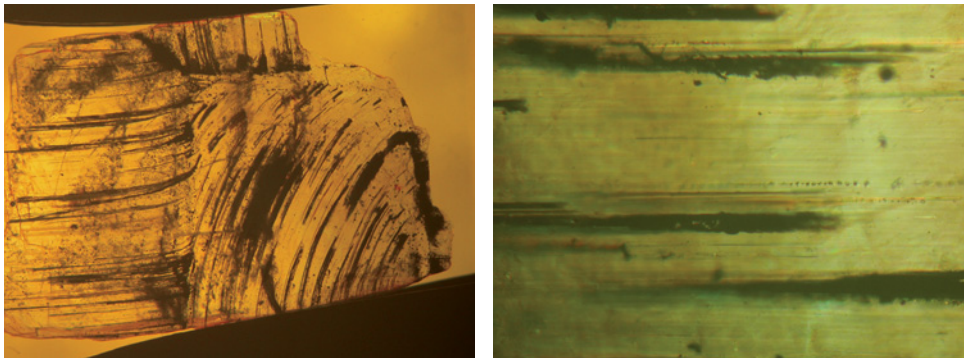

Figure 11. Type 2 curved inclusions consist of tubes that are filled with a black material. In some samples, groups of these tubes were oriented in various directions (left). At higher magnification, the black material appears granular (right). Photomicrographs by G. Choudhary; magnified 30× (left, in immersion) and 80× (right).

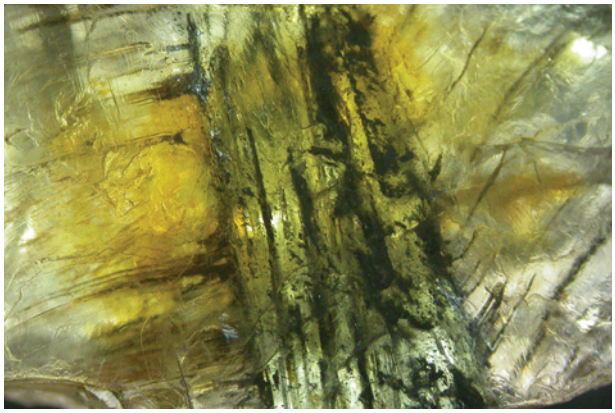

Figure 12. In a few chiastolite specimens, a green core contained tubes oriented parallel to the c-axis, while the surrounding area hosted tubes in a radiating pattern. Similar patterns of black tubes have been observed previously in chiastolite by the authors. Photomicrograph by G. Choudhary; magnified 25×.

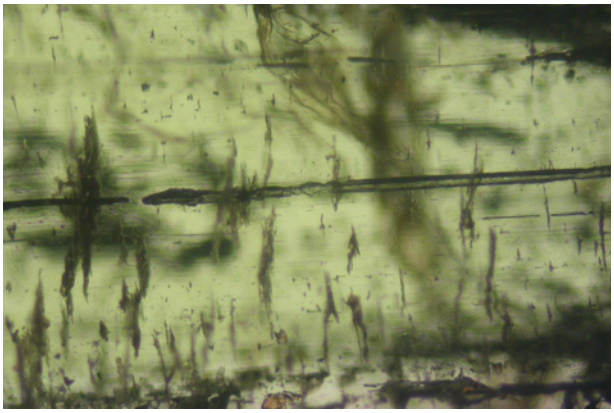

Figure 13. Straight tubes with wavy surfaces, oriented parallel to the c-axis, were present in some of the andalusite samples. Photomicrograph by G. Choudhary; magnified 60×.

a black granular material (figure 11, right). Similar inclusions have been reported in "trapiche" tourmaline (Hainschwang et al., 2007), where growth channels are oriented in two directions. In our chiastolite specimens, the varying orientations of the tubes may be attributed to twinning or different stages of growth, as also indicated by the sharp growth zoning described below.

The angle of curvature in both types of inclusions typically was almost 90° (e.g., figure 10), while some appeared closer to 45°, as if originating from pyramidal faces. Most of the inclusions were oriented parallel to the c-axis.

A few samples displayed an interesting pattern of type 2 tubes (figure 12). A central green core exhibited curved tubes parallel to the c-axis, while the surrounding portions contained tubes that radiated from the boundary with the core. The authors have previously observed a similar pattern of black tubes in chiastolites. Such a growth pattern indicates different growth stages and directions of the overgrown areas, and is a characteristic of chiastolite.

Straight tubes with slightly wavy surfaces (figure 13), oriented parallel to the c-axis, were also observed in the yellow-green and bicolored samples, as well as in the chiastolite with green cores.

Figure 14. The andalusites commonly contained film or platelet-like inclusions that appeared to be oriented along the c-axis (vertical in this view), giving a stringer-like pattern as in figure 10 (left). Photomicrograph by G. Choudhary; magnified 65×.

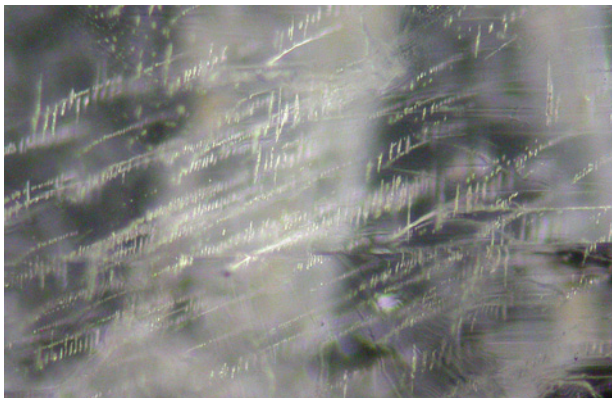

Figure 15. In one sample, small films/fractures were associated in places with conical tube-like features (similar to nail-head spicules). These films were oriented roughly along the basal plane (horizontal in this view), while the conical "tubes" were along the c-axis. Also note the growth zoning parallel to the c-axis. In addition, many scattered tiny inclusions were visible that could not be resolved clearly. Photomicrograph by G. Choudhary; magnified 80×.

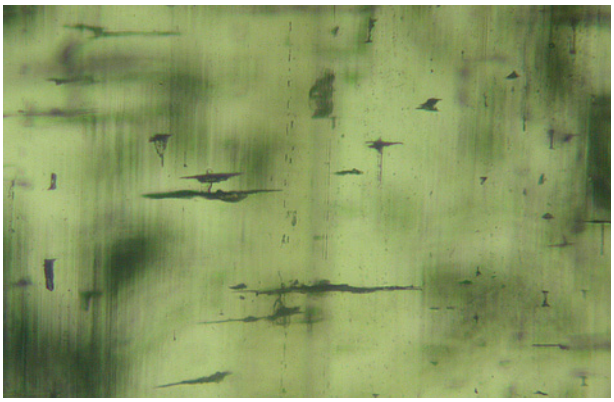

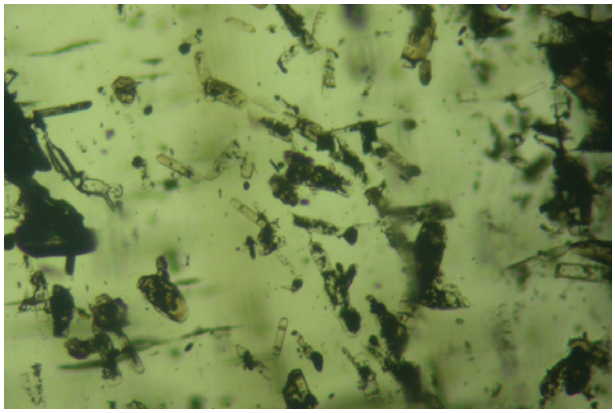

Figure 16. Scattered crystalline inclusions were present in the andalusites. Some of these inclusions were birefringent between crossed polarizers. Photomicrograph by G. Choudhary; magnified 80×.

Films and Discs. Many of the samples had rows of small films or discs oriented along the c-axis in a "stringer"-like pattern (figure 14) similar to the "fringes" associated with the type 1 curved inclusions discussed above. In one of the samples, some films were associated with small conical tube-like features that resembled nail-head spicules (figure 15). These films were oriented roughly along the basal plane, while the conical tubes were oriented along the c-axis. Although nail-head spicules are commonly associated with synthetic gems grown by hydrothermal or flux processes, they have also been reported in a few natural stones such as sapphire and emerald (Choudhary and Golecha, 2007).

Mineral Inclusions. The cross pattern of black granular inclusions in chiastolite is the result of rapid growth of the prism faces, which pushed the black material to the edges. Although we did not analyze them for this study, similar black inclusions in chiastolite have been identified as graphite (Johnson and Koivula, 1998; Hlaing, 2000).

Scattered colorless to brown and black crystals (figure 16) were also present. Many of these inclusions were elongated and birefringent between crossed polarizers, and some displayed cleavage-like features oriented perpendicular to their length. They were confined to two directional planes intersecting at 90° to form a square or rectangular outline. This orientation indicated that different growth sectors were separated by these crystal inclusions. This inclusion pattern has not been reported previously for chiastolite. However, such features are not expected in a faceted andalusite since a cutter would surely exclude them.

Also seen were brownish birefringent platelets oriented in planes. In the green and brownish pink varieties they appeared scattered, while they were more defined (i.e., along the planes of the core) in the chiastolitic material.

Fingerprints. A few stones had "fingerprint" inclusions forming a crisscross veil-like pattern (figure 17). These appeared to be composed of crystals rather than fluid, judging from the sharp edges of the individual inclusions.

Pinpoints. We observed whitish pinpoints in a few samples. These pinpoints were restricted to straight, wavy, and curved zones (figure 18) that appeared white and were mostly oriented parallel to the c-axis.

Growth Features. The study samples displayed a wide range of growth features, some of which were quite complex. Many exhibited distinct color zones when viewed with the unaided eye, and also revealed unusual and interesting patterns with magnification. In one case, two colors—green and light pink—were separated by a brown zone that appeared to be composed of tiny crystals (as it appeared granular; see figure 8). In a few specimens, distinct brownish pink and green zones were separated by sharp planes, often containing some mineral inclusions (again, see figure 9, left). This suggests two stages of growth with different chemical compositions, as is the case for color-zoned sapphire or bicolored tourmaline; both color components also displayed a strong degree of pleochroism (again, see figure 9). Such bicolored andalusite specimens, when viewed along the c-axis, had the central green core and light brownish pink to red to almost colorless outer layers

Figure 17. A few andalusite samples displayed veil-like "fingerprints" that appeared to be composed of crystals. Photomicrograph by G. Choudhary; magnified 60×.

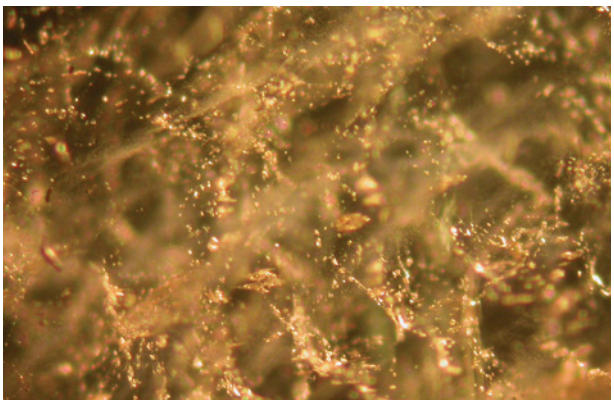

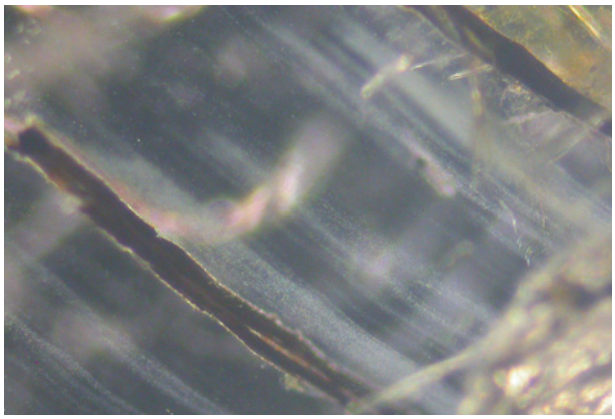

Figure 18. Fine whitish pinpoints arranged in straight, curved, or wavy zones were observed in a few andalusite samples. Photomicrograph by G. Choudhary; magnified 65×.

following the crystal shape with a square-to-rectangular profile.

Many samples also displayed growth zones that were oriented parallel to the prism face or the c-axis (again, see figure 15). Some of the chiastolite samples also exhibited wavy alternating yellow and brown color and growth zones.

EDXRF Analysis. Qualitative EDXRF analysis was performed on polished samples as well as preforms. The samples were oriented to analyze both brownish pink and green areas to check for variations in chemical composition; this included color-zoned samples as well as those of different homogeneous bodycolors. However, no chemical variations were observed. The analyses revealed the presence of Al and Si, as expected for andalusite. A minor amount of Fe was also detected, along with traces of Ca and Cr. Manganese was not detected in any of the samples, consistent with the low birefringence and the RI values.

FTIR Spectroscopy. The FTIR spectra displayed complete absorption below 2100 cm^{-1} and a number of bands of varying intensity in the 3800–3000 cm^{-1} region (figure 19): three at ~3687, 3652, and 3624 cm^{-1} in most samples; a pair at about 3520 and 3460 cm^{-1} in almost all samples; two bands at ~3280 and 3095 cm^{-1} in most samples; and weak features at ~3380 and 3170 cm^{-1}.

All the features recorded in this study are in the water region of the IR spectrum and correspond to vibrations and stretching of OH molecules (Busigny et al., 2004; Balan et al., 2006). Although andalusite is considered an anhydrous mineral, this suggests the presence of some water (H_2O or OH), either in the structure or in inclusions. The bands at 3520 and 3460 cm^{-1} suggest that OH dipoles lie within the {001} basal plane of andalusite (Burt et al., 2007); these two features appeared much stronger when the spectra were collected along the c-axis or in the brownish pink direction.

Raman Analysis. No directional variations were recorded in the Raman spectra. There were several sharp peaks at ~1063, 917, 550, 463, 356, 325, and 290 cm^{-1}, with smaller peaks at ~1120, 850, and 717 cm^{-1}. The spectral pattern is similar to those reported for andalusites in the RRUFF project database (www.rruff.info). Peaks in the 1150–800 cm^{-1} region arise from Si-O stretching, while those below 600 cm^{-1} are due to complex motions between O, OH, and SiO_4 (Wang et al., 2002), suggesting the presence of OH in the structure of the andalusite.

Treatment Experiments. Heat treatment at 350°C and 550°C yielded no noticeable change in color; heating at 800°C resulted in only a subtle lightening of the bodycolor, though it has been reported previously that "olive" green andalusite from Brazil changes to pink and brown, and then to colorless, at 800°C (Nassau, 1994).

Microscopic examination of the samples heated at the lower temperatures did not reveal any observable effects. In the samples that were heated to 800°C, however, some changes were observed, though they

Figure 19. The infrared absorption spectra revealed a number of weak-to-strong peaks in the 3800–3000 cm^{-1} region in both pleochroic directions. The peaks at 3520 and 3460 cm^{-1} were much stronger in the brownish pink direction (parallel to the c-axis), suggesting the presence of OH dipoles in the basal plane.

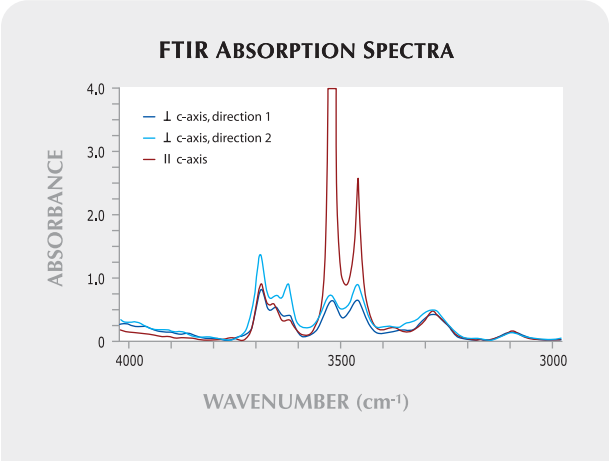

were not distinct enough to be considered diagnostic evidence of heating. These samples developed some stress fractures oriented in one direction along the prism faces, indicating the expansion of cleavage planes due to heat. Samples containing tube-like inclusions with brownish material also displayed some changes; the brown material burst from within the tubes and concentrated in associated fractures, thereby giving the effect of iron-stained films or fractures. Some samples also developed similar patches or films on the surface, possibly resulting from the oxidation of Fe in the structure of andalusite.

The three specimens subjected to fracture filling with resin showed an obvious improvement in apparent clarity, while the two filled with oil displayed only a minute change in the visibility of inclusions. The resin filling was detectable in the infrared spectra, which displayed a characteristic band at 3046 cm^{-1}, as well as peaks at 2926 and 2854 cm^{-1}. The latter bands are associated with oils and epoxy prepolymers (Johnson et al., 1999). The stones filled with oil also displayed the characteristic 2926 and 2854 cm^{-1} bands.

CONCLUSION

The color range of the Brazilian andalusite study samples varied from yellowish green to green to brownish pink, with some bicolored green and brownish pink. The transparent chiastolite samples were quite unusual for this gem variety. Gemological properties such as RI and SG, along with a characteristically strong pleochroism, easily distinguish andalusite from other gems such as tourmaline (which has weaker pleochroism and is uniaxial). EDXRF analysis revealed the presence of Fe, Ca, and Cr, in addition to Al and Si; no Mn was detected in any of the samples, consistent with the low RI and birefringence values. In addition to these properties, FTIR and Raman analysis revealed peaks in the 3800–3000 cm^{-1} and 1100–200 cm^{-1} regions, respectively. These features indicated vibrations or stretching of OH and SiO_4 molecules in this primarily anhydrous mineral. The most unusual findings of the inclusion study were the curved inclusions seen in many of the samples and the growth patterns associated with the bicolored stones.

ABOUT THE AUTHORS

Ms. Fernandes is project consultant with the Indian Institute of Jewellery in Mumbai and proprietor of SF Gem Labs in Jaipur. Mr. Choudhary (gtl@gjepcindia.com) is assistant director of the Gem Testing Laboratory in Jaipur.

ACKNOWLEDGMENTS

The authors are grateful to Frank Fernandes of M/s. Neethi's in Jaipur for loaning the samples for study, some of which he also cut and polished, as well as for helpful discussions on determining the refractive index variations according to crystal orientation. The authors also express their gratitude to the Indian Institute of Jewellery in Mumbai for collecting Raman spectra at their facility.

REFERENCES

Balan E., Lazzeri M., Mauri F. (2006) Infrared spectrum of hydrous minerals from first-principles calculations. *Ab Initio (from Electronic Structure) Calculation of Complex Processes in Materials*, No. 75, pp. 143–150, www.psik.org/newsletters/News_75/newsletter_75.pdf.

Burt J.B., Ross N.L., Gibbs G.V., Rossman G.R., Rosso K.M. (2007) Potential protonation sites in the Al_2SiO_5 polymorphs based on polarized FTIR spectroscopy and bond critical point properties. *Physics and Chemistry of Minerals*, Vol. 34, pp. 295–306.

Busigny V., Cartigny P., Philipot P., Javoy M. (2004) Quantitative analysis of ammonium in biotite using infrared spectroscopy. *American Mineralogist*, Vol. 89, pp. 1625–1630.

Choudhary G., Golecha C. (2007) A study of nail-head spicule inclusions in natural gemstones. *G&G*, Vol. 43, No. 3, pp. 228–235.

Dana E.S., Ford W.E. (1992) *A Textbook of Mineralogy with an Extended Treatise on Crystallography and Physical Mineralogy*, 4th ed. Wiley Eastern Ltd., New Delhi, India.

Gübelin E.J., Koivula J.I. (2008) *Photoatlas of Inclusions in Gemstones*, Vol. 3. Opinio Publishers, Basel, Switzerland.

Hainschwang T., Notari F., Anckar B. (2007) Trapiche tourmaline from Zambia. *G&G*, Vol. 43, No. 1, pp. 36–46.

Hlaing T. (2000) Chiastolite from Kyaukse, Myanmar. *Australian Gemmologist*, Vol. 20, No. 11, pp. 479–480.

Johnson M.L., Koivula J.I., Eds. (1998) Gem News: Andalusite (chiastolite) sphere. *G&G*, Vol. 34, No. 1, p. 51.

Johnson M.L., Elen S., Muhlmeister S. (1999) On the identification of various emerald filling substances. *G&G*, Vol. 35, No. 2, pp. 82–107.

Kerr P.F. (1959) *Optical Mineralogy*. McGraw-Hill Book Co., London.

Liu G. (2006) *Fine Minerals of China: A Guide to Mineral Localities*. AAA Minerals AG, Zug, Switzerland.

Nassau K. (1994) *Gemstone Enhancement: History, Science and State of the Art*, 2nd ed. Butterworth-Heinemann, Oxford, UK.

O'Donoghue M., Ed. (2006) *Gems*, 6th ed. Butterworth-Heinemann, Oxford, UK.

Phillips W.M., Griffen D.T. (1986) *Optical Mineralogy: The Nonopaque Minerals*, 1st Indian ed. CBS Publishers & Distributors, New Delhi, India.

Wang A., Freeman J., Kuebler K.E. (2002) Raman spectroscopic characterization of phyllosilicates. *33rd Lunar and Planetary Science Conference*, March 11–15, League City, Texas, Abstract 1374, www.lpi.usra.edu/meetings/lpsc2002/pdf/1374.pdf.

Webster R. (1994) *Gems: Their Sources, Descriptions, and Identification*, 5th ed. Revised by P.G. Read, Butterworth-Heinemann, Oxford, UK.

Characterization of Peridot from Sardinia, Italy

Ilaria Adamo, Rosangela Bocchio, Alessandro Pavese, and Loredana Prosperi

Gem-quality peridot is occasionally found as mantle xenoliths within basalts near Pozzomaggiore, in northwestern Sardinia, Italy. The gemological properties and spectroscopic features of this material are consistent with the measured chemical composition of $Fo_{91}Fa_9$, typical of peridot from other localities worldwide. Although not yet mined commercially, this stone represents a promising gem material.

Peridot has been reported from many sources worldwide, but the localities with historical or contemporary commercial importance are Zabargad (Egypt), Arizona (United States), Myanmar, China, Vietnam, Ethiopia, Tanzania, and Pakistan (Shigley et al., 1990, 2000; Kane, 2004).

Figure 1. These peridots from Sardinia (0.31–2.53 ct) are among the samples investigated for this report. Photo by Kevin Schumacher.

Some attractive peridot has also been found in Italy (Bianchi Potenza et al., 1989, 1991). Gem-quality stones (e.g., figure 1), typically <3 ct when faceted, have been recovered from an area near Pozzomaggiore, close to the city of Sassari, in northwestern Sardinia (figure 2). The olivine occurs in peridotite mantle xenoliths (figure 3) embedded in Plio-Pleistocene alkali basalts (Dupuy et al., 1987). These nodules range up to 30 cm in diameter and contain a typical peridotite assemblage of olivine, orthopyroxene, clinopyroxene, and spinel (Dupuy et al., 1987). The nodules are clearly visible in great abundance in this area, especially in excavations made for road construction and also in blocks used as building materials (Bianchi Potenza et al., 1991). The olivine-bearing basalts have been well known to Italian mineral collectors for years, though there are no reliable records of the amount of gem material recovered to date. The present study provides a detailed characterization of this Sardinian peridot.

Materials and Methods. We examined 10 faceted gems ranging from 0.14 to 2.53 ct (see, e.g., figure 1) and two pieces of rough measuring approximately 0.5–1 cm, all obtained from six fragments sampled in nodules recovered *in situ* from basaltic rocks near Pozzomaggiore. All the faceted samples were examined by standard gemological methods to determine their optical properties, specific gravity, UV fluorescence, and microscopic features.

Quantitative chemical analyses of major and minor elements (Mg, Si, Mn, Fe, and Ni) were performed on polished surfaces of two rough samples using an ARL electron microprobe in wavelength-dispersive mode. We determined trace elements (Li, B, Na, Ca, Sc, Ti, V, Cr, Co, Zn) in the same samples by laser ablation–inductively coupled plasma–mass spectrometry (LA-ICP-MS).

Mid-infrared (4000–400 cm^{-1}) spectra were collected from two rough samples in transmission mode using a Nicolet Nexus FTIR spectrometer. Powdered samples

See end of article for About the Authors and Acknowledgments.
Gems & Gemology, Vol. 45, No. 2, pp. 130–133.

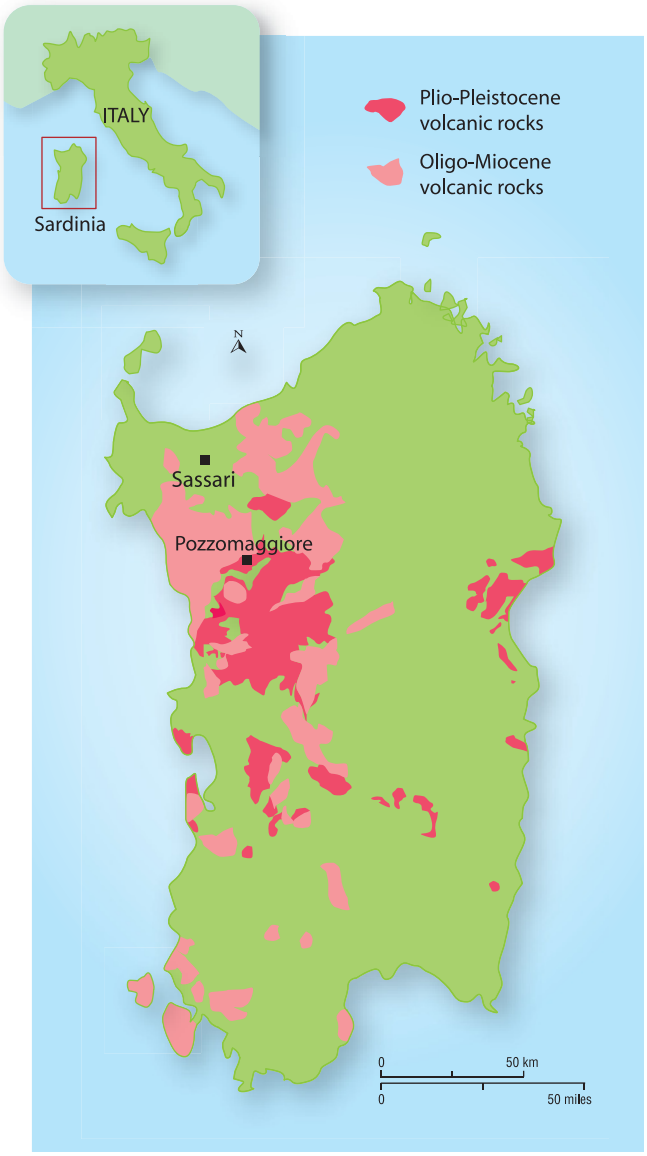

Figure 2. Gem-quality peridot is found in northwestern Sardinia, near the town of Pozzomaggiore.

were compressed into KBr pellets with a sample-to-KBr weight ratio of 1:100.

Unpolarized UV-Vis-NIR spectra were taken from two faceted samples (6.82 × 3.88 × 1.77 mm and 4.33 × 3.86 × 2.04 mm) with a PerkinElmer Lambda 950 spectrometer, equipped with an integrating sphere, over the 300–1300 nm range.

Results and Discussion. The gemological properties of the faceted samples (table 1) agree with those previously reported by Bianchi Potenza et al. (1991) for samples from the same area, and they are consistent with those of peridot from other geographic localities (Gübelin, 1981; Koivula, 1981; Koivula and Fryer, 1986; Führbach, 1998; Kane, 2004). For the most part, the samples appeared clean, with few internal features. The most common inclusions, present in

Figure 3. Olivine-rich nodules containing pyroxene and spinel are hosted by basalts of Plio-Pleistocene age at the Sardinia locality. Photo by R. Bocchio.

almost all samples, were partially healed fractures (figure 4, left) and liquid inclusions. Four samples also contained some roughly round- to oval-shaped decrepitation halo cleavages, commonly known as "lily pad" inclusions (figure 4, right). More rarely observed were minute dark crystals (probably spinel, seen in three samples), parallel twinning (in two samples), and growth planes (in one sample).

Peridot is the gem variety of olivine that compositionally falls within the forsterite [abbreviated Fo; $Mg_2(SiO_4)$] – fayalite [Fa; $Fe_2(SiO_4)$] solid-solution series. Most gem peridots lie within the $Fo_{80–95}Fa_{20–5}$ range (Gübelin, 1981; Nassau, 1994; Krzemnicki and Groenenboom, 2008). Chemical analysis of the two rough samples (table 2) indicated a composition of $Fo_{91}Fa_9$ for both, which is consistent with that previously reported by Bianchi Potenza et al. (1991) and is typical of peridot from various localities (e.g., Stockton and Manson, 1983; Gunawardene, 1985; Führbach, 1998). The MnO content was low in both samples (average 0.13 wt.%), whereas the NiO average of 0.39 wt.% was close to the

TABLE 1. Gemological properties of peridot from Sardinia, Italy.

Color	Yellowish green
Pleochroism	Weak to moderate: α, β = green; γ = yellow-green
Optic character	Biaxial positive
Refractive indices	n_α = 1.650–1.652 n_β = 1.669–1.670 n_γ = 1.688–1.690
Birefringence	0.038–0.039
Specific gravity	3.32–3.36
UV fluorescence	Inert
Internal features	Partially healed fractures, liquid inclusions, "lily pad" inclusions, crystals, growth planes, traces of parallel twinning

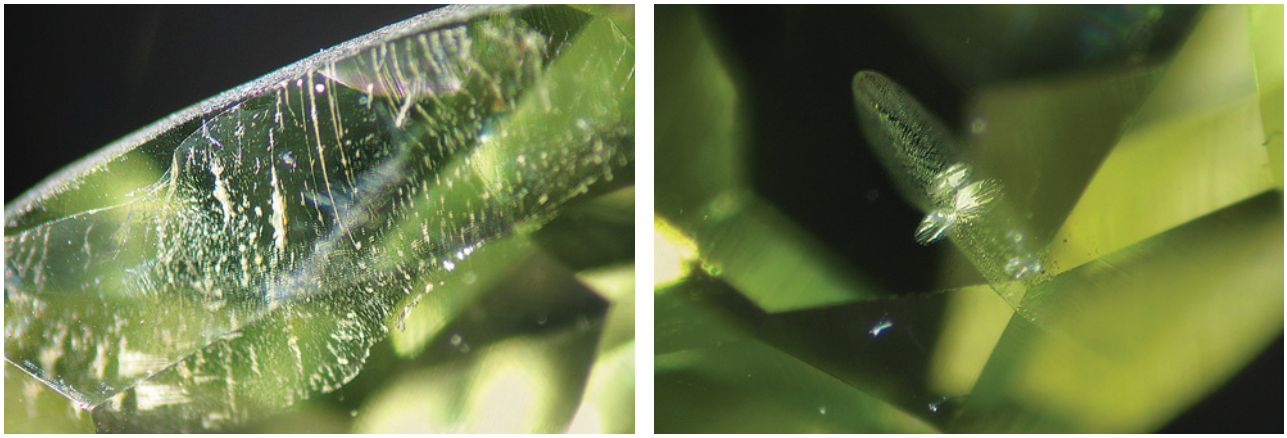

Figure 4. Sardinian peridot commonly contains partially healed fractures (left, magnified 30×). Decrepitation halo cleavages were present in some of the samples (right, magnified 45×). Photomicrographs by I. Adamo.

TABLE 2. Chemical composition of two peridots from Sardinia, Italy.

Chemical composition	Sample 1	Sample 2
Oxide (wt.%)[a]		
SiO_2	40.83	40.69
FeO	8.98	8.77
MgO	50.15	50.17
MnO	0.15	0.11
NiO	0.39	0.38
Total	100.50	100.12
Ions on the basis of 4 O atoms		
Si	0.994	0.993
Fe	0.183	0.179
Mg	1.819	1.825
Mn	0.003	0.002
Ni	0.008	0.007
Sum cations	3.007	3.006
Mol% end members[b]		
Fo	91	91
Fa	9	9
Trace elements (ppm)[c]		
Li	2.30	1.99
B	34.48	38.24
Na	95.67	73.21
Ca	548.50	453.94
Sc	4.87	6.35
Ti	10.51	8.81
V	4.18	4.15
Cr	157.51	181.35
Co	213.93	216.77
Zn	80.73	73.38

[a] *Obtained by electron microprobe analysis. Operating conditions: accelerating voltage = 15 kV, sample current = 15 nA, count time = 20 sec on peaks and 5 sec on background. Standards: forsterite (for Mg and Si), spessartine (for Mn and Fe), nickeline (for Ni), and kaersutite (for Na, K, and Ti). Na, K, and Ti were below the detection limit (0.01 wt.% oxide).*
[b] *Fo and Fa calculations omitted minor elements.*
[c] *Obtained by LA-ICP-MS; instrumental configuration and operating conditions are reported in Tiepolo et al. (2003). Rb, Sr, Y, Zr, Nb, Cs, Ba, and rare-earth elements were analyzed for but not detected.*

typical value of 0.40 wt.% reported in the literature for mantle olivine at ~$Fo_{90}Fa_{10}$ (Ishimaru and Arai, 2008). Our microprobe results are consistent with values estimated from the refractive indices, following Deer et al. (1982). Ca was the most abundant trace element found, followed in order of abundance by Co, Cr, Na, Zn, B, Ti, Sc, V, and Li, similar to the composition reported by Dupuy et al. (1987) for olivine from peridotite xenoliths of the Pozzomaggiore area.

The mid-IR spectra of both samples analyzed exhibited several absorption bands, located at about 982, 954, 885, 838, 605, 503, 469, and 415 cm^{-1} (figure 5). Their positions, known to be composition dependent (Duke and Stephens, 1964; Burns and Huggins, 1972), agreed with the Fe content of the samples.

The UV-Vis-NIR absorption spectra of our samples were characterized by a broad band at 1050 nm, with a shoulder at ~830 nm, in the near-IR range, and an increasing absorption toward the UV region (figure 6). Weak bands were also present at 403, 450, 473, 490, and 635 nm. The bands at 450,

Figure 5. Sardinian peridot's mid-IR spectrum in the 1200–400 cm^{-1} range is characterized by absorption bands with composition-dependent frequencies.

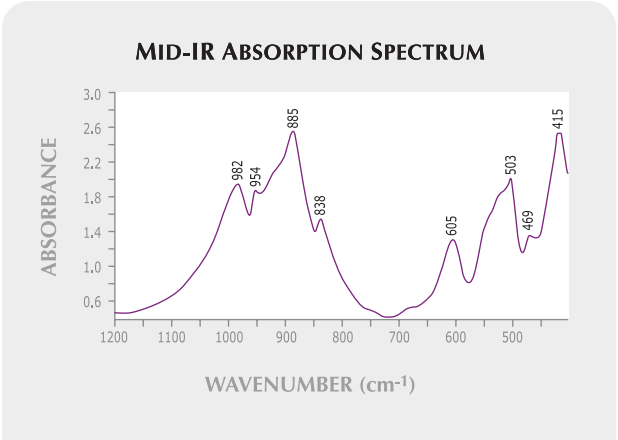

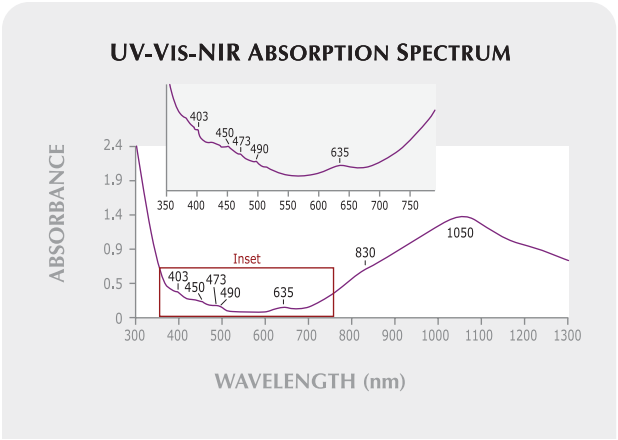

Figure 6. The UV-Vis-NIR spectrum of Sardinian peridot is mainly characterized by Fe^{2+} absorption features.

473, and 490 nm were visible with a hand spectroscope as well, with total absorption below ~440 nm. All these spectral features, which have been observed in peridot from other localities (see, e.g., Kammerling and Koivula, 1995; Führbach, 1998), are due to the presence of Fe^{2+} (Burns, 1970), confirming that iron is mainly responsible for the coloration. However, some absorption bands could also be contributed by the other chromophores in our samples, such as chromium (Rossman, 1988).

On the basis of the samples examined, the Sardinian peridot cannot be distinguished from peridot of other known localities.

Conclusions. The physical and chemical properties of peridot from near the town of Pozzomaggiore in northwestern Sardinia lie within the range of those reported for peridot specimens sampled worldwide. Thus far, because of the greater availability and larger sizes of peridot from other localities, the Sardinian material has remained within the Italian gemological community. The results of this study indicate that Sardinian peridot is worthy of attention as a gem material, and might have a market niche if properly mined and distributed.

ABOUT THE AUTHORS

Dr. Adamo (ilaria.adamo@unimi.it) is a postdoctoral fellow, and Drs. Bocchio and Pavese are professors of mineralogy, at the University of Milan, Italy. Dr. Prosperi is director of the Italian Gemological Institute laboratory in Milan.

ACKNOWLEDGMENTS

The authors are grateful to Dr. Massimo Tiepolo (CNR—Geosciences and Georesources Institute, Pavia, Italy) for LA-ICP-MS analyses, and Drs. Valentina Palanza and Giorgio Spinolo (University of Milan–Bicocca, Italy) for UV-Vis-NIR spectroscopy. The Geosciences and Geotechnologies Department of the University of Milan–Bicocca, and Dr. Vanda Rolandi, are acknowledged for assistance with taking photomicrographs. The manuscript benefited from the critical reviews of Drs. Lore Kiefert and Mary L. Johnson.

REFERENCES

Bianchi Potenza B., De Michele V., Liborio G., Nana G.P. (1989) Olivine from Val Malenco (Sondrio), Italy: A material of gemmological interest. *La Gemmologia*, Vol. 14, No. 3–4, pp. 23–33 [in Italian].

Bianchi Potenza B., De Michele V., Liborio G., Rizzo R. (1991) Olivines from Sardinia (Italy): A material of gemmological interest. *La Gemmologia*, Vol. 16, pp. 17–28 [in Italian].

Burns R.G. (1970) Crystal field spectra and evidence of cation ordering in olivine minerals. *American Mineralogist*, Vol. 55, No. 9/10, pp. 1608–1632.

Burns R.G., Huggins F.E. (1972) Cation determinative curves for Mg-Fe-Mn olivines from vibrational spectra. *American Mineralogist*, Vol. 57, No. 5/6, pp. 967–985.

Deer W.A., Howie R.A., Zussman J. (1982) Orthosilicates. *Rock-Forming Minerals*, Vol. 1A, 2nd ed. Longman, London, pp. 3–336.

Duke D.A., Stephens J.D. (1964) Infrared investigation of the olivine group minerals. *American Mineralogist*, Vol. 49, No. 9/10, pp. 1388–1406.

Dupuy C., Dostal J., Bodinier J.-L. (1987) Geochemistry of spinel peridotite inclusions in basalts from Sardinia. *Mineralogical Magazine*, Vol. 51, No. 362, pp. 561–568.

Führbach J.R. (1998) Peridot from the Black Rock Summit lava flow, Nye County, Nevada, USA. *Journal of Gemmology*, Vol. 26, No. 2, pp. 86–102.

Gübelin E. (1981) Zabargad: The ancient peridot island in the Red Sea. *G&G*, Vol. 17, No. 1, pp. 2–8.

Gunawardene M. (1985) Peridot from Ratnapura district, Sri Lanka. *Journal of Gemmology*, Vol. 19, No. 8, pp. 692–702.

Ishimaru S., Arai S. (2008) Nickel enrichment in mantle olivine beneath a volcanic front. *Contributions to Mineralogy and Petrology*, Vol. 156, No. 1, pp. 119–131.

Kane R.E. (2004) The creation of a magnificent suite of peridot jewelry: From the Himalayas to Fifth Avenue. *G&G*, Vol. 40, No. 4, pp. 288–302.

Kammerling R.C., Koivula J.I. (1995) An examination of peridot from Ethiopia. *Australian Gemmologist*, Vol. 19, No. 4, pp. 190–194.

Koivula J.I. (1981) San Carlos peridot. *G&G*, Vol. 17, No. 4, pp. 205–214.

Koivula J.I., Fryer C.W. (1986) The gemological characteristics of Chinese peridot. *G&G*, Vol. 22, No. 1, pp. 38–40.

Krzemnicki M.S., Groenenboom P. (2008) Gem News International: Colorless forsterite from Mogok, Myanmar. *G&G*, Vol. 44, No. 3, pp. 263–265.

Nassau K. (1994) Synthetic forsterite and synthetic peridot. *G&G*, Vol. 30, No. 2, pp. 102–108.

Rossman G.R. (1988) Optical spectroscopy. In F. C. Hawthorne, Ed., *Spectroscopic Methods in Mineralogy and Geology*, Reviews in Mineralogy, Vol. 18, Mineralogical Society of America, Washington, DC, pp. 207–254.

Shigley J.E., Dirlam D.M., Laurs B.M., Boehm E.W., Bosshart G., Larson W.F. (2000) Gem localities of the 1990s. *G&G*, Vol. 36, No. 4, pp. 292–335.

Shigley J.E., Dirlam D.M., Schmetzer K., Jobbins E.A. (1990) Gem localities of the 1980s. *G&G*, Vol. 26, No. 1, pp. 4–31.

Stockton C.M., Manson D.V. (1983) Peridot from Tanzania. *G&G*, Vol. 19, No. 2, pp. 103–107.

Tiepolo M., Bottazzi P., Palenzona M., Vannucci R. (2003) A laser probe coupled with ICP-double focusing sector-field mass spectrometer for in situ analysis of geological samples and U-Pb dating of zircon. *Canadian Mineralogist*, Vol. 41, No. 2, pp. 259–272.

2009 LAB NOTES

Editors
Thomas M. Moses and
Shane F. McClure
GIA Laboratory

DIAMOND

Bicolored Diamond

GIA only rarely encounters faceted diamonds that merit two color grades because of the presence of two distinct colored areas (e.g., Winter 1989 Lab Notes, p. 237). Recently, the New York laboratory had the chance to examine just such a stone, when the 1.79 ct rectangular step cut in figure 1 was submitted for grading. The diamond was assigned two color grades: Fancy Dark orangy brown and near-colorless, both confirmed to be of natural origin. The pronounced orangy brown color was confined to one half of the stone; a sharp boundary separated it from the near-colorless half. Some fractures extended across the boundary, but the (highly reflective) mineral inclusions indicative of a natural type Ib diamond were observed only in the orangy brown region. Both regions fluoresced moderate blue to long-wave ultraviolet radiation; however, the near-colorless region displayed stronger yellow fluorescence to short-wave UV than the orangy brown region. No phosphorescence was observed.

Figure 1. This unusual diamond (1.79 ct) proved to be a mixed-type IaA/Ib, with the two types corresponding to the near-colorless and Fancy Dark orangy brown regions, respectively.

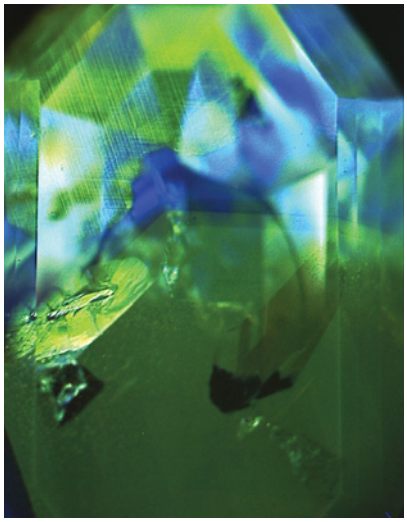

Figure 2. In the DiamondView, the diamond in figure 1 showed two distinct areas of growth, again corresponding to the different colors (near-colorless, top; orangy brown, bottom).

Infrared absorption spectra collected from the two regions also revealed clear differences. The near-colorless region showed a characteristic type IaA spectrum with a very low concentration of nitrogen and a very weak hydrogen-related absorption at 3107 cm^{-1}. In contrast, the orangy brown section showed the "irregular" features usually observed in natural yellow-orange diamonds colored by the lattice defect referred to as the "480 nm band" (e.g., Spring 2007 Lab Notes, pp. 49–50), as well as trace amounts of isolated nitrogen. In addition to the 3107 cm^{-1} peak, sharp lines at 3313, 3299, 3272, 3191, 3182, and 3144 cm^{-1} were recorded. All these observations indicated that the orangy brown color was due to the 480 nm band defect and isolated nitrogen. None of these features were detected in the infrared spectrum from the near-colorless region.

Most natural diamonds are type Ia, with the majority of nitrogen pres-

Editors' note: All items were written by staff members of the GIA Laboratory.

GEMS & GEMOLOGY, *Vol. 45, No. 2, pp. 134–140.*

ent as IaA aggregates. Type Ib singly substituted nitrogen rarely occurs in natural diamonds. When present in natural stones, it can cause an orange-yellow ("canary") color, occasionally with brownish or, rarely, reddish modifiers (e.g., Fall 2008 Lab Notes, pp. 255–256). This bicolored diamond contained both type Ia aggregated nitrogen and type Ib isolated nitrogen. While it is not unusual for a diamond to contain different forms of nitrogen aggregates, the sharply defined distribution of these defects with respect to the distinct color zones is unusual.

DiamondView imaging indicated that this stone may have crystallized during two different periods of growth and in two different growth environments (figure 2). Distinct differences in defect configuration between the two sections also suggest that the nitrogen aggregation process after diamond crystallization in the mantle may have been affected by factors (e.g., occurrence of other lattice defects) in addition to temperature and duration.

Erica Emerson, Paul Johnson, and Wai Win

"Black" Diamond with Deep Violet Color

Black diamonds are not uncommon in the gem trade, but naturally colored examples are relatively rare. Most black diamonds currently in the market are produced by the heating of fractured diamond to high temperatures in a vacuum to induce graphitization of the feathers and inclusions. The result is a nearly opaque stone that contains so much graphite that the diamond will conduct an electric current. In the past, treatments involving heavy-dose irradiation or irradiation plus annealing have also been used to produce black diamonds that are, in reality, very dark green when viewed with strong fiber-optic illumination. On occasion, we have seen other very dark colors, such as orange and blue. Naturally colored black diamonds typically contain abundant dark inclusions (sometimes graphite) that cause the stones to appear black when viewed face-up. Dense, dark-colored hydrogen clouds have also been reported as a natural cause of black color in diamonds (see Lab Notes: Fall 2008, p. 254; Spring 2009, pp. 54–55).

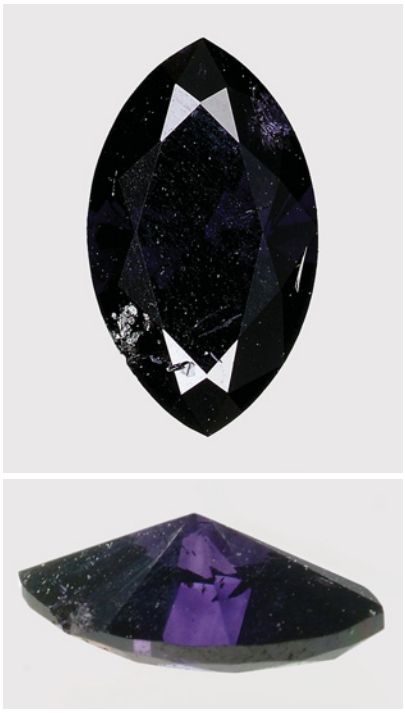

Figure 3. This 0.4 ct diamond was graded Fancy black. When viewed through the pavilion (bottom), the stone shows deep violet color.

Recently, we examined an interesting 0.4 ct marquise brilliant in the Carlsbad laboratory. The tone of the diamond was so dark when it was viewed face-up that the stone was graded Fancy black (figure 3, top). Table-down examination in a white tray, however, revealed that the body-color of the diamond was in fact a very deep violet (figure 3, bottom). This is remarkable because we had not previously seen a violet diamond with such a dark tone.

The diamond's infrared absorption spectrum (see the *G&G* Data Depository at www.gia.edu/gandg) showed that it was type Ia with very high concentrations of nitrogen and hydrogen impurities. As is typical of natural hydrogen-rich violet diamonds, the stone contained shallow etch pits and cavities, and fluoresced yellow to both long- and short-wave UV radiation (C. van der Bogert et al., "Gray-to-blue-to-violet hydrogen-rich diamonds from the Argyle mine, Australia," Spring 2009 *G&G*, pp. 20–37).

This marquise cut represents an extremely rare type of black diamond. It was issued a "natural" color origin report.

Christopher M. Breeding and Kimberly M. Rockwell

Carved Diamond Crucifix

It is not unusual to see carved diamonds submitted to the laboratory for identification. Over the years, they have come in many forms, such as carved fish (Spring 1983 Lab Notes, p. 73) or dice (Fall 1985 Lab Notes, p. 172). Carved diamonds with religious themes have also been submitted, including one fashioned as a Hamsa, symbolizing the protective hand of the creator (Fall 2001 Lab Notes, p. 214), and another cut in the image of the Buddha (Fall 1996 Gem News, p. 215). In reviewing our records, however, it does not appear that we have previously examined a crucifix such as the one shown in figure 4.

This piece consisted of a carving of Christ on a white metal cross; the Christ figure was determined to be diamond by Raman analysis. The grayish appearance of the diamond was due to numerous graphite-containing fractures. There was also evidence of the rough diamond crystal at one point on the carving, a corner of a trigon and some striations.

While many diamond carvings today are created using lasers, the client stated that this crucifix had been fashioned by a now-deceased Indian master carver using just hand tools. Only a skilled craftsman with exceptional patience could perform this type of carving, in this detail. To our knowledge, this diamond crucifix is unique.

Garry Du Toit

Figure 4. This unique crucifix (27.12 × 7.24 × 4.25 mm) consisted of a carved diamond set on a white metal cross.

Rare Type IIb Gray-Green Diamond

Natural type IIb diamonds are very rare. Among those we have examined in the GIA Laboratory, only about half showed a pure blue color, with the other half displaying an additional gray component due to varying levels of saturation. Two of the most famous type IIb diamonds, the Hope and the Wittelsbach, were color graded Fancy Deep grayish blue. Occasionally, brown diamonds with type IIb characteristics have also been seen (e.g., Summer 1977 Lab Notes, p. 307; Winter 2008 Lab Notes, pp. 364–365). Recently, staff members in the New York laboratory had the opportunity to examine an extremely rare type IIb diamond for which the dominant color was green.

The 5.41 ct marquise brilliant cut in figure 5 was color graded Fancy Dark gray-green. With magnification, the diamond showed only minor fractures reaching the surface. It had no reaction to either long- or short-wave UV radiation, which is characteristic of type IIb diamonds. When examined under the strong short-wave UV radiation of the DiamondView, it showed moderately strong blue florescence and weak red phosphorescence.

Infrared and photoluminescence spectroscopy revealed features observed in other natural type IIb diamonds. No evidence of artificial irradiation was detected. However, some unusual features were observed in the ultraviolet-visible–near infrared region (see the spectrum in the *G&G* Data Depository at www.gia.edu/gandg). In contrast to typical blue IIb diamonds, which often show a uniform increase in absorption from the UV toward the lower energy/longer wavelength side, this diamond displayed increasing absorption from ~500 nm toward the higher energy/shorter wavelength side. As a result, a transmission window was created from ~500 to 525 nm, leading to the dominant green hue. This increase in absorption from ~500 nm to shorter wavelengths is very likely caused by plastic deformation of the crystal lattice, a common feature in many natural diamonds.

Figure 5. This highly unusual Fancy Dark gray-green diamond (16.54 × 9.13 × 5.87 mm) proved to be type IIb.

A natural type IIb diamond with a dominant green hue is extremely rare. This unusual color is a result of the right combination of boron concentration, intensity of plastic deformation, and influence of the cut style.

Paul Johnson and Jason Darley

Unconventional Diamond Cuts

In March, the New York lab received a number of diamonds with unusual and unconventional facet distributions. They ranged in shape from round and cushion to pear and rectangular, but all had one feature in common: a fully faceted dome-shaped crown, with either no table at all or only a tiny "culet"-style facet in the center of the crown (figure 6). We were surprised to see these experimental cuts being applied to fairly large diamonds, most of them between 2 and 7 ct, as well as to diamonds of different colors.

Diamond cuts that lack a table facet invariably pose challenges for calculating overall dimensions and crown and pavilion angles, since typically the table serves as the basic reference plane against which these angles are measured. The cut description (shape and cutting style) also becomes more difficult, because none

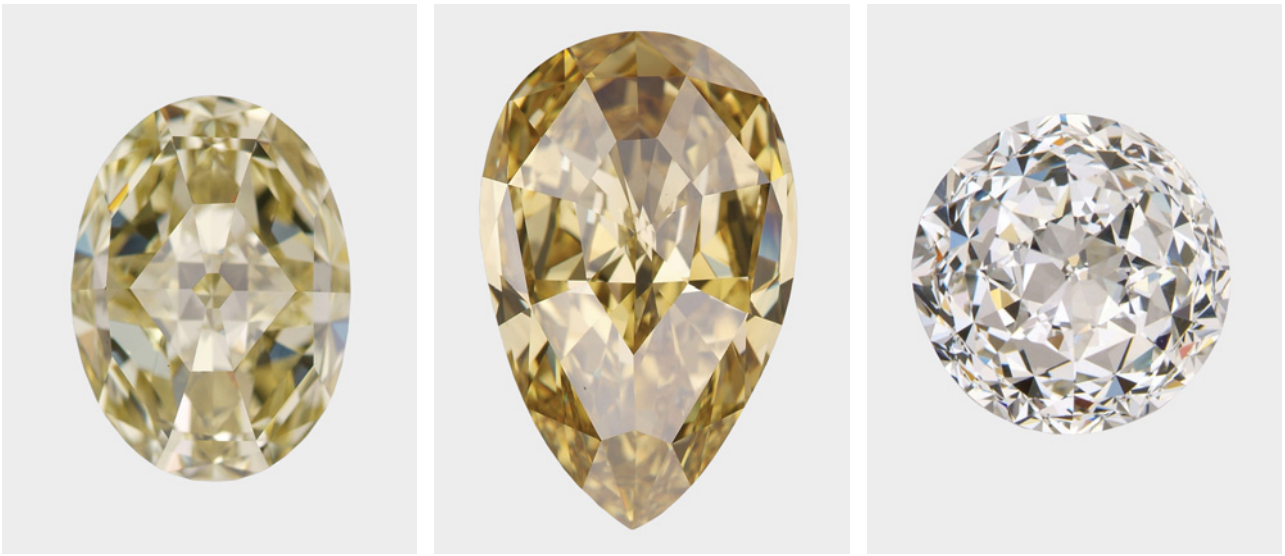

Figure 6. The Antwerp Twins cut is used on different shapes, such as those shown here (2.27, 4.17, and 2.08 ct). Note the fully faceted crown on each diamond and the small culet-style facet in the center of the yellow oval.

of the standard terms in the GIA lexicon fully explain these designs.

We were pleasantly surprised, however, to see that a number of the stones showed a balanced contrast pattern, which is very unusual for nontraditional diamond cuts (and even for the standard fancy cuts). When we compared one of the round shapes with a round brilliant cut (graded by GIA as "Excellent") of the same diameter, the latter appeared darker overall, with a less subtle contrast pattern. We have not analyzed the light path by ray tracing, but we believe that the fragmented specular reflection or glare of the additional crown facets, in combination with an efficient light-path migration inside the diamond, results in this brighter and more sparkly look.

We contacted the client and learned that this new cut has been patented and will be marketed as "Antwerp Twins." The name was chosen to reflect the cut's city of origin and the fact that these diamonds have two "dome-faceted" sides (crown and pavilion), as shown in figure 7.

While unconventional cuts can be challenging to measure, classify, and grade, we appreciate the opportunity to view the results of this type of innovation.

Ronnie Geurts

Figure 7. This side view of the 2.08 ct round-cut Antwerp Twins diamond in figure 6 shows the unusual "dome" faceting of the crown and pavilion.

Pink CVD SYNTHETIC DIAMOND

Gem-quality synthetic diamonds grown by chemical vapor deposition (CVD) were introduced to the jewelry market several years ago, but only a limited number of stones have been submitted to the GIA Laboratory for testing, and those have been near-colorless or brown (see, e.g., Lab Notes: Spring 2008, pp. 67–69; Summer 2008, pp. 158–159; Winter 2008, pp. 365–367). Recently, however, we identified a rare CVD synthetic diamond with a distinct pink coloration.

This 0.54 ct cushion cut, originally submitted for a colored diamond grading report, was graded Fancy brownish pink (figure 8). Although comparable to that seen in many natural counter-

Figure 8. This 0.54 ct Fancy brownish pink cushion cut (4.97 × 4.90 × 2.60 mm) was identified as a CVD synthetic diamond.

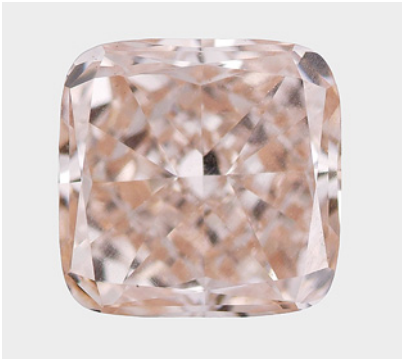

parts, this color is rare in synthetic diamonds. The color was evenly distributed throughout. With magnification, the gem displayed strong dislocation-related graining in a linear arrangement. Except for one black "pinpoint" (likely graphite), no other inclusions or fractures were observed.

We detected weak orange-yellow fluorescence to both long- and short-wave UV radiation. Under the ultra short-wave UV radiation of the DiamondView, the cushion cut displayed strong, uniform orange-red fluorescence, as well as moderately strong, evenly distributed yellow phosphorescence. We did not observe the irregularly distributed blue fluorescence seen in many CVD synthetic diamonds. In addition, the characteristically striated growth structure of CVD synthetics (P. Martineau et al., "Identification of synthetic diamond grown using chemical vapor deposition [CVD]," Spring 2004 *G&G*, pp. 2–25; W. Wang et al., "Latest-generation CVD-grown synthetic diamonds from Apollo Diamond Inc.," Winter 2007 *G&G*, pp. 294–312) was less pronounced.

Infrared absorption spectroscopy revealed typical type IIa features, with no detectable absorption in the one-phonon region. Noticeable features included weak but sharp absorptions at 7804, 5219, 4888, 4767, 4648, 4587, 4337, and 3123 cm^{-1}. These absorptions are specific to CVD synthetic diamonds and have been reported in other pink samples (Wang et al., 2007). Notable features in the UV-Vis-NIR absorption spectrum (collected at liquid-nitrogen temperature) included a moderately strong broad band centered at ~520 nm that is the main cause of pink coloration, a sharp absorption doublet at 736.5/736.9 nm from a Si-related defect, and sharp peaks at 753.0 and 850.2 nm (figure 9). Assignment of the 753.0 and 850.2 nm peaks is ambiguous, but they have not been reported in natural diamonds. The color of most natural pink diamonds is caused by a broad absorption band centered at ~550 nm, slightly higher than the 520 nm band in this CVD synthetic diamond.

The photoluminescence (PL) spectrum was dominated by emissions of N-V centers (ZPL at 574.9 nm and 637.0 nm) and a Si-related defect (736.5/736.9 nm doublet). In addition, numerous weak and sharp peaks were detected in the 460–530, 670–700, and 740–780 nm regions.

Pink CVD synthetic diamonds are rarely encountered in the gem market. Despite their many close similarities with natural pink diamonds, they can be identified reliably by spectroscopic features such as the H-related 3123 cm^{-1} absorption in the infrared region and the Si-related 736.5/736.9 nm doublet seen with both absorption and PL spectroscopy.

Wuyi Wang

Figure 9. The UV-Vis-NIR absorption spectrum of the CVD synthetic diamond in figure 8 displayed a moderately strong broad band centered at ~520 nm (not shown), which is the main cause of the pink coloration. In the NIR region (shown), a sharp absorption doublet at 736.5/736.9 nm from a Si-related defect was observed, along with sharp peaks at 753.0 and 850.2 nm.

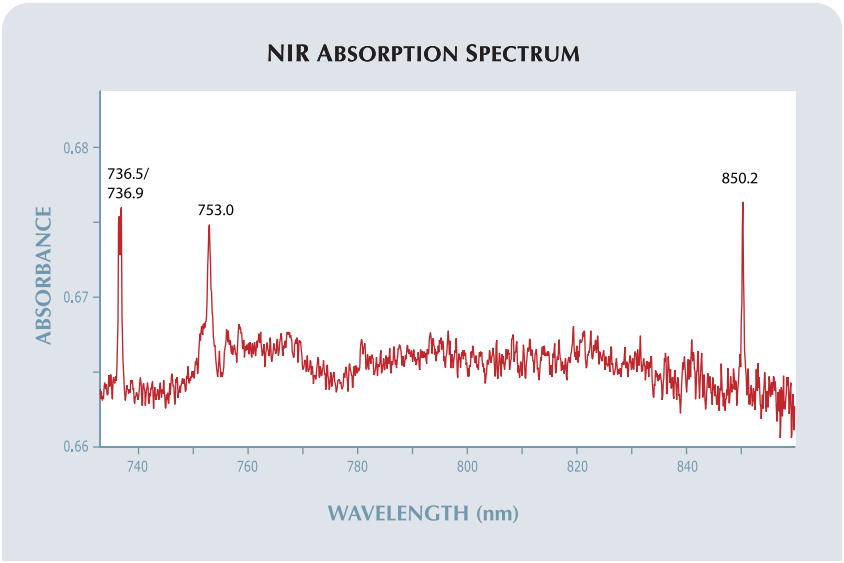

Rare Star PERIDOT

Cat's-eye peridot is rare, and star peridot is rarer still. Only two examples of the latter have been reported by the GIA Laboratory (Spring 1960 Highlights at the Gem Trade Lab in Los Angeles, p. 3; Summer 1987 Lab Notes, p. 106). The first was described as having a "well-defined four-rayed star reflected from tiny needlelike oriented inclusions," the second as having a star with two strong arms and two weaker arms. Recently, we were loaned for examination a 22.21 ct oval peridot with a uniformly distinct four-rayed star (figure 10).

Standard gemological testing confirmed the stated identity and gave the following properties: diaphaneity/color—transparent to semitransparent brownish green; spot RI—1.65; hydrostatic SG—3.32; and absorption bands observed at 453, 477, and 497 nm in the desk-model spectroscope. Despite the stone's relatively high transparency, examination with a gemological microscope revealed that it was filled with inclusions. "Fingerprints" and brown platelets were the most obvious internal features (figure 11, left). With fiber-optic illumination, oriented fine iridescent thin films, tiny needles, and short strings of reflective particles were observed

Figure 10. This unusual 22.21 ct peridot displayed a distinct four-rayed star.

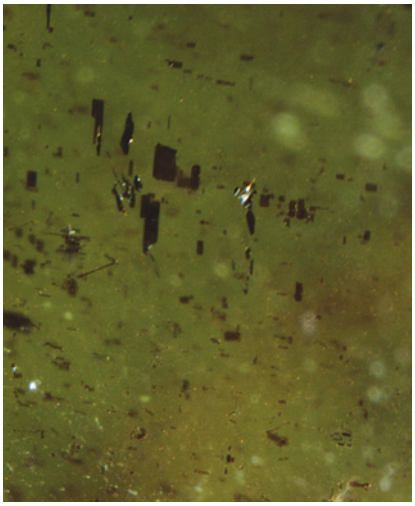

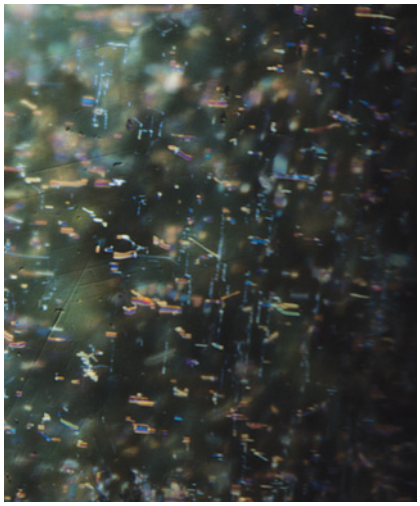

Figure 11. The star peridot had numerous inclusions of brown platelets (left, magnified 75×), though these could not be identified by Raman spectroscopy. Fiber-optic illumination revealed the abundant fine needles, thin films, and particle strings (right, magnified 85×) that caused the peridot's asterism.

throughout (figure 11, right); these abundant inclusions were the cause of the asterism. We performed Raman spectroscopy in an attempt to identify the platelets, but the spectra showed too much interference from the host peridot. As many of the platelets appeared brown in transmitted light, the possibilities include phlogopite, biotite, or even the ilmenite that was suggested for the peridot in the Summer 1987 Lab Note.

Accurately photographing the asterism proved quite challenging. As a result, the image in figure 10 is a composite of two digital photos—one focusing on the star, the other on the outline of the cabochon.

Donna Beaton

TOURMALINE with Silver and Gold Chatoyancy

In the Fall 2001 Lab Notes (pp. 218–219), we reported on a 1.51 ct star sapphire double cabochon that displayed a six-rayed "silvery" star on one side and a six-rayed "golden" star on the opposite side. This effect was due primarily to color zoning and the distance of the phenomenon-causing inclusions from the surface of the gem.

We recently had the opportunity to examine a cat's-eye tourmaline, said to be from Mozambique, that displayed a similar dual-color phenomenon. The 5.44 ct double cabochon (figure 12) was loaned for examination by Leon M. Agee (Agee Lapidary, Deer Park, Washington). The 12.01 × 10.59 × 5.46 mm gem displayed a strong silvery white eye on one side and a deep golden brown eye of almost equal intensity and sharpness on the other. When the cabochon was positioned between two light sources and then rotated, both eyes could be made to open and close dramatically, as would be expected in a fine cat's-eye chrysoberyl.

Microscopic examination revealed very strong color zoning, with a golden brownish yellow zone positioned parallel to a near-colorless achroite layer. The near-colorless side contained numerous very fine, uniformly distributed growth tubes of the sort required to produce strong chatoyancy. Reflections from these inclusions

Figure 12. Fashioned from tourmaline reportedly mined in Mozambique, this 5.44 ct double cabochon displays silver chatoyancy on one side and a golden eye on the other.

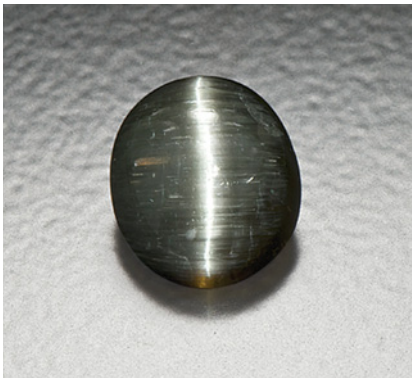

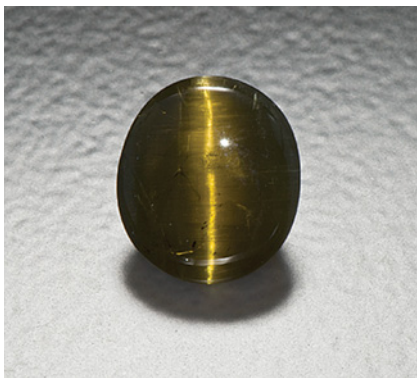

were responsible for the silvery white eye (figure 12, left). The growth tubes did not extend into the brownish yellow color-zoned area; instead this side gained its golden chatoyancy by reflections from the tubes in the near-colorless zone, which were projected through the color layer (figure 12, right).

This is the first time we have encountered a tourmaline displaying this dual-color phenomenon. The most logical way to set such a gem would be in a pendant with a simple bezel, leaving both sides exposed so that either cat's-eye could be enjoyed.

John I. Koivula

Eljen Treated TURQUOISE

In 2004, turquoise treated by a proprietary process developed by Eljen Stones (Reno, Nevada) first appeared on the market. According to the treater, Elven Jennings, his company has processed approximately 6 tonnes of rough material since then. In the last three years, about 1.4 million carats of finished goods were cut from ~1.4 tonnes of treated material. Mr. Jennings claims that his proprietary process transforms soft, chalky turquoise into harder material that takes a better polish with little or none of the weight gain he has experienced with stabilized turquoise, and without using any dyes or surface coatings.

We examined three rough samples (10.23–24.06 g) and five cabochons (5.93–12.62 ct; e.g., figure 13) of turquoise treated by the Eljen process and donated to GIA by Mr. Jennings and Dayton Simmons. The samples were greenish blue to blue, some with brown matrix. The polished stones had good to very good luster. Standard gemological testing revealed Spot RIs ranging from 1.60 to 1.62 and SG values of 2.27–2.85.

The IR spectra of all the samples resembled those of polymer-impregnated turquoise. We did not detect any evidence of Zachary treatment, such as the presence of abnormally high concentrations of potassium, with energy-dispersive X-ray fluorescence (EDXRF) spectroscopy. UV-Vis spectroscopy showed a standard turquoise spectrum and no evidence of dye. When exposed to long-wave UV radiation, all the samples fluoresced weak-to-moderate blue and several showed zoned fluorescence at the boundary between the turquoise and the interstitial matrix. The boundary region appeared strong yellow, while the turquoise itself fluoresced a moderate blue.

The samples had a Mohs hardness of 5–6, similar to high-quality (untreated) turquoise. By comparison, most polymer-impregnated turquoise can be indented with a metal probe (Mohs hardness of 5). Additionally, a hot point can char or blacken a polymer-impregnated stone and release an acrid odor; if wax is present, the stone may react by sweating. When the Eljen-treated samples were tested with a hot point, the turquoise gave no reaction or only a very weak one (some sweating was seen in samples with matrix).

Three of the cabochons tested had been cut and polished by one of us (PAO). During preforming on the coarse grinding wheel, the material seemed harder than typical stabilized turquoise. The good luster of the polished stones was probably due to the greater hardness. Although the matrix was slightly softer than the turquoise, these specimens had less undercutting than typical polymer-impregnated material. A thin (0.7 mm) sample was cut and polished to test the strength and behavior of thin edges during fashioning; the sample did not fracture and could be polished to a sharp edge.

The Eljen samples we studied were consistent with the treater's claims regarding hardness, durability, ease of cutting, and quality of polish. Although we did not attempt to identify the specific substance used in this treatment, IR spectroscopy did reveal the presence of a polymer. Therefore, the GIA Laboratory would identify this material as "impregnated natural turquoise."

Philip A. Owens and Sally Eaton-Magaña

Figure 13. These three cabochons (5.93–8.08 ct) were treated by the Eljen process and studied for this report.

PHOTO CREDITS
Jian Xin (Jae) Liao—1, 5, 6–8; Paul Johnson—2; Robison McMurtry—3; Shashikant Shah—4; Robert Weldon—10, 12, 13; Donna Beaton—11.

Thank You Donors

GIA appreciates gifts to its permanent collection, as well as gemstones, library materials, and other non-cash assets to be used in GIA's educational and research activities. These contributions help GIA further its public service mission while offering donors philanthropic benefits. We extend sincere thanks to all 2008 contributors.

If you are interested in making a donation and receiving tax benefits information, please contact Kimberly Vagner at (800) 421-7250, ext. 4150. From outside the U.S., call (760) 603-4150, fax (760) 603-4199, or e-mail kimberly.vagner@gia.edu.

Circle of Honor *

$100,000 and higher

The Aaron Group
Dr. Suman Agrawal
Almaza Jewelers (Ziad H. Noshie)
American Pearl Company
Amsterdam Sauer
Aurafin Oro America
Banks International Gemology, Inc. (Daniel & Bo Banks)
The Bell Group/Rio Grande
Allan Caplan
Chatham Created Gems, Inc. (Thomas H. Chatham)
PierLuigi Dalla Rovere
The De Beers Group
Debbie and Mark Ebert
Fabricjewelry
Dallas R. Hales
Dr. H. Tracy Hall
Dr. Gary R. and Barbara E. Hansen
James Y. Hung, M.D.
Inta Gems Inc.
J.O. Crystal Company, Inc. (Judith Osmer)
JewelAmerica, Inc. (Zvi & Rachel Wertheimer)
Kazanjian Bros, Inc.
KCB Natural Pearls (K.C. Bell)
William F. & Jeanne H. Larson
Honoring Betty H. Llewellyn
Stephen Lentz
Sophie Leu
Marshall and Janella Martin
Roz & Gene Meieran
Nancy B & Company
Kurt Nassau, Ph.D.
John & Laura Ramsey
R. Ed Romack
Art Sexauer
Shades of the Earth (Laura & Wayne Thompson)
Ambaji Shinde
S.H. Silver Company (Stephen & Eileen Silver)
Dr. Geoffrey A. Smith
D. Swarovski & Co
Touraine Family Trust
United States Pearl Co. (James & Venetia Peach)
Robert H. Vanderkay
Vicenza Fair

2008 Donors *

$50,000 to $99,999

Custom and Estate Jewels (Mona Lee Nesseth, G.G.)
Zultanite Gems LLC

$10,000 to $49,999

Cos Altobelli
American Gem Trade Association
Jerry Bearman
Dudley Blauwet
George Brooks
Fine Gems International (Robert E. Kane)
Scott Isslieb
Christopher L. Johnston
Dona Leicht
Dimitri Mantheakis
Mark Mauthner
Mayfield's
Donald & Ruth Milliken
Joe & Anne Ondraka
Tommy Wu
Mary E. Wurst, A.J.P.

$5,000 to $9,999

Colgem Coldiam (Israel and Oren Eliezri)
House of Onyx, Inc.
Alice Keller
Nick & Marguerita Michailidis
Robert J. Mulligan
Jose Guillermo Ortiz
Abe Suleman

$2,500 to $4,999

Barker & Co.
Scott Davies
Henry Dunay Designs
Syed Iftikhar Hussain
Patricia MB Gotthilf
Nanda Kulathunga
Michael LaBate II
Levisons Jewelry Inc.
Minerales y Metales del Oriente (Ramiro Rivero)
New Era Gems
Hussain Rezayee
Don & Barbara Waisman
Wild & Petsch Lapidaries

$1,000 to $2,499

Aurora Gems Inc. (Alan Bronstein)
Si & Ann Frazier
JOEB Enterprises (Edward Boehm)
Dr. Mary Johnson
Nature's Geometry (Brian Cook)
Nitin N. Pattni
Joseph A. Rott
Hal Stewart Jr.
Thomas & Lisa Trozzo

$500 to $999

Pirapan Belmont
Dr. Jaroslav Hyršl
Dr. A. J. A. (Bram) Janse
Kaufman Enterprises (Mark Kaufman)
Mary Healey's Fine Jewelry
Michael Beaudry, Inc.
microWorld of Gems (Kristi A. Koivula)
Moyer Jewelers, Inc.
David & Marydean Patterson
Platinum Guild International
Schramsberg Vineyards
Steve Stribling

Under $500

AmbarAzul, LCC
Zohreh Amini
Neda Baraati
Beth Bayard
Mr. & Mrs. James E. Bie
John Clyma, G.G.
Cornell's Jewelers
Fabrice Danet
Janet Davidi
Dawson's Fine Jewelry, Ltd. (Gregg W. Dawson)
Mahkmout Douman
Elegant Gems Ltd. (Brent Malgarin, G.G.)
Garrard & Co.
Gem & Jewelry Institute of Thailand
The Gem Trader (Bradley J. Payne)
Gems Foundation
Geological Survey of Namibia
Al Gilbertson
Aura Godoy
Harold Ha
David Anthony Hayes
Frank W. Heiser
Than Htike
Dr. Arunas Kleismantus
Kim Knox
Alf Larsson
Michele Macri
Mariana Magtaz
Marle's Gemstone Service
Mawingu Gems
Virginia Mizgiriene
Kazimeras Mizgiris
Oceanview Mines, LLC
Randy Joe Peach
Randy Price
Norb & Jean Rau
Restifo's Jewelry (Vincent A. Restifo)
Rio Tinto Diamonds
Sara Ritchie
Rockland Kenya Ltd.
Nora & Norma Stevens
Donald N. & Judith Stone Family
Bharat Thakarar
Greta Helene Wasserman/Goodman
M. Yoshizawa

*** All are cumulative donations**

GEM NEWS INTERNATIONAL 2009

COLORED STONES AND ORGANIC MATERIALS

Andradite from Erzincan, eastern Turkey. In October 2007, Alexandra Woodmansee (Rock Logic, Glencoe, Minnesota) informed GIA about a new find of demantoid in Turkey. She obtained some rough and cut samples of this material in time for the 2008 Tucson gem shows, and loaned several pieces to GIA for examination. Her supplier, Kerem Özütemiz (Truva Mining Ltd., Ankara, Turkey), also exhibited the garnet in Tucson, in both 2008 and 2009. He informed one of us (BML) that he owned the claim, located near Erzincan, 700 km east of Ankara. Due to the long and severe winters, he mines the area for only three months of the year (June through August). Using a pneumatic hammer and hand tools, he produced ~300 g of cuttable material in 2007, and ~120 g in 2008, although most was fairly small and included. To date, he has had about 20 stones cut (in Germany) that range from 0.5 to 1.2 ct, as well as an abundance of melee-sized material, totaling ~300 carats.

A gemological examination of 13 stones that Mrs. Woodmansee obtained from Mr. Özütemiz showed that six were andradite (including some demantoid) and seven were grossular (tsavorite). The presence of grossular could not be explained, but Mr. Özütemiz indicated that those stones may have been introduced into the parcel at the cutting factory. The six andradite samples (figure 1; 0.15–0.38 ct) were characterized for this report: color—orangy brown, brownish yellow, yellow-green, and yellowish green (the four yellow-green to yellowish green samples were demantoid); RI—>1.81; hydrostatic SG—3.82–3.93 (brown/yellow samples) and 4.17–4.43 (green samples); inert to both long- and short-wave UV radiation; and a 440 nm cutoff visible with the desk-model spectroscope. Microscopic examination revealed radiating curved fibrous needles with associated fractures (some of which contained a transparent filler or partially dried residue), blocky "fingerprints," and cubic growth zoning. Except for the high SG values, these properties are typical for andradite (e.g., M. O'Donoghue, Ed., *Gems*, 6th ed., Butterworth-Heinemann, Oxford, UK, 2006, pp. 206–210). In addition, the demantoid samples had distinct brown and green cubic color zoning, similar to that seen previously in two samples of andradite from Iran (see Spring 2007 Gem News International [GNI], pp. 65–67).

Quantitative chemical analysis of the six andradites was performed by electron microprobe at the University of Oklahoma (see details in the *G&G* Data Depository at www.gia.edu/gandg), and revealed the garnets contained 93.4–98.9 mol% andradite component. The demantoid samples contained significant levels of Cr (0.09–1.45 wt.% Cr_2O_3), while the orangy brown andradite had the highest Ti content (0.13 wt.% TiO_2).

Alethea Inns (alethea.inns@gia.edu)
GIA Laboratory, Carlsbad
Brendan M. Laurs

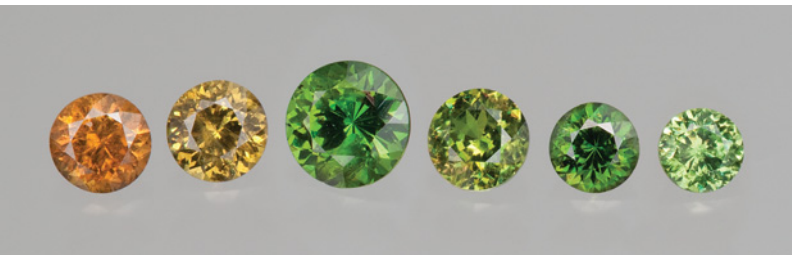

Figure 1. These andradites (0.15–0.38 ct) were reportedly cut from rough produced in eastern Turkey in mid-2007. Photo by Kevin Schumacher.

Editor's note: Interested contributors should send information and illustrations to Brendan Laurs at blaurs@gia.edu or GIA, The Robert Mouawad Campus, 5345 Armada Drive, Carlsbad, CA 92008. Original photos will be returned after consideration or publication.

GEMS & GEMOLOGY, Vol. 45, No. 2, pp. 142–155

Figure 2. This 5.63 ct star apatite was sold as aquamarine. Photo by K. Sieber.

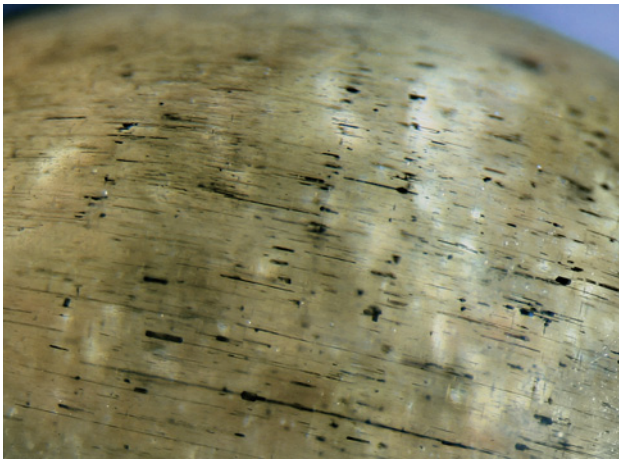

Figure 3. Parallel channel-like inclusions with irregular shapes and perpendicularly oriented tiny cracks are responsible for the asterism in the star apatite. Photomicrograph by K. Sieber; image width 8.8 mm.

Star apatite—first occurrence in the gem world. At the 2004 Tucson gem shows, one of these contributors (MPS) purchased a few stones represented as star aquamarine from an Indian company based in Bangkok. The gems reportedly came from India or Sri Lanka.

Although chatoyant aquamarine is relatively common, aquamarine with a four- or six-rayed star is very rare (see J. Hyršl, "Some new unusual cat's-eyes and star stones," *Journal of Gemmology*, Vol. 27, No. 8, 2001, pp. 456–460). Two of the so-called star aquamarines appeared somewhat different, prompting further examination.

The two medium brownish green cabochons (5.63 and 6.65 ct) were examined at the German Gemmological Institute (EPI). Under spot illumination, they showed four distinct rays (e.g., figure 2). Standard gemological testing gave a spot RI of 1.64 and an SG of 3.18. Neither reading fit aquamarine, and the Mohs hardness of 5 (tested on the back of the cabochons) showed that they were softer than beryl. With the handheld spectroscope, a clear absorption doublet in the yellow region was visible. In the polariscope, the specimens were transparent enough to show a uniaxial optic figure. Colorless to yellowish green dichroism was fairly strong. These properties identified the two samples as apatite.

With magnification, it was apparent that a parallel network of narrow, irregularly shaped tubes and perpendicularly oriented tiny cracks were responsible for the asterism (figure 3). To further characterize these unusual apatites, energy-dispersive X-ray fluorescence spectroscopy (EDXRF) and Raman analyses were performed on both stones by the SSEF Swiss Gemmological Institute in Basel. EDXRF detected major amounts of Ca and P, with traces of Cl. This result pointed to apatite-(CaCl), formerly known as *chlorapatite*. Raman analysis confirmed the identification, with distinct peaks at 1058, 1030, 963, 579, and 446 cm^{-1} that matched the reference spectrum for apatite.

Apatite occurs in a wide range of colors, such as white, yellow, green, blue, brown, violet, and black. While cat's-eye apatite has been found in Brazil, India, Russia, Sri Lanka, and Tanzania, to the best of our knowledge star apatite has not been previously reported.

Martin P. Steinbach (gstargems@aol.com)
Steinbach–Gems with a Star
Idar-Oberstein, Germany

Bernhard Bruder
German Gemmological Institute
Ohlsbach, Germany

A chalcedony-opal cameo with remarkable inclusions. A cameo believed to be carnelian (red-orange chalcedony) was borrowed from the Dobrée Archaeological Museum in Nantes, France, for examination. The ~2.7 × 2.3 cm gem, set in a gold tie pin, depicted the right profile of a bearded male figure with a headband (figure 4). Little is known of the cameo's history except that it appeared to be of classical Greek manufacture. The headband and background were brown in reflected light, while the rest of the carving was predominantly dark orange.

The RI, measured with some difficulty using the spot method, ranged from 1.53 to 1.55, a little low for chalcedony; the SG could not be determined because of the mounting. The cameo luminesced very weak greenish yellow to long-wave UV radiation and bright yellowish green to short-wave UV. While pure chalcedony is normally inert, this luminescence behavior is typical of uranium-bearing common opal, raising the possibility of a chalcedony-opal mixture.

To test this hypothesis, we obtained a Raman spectrum (using a Bruker RFS 100 Fourier-transform spectrometer) and compared it to that of a reference gray chalcedony. The positions of the sharp peaks were identical, but there was a broad underlying signal below the typical chalcedony peaks in the cameo spectrum. Subtracting the reference spectrum from the cameo pattern resulted in a signal with a broad band around 335 cm^{-1} and an even broader one around 3000 cm^{-1}, consistent with

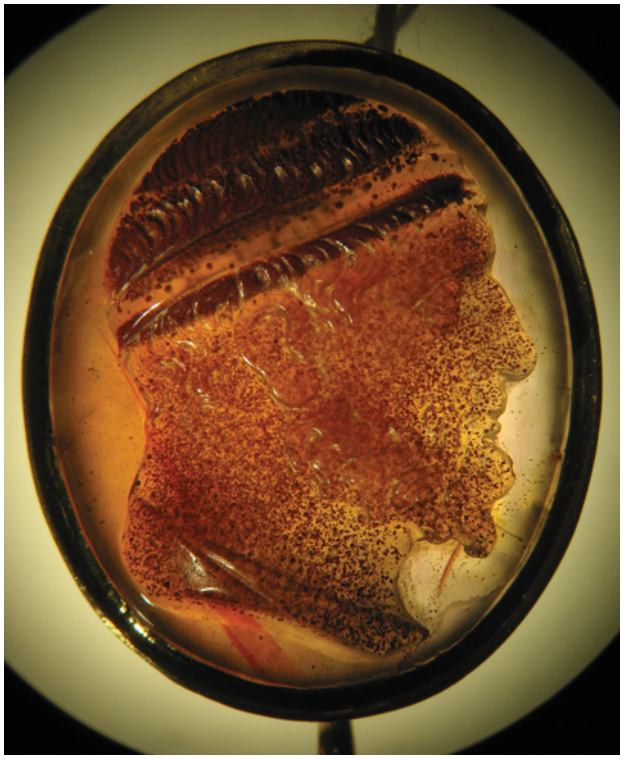

Figure 4. In transmitted light, this unusual chalcedony-opal cameo (~2.7 × 2.3 cm; Dobrée Archaeological Museum no. 927.1.1438) shows banding due to the variable density of near-spherical red-orange inclusions, probably hematite. Photomicrograph by E. Fritsch.

opal-CT. We performed additional luminescence analysis with a Jobin-Yvon Fluorolog 3 spectrometer with 315 nm excitation, and compared the cameo's emission spectrum to reference luminescence spectra for opal. The spectra had similar shape and peak positions at about 415 nm (intrinsic opal luminescence, never observed in chalcedony), 504, 524, 548, and 574 nm (uranyl emission in opal), further indication that the luminescence indeed originated from an opal component (E. Fritsch et al., "Luminescence of oxidized porous silicon: Surface-induced emissions from disordered silica micro- to nano-textures," *Journal of Applied Physics*, Vol. 90, No. 9, 2001, pp. 4777–4782).

We therefore believe that the cameo was fashioned from a chalcedony-opal mixture, primarily the former, with the small opal component responsible for the luminescence behavior and slightly lower RI as well as the extra Raman signal. Chalcedony with similar luminescence is known from Mexico, but whether such material is actually a mixture with opal has not been determined (John I. Koivula, pers. comm., 2009).

The cameo was also remarkable for its inclusions. Although it was not apparent in reflected light, transmitted light demonstrated that the color zoning was due to variations in the density of red-orange, near-spherical inclusions (again, see figure 4). These likely consisted of hematite (see E. J. Gübelin and J. I. Koivula, *Photoatlas of Inclusions in Gemstones*, Vol. 2, Opinio Publishers, Basel, Switzerland, 2005, p. 360). They ranged from 0.01 to 0.4 mm in diameter, and some were striated like circled pearls. A few of the inclusions were flat with an empty core, causing them to appear crescent-shaped or circular (figure 5). Considering the size range of these inclusions, the hematite that formed them must have been quite finely divided, as shown by their red-orange (rather than metallic gray) appearance. The headband and background of the cameo contained very few inclusions, while the face and especially the hair layers were densely populated with them. A coloration by hematite inclusions is consistent with the carnelian-like appearance of the cameo.

Emmanuel Fritsch
Clothilde Feydieu and Julie Fauran
Bordeaux University, France
Yves Lulzac
Centre de Recherche Gemmologique, Nantes, France
Benjamin Rondeau
CNRS Team 6112, Laboratoire de Planétologie et Géodynamique, University of Nantes, France

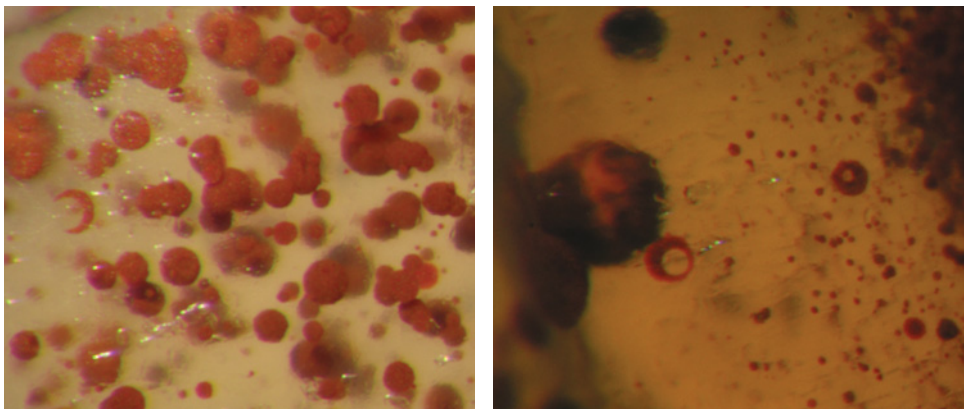

Figure 5. A few of the inclusions in the cameo are flat and lack a core, giving rise to a crescent-shaped (left) or circular appearance (right). Photomicrographs by E. Fritsch; magnified 180×.

Citrine from Andongologo, Madagascar. Deposits of natural citrine are not common, and most citrine is produced by heat treating amethyst. A new source of untreated citrine has been found in central Madagascar, at Andongologo, located 24 km southwest of Antsirabe at coordinates 19°59.510′ S, 46°50.884′ E. The deposit has been mined for rock crystal for a few years, but in February 2009 some new veins were found that contain citrine and smoky quartz. Using simple hand tools, 14 miners have excavated tunnels and shafts down to 15 m. So far, 300 kg of citrine have been produced.

The citrine is mined from quartz veins hosted by weathered Precambrian quartzites. The veins range up to 0.5 m wide, and locally contain cavities filled with prismatic crystals of smoky quartz and citrine. The crystals are well formed (some are doubly terminated) and range up to 30 cm long (e.g., figure 6). The crystal terminations and rims are smoky, whereas their core is brownish yellow. To this contributor's knowledge, quartz is the only mineral found in the cavities.

Much of the citrine is transparent, and this contributor is aware of faceted stones ranging from 30 to 385 ct from ~4,000 carats that have been cut. The color of the faceted stones varies from light-to-medium pale yellow to brownish yellow (e.g., figure 7). The material shows moderate dichroism, and RI measurements of 17 stones gave values of 1.544–1.553 (birefringence 0.009). No inclusions were seen in the cut samples examined.

Historically, the main source of citrine in Madagascar is located 110 km west of Antsirabe, on top of Bevitsika ("lots of ants") Mountain. The Bevitsika citrine is also hosted by quartz veins in Precambrian quartzites. For at least 20 years, large amounts of natural citrine and rock crystal have been mined there sporadically during the dry season (May to November). However, there has been no production at Bevitsika for the past two years.

Fabrice Danet (fabdanet@moov.mg)
Style Gems, Antsirabe, Madagascar

Figure 7. These faceted citrines from Andongologo weigh 83 and 138 ct. Photo by F. Danet.

Figure 6. The quartz from Andongologo (here, up to 25 cm long) typically has smoky outer zones and citrine cores. Some of the crystals are doubly terminated, as shown in the inset (30 cm long). Photos by F. Danet.

"Sugarcane Emerald" from Brazil. In 2007, some unusual beryl crystals (e.g., figure 8) were found during mining operations in northern Bahia State, Brazil, by John Papajohn and Cesar Menezes of JP International Rough Mining & Colored Gemstones Inc. (Campo Formoso, Bahia). The find occurred at 180 m depth and yielded ~1 tonne of material, including 600 kg of well-formed crystals. The company's five mines in the mountains of Serra de Jacobina at Carnaíba near Campo Formoso had previously produced mostly dark-colored emeralds and mineral specimens in mica schist. However, the material from this find was translucent bluish green, with white mottled veins and a bamboo stalk–like appearance. Many of the well-developed

Figure 8. These crystals of "Sugarcane Emerald" (104 and 77.6 g) were recovered from Bahia State, Brazil. Photo by H. Serras-Herman.

Figure 9. Some of the fashioned "Sugarcane Emerald" has been set into distinctive jewelry pieces such as this necklace, which features an 88.0 ct polished slice and 430.0 carats of beads, along with accents of black opal and fire opal. Designed, created, and photographed by H. Serras-Herman.

hexagonal crystals also showed pronounced whitish bands of hexagonal zoning. At first glance, the material resembled amazonite, but it had a higher polish luster due to beryl's greater hardness.

JP International had most of the material fashioned into beads, as well as polished slices and carvings. Together with some crystal specimens, they debuted the gem material at the 2008 Tucson gem shows under the trade name "Sugarcane Emerald." This contributor purchased some of the stones and incorporated them into a jewelry collection introduced at the 2009 Tucson shows (e.g., figure 9).

Although JP International has continued prospecting for similar material, so far no more of this beryl has been found. For now, the "Sugarcane Emerald" can be considered an oddity of nature, one of those rare gem occurrences perhaps never to be seen again.

Helen Serras-Herman (helen@gemartcenter.com)
Rio Rico, Arizona

Orange kyanite from Tanzania. Kyanite derives its name from the Greek word for blue, due to its typical color. Gem-quality green kyanite has also been seen (e.g., Winter 2001 GNI, pp. 337–338), and colorless or yellow varieties have occasionally been faceted. Recently, however, orange kyanite has appeared in the gem market. The material was mined at Loliondo, Tanzania, near the area that recently produced fine crystals of spessartine (see, e.g., Spring 2008 GNI, pp. 76–78).

Brad Payne of The Gem Trader (Surprise, Arizona) loaned GIA three faceted specimens (0.63–1.26 ct; figure 10) of this kyanite for examination. Additionally, one of these contributors (GRR) obtained two crystal fragments of orange kyanite, one from Loliondo and the other from Mautia Hill, Kongwa, also in Tanzania (again, see figure 10). The latter sample was procured in the late 1980s; both were polished on parallel sides for spectroscopy.

Examination of the cut stones gave the following properties: color—medium yellow-orange to yellowish orange; pleochroism—weak yellow-orange and yellowish orange; RI—n_α = 1.718 and n_γ = 1.734–1.735; birefringence—0.016–0.017; optic sign—biaxial negative; hydrostatic SG—3.69–3.73; no UV fluorescence or Chelsea filter reaction; and a line observed at ~550 nm, plus a band at ~460–500 nm, seen with the desk-model spectroscope. The RI and SG values were similar to the upper ranges for blue/green kyanite given by M. O'Donoghue, Ed. (*Gems*, 6th ed., Butterworth-Heinemann, Oxford, UK, 2006, p. 422). All of the observations are also consistent with those presented by J.-M. Arlabosse for orange kyanite from Loliondo ("Kyanite orange Tanzanie," Gemmologie FlashData, No. 35, www.geminterest.com/articlist.php, Dec. 9, 2008). Microscopic examination of the cut stones revealed cleavage fractures, globular-to-angular brown rutile crystals, rounded colorless high-relief zircon crystals, and globular colorless low-relief crystals of mica (probably muscovite) and quartz—all identified by Raman analysis.

The two polished fragments gave the following properties: color—light yellow-orange (Mautia Hill) and medium yellowish orange (Loliondo); and no UV fluorescence or Chelsea filter reaction. With the desk-model spectroscope,

Figure 10. These kyanites from Tanzania have a distinctive orange color. The faceted stones (0.63–1.26 ct) are from Loliondo, and the polished fragments are from Loliondo (left, no. CIT15871) and Mautia Hill (bottom center, no. GRR544). Photo by Kevin Schumacher.

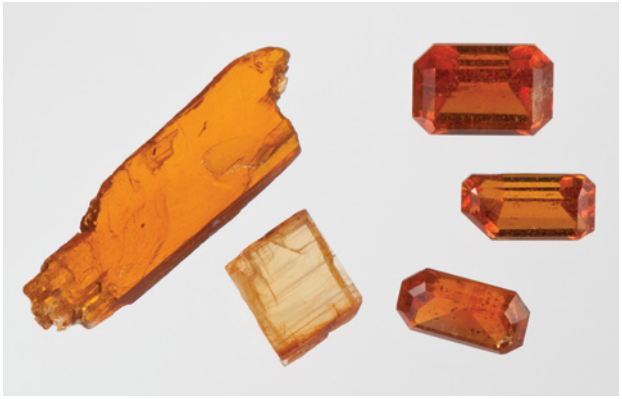

a line was observed in the Loliondo sample at ~550 nm, with extinction below ~500 and above ~680 nm; no features were seen in the Mautia Hill sample. Rutile, zircon, (both confirmed by Raman analysis) and mica/quartz inclusions were also noted in the Loliondo sample.

UV-Vis-NIR spectroscopy of the polished fragments (figure 11) indicated that their orange color resulted from a transmission window with minima at approximately 645–755 nm; the adjacent absorption bands arise from Mn^{3+}. The Mautia Hill sample—which displayed a lighter, yellower bodycolor—showed a similar, but lower-amplitude, absorbance trace compared to the Loliondo sample. Narrow peaks at ~380, 433, and 447 nm in the Mautia Hill spectra were due to Fe^{3+}.

Laser ablation–inductively coupled plasma–mass spectrometry (LA-ICP-MS) analysis of both slabs by GIA research scientist Dr. Mike Breeding confirmed manganese as the cause of color. The Mn concentration of the Loliondo sample (CIT15871) was ~10 times higher than that of the Mautia Hill specimen (GRR544; table 1). Iron content was similar in the two samples, but slightly greater in the one from Loliondo. A third orange kyanite—no. GNI555, a light-to-medium yellowish orange Loliondo crystal donated to GIA by Werner Radl (Mawingu Gems, Niederwörresbach, Germany)—was also analyzed. The concentrations of all elements except Fe in this specimen fell between those for Mautia Hill and the Loliondo sample.

In the mid-1970s, small crystals of orange-yellow kyanite were synthesized in experiments using Mn^{3+} in the form of Mn_2O_3 in conjunction with SiO_2 and gem-quality andalusite (a polymorph of kyanite; I. Abs-Wurmbach and K. Langer, "Synthetic Mn^{3+}-kyanite and viridine, $[Al_{2-x}Mn^{3+}_x]SiO_5$, in the system Al_2O_3–MnO–MnO_2–SiO_2," *Contributions to Mineralogy and Petrology*, Vol. 49, 1975, pp. 21–38). That research supports our observations, which indicate that Mn^{3+} is the chromophore responsible for the orange color of these Tanzanian kyanites.

Karen M. Chadwick (karen.chadwick@gia.edu)
GIA Laboratory, Carlsbad
George R. Rossman
California Institute of Technology
Pasadena, California

TABLE 1. Average trace-element composition by LA-ICP-MS of orange kyanite from Tanzania.[a]

Sample	Locality	Mg	Ti	Cr	Mn	Fe	Zn	Ga
CIT15871	Loliondo	72.9	4.2	35.8	1893	3547	bdl	8.8
GNI555	Loliondo	62.1	8.5	22.2	655	4167	bdl	11.1
GRR544	Mautia Hill	29.4	12.4	bdl	190	3207	2.0	13.6

[a] *Values expressed in parts per million by weight, and collected using a Thermo X-Series II ICP-MS equipped with a New Wave 213 nm laser-ablation system. Parameters used were 40 µm spot size, 7 Hz repetition rate, and ~10 J/cm² laser fluence. The values represent the average of three spots (CIT15871 and GRR544) or two spots (GNI555). Abbreviation: bdl = below detection limit.*

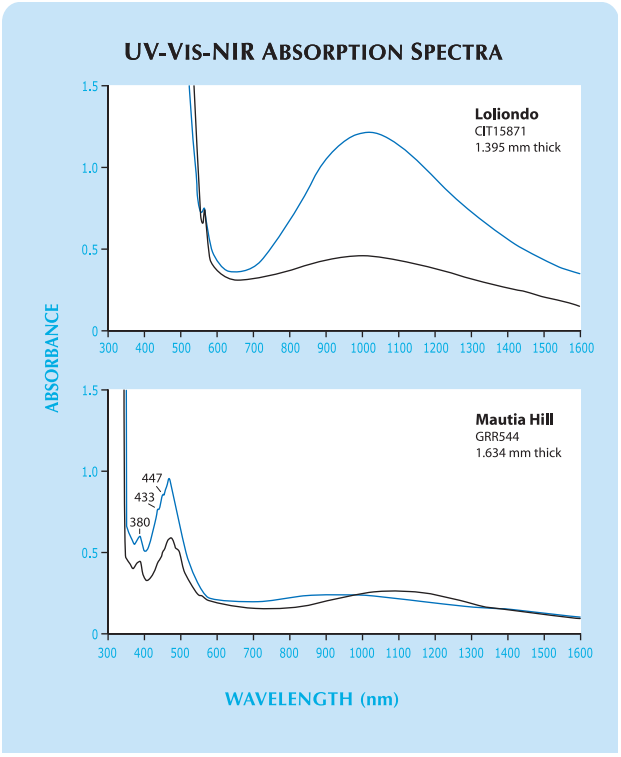

Figure 11. UV-Vis-NIR spectra of the polished fragments of orange kyanite show a transmission window at ~645–755 nm, which accounts for their orange color. The window is defined by Mn^{3+} absorption bands on either side. Also present in the Mautia Hill sample are some minor features at ~380, 433, and 447 nm due to Fe^{3+}. The two spectra display two polarizations that correspond, approximately, to the Y = β (black lines) and Z = γ (blue lines) orientations.

Rare optical phenomenon in play-of-color opal. We recently examined a 4.43 ct oval cabochon of translucent white play-of-color opal provided by Francesco Mazzero (Opalinda, Paris, France). The stone came from the new Wegel Tena deposit in the Welo Province of Ethiopia (see Spring 2009 GNI, pp. 59–60). Typical play-of-color opal displays patches of pure spectral colors that result from the diffraction of visible light by the network of silica spheres (E. Fritsch and G. R. Rossman, "An update on colors in gems, part 3: Colors caused by band gaps and physical phenomena," Summer 1988 *G&G*, pp. 81–102). This sample, however, displayed several discrete spots of spectral colors that were distributed across the entire stone (figure 12). The effect was seen most clearly when a point (e.g., fiber optic) light source was used; the colored spots moved together around the stone as the light source changed position. This phenomenon is best seen in a video, available at http://gemnantes.fr/recherche/opale/index.php#reciproque. Even more interesting, the color of each spot progressively changed (e.g., from yellow to red) with the position of the illumination—sometimes very slightly, sometimes noticeably. Since the cabochon was poorly cut, the spots

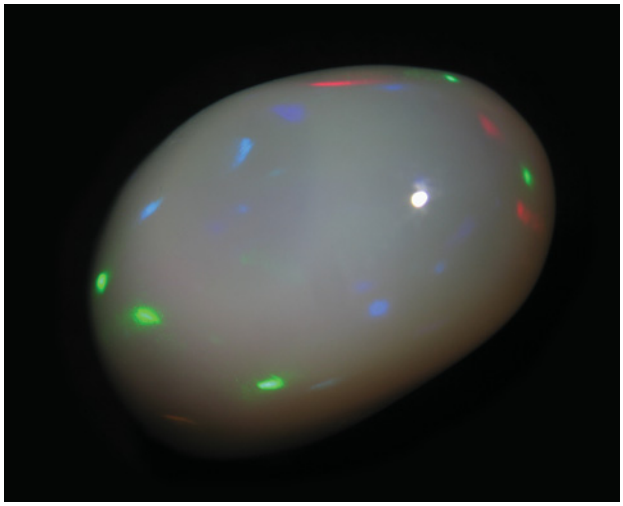

Figure 12. Rather than showing immobile patches of pure spectral colors, this unusual opal cabochon (15 × 7.5 × 6 mm) diffracts visible light as colored spots moving with the point light source (the source's reflection is visible as the white spot). Photo by B. Rondeau.

sometimes stretched into small patches over a flatter area.

According to diffraction theory, radiation diffracting on a perfect network should produce spots. Hence, for a perfect network of silica spheres constituting opal, one would expect diffraction of visible light to produce discrete colored spots—which is what we observed in this sample. For those interested in physics, this corresponds to the physical expression of the reciprocal lattice (see, e.g., http://en.wikipedia.org/wiki/reciprocal_lattice). Typically, however, the opal network is not regular enough to show this effect; instead, the spots spread out to become color patches. Each patch corresponds to small domains in which a single spot is stretched through deformation or irregularities in the network, and therefore represents an "average" direction of diffraction. The orientation of the network varies from one patch to the next. No matter what an opal looks like, the rules of diffraction remain the same.

The extraordinary optical phenomenon we report here is very rarely observed. It implies a perfect network extending throughout the entire stone (that is, over a centimeter), and hence a very regular stacking of spheres over a relatively large distance. This is only possible in a formation environment that is geologically very quiet.

Emmanuel Fritsch and Benjamin Rondeau

Figure 13. These attractive variously colored cultured pearls (up to 14.7 mm in diameter) are from Vanua Levu in Fiji. Courtesy of Gerhard Hahn Pearl AG.

Cultured pearls from Fiji. At the BaselWorld Watch and Jewellery Show in April 2008, Gerhard Hahn Pearl AG (Düsseldorf, Germany) displayed some variously colored cultured pearls (figure 13) from a relatively new source, the South Pacific island nation of Fiji. So far, Fijian production has been limited, coming from two pearl farms located ~60 km apart on the island of Vanua Levu, in Savusavu Bay and Buca Bay. The cultured pearls are harvested from *Pinctada margaritifera* oysters, which are grown from spat collected in waters of the Savusavu area. The oysters are implanted with round bead nuclei (minimum 7.5 mm in diameter) and harvested 12–18 months later. They average 10.8 mm in diameter at first harvest (i.e., before reinsertion of beads for a second harvest). They mostly range from light bluish green to the popular "chocolate" brown, and Gerhard Hahn Pearl AG indicated that their colors do not result from treatment; only standard post-harvest processing such as cleaning is performed.

Up to 65% of the production show lighter colors than those that are typical of *P. margaritifera* cultured pearls. Since some resemble bleached *P. margaritifera* products (see, e.g., Summer 2008 Lab Notes, pp. 159–160), Gerhard Hahn Pearl AG donated 20 samples to GIA for documentation purposes, and they were studied at the New York Laboratory by Akira Hyatt and Dr. Wuyi Wang.

Based on GIA's examination over the years of many thousands of *P. margaritifera* cultured pearls, the broad range of bodycolors in this relatively small sample set was remarkable. The hues ranged from blue and green (cool hues) to orange and yellow (warm hues), with many samples showing strong saturation. *P. margaritifera* cultured pearls typically occur in the cooler hues, with darker tones showing higher saturation and lighter tones showing lower saturation. In contrast, those from the *Pinctada maxima* oyster typically show warm hues, with higher saturation in the lighter tones and lower saturation in the darker tones. The Fijian cultured pearls were split between warm and cool hues, and many of the cool hues exhibited a lighter tone, often with relatively high saturation. Some also exhibited colors generally seen in *P. maxima* cultured pearls (i.e., yellows, but with darker tone and stronger saturation), while others resembled treated "chocolate" pearls (orangy/pinkish browns) from *P. margaritifera*. (Note that in lower saturations, warm hues appear brown or brownish, while cool hues appear gray or grayish.) The

Figure 14. The shells of the P. margaritifera *oysters that are used to produce the Fijian cultured pearls show a diversity of colors. Courtesy of J. Hunter Pearls.*

diverse color range of the cultured pearls is also seen in the host *P. margaritifera* shells (e.g., figure 14).

UV-Vis-NIR reflectance spectra are given in figure 15 for four categories of the Fijian cultured pearls: brown (five samples), yellow (seven), green (five), and blue (three). The brown samples showed decreases in reflectance due to absorptions at 290, 495, and 700 nm—believed to be related to organic pigments—that were superimposed on a nearly flat background. These spectral features are similar to those of naturally colored brown Tahitian cultured pearls. The absorptions at 290, 495, and 700 nm were also distinct for the yellow samples, but the overall spectra were sloped toward lower wavelengths. The absorptions at 495 and 700 nm were very weak in the green samples, but the 295 nm band was consistently strong. In addition, the slope of the spectra in the 400–700 nm region for the green samples was opposite that of the yellow samples. In the blue cultured pearls, the three bands related to organic pigments were clearly observed, and in general the reflectance increased with decreasing wavelength. The spectroscopic data indicate that all of the tested cultured pearls were of natural color. X-radiography showed that they were bead cultured, as represented by Gerhard Hahn Pearl AG.

Figure 15. UV-Vis-NIR reflectance spectroscopy of brown, yellow, green, and blue cultured pearls from Fiji indicated that all these colors are natural. Photos by Sood Oil Chia.

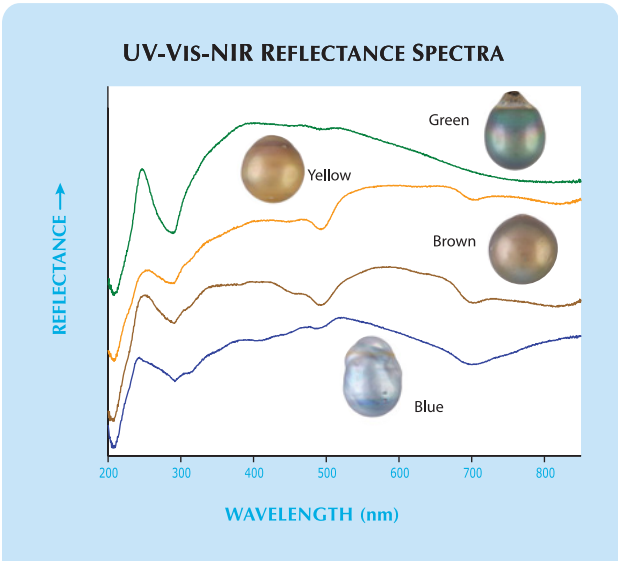

The Fijian farms together produce ~40,000 cultured pearls (or 125 kg) yearly and have ~100,000 oysters under cultivation. The farms are operated by the J. Hunter Pearls Fiji Pearling Conservancy under the country's Environmental Code of Practice, to ensure that any negative environmental impact is minimized.

Marisa Zachovay (marisa@hotpebbles.com)
Pebbles LLC, Delray Beach, Florida

Rare necklace made of natural pearls from different mollusks. The Gübelin Gem Lab recently received a necklace consisting of 29 larger pearls and numerous smaller pearls and diamonds for routine gemological identification (figure 16). Ten of the larger pearls were "cream" colored, and 19 were various shades of purple; they were near-spherical to button to baroque shaped, and they ranged from 4.6 to 20.7 mm in longest dimension. Five of the purple pearls had a nacreous appearance, while all the others were porcelaneous. Ultraviolet fluorescence, Raman spectra, spot refractive index readings, EDXRF chemical data, and microscopic characteristics of all samples were consistent with saltwater pearls. The natural origin of these pearls was indicated by the fact that they originated from mollusks that are not used for cultivation.

One of the cream-colored pearls showed a flame structure, as observed in pearls produced by mollusks such as *Tridacna* species and Veneridae family bivalves, as well as by some gastropods. The nine other cream-colored pearls did not reveal any structure, as was the case for the Veneridae pearls described in the Winter 2008 GNI section (pp. 374–375), as well as for natural pearls from other mollusks.

Five of the 19 purple pearls revealed a honeycomb structure in the microscope (figure 17). Raman spectra showed aragonite peaks, along with bands at about 1520 and 1130 cm^{-1} due to a mixture of polyacetylenic pigments. To our knowledge, purple-hued pearls with these color, structure, and Raman characteristics only come from bivalves belonging to the Veneridae family. Four other purple pearls of comparable shape and color had similar Raman spectra; however, they did not show a honeycomb structure, as also documented in Veneridae pearls (see GNI entry cited above). These observations suggest that nine of the 19 colored pearls were from Veneridae family mollusks.

Five of the remaining 10 purple pearls had a nacreous structure (figure 18), but they lacked strong overtones. This is probably because the aragonite layers were thicker than is commonly observed in nacreous pearls, both natural and

Figure 16. This necklace contains 29 pearls (4.6–20.7 mm in largest dimension) that proved to be from at least two different mollusk families. Courtesy of Boghossian S.A., Geneva; photo by Evelyne Murer.

cultured. Raman spectra showed aragonite peaks, as well as bands at about 1490 and 1100 cm^{-1}. The positions of these bands suggest that this coloration is also due to a mixture of polyacetylenic pigments, but with a larger polyenic chain than has been documented in Veneridae pearls. To our knowledge, the only pearls with similar color, Raman spectra, and nacreous structure are those from the Mytilidae family. The other five purple pearls, which were non-nacreous, had similar Raman spectra. They also appear to originate from a mollusk of the Mytilidae family, as such pearls may have a porcelain-like appearance.

To our knowledge, this is the first time that mixed purple-hued pearls from the Veneridae and Mytilidae families have been observed in the same necklace. A combination of classical and advanced gemological analysis appears to be a promising approach for the identification of the mollusk family to which a pearl belongs.

Stefanos Karampelas
(s.karampelas@gubelingemlab.ch) and Eric Erel
Gübelin Gem Lab, Lucerne, Switzerland

Colorless petalite and pollucite from Laghman, Afghanistan. Farooq Hashmi (Intimate Gems, Jamaica, New York) recently loaned GIA three colorless stones (figure 19), which he believed to be petalite (14.98 ct) and pollucite (11.30 and 12.10 ct) from Laghman Province, Afghanistan. He purchased the rough in Peshawar, Pakistan, between 2007 and 2008. The stones were reportedly byproducts of pegmatite mining for tourmaline and other gems. Mr. Hashmi said he saw several kilograms of both gem materials in the Peshawar market, but he understands from local gem dealers that neither of them is being actively mined.

Petalite and pollucite are both known to be hosted in lithium-rich granitic pegmatites, and they have a Mohs hard-

Figure 17. The honeycomb structure observed in this non-nacreous pearl can be attributed to a simple prismatic arrangement of aragonite formed by parallel and adjacent prisms that do not strongly interlock along their mutual boundaries. Photomicrograph by E. Erel; field of view ~3.0 mm high.

Figure 18. Nacreous structures on this pearl form a layered aragonitic structure consisting of polygonal to rounded tablets arranged in broad, regularly formed parallel sheets. Photomicrograph by E. Erel; field of view ~3.4 mm high.

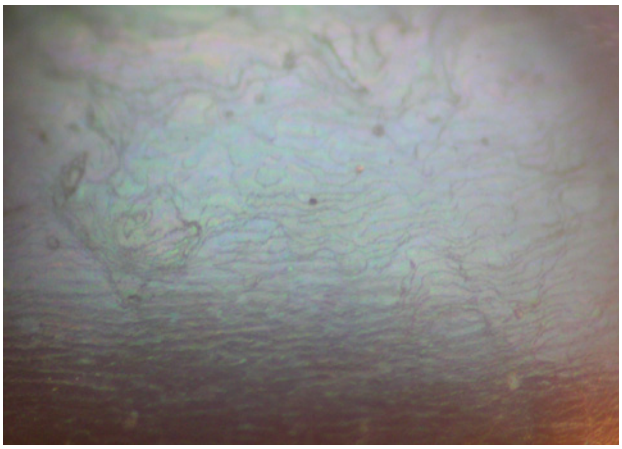

ness of 6.5. Petalite (also known as castorite) is a lithium aluminum tectosilicate ($LiAlSi_4O_{10}$) and a member of the feldspathoid group. An important lithium ore, it occurs with spodumene, lepidolite, and tourmaline in tabular crystals and columnar masses that range from colorless to gray and yellow. Pollucite, $(Cs,Na)(AlSi_2O_6)\cdot nH_2O$, is a zeolite that forms a solid-solution series with analcime and commonly occurs with quartz, spodumene, petalite, and tourmaline, among other pegmatite minerals. Isometric crystals ranging from colorless to white and occasionally pale pink can be found, though well-formed examples are rare.

Standard gemological testing produced the following properties (with those of petalite listed first, then the 11.30 and 12.10 ct pollucites, respectively): RI—1.505–1.515, and 1.518–1.519 or 1.517–1.518; birefringence—0.010 and 0.001 (pollucite can be weakly anisotropic); SG—2.40 and 2.90; UV fluorescence—all three samples were inert to both long- and short-wave UV radiation. No bands or lines were observed with the desk-model spectroscope. Microscopic examination of the petalite only revealed two feathers. No inclusions were observed in the 12.10 ct pollucite, but the 11.30 ct stone contained colorless inclusions of pollucite (identified by Raman spectroscopy) and a plane of crystals in the pavilion (figure 20) that had a Raman pattern similar to that of muscovite.

EDXRF analyses of the petalite showed major amounts of Si and Al, and traces of Fe, Ge, Cs, and Sm. Analyses of the pollucite samples revealed major Si, Al, and Cs, low amounts of Rb, Rh, Yb, and La, and traces of Ti.

We performed infrared (see *G&G* Data Depository) and Raman spectroscopy to further characterize these unusual stones. The IR spectra for the petalite showed bands at ~3358, 3270.6, 3037, and 2591 cm^{-1}, and broad absorption below ~2390 cm^{-1}. The IR spectra for the pollucite samples showed a band at ~4720 cm^{-1} and broad absorption between ~5321 and 5162, ~4141 and 3140, and below ~2325 cm^{-1}. The Raman spectra matched those of petalite and pollucite in our Raman database.

Figure 20. The 11.30 ct pollucite sample contained a plane of inclusions. The larger ones gave a Raman pattern similar to that of muscovite. Photomicrograph by J. Darley; magnified 40×.

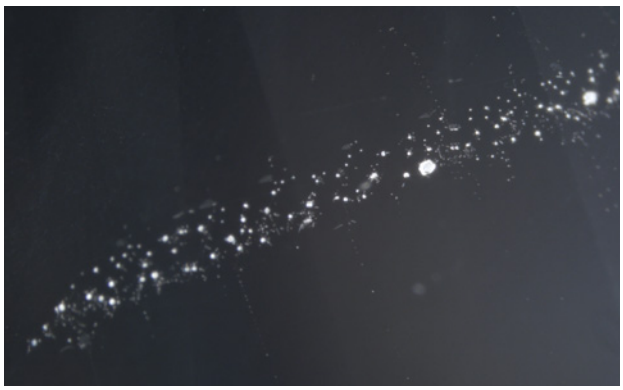

Figure 19. These unusual colorless gems are petalite (14.98 ct, left) and pollucite (11.30 and 12.10 ct, center and right), reportedly from Laghman Province, Afghanistan. Faceted by Robert C. Buchannan, Hendersonville, Tennessee; photo by Robert Weldon.

A pink cat's-eye petalite from South Africa (Winter 1986 Lab Notes, pp. 239–240) had properties similar to the colorless petalite from Afghanistan, except for its dull red fluorescence to UV radiation and its lower SG (2.34). Both the petalite and pollucite we studied had properties analogous to those reported by M. O'Donoghue (*Gems*, 6th ed., Butterworth-Heinemann, Oxford, UK, 2006, pp. 436–438), although the birefringence of petalite was slightly higher (0.013) in that publication.

Erica Emerson (eemerson@gia.edu) and Paul Johnson
GIA Laboratory, New York

Serpentine cat's-eye. Recently, the Gem Testing Laboratory in Jaipur, India, had the opportunity to examine an unusual opaque bluish green cabochon (36.63 ct; figure 21) that had a broad but distinct chatoyant band. The color, greasy-to-dull luster, and low heft suggested it was serpentine.

Standard gemological testing gave the following results: spot RI—approximately 1.57 with no distinct birefringence blink; hydrostatic SG—2.60; fluorescence—weak yellow to long-wave UV; and absorption spectrum—weak bands in the green (~490 nm) and blue (~460 nm) regions seen with the desk-model spectroscope. In addition, the luster indicated low hardness, which was confirmed by scratching with a fluorite crystal on an inconspicuous part of the sample. These properties are consistent with those reported for serpentine (e.g., R. Webster, *Gems*, 5th ed., revised by P. G. Read, Butterworth-Heinemann, Oxford, UK, 1994, pp. 369–372).

Serpentine is a common ornamental stone that is sometimes used as an imitation of jadeite and nephrite because of its similar aggregate structure and color appearance. It is usually seen in variable hues of blue, green, and yellow. It comprises species such as antigorite, chrysotile, and lizardite, and varieties such as bowenite, williamsite, and ricolite. Chatoyant serpentine, however, is quite rare. "Satelite," a fibrous variety exhibiting chatoyancy, has been reported from Maryland and California in the U.S. (Webster, 1994) and from Sichuan Province in China (B.-q. Lu et al., "Infrared absorption spectra of serpentine cat's eye

Figure 21. This bluish green cat's-eye cabochon (36.63 ct) proved to be serpentine. Photo by G. Choudhary.

from Sichuan Province of China," *Journal of Shanghai University*, Vol. 9, No. 4, 2005, pp. 365–368).

When the cabochon was examined with a microscope, thin parallel planes were visible. These appeared to be composed of fine films oriented perpendicular to the chatoyant band (figure 22, left), and were thus responsible for the cat's-eye effect. In addition, a few scattered brown dendritic crystals (figure 22, right) and white cloudy patches were present; this contributor has previously observed such inclusions in serpentine.

Because serpentine is a hydrous material, the FTIR spectrum in the 6000–400 cm^{-1} range exhibited complete absorption from 4500 to 400 cm^{-1} and there were two bands around 5000 and 4700 cm^{-1}. This pattern was similar to those of serpentine samples in our reference database. EDXRF analyses revealed the presence of Mg, Si, Cr, Fe, and Ni, which is consistent with the elements expected to be detected in serpentine.

This was the first time this contributor has encountered this rare variety of serpentine. The origin of this specimen is not known.

Gagan Choudhary (gtl@gjepcindia.com)
Gem Testing Laboratory, Jaipur, India

Zircon mining in Cambodia. In April 2009, these contributors visited Ratanakiri (or Rattanakiri, Rotanah Kiri) Province, Cambodia, ~600 km by road northeast of Phnom Penh. Ratanakiri is the world's major source of fine heated blue zircon. Blue is not known to occur naturally in zircon, but heat treatment of brown to reddish brown material from Indochina will produce light blue stones, and many gem enthusiasts believe that the finest blue colors are produced by heating the dark brown material from Ratanakiri (e.g., figure 23). It is likely that these deposits were not exploited until the early 20th century, when the potential for this heat treatment was discovered.

The zircon is found in an area of extensive volcanism consisting of flood basalts and scattered volcanic cones. Zircon-bearing alkaline basalts are confined to the intersection of brittle crustal structures, so the occurrences are small and discontinuous. We were told by a local zircon dealer that there are more than 100 deposits in Ratanakiri, but because the gem-bearing areas are small and remote, and many are worked seasonally, it is difficult to determine the number of miners or the annual production of zircon. We saw about 70 active shafts in the four small mining areas we visited, each employing two to four people. We estimate that those four mining areas produced about 500 g of gem-grade material per day during our visit.

Mining is performed by sinking a shaft through the overburden to the zircon-bearing horizon, which lies 2–15 m below the surface (figure 24, left). In some mines, the basalt has decomposed to loose red soil, and the gems can be separated by combing through the excavated earth by hand. In others, basalt cobbles remain as gravel, and the material must be washed (figure 24, right).

In addition, since 2005, the Cambodian government has granted three large concessions—totaling 19 km^2—in Ratanakiri: Ultra Marine Kiri Co. Ltd., Seoul Digem (Cambodia) Co. Ltd., and Ratanak Chhorpoan (Cambodia) Ltd. We visited the first two, but both were inactive.

The gems we saw during our visit consisted almost exclusively of zircon that ranged from nearly colorless to dark brown, and was occasionally reddish brown. Many crystals showed remnants of their tetragonal shape, and

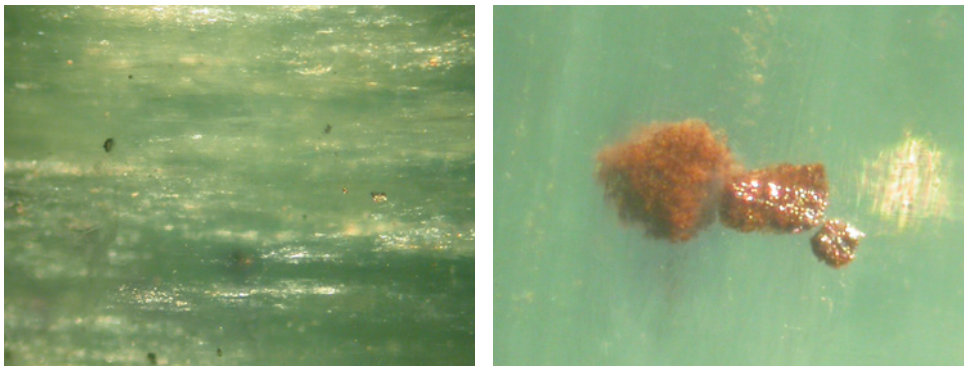

Figure 22. Parallel planes consisting of fine films were responsible for the chatoyancy of the stone in figure 21 (left). Brownish dendritic crystalline inclusions were also present (right); these are commonly seen in serpentine. Photomicrographs by G. Choudhary; magnified 30× and 45×.

most had a shiny "melted" surface (again, see figure 23) from partial resorption during transport in the basalt. A significant portion also exhibited tenebrescence: After being kept in darkness for several days, they were a bright orange to red that changed to brown with several minutes' exposure to sunlight. This photochromism is reversible and repeatable. The rough generally weighed 0.1–5 g, although we saw non-gem-grade specimens up to 100 g. Rough that will produce clean gems in excess of 10 ct is unusual, although cut stones larger than 100 ct are known.

Most of the rough is sent to Phnom Penh or Thailand for heating and cutting, although some is processed in Ratanakiri. The stones are heated in a reducing atmosphere at 900–1000°C for ~1 hour. Almost all brown zircon from this source will turn blue with heating (e.g., figure 25); a light blue color can sometimes be produced from stones that were originally colorless.

Additional images from this expedition are available in the *G&G* Data Depository.

Mark H. Smith
Thai Lanka Trading Ltd. Part., Bangkok, Thailand
Walter A. Balmer
Department of Geology (Faculty of Science)
Chulalongkorn University, Bangkok, Thailand

Figure 23. These rough zircons were recovered from Ratanakiri Province, Cambodia. The blue rough (up to 7 g) was produced by heating brown stones such as those on the left (up to 24 g). Photo by Prasit Prachagool.

Figure 24. The best-known Cambodian zircon deposit is at Bo Keo (left), where there are ~30 active mines. The shafts in this region are typically about 15 m deep. At Bo Kalap (below), there are ~10 active pits; the excavated material contains basalt cobbles and requires washing to recover the zircon. Photos by M. H. Smith.

Figure 25. With heat treatment, most Ratanakiri zircon turns blue. The large emerald cut weighs 30.45 ct. Courtesy of Thai Lanka Trading.

CONFERENCE REPORTS

GIT 2008. After being postponed in December 2008 due to political unrest in Bangkok, the second Gem and Jewelry Institute of Thailand (GIT) conference, GIT 2008, was held March 9–12, 2009. Some 500 participants attended the two-day conference, which was followed by a two-day field trip to Kanchanaburi and the Bo Phloi sapphire mine. Parallel sessions saw 50 speakers, and there were approximately the same number of posters on display. Only selected oral presentations are mentioned in this report, since these authors were unable to attend all sessions. The conference proceedings (extended abstracts) are available in book or CD-ROM format by contacting the GIT at www.git.or.th.

After the opening ceremony, hosted by GIT Director **Dr. Wilawan Atichat** and Thai Deputy Minister of Commerce **Alongkorn Ponlaboot**, the conference started with three keynote speakers. **Vichai Assarasakorn**, president of the Thai Gem and Jewelry Traders Association, gave an impressive overview of the Thai gem and jewelry business. He was followed by **Massimo Zucchi** (Studio Zucchi Design, Milan, Italy), who discussed globalization and branding, and **Dr. Joerg Fischer-Buehner** (Legor Group SRL, Bressanvido, Italy), who lectured on palladium casting for jewelry.

Strategic marketing in emerging markets was discussed by **Dr. Krittinee Nuttavuthisit** (Chulalongkorn University, Bangkok), and the new era of jewelry design in Thailand was reviewed by **Dr. Veerawat Sirivesmas** (Silpakorn University, Bangkok). One of these contributors **(LK)** presented an overview of the Tom Lantos JADE Act, its implications for the trade, and possible alternative ruby sources.

Hyun Min Choi (Hanmi Lab, Seoul, Korea) examined photoluminescence characteristics of HPHT-processed natural type IIa diamonds. **Dr. Walter Balmer** (Chulalongkorn University) gave a presentation on behalf of Swiss gemologist **George Bosshart**, who was unable to attend. Mr. Bosshart's research focuses on distinguishing natural from artificially colored green diamonds; the presentation introduced the properties of untreated green diamonds and the natural radiation mechanisms that produce this color.

An interesting report on rubies from Fiskenæsset, Greenland, was given by **Pornsawat Wathanakul** of GIT (for **Greg Davison** of True North Gems, Vancouver, British Columbia, Canada, who could not attend). A pair of garnet lectures was given by **Dr. Karl Schmetzer** (Petershausen, Germany) and GIT's **Dr. Visut Pisutha-Arnond**. **Dr. Claudio Milisenda** (German Gemmological Association, Idar-Oberstein) reported on his study of red labradorite-andesine feldspars and offered some promising results based on FTIR data on the distinction of treated versus untreated stones. A thought-provoking talk about experimental heating of Cu-bearing tourmaline was given by **Thanong Leelawatanasuk** (GIT). **Boontawee Sriprasert** (Department of Mineral Resources, Bangkok) discussed heat-treatment experiments on red spinel from Myanmar. **Dr. Chakkaphan Sutthirat** (Chulalongkorn University) gave an introduction to heat-treatment experiments on sapphire from the Awissawella deposit in Sri Lanka. **Dr. Ahmadjan Abduriyim** (Gemmological Association of All Japan—Zenhokyo, Tokyo) presented his findings on treated green amber.

The SSEF Swiss Gemmological Institute's **Dr. Michael Krzemnicki** described modern, portable instruments for advanced testing in the gemological laboratory, including UV-Vis and laser-induced breakdown spectrometers. **Dominic Mok** (AGIL Ltd., Hong Kong) gave a controversial lecture on advanced testing of jadeite jade (called *Fei Cui* by the Chinese). After describing the different colors of jadeite, he mentioned that kosmochlor and omphacite are also called *Fei Cui* in the Chinese market. This brought strong reactions from some attendees, as these two materials are considered much less valuable than true jadeite.

Dr. Henry Hänni (SSEF) delivered an overview of the different types of cultured pearls, and **Kenneth Scarratt** (GIA Thailand) discussed nautilus pearls.

After the conference, the two-day field trip took approximately 80 participants to the Bo Phloi gem field about 170 km northwest of Bangkok. The field lies within Quaternary sediments and covers an area of about 1200 km^2. The largest sapphire deposit in Thailand's western region, it is operated by SAP Mining Co. Ltd. as an open-pit mine. The gem-bearing layers are 1–8 m thick at depths of 6–19 m. The gravel is brought to a washing site to concentrate the gem corundum before it is hand-sorted. In addition to sapphire, miners have recovered black spinel, black pyroxene, and red garnet.

Lore Kiefert (lkiefert@agta-gtc.org)
AGTA Gemological Testing Center, New York
Evan Caplan
Omi Gems, Los Angeles

Sinkankas Spinel Symposium. The seventh annual symposium in honor of John Sinkankas took place April 18, 2009, at GIA in Carlsbad. Co-hosted by GIA and the San Diego Mineral and Gem Society, the sold-out event was attended by 152 people.

After opening remarks by convener **Roger Merk** (Merk's Jade, San Diego, California), **Si Frazier** (El Cerrito, California) reviewed historical spinels and noted that some of them were quite large, such as the ~400 ct red spinel that was set in Catherine II's (Russian) crown. **Edward Boehm** (Joeb Enterprises, Solana Beach, California) indicated that the ~500 ct Sumerian Spinel in the Iranian crown jewels most likely came from the old mines in present-day Tajikistan. He also illustrated how most famous "rubies" in royal and ecclesiastical regalia are actually spinels. If not for spinel, ruby would not have achieved the fame it enjoys today.

Dr. William B. "Skip" Simmons (University of New Orleans) covered the mineralogy and crystallography of the spinel group. Of the 22 spinel species recognized by the International Mineralogical Association, only one (spinel *sensu stricto*) is an important gem material. **Jennifer L. Stone-Sundberg** (Saint-Gobain Crystals, Washougal, Washington) reviewed the historical and contemporary growth of synthetic spinel. Today the material produced for gem use comes mainly from China and Russia; it can be identified by its higher RI values (for Verneuil- and Czochralski-grown products), inclusions (for flux-grown as well as the flame-fusion products), chemical composition, fluorescence, and Raman spectroscopy.

Jo Ellen Cole (Cole Appraisal Services, Vista, California) examined spinel pricing, and noted that there was a sharp increase in the cost of rough/cut material during 2000–2002; prices have continued to rise since then. **Bill Larson** (Pala International, Fallbrook, California) reviewed the main sources of spinel: Tajikistan (Kukh-i-Lal), Myanmar (Mogok and Nanyaseik), Sri Lanka, Vietnam (Luc Yen), and Tanzania (Morogoro, Tunduru, and Mahenge). The rare Co-colored blue spinel comes from Sri Lanka and Tunduru.

Meg Berry (Mega Gem, Fallbrook, California) illustrated the recutting of spinel, in which she improved lopsided, windowed, and damaged stones by keeping the original tables and paying attention to spinel's ~40° critical angle; major improvements in appearance were attained, with a cutting yield of 56%–76%. **Robert Weldon** (GIA, Carlsbad) provided suggestions for photographing spinel—applicable to other gems as well—that include using shallow depth-of-field to highlight interesting inclusions, positioning a reflector to help eliminate a "bow-tie" effect in problematic cuts, and, in asteriated stones, placing the reflection from a pinpoint light source in the center of the stars.

John Koivula (GIA, Carlsbad) reviewed the variety of internal features found in spinel, including mineral inclusions (e.g., rutile, carbonates, graphite, hematite, högbomite, Fe-sulfides, sphene, uraninite, and zircon) and fluid inclusions (both secondary and primary). He also noted that spinel forms inclusions in other gems, such as in sapphire and grossular (hessonite) from Sri Lanka. **Dr. George Rossman** (California Institute of Technology, Pasadena) reviewed the primary causes of color in spinel: Cr^{3+} (pink-to-red), Co^{2+} (blue), and Fe^{3+} (usually with Fe^{2+}; blue to green to lavender). Also, the following colorants have been used in synthetic spinel: Mn^{3+} (yellow), Cu^{2+} (blue), and Ti^{3+} (blue-green).

The theme of next year's Sinkankas Symposium (date to be determined) will be feldspar.

Brendan M. Laurs

ANNOUNCEMENTS

Gems issue of *Elements*. The June 2009 issue of the earth sciences magazine *Elements* focuses on key aspects of gemology: how gems occur in nature, the role of geochemistry in characterizing them, the challenge of nondestructively identifying faceted samples, the detection of treatments and synthetics, and the use of pearls and corals as organic gem materials. The issue's guest editors are *G&G* contributors Emmanuel Fritsch and Benjamin Rondeau. Visit www.elementsmagazine.org.

Responsible Jewellery Council announces Code of Practice. The Responsible Jewellery Council (RJC; formerly the Committee for Responsible Jewellery Practices) outlined its supply chain Code of Practice certification system at a March 25 news conference at the BaselWorld Fair. The RJC certifies mine-to-market activities in areas of sustainable mining practices, including fair wages, benefits to local communities, health and safety standards, ethical trading, and environmental respect. During the second half of 2009, the RJC will make independent auditors available to verify each member firm's adherence to Code of Practice standards and issue the appropriate certificate. The RJC has 85 members (including GIA) in the diamond and gold mining, manufacturing, and retailing sectors. More information can be obtained at www.responsiblejewellery.com.

ERRATA

The Spring 2009 article by F. Farges et al., "The French Blue and the Hope: New data from the discovery of a historical lead cast," contained the following errors.

1. The estimated error of the density of the lead cast on p. 13 should have been given as 11.2 ± 0.1 g/cm^3.
2. The entries for footnotes *a* and *b* in table 1 on p. 10 were inadvertently switched, and the entry for footnote *b* is incorrect. Footnote *a* should read *1* grain, poids de marc ≈ *0.0531147 g ≈ 0.2655735 ct (Lionet, 1820)*. Footnote *b* should read *1 ligne = 2.2558 mm (Morel, 1988)*.
3. The name of the company that performed the scanning, Matrix Diamond Technology, was incorrect.

Gem & Gemology regrets the errors.

LETTERS/BOOK REVIEWS/GEMOLOGICAL ABSTRACTS

The *Gems & Gemology* Letters, Book Reviews, and Gemological Abstracts sections are available only in electronic (PDF) format. These sections are available free of charge both on the *G&G* web site (www.gia.edu/gemsandgemology) and as part of *G&G* Online (gia.metapress.com), and are paginated separately from the rest of the issue.

These sections are also included in this full-issue PDF. Accordingly, the Table of Contents included in this file lists these additional sections, and thus differs from the Table of Contents in the print version. For these reasons, this PDF is *not* the official version of this issue—the "journal of record" for this issue is the combined print/online version that was released to subscribers.

09 Letters

MORE ON D-to-Z DIAMOND COLOR GRADING

I enjoyed reading "Color Grading 'D-to-Z' Diamonds at the GIA Laboratory" (Winter 2008, pp. 296–321). It is always great to learn how things are done at the GIA lab. Although I feel it would have been better to present and discuss much of this information at least eight years ago, it is nonetheless good to see the lab publish its standards for policy, procedures, and equipment.

That said, I write to say how strongly I disagree with the authors' conclusion that "a standard light source for diamond color grading should have key characteristics of daylight, *including a UV component*" (p. 320, italics mine). In their introduction, the authors stress the impact of color grade on the price of diamonds, and they go on to review the development of the GIA system and the various modifications that have occurred since the mid-1950s. Then they admit that, "at times, the resulting adjustments *have appeared to conflict with earlier statements*" (p. 296, italics mine). As the authors point out, all of the early literature, including that from GIA, indicated that the "true bodycolor" of a diamond should be determined in light that is similar to indirect northern daylight but with a minimum of UV radiation.

I began working at the GIA lab (on San Vicente Blvd. in Los Angeles) in 1975, shortly after GIA Gem Instruments introduced the new DiamondLite with Verilux lamps, which had "a new coating that minimized UV emission as compared to similar lamps. . . ." (p. 302). And yes, as a GIA lab employee for the next three years, I "often promoted the minimized UV emission in these lamps" (p. 302), generally to diamond dealers who had submitted stones for grading and thought the color grade should have been higher. If the stone had medium blue or stronger fluorescence, I would explain that it probably appeared to have a higher color grade in the lighting environment the dealer used because of UV emission, and that we, at the GIA lab, were using specially developed, standardized lamps with a minimum of UV emissions to determine each diamond's true bodycolor.

When I became aware, in 1995, that the Verilux lamps in the GIA DiamondLite emitted a good deal of UV radiation, I assumed that the lamps had undergone a change in manufacture, and were not the same as those used in 1974 (see T. E. Tashey, "The effect of fluorescence on the color grading and appearance of white and off-white diamonds," *The Professional Gemologist*, Vol. 3, No. 1, 2000, pp. 5–7). The authors seem to disagree: "Indeed, the lamps chosen in the '70s had a small, *but not negligible*, UV component. And we continue to see this UV component in lamps chosen since then" (p. 306, italics mine). Not negligible, indeed. If the authors are correct—that the Verilux lamps, even the original ones from 1974, have such a strong UV component—I would have to conclude that a lot of fluorescent diamonds were misgraded between 1974 and 2000.

The authors emphasize that millions of diamonds (fluorescent and not) have been graded under the procedures they describe and that it would be wrong to change grades, based on new procedures, for all of the possible resubmissions of previously graded diamonds. Personally, I don't know. The authors emphasize how careful the graders are and how procedures are designed to be repeatable so that the lab will always get the correct color grade of a diamond, and how their "research has shown that skilled graders reach a point of visual tolerance (i.e. the range of repeatability) . . . at slightly less than one-fifth of a grade at best" (p. 308). Such repeatable consistency for a lab would be commendable. And yet a strongly fluorescent diamond, which in my experience (see Tashey, 2000) can have its apparent color lowered by two to four letter grades when using a UV filter (see below) in the standard viewing environment used by GIA, is not considered to be of any significance? Is this lower grade not the *true bodycolor* of the diamond, which all historical literature has advised should be used to determine the real value of a diamond?

The authors acknowledge that the blue fluorescence of some diamonds can alter their appearance in certain lighting environments by canceling out a portion of their yellow bodycolor. They propose to standardize the amount of UV emissions for the effective color grading of diamonds. They do this by using a standard lamp with a standard level of UV emission (though this level may decay over time) and defining a standard viewing distance:

> For consistency, we use a distance of 8–10 in. (20–25 cm) between the lamps and the diamond. Bringing a fluorescent diamond closer to the lamps may result in a stronger fluorescent impact. For instance, a yellow diamond with strong blue fluorescence could appear less yellow (i.e., to have a higher color grade) as it gets closer to the lamps. Moving the same diamond more than 10 in. from the lamps will have the opposite effect; that is, the color will appear more yellow (a lower color grade) (p. 304).

While this is indeed a standard, is it the best possible standard for the evaluation of a diamond's color grade?

I personally think not, considering the high amount of UV emission in this proposed standard lighting environment, unless one also includes on the grading report a letter grade determined in a similar standard viewing environment with no UV component.

I was shocked when I first discovered in 1995, by shielding the Verilux lamps in the GIA DiamondLite with a clear Makrolon plastic film (which acts as a UV filter), that stones with very strong blue fluorescence could appear three or four letter grades lower in color. Similarly, after sharing my findings and offering others some Makrolon film for their own experiments, several of my colleagues and former associates were as shocked as I was to see these dramatic color shifts in strongly fluorescent diamonds. I believe this to be a very significant issue in the accurate color grading of D-to-Z diamonds, and I cannot accept GIA's recommendation for their standard viewing environment.

As a consultant to the World Gemological Institute in Israel from 2005 to 2007, I oversaw that lab's transition from the GIA DiamondLite (DL) to the GIA DiamondDock (DD) as the standard environment for color grading. During the transition, over a three- to four-week period, all stones were observed in both environments to check for any discrepancies. As a UV filter was used with the DL to grade diamonds with medium or stronger blue UV fluorescence, we also used it with the DD. Because the distance from the lamp to the grading tray is greater in the DD than in the DL, one can imagine that the UV component might be somewhat reduced. We found that stones with medium or stronger blue fluorescence had the same color in the DL and the DD when viewed without a UV filter. They shifted to the same lower grades when examined with the filter. It should be noted that the Verilux lamps in the DD are thicker and have more than twice the wattage of the lamps in the DL.

I think the GIA DiamondDock has made significant improvements over the DiamondLite, and, except for the issue of the high UV emission from its Verilux lamps, it makes a very good standard viewing environment for diamond color grading. It is larger and more grader friendly; it has a neutral gray background for better color discrimination and less grader eye fatigue; the distance from the lamps to the grading shelf is greater (from approximately 5 inches in the DL to approximately 7 inches in the DD); and it provides a vastly improved grading tray. This is a large, very white, nonfluorescent plastic, pivotable, V-shaped tray that will hold a complete master set of 10 to 12 stones and still have plenty of working distance between stones for accurate color discrimination.

I'll conclude with the description of a diamond my laboratory examined in October 2008: a 0.89 ct marquise brilliant with very strong blue fluorescence. In the DL without a UV filter, the stone was graded table-down as a high D. In the face-up position, compared to the face-up appearance of a 1.0 ct E master stone, the E master looked very slightly yellow. But with the UV filter in place, when graded table-down, the color grade shifted to a low H. In the face-up position, because the diamond was a marquise brilliant (a fancy cut that will generally show more color face-up than a round brilliant of the same size and bodycolor), it was very slightly less yellow than a 1.0 ct J master in its face-up position, and considerably more yellow than the 1.0 ct H master. The diamond was also examined in a DiamondLite modified by Dazor Inc. to use LED lighting. We found that the diamond appeared the same in this LED lighting environment, in both the face-up and table-down positions, as it did in the DiamondLite with a UV filter.

How is such a diamond to be described and graded with consistency and accuracy? I have concluded that the best procedure for strongly fluorescent diamonds, going forward, would be to issue a report listing two different color grades in two different standard lighting environments, both similar to natural daylight, but one with and one without a UV component (of course, natural daylight has a UV component, but the strength of that component differs significantly from direct sunlight to northern, indirect daylight). This additional information would be useful to the owners of strong blue fluorescent diamonds, alerting them to the fact that the diamond may look different in different lighting environments.

My lab graded the 0.89 ct marquise-cut diamond as G color, as in our opinion this was a fair compromise. I wonder how the GIA Lab would grade it. How is this diamond, and how are other strongly fluorescent diamonds, to be valued? Based on the higher color grade, with a large deduction for the strong blue fluorescence? Or based on the lower color grade, with a large premium for the strong blue fluorescence? Personally I prefer, and professionally I practice, the latter.

Thomas E. Tashey Jr.
Professional Gem Sciences
Chicago, Illlinois

MORE ON THE WITTELSBACH BLUE

In our recent article on the Wittelsbach Blue (Winter 2008, pp. 348–363), we noted that despite "exhaustive efforts" we had been unable to locate the "Dr. Klaus Schneider" whose research was the basis for much of K. de Smet's book, *The Great Blue Diamond* (1963). This work has been used as an important source for historical information on the Wittelsbach Blue by many authors (e.g., Tillander, 1965, 1996; Heiniger, 1974; Legrand, 1980; Khalidi, 1999; Balfour, 2001; Bari and Sautter, 2001; Bharadwaj, 2002; Manutchehr-Danai, 2005; Erichsen, 2006; Christie's, 2008). During our research, however, we discovered that many of the statements therein had no archival basis, and we sought to contact Schneider or at least review his records in hopes of clarifying these inconsistencies. Although we had met with no success at the time the *G&G* article went to press, we wish to report that further work has finally cleared up this mystery.

Some background here is useful. As we discussed, de Smet's book was commissioned by Jozef Komkommer, who bought the diamond in 1961. In it, Schneider is described as a "final-year student of history" and "Dr. Klaus Schneider," whom an associate of Komkommer's recruited from a Munich student work organization to assist with the book.

Our initial research determined that Schneider sought access to the Bavarian Secret House Archives (BSHA) in Munich in September 1961. Schneider's research proposal gave his Munich address (Zieblandstrasse 11), his student status ("stud. phil.," or student at the faculty of philosophy) and his academic degree ("Diplom-Volkswirt" or diploma in national economics). Dr. Hans Rall, head of the Archives and professor at the Ludwig-Maximilian University (LMU), Munich, contacted the Wittelsbach Equity Foundation about Schneider's request, as only the head of the House of Wittelsbach, Duke Albrecht of Bavaria, could give such permission. In October 1961, Dr. Rall informed Schneider that his proposal could not be addressed because Duke Albrecht was on a vacation in the mountains. There is no evidence Schneider ever gained access to this archive.

Later in October 1961, Schneider visited the Austrian State Archive in Vienna. The record of his visit (figure 1) is quite interesting, because in it he is described as "Dr. phil. Klaus Schneider" and his signature ("Unterschrift") appears as "Dr. Klaus Schneider" at the lower part of the form. His Munich address also appears, as does an identification as "Assistant to Prof. Rall, Munich." This latter designation was not an informal or unimportant appellation: In the German university system, employment as a professor's assistant is one of the possible first steps to achieve the rank of professor.

From 2006 to 2008, we attempted in vain to locate any further records of Schneider's activities. LMU had no record of a student of that name. We contacted both Dr. Rall's widow and two former colleagues, none of whom recalled a Klaus Schneider working as Dr. Rall's assistant during 1961–1964 (though this is not terribly surprising after the passage of 40 years). One of us (JE) inspected Professor Rall's private library, which is now stored at the BSHA; we also requested records from the register of citizens of the City of Munich for a "Klaus Schneider" or a "Dr. Klaus Schneider" living at Zieblandstrasse 11 during this period. Nothing was found.

However, in January 2009, one of us (BB) came across a record of a "Johannes Nikolaus Paul Anton Schneider" at the register of citizens of the City of Düsseldorf. This was significant because *Klaus* is a German short form of *Nikolaus*. A new request to the City of Munich using this name was successful: a "Nikolaus Johannes Schneider" indeed lived at Zieblandstrasse 11 during this period. Unfortunately, we also learned that Schneider had passed away in 1996 in Wuppertal. His death certificate identifies him as "Dipl.-Volkswirt Johannes Nikolaus Paul Anton Schneider" (indicating that he had earned only an undergraduate degree, not a doctorate), born in Düsseldorf in 1935. In March 2009, author JE succeeded in locating this Schneider's ex-wife, who recalled that her ex-husband had indeed visited the General Archive of the Royal Palace in Madrid in 1962 as stated in de Smet. Thus, we can be certain that we located the correct individual.

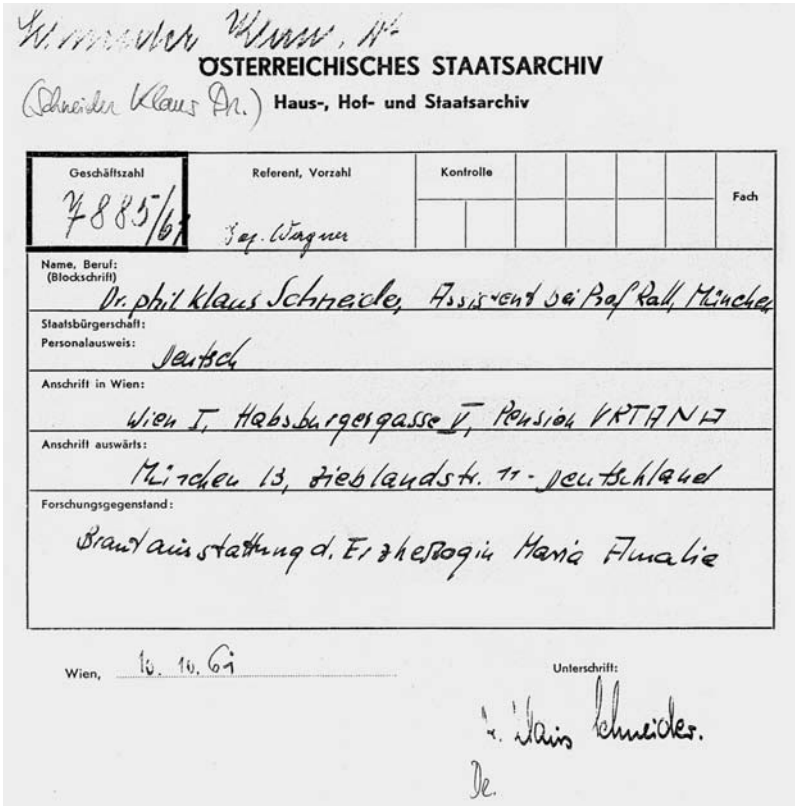
ÖSTERREICHISCHES STAATSARCHIV
Haus-, Hof- und Staatsarchiv
Geschäftszahl 7885/61
Referent, Vorzahl Kontrolle Fach
Name, Beruf: (Blockschrift) Dr. phil Klaus Schneider, Assistent bei Prof Rall, München
Staatsbürgerschaft:
Personalausweis: Deutsch
Anschrift in Wien: Wien I, Habsburgergasse 7, Pension VRTANA
Anschrift auswärts: München 13, Zieblandstr. 11 - Deutschland
Forschungsgegenstand: Brautausstattung d. Erzherzogin Maria Amalie
Wien, 16. 10. 61
Unterschrift: Klaus Schneider.

Figure 1. This page from the records of Schneider's visit to the Austrian State Archive in Vienna in October 1961 identifies him as "Dr. phil. Klaus Schneider" and the assistant of Professor Hans Rall at Ludwig Maximilian University, Munich. At the lower part of the figure his signature, "Dr. Klaus Schneider," is shown. The three statements were false.

A request to the LMU administration in March 2009 using the correct name at last succeeded in locating Schneider's student records. He entered LMU in 1959 to study national economics ("Volkswirtschaft") and graduated in 1963. On the basis of this, it is clear that Schneider performed his work for Komkommer in 1961 and 1962 not as a doctoral student in history but as an undergraduate student in economics. It is a fair question to ask whether Schneider misrepresented himself (again, see figure 1) in order to get the job for the historical research on the Wittelsbach Blue.

Bernd Beneke
City of Düsseldorf

Rudolf Dröschel, Jürgen Evers, and Hans Ottomeyer

The authors wish to thank Regierungsdirektor S. Conrad, Prof. H. Glaser, Dr. A. Neuhoff, and Prof. G. A. Ritter,

Ludwig-Maximilian University, Munich; Dr. G. Gonsa, Austrian State Archive, Vienna; Mr. P. Gutmann, Munich; Dr. G. Immler and Archivoberinspektor A. Leipnitz, Bavarian Secret House Archive, Munich; Mrs. M. Rall and Mrs. A. Ludden, Munich; AOR G. Reiprich, Bavarian State Archive, Munich; Mrs. B. Schneider, Hamburg; and MR G. Tiesel, Bavarian State Ministry of Justice and Consumer Protection.

REFERENCES

Balfour I. (2001) *Famous Diamonds*. Christie, Manson & Woods, London.

Bari H., Sautter V. (2001) *Diamonds: In the Heart of the Earth, in the Heart of the Stars, at the Heart of Power*. Vilo International, Paris.

Bharadwaj M. (2002) *Great Diamonds of India*. India Book House Pvt., Nariman Point, Mumbai.

Christie's (2008) Jewels: The London Sale (10 December 2008). Auction catalogue, Christie, Manson & Woods, London.

Erichsen J.K., Heinemann K. (2006) *Bayerns Krone 1806, 200 Jahre Königreich Bayern* [*Bavaria's Crown 1806, 200 Years Kingdom Bavaria*]. Bavarian Administration of Castles, Gardens and Lakes, Munich.

Heiniger E.A., Heiniger J. (1974) *The Great Book of Jewels*. New York Graphic Society, Boston.

Khalidi O. (1999) *Romance of the Golconda Diamonds*. Grantha Corp., Middletown, NJ, in association with Mapin Publishing, Ahmedabad, India.

Legrand J. (1981) *Der Diamant, Mythos, Magie und Wirklichkeit* [*Diamond: Myth, Magic and Reality*]. Herder, Freiburg, Germany.

Manutchehr-Danai M. (2005) *Dictionary of Gems and Gemology*. Springer-Verlag, Berlin, Germany.

de Smet K. (1963) *The Great Blue Diamond: The Wittelsbacher, Crown Witness to Three Centuries of European History*. Standaard-Boekhandel, Antwerp-Amsterdam.

Tillander H. (1965) Six centuries of diamond design. *Journal of Gemmology*, Vol. 9, No. 11, pp. 380–401.

Tillander H. (1995) *Diamond Cuts in Historic Jewellery*. Art Books International, London.

INCONSISTENCIES IN "THE FRENCH BLUE AND THE HOPE"

In their article presenting a new model of the French Blue (Spring *G&G*, pp. 4–19), Farges et al. used a newly discovered lead cast to confirm the possibility of the Hope diamond being cut from the French Blue. During their research, they created a three-dimensional model of the cast based on the shadow projections obtained by an Octonus Helium Rough 1:4 scanner operated by Matrix Diamond Technology. The dimensions of the model are $30.37 \times 25.50 \times 12.87$ mm, which match those of the lead cast within 20 microns accuracy. (This model is available at www.octonus.com/oct/projects/frenchblue.phtml.)

From my analysis of the 3D model, I disagree with some of the statements made in the article. First, it is clear that its maximum diameter is actually 30.44 mm: The inclination of the maximum diameter to the direction of the length measurement is 4.4°, as illustrated in figure 1. If Brisson (1787) measured this true maximum diameter, and the edges of the lead cast have indeed been rounded and worn down over two centuries, then Brisson's data match the lead model in this dimension much better than the authors believed because of their assumption that Brisson measured a smaller, "non-tilted" diameter.

Next, the authors estimate the French Blue's dimensions as $29.99 \times 23.96 \times 12.11$ mm on the basis of Brisson's mistakes in measuring the Regent diamond. However, the authors did not specify their correction factor and method. Taking into account that the correction factors for the Regent are in the 1.028–1.035 range, while the correction factors for the French Blue height and width used by the authors were 1.034–1.035, a height of 12.11 requires a correction factor of 1.055. Using the 1.034–1.035 correction factor, the height would be 12.35 mm.

Finally, to correct the weight of the French Blue based on the lead cast, the authors used historical data after Bion (1791) and Brisson (1787). The weight was used as a main criterion to determine the model's accuracy. The authors used results after Morel and converted 268⅛ grains (Bion) and 260 grains (Brisson) to 69.00 ± 0.05 modern carats, as their weight estimate; this estimate was used later to adjust the dimensions of the lead cast to match the diamond's presumed weight. To obtain the weight represented by the reduced lead cast, the authors used the weight of the lead cast (which is not given in the article), the cast's density (which was determined by chemical analysis of the metal surface), and the density of the French Blue according to Brisson. This resulted in 68.3 ± 0.2 ct. The discrepancy in the estimates was explained by different factors of the lead cast's production and storage. As a result, the conclusion was made that the lead cast models the French Blue well.

However, there are several problems with this approach.

First, 268⅛ grains (Bion) equal 71.22 modern carats, while 260 grains (Brisson) correspond to 69.05 modern carats. The authors do not explain why different ratios were used for recalculation of grains into carats for the Bion and Brisson data.

Second, the 3D model developed on the basis of the lead cast obtained by an Octonus Helium Rough 1:4 scanner operated by Matrix Diamond Technology resulted in 71.4 ± 0.2 modern carats; this was not mentioned by the authors at all.

Third, the discrepancy between the dimensions of the lead cast and Brisson's data is as much as 0.6 mm, and the authors' data had a final error range of up to 1.5 mm.

Last, the chemical composition of the lead cast's surface could differ significantly from its internal chemical composition. If the authors chose not to rely on the weight calculated on the basis of the 3D model, they should have measured the lead cast volume by, for example, hydrostatic weighing. This would have provided a more reliable weight estimate to reduce the diamond density.

The issues above compel one of two conclusions: Either the French Blue weighed more than 71 ct or, if the authors consider 69 ct to be the true weight, then the 3D model based on the lead cast should be reduced to a size corresponding to 69 ct before the comparison with the models of the French Blue and Hope Diamond. However, this decrease in model parameters would make the conclusion that the Hope Diamond could have been recut from the French Blue doubtful (figure 2).

In order to increase the accuracy and reliability of the analysis, I suggest it is necessary to use the 3D models of these objects directly, not by comparison with 2D projections (which have an accuracy of only 43 pixels/mm). For a 3D model comparison, there are programs like AutoCad, Solidworks, or software for rough diamond allocation, such as PacorClient developed by OctoNus, whose products were used by the authors in the course of their research.

Sergey Sivovolenko
OctoNus Finland OY
Tampere, Finland

Reply

We welcome Dr. Sivovolenko's comments. We do wish to point out that, for space reasons, the published version of the paper was shorter than the version that was originally submitted, so it was not possible to include all relevant details.

First, we do not feel it is appropriate in such a paper to argue that one type of software is better than another. Second, a difference of 2.5 ct (out of 69 ct, following Brisson, 1787), depending on the software used, corresponds to an error of 0.3 mm in the dimensions of the cast, which is surely within the error range resulting from wear or shrinkage given its manufacture sometime before 1812. Third, we have no doubt that Brisson's 1787 measurements are accurate to the 0.03 ct level and $^{2}/_{10}$ of a millimeter based on comparison of his reports of the Regent and Hortensia diamonds with modern measurements.

Our goal was not to conduct an analytical study of the lead cast per se but to help reconstruct a mythic diamond. The lead cast is the best model known to date of the French Blue, as it has unique features (such as asymmetries) that are also present in the 1889 drawing. There is no record of any other diamond of that size with that peculiar cut, so there is no doubt that this cast is a replica of the French Blue and the only remaining artifact of the largest blue diamond ever cut.

Our research is now focusing on a second lead cast of another well-known (and lost) diamond and that of a mythic sapphire (also recut) that were found in the same set of donations.

François Farges
MNHN, Paris
Scott Sucher
Tijeras, New Mexico

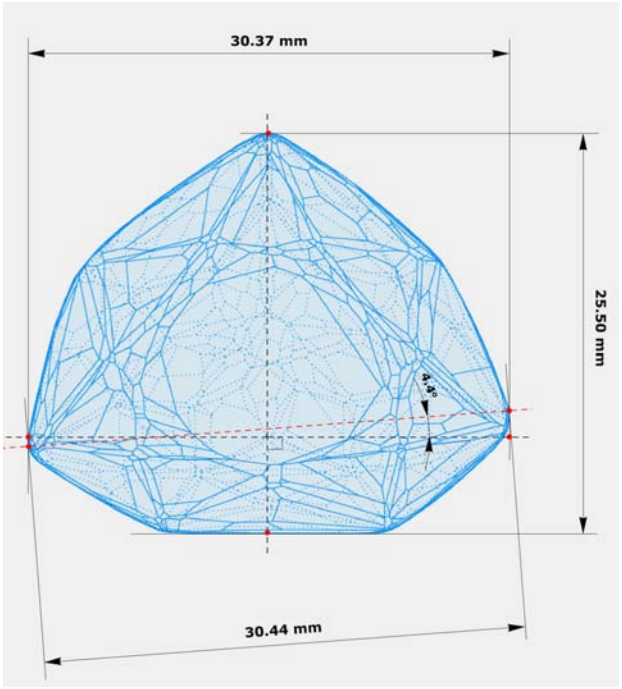

Figure 1. The maximum diameter of the French Blue model is actually 30.44 mm, if the measurement is taken in a direction slightly inclined from a line directly across the table.

Figure 2. Based on the Helium 3D model, the weight of the French Blue would be at least 71.38 ct. Reducing the weight to 69.05 ct, as given in Farges et al., would require reducing the dimensions as shown.

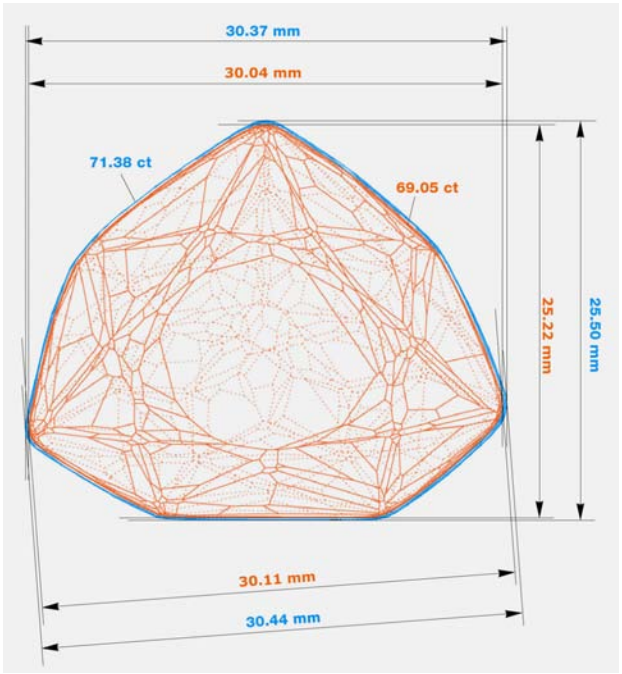

BOOK Reviews 09

Mikimoto

By Nick Foulkes, 80 pp., illus., publ. by Assouline Publishing [www.assouline.com], New York, 2008. US$18.95

Assouline Publishing has a reputation for releasing sparkling and glamorous books with pretty pictures worthy of the coffee table, and its profile of Mikimoto is no different. This slim book is equal parts biography of Kokichi Mikimoto (1858–1954), timeline of the company he founded at the turn of the 20th century, and broad history of the pearl itself. Nick Foulkes, the British journalist and historian known as much for his dapper appearance as for his reporting, has written on luxe topics such as trench coats, the Marbella Club, Bentleys, and the rise of America's upper class. And with Mikimoto's pearls, Foulkes imparts the same nostalgic sheen with which he inevitably coats each of his subjects.

Foulkes begins with a comprehensive overview of the pearl throughout history, focusing on its myths and legends, its literary and artistic references, and its popularity among rulers of all cultures and civilizations. In fact, his detailed account of the various queens and kings who worshipped the pearl may draw more attention than Mikimoto's own life and company history. Did you know, for example, that Cleopatra had a taste for pearls dissolved in vinegar?

Foulkes then delves into Kokichi Mikimoto's childhood and early youth, highlighting his humble origins as the son of a noodle maker, his involvement in "marine product" (the arrangement of pearl, mother-of-pearl, and shellfish displays), and his marriage to Ume, a member of the samurai social elite. It is said that the untimely death of Ume at the age of 32 propelled him to work tirelessly at perfecting his brand and product in the ensuing years.

The history of the company is described as a quick ebb and flow of successes and setbacks: Mikimoto and Ume creating their first cultured pearls in 1893 (despite a devastating case of red tide that had killed more than 5,000 oysters the previous year), his first success in culturing perfectly spherical pearls, the opening of his first shop—in Tokyo's Ginza district—in 1899, the company's difficulties during World War II, and its swift resurgence afterward.

What is absent from the history of Mikimoto's pearl business is any discussion of his competition. Foulkes says that Mikimoto was backed by naval officer Yanagi, and relied on previous studies by Professor Kakichi Mitsukuri in his quest to assist nature in culturing pearls, but he does not mention the work of others such as Tokichi Nishikawa or Tatsuhei Mise. Likewise, his discussion of the company's grading scale and practices is never balanced by any perspective from authorities outside the Mikimoto organization.

The second half of the book is composed solely of photos, provided by Mikimoto or taken from fashion magazines, that highlight cultured pearl trends over the 20th century. These photos are the most worthwhile element of the book, as they include some of Mikimoto's most famous and exquisite designs, such as Yagurama ("Wheels of Arrows") from the World Exposition of Paris in 1937, shown in both its deconstructed form and its assemblage as a sash clip.

The book appeals to the same audience as every other volume in Assouline's inventory: the social elite and those aspiring to the top. Foulkes is no stranger to this audience, and judging from the way he praises the brand's quality and immortality, it seems that he might sell a strand of Mikimoto's cultured pearls better than any sales clerk at Saks or Bergdorf.

SHANNON ADDUCCI
New York

The Occurrence of Diamonds in South Africa

By M. G. C. Wilson, N. McKenna, and M. D. Lynn; 105 pp. with two wall charts, illus., publ. by Council for Geoscience [www.geoscience.org.za], Pretoria, South Africa, 2007. US$68.00

This is a slim softcover book on diamond occurrences in South Africa. It does not focus on the geology of diamond deposits or the mineralogy and chemistry of kimberlite or the crystallography of diamond, but rather it describes the various deposits in South Africa, both primary and secondary, where diamonds have been found. The first 20 pages present a good summary of our general knowledge of diamond: physical properties;

classification of gem, industrial, and synthetic diamonds; the history of diamond discoveries; the diamond market; classification and genetic models of diamond deposits; ages of intrusion of kimberlites; and methods of exploration for kimberlites and alluvial diamond deposits. Not discussed are the subjects of nitrogen atoms in the diamond lattice, the division of diamonds into different types, and carbon and nitrogen isotopes in diamond. Further, the two kimberlite groups (I and II) and the role of indicator minerals in diamond exploration are only briefly mentioned. However, these omissions are unavoidable in a concise, easily understood text.

There are, however, errors that should have been avoidable. In the section on history of discoveries, it is correct that the town of Kimberley was named in 1873 after Lord John Wodehouse, the first earl of Kimberley, who was at the time the Secretary for the Colonies in London. He was not, as is stated on page 8, the governor of South Africa and high commissioner for southern Africa. Nor was the first diamond found on the farm Dorstfontein. In April 1860, that large farm had been divided into Dutoitspan, Bultfontein, and Vooruitzigt, and the first diamond was found in the mortar of the farm house on Dutoitspan.

The section on primary sources contains two beautiful and instructive full-page color illustrations (figures 2 and 5 on pp. 13 and 16) on the origin of diamond and the intrusion of kimberlite pipes. However, it appears that the color coding for the shale and sandstone in the stratigraphic profile in figure 4 (p. 15) has been reversed. Also, it is difficult to distinguish the color coding of the maps in figure 6 (p. 19) and figure 7 (p. 22), depicting the different groups of kimberlite and their ages; nor is it adequately explained what the symbols K1, K2, K12, and K21 represent. It also comes as a surprise to see in figure 8 (p. 22) that 67% of the South African kimberlites fall in the 120 Ma age group, as all the traditionally known and economic kimberlites around Kimberley are in the 80–85 Ma group. The editor should have spotted that the y-axis of figure 9 (on p. 30), representing South Africa's percentage of world production, goes up to the 120% mark.

The sections on the distribution of kimberlites in relation to structural/tectonic features and on the genesis of alluvial deposits and their methods of exploration are well described and easy to understand. While primary deposits are discussed in just 20 pages, alluvial deposits receive a 50-page treatment, since the book is aimed at those who might invest in the less capital-intensive alluvial mining sector.

The book is accompanied by two large maps printed on sturdy, glossy paper. The main map, "Diamond Deposits and Kimberlites of South Africa, Lesotho and Swaziland," is derived from the De Beers database for this area. Simplified geology is shown in color on the map and in the legend, and every diamondiferous kimberlite and alluvial diamond deposit appears on the map and in the legend. The symbols for kimberlites are color coded (K1, K2, etc.) but again difficult to distinguish and inadequately explained. The second map, "Alluvial-Diamond Occurrences of the Northwest Province," highlights farms on which mining licenses have been issued, historical production is recorded, and recent workings have been confirmed by field visits. This is the region between Mafikeng-Lichtenburg-Ventersdorp to Potchefstroom in the north and Schweizer Reneke-Wolmaransstad to Bloemhof in the south. Scrutinizing the map and the text, one can see that that not all alluvial deposits have been investigated in detail and additional economic ventures may await.

In summary, this is a most useful book for readers familiar with South Africa. For casual readers, the information on individual occurrences is perhaps a bit too specific and detailed.

A. J. A. (BRAM) JANSE
Archon Exploration
Perth, Western Australia

Gemlore: Ancient Secrets and Modern Myths from the Stone Age to the Rock Age

By Diane Morgan, 232 pp., publ. by Greenwood Press [www.greenwood.com], Westport, CT, 2008. US$55.00

Gem lore arises from a constellation of sociocultural beliefs and traditions. The universally appealing mystique that surrounds gems springs from imagination and magical thinking that morphs and mutates on contact with real people and events. *Gemlore* compiles many of gems' greatest fables and twice-told tales, multiplied exponentially over the ages.

Prolific author Diane Morgan is adjunct professor of religion and philosophy at Pennsylvania's Wilson College. She has written many books on related subjects, such as emerald's mystique and Eastern religious experiences in American life. As she conveys in her excellent introduction, Morgan appreciates the power of belief as perhaps the strongest magic of all.

Morgan chooses to profile 34 gems long associated with mythical powers—most of which were well known to the world's ancient and distant civilizations—such as lapis lazuli, peridot, and the chalcedonies. Whether a gem is revered by denizens of the 21st century or has been relegated to the dungeons of fashion, the author addresses each with humility and respect.

Each chapter begins with a synopsis of the gem's hardness, chemical composition, geographic distribution, and other physical information. Next are the stone's mystical links with planetary bodies, zodiac signs, anniversaries, chakras, and dream meanings.

Morgan's narrative provides cross-cultural accounts of each gem's lore as it courses through ancient civilizations to modern crystal healers. While many of these tales will be familiar to gem and birthstone enthusiasts, Morgan entertains readers with obscure associations, historical quotes, and tidbits of medical anthropology. Contemporary gem and crystal healers

give older tales a modern-to-occult twist, thereby tweaking each stone's lore with a new spin that may seed further myth and mystery for future generations.

The author's unconventional sourcing style contributes to a sometimes staccato narrative. Shunning footnotes, Morgan instead employs frequent quotation marks and repetitive attributions to her short list of references. In contrast to each chapter's synoptic opening, the narrative drifts between epochs and occasionally loses organizational structure. References to the teachings of Greco-Roman physician Galen are followed in nearly the same breath by comments from a modern crystal writer who calls herself Melody. Are they truly all the same?

Morgan relies heavily on the *Book of Secrets*, a text the author calls a compendium of 2,000 years of gossip, which may date to at least the 13th century. While the brief bibliography gives modern sources—heavily represented by crystal therapists—no reference to *Secrets* is provided. The book's index, however, is commendable.

Gem enthusiasts and those interested in the symbolic allure of gems should find this book enjoyable, if not indispensable. Morgan's wry and often unexpected wit adds a dose of humor, while her informed perspective provides readers with an engaging roundup of gem magic's relentless grip on our collective imagination.

MATILDE PARENTE
Libertine
Indian Wells, California

Gems & Jewelry Appraising: Techniques of Professional Practice, 3rd Ed.

By Anna M. Miller, edited by Gail Brett Levine, 235 pp., illus., publ. by Gemstone Press [www.gemstone-press.com], Woodstock, VT, 2009. $39.99

This third edition of the late Anna Miller's classic guide is better described as a new-century update, and it does an admirable job of bringing one of the first "how-to-be-an-appraiser" books up to the present day. Edited by Gail Brett Levine, a renowned jewelry appraiser in her own right and a self-described protégé of Miller's, this latest edition follows the organization of its predecessors, eliminating most obsolete entries and adding important new information. The subtitle is what the book is really about—it lays out much of what a jewelry appraiser may encounter in the daily, weekly, or monthly practice of the profession.

In speaking to the novice, the book discusses what a professional appraiser is, explains how to open a practice, and answers key questions for the uninitiated. It continues with the basic appraisal concepts of purpose and function and limiting conditions, and handling the typical insurance appraisal. Most of the significant elements of the process are addressed, section by section, with new information superseding that from previous editions. For example, the discussion of digital photography, which did not exist in the first edition and was only in its infancy in the second, now reflects the current state of the art.

The characteristics of value in various gem categories have been updated where necessary (i.e., treatments, synthetics, etc.), with an expanded section on pearls to reflect how much that sector of the trade has grown. Not surprisingly, the sections on period and ethnic jewelry are largely unchanged, but there have been revisions to the sections on coins and silver flatware and hollowware. The appendix with charts, tables, and sample reports has been expanded, as have the glossary and bibliography. One disappointing element is that the same black-and-white photographs from the first edition are still being used, with a few more added in the new sections.

Where the book falls short is in reminding the reader about the importance of actual *experience* in the trade. Seemingly hidden among the pages are a few key statements, such as, "Recognizing the limits of your knowledge and getting help when needed will keep you out of trouble" (p. 127). The danger of not repeating this idea regularly is that it might lead novices to think they only need to read a "how-to" book, take a few classes on theory, and do some online research to somehow bypass the many years, if not decades, of trade experience required to become a true professional appraiser.

Overall, this new edition for the 21st century provides a good starting point for the novice and a wealth of reference information for the veteran appraiser.

CHARLES I. CARMONA
Guild Laboratories, Inc.
Los Angeles

OTHER BOOKS RECEIVED

The Opal Story: A Guidebook. *By Andrew Cody and Damien Cody, 39 pp. with DVD supplement, illus., publ. by the authors [www.nationalopal.com], Melbourne, Australia, 2008, US$37.00.* This wonderful, beautifully illustrated and produced little book is best described as a love letter to opal. Into less than 40 pages, the authors have packed virtually everything the beginning opal enthusiast could want to know about this stone's history, formation, mining, production, characteristics, care, and basic valuation. A seven-minute DVD supplement is included.

TWO

Growth and Morphology of Quartz Crystals Natural and Synthetic. *By Ichiro Sunagawa, Hideo Iwasaki, and Fumiko Iwasaki, 202 pp., illus., publ. by Terrapub [www.terrapub.co.jp], Tokyo, 2009, ¥7500.* This book details the growth and morphology of natural and synthetic quartz. The growth of chalcedony and opal is also addressed.

TWO

09 GEMOLOGICAL Abstracts

COLORED STONES AND ORGANIC MATERIALS

Einige Gedanken zu Jadeit-Jade [Some thoughts about jadeite-jade]. H. A. Hänni [h.a.haenni@freesurf.ch], *Gemmologie: Zeitschrift der Deutschen Gemmologischen Gesellschaft*, Vol. 57, No. 1–2, 2008, pp. 5–12 [in German].

This article addresses three issues: Why is jadeite not transparent? Why is most jadeite green? Why is the chemical composition not always constant? The answer to the first question is the polycrystalline structure of jadeite: Light is scattered at the grain boundaries. The transparency of the stone is essentially influenced by the size and homogeneity of the grains, and can be clearly enhanced by filling of the pores. The answer to the other two questions can be found in the fact that jadeite, $NaAlSi_2O_6$, forms a solid-solution series with kosmochlor, $NaCrSi_2O_6$. Isomorphic replacement of Al by Cr in jadeite correlates with increasing green color. Jadeite also forms a solution series with omphacite, a Ca- and Fe-bearing clinopyroxene. Variations in jadeite composition are due to isomorphic replacement by kosmochlor and omphacite components. A new standard introduced in Hong Kong allows for small amounts of these impurities in jadeite, as long as a specific gravity of 3.4 and a refractive index of 1.688 are not exceeded. This type of jadeite is called *Fei Cui* in China. *RT*

The geochemistry of gem opals as evidence of their origin. E. Gaillou [eloise.gaillou@cnrs-imn.fr], A. Delaunay, B. Rondeau, M. Bouhnik-le-Coz, E. Fritsch, G. Cornen, and C. Monnier, *Ore Geology Reviews*, Vol. 34, 2008, pp. 113–126.

The authors provide evidence that the geologic and geo-

This section is designed to provide as complete a record as practical of the recent literature on gems and gemology. Articles are selected for abstracting solely at the discretion of the section editors and their abstractors, and space limitations may require that we include only those articles that we feel will be of greatest interest to our readership.

Requests for reprints of articles abstracted must be addressed to the author or publisher of the original material.

The abstractor of each article is identified by his or her initials at the end of each abstract. Guest abstractors are identified by their full names. Opinions expressed in an abstract belong to the abstractor and in no way reflect the position of Gems & Gemology *or GIA.*

graphic origin of opals can be deduced from the concentrations of the main impurities (defined as >500 ppm) and trace elements (<500 ppm) they contain. Based on a study of 77 gem-quality opals and 10 host rocks from 10 countries, they concluded that the chemical composition of an opal is genetically linked to that of its host rock. This conclusion appears to hold true for both forms of play-of-color opal (amorphous opal-A and poorly crystalline opal-CT), regardless of the amount of weathering the host rock has endured. The Ba and rare-earth element (REE) concentrations of the gem opals and their host rocks were nearly identical, suggesting that the opals were derived from fluids that circulated through those same rocks. Opals from sedimentary environments were shown to have relatively high Ba concentrations (118–300 ppm) and "typical" REE patterns (depletion from light REE to heavy REE, without any noticeable Eu or Ce anomalies). Opals with volcanic origins had lower Ba concentrations (<110 ppm) and typical REE patterns, along with a negative anomaly for Eu and, depending on oxidation conditions, a positive or negative anomaly for Ce. Geochemical data for Mexican opals from volcanic host rocks and Australian opals from sedimentary sources are used to illustrate these relationships.

While there are sufficient differences in geochemical signatures to determine opal provenance at the regional scale, identifying more specific geographic sources (such as mines) within the same geologic setting requires further study. With additional geochemical data on more samples, along with other observations such as inclusion analysis, the approach described here could be developed into a method for fingerprinting the provenance of play-of-color opals. Other observations linked a high iron concentration (>1000 ppm) to suppressed luminescence and darker colors (from yellow to brown) in opal. Green luminescence in opal is associated with minute amounts of uranium (<1 ppm).

KAM

Identification visuelle des différents ivoires [Visual identification of different types of ivory]. I. Reyjal, *Revue de Gemmologie*, No. 164, June 2008, pp. 22–27 [in French].

Ivory is defined as material originating from the dentition of one of seven animal species: elephant, mammoth, warthog, hippopotamus, walrus, sperm whale, and narwhal. The visual characteristics of ivory from each of these sources are described, including size, color, polish, growth patterns and lines, and Schreger angles (the angles between the cross-hatched lines seen in cross section). These characteristics help identify ivory and distinguish its origin. Two frequent ivory substitutes are also described: the endosperms of tagua palm trees (vegetable or palm ivory) and the casques of helmeted hornbill birds (hornbill ivory). *RT*

Inside rubies. C. P. Smith, C. R. Beesley, E. Q. Darenius, and W. M. Mayerson, *Rapaport Diamond Report*, Vol. 37, No. 47, 2008, pp. 140–148.

Fine-quality Burmese rubies set the standard by which rubies from other parts of the world are judged. However, Burmese rubies recently became a subject of U.S. legislation—the Tom Lantos Block Burmese JADE (Junta's Anti-Democratic Efforts) Act of 2008.

Dealers prohibited from supplying Burmese rubies to the U.S. market are looking for alternate ruby sources, and the authors indicate there are about 20 other countries. These deposits are concentrated in two regions where major orogenic episodes have occurred. One of these events produced the Himalayas and several associated mountain chains ~55 million years ago (Ma); this ruby-bearing region extends from Afghanistan, Pakistan, and Tajikistan, into Nepal and east to Myanmar and Vietnam. The other event, the Pan-African Orogeny (800–450 Ma), is responsible for ruby deposits in southern India, Sri Lanka, Madagascar, and East Africa. Rubies that formed during orogenic episodes are typically related to metamorphic growth conditions, with the finest-quality stones hosted by marbles. However, some deposits have a magmatic origin; that is, the rubies formed in the mantle and then were transported to the surface during eruptive events.

One of the authors (CPS) devised a ruby classification scheme to differentiate rubies' geologic origins—metamorphic or magmatic—based on their gemological features. The latter pages of the article illustrate this scheme, with photomicrographs of (1) internal features that differentiate stones from various localities and (2) the principal treatments used on rubies. *AB*

Weight of production of emeralds, rubies, sapphires, and tanzanite from 1995 through 2005. T. R. Yager, W. D. Menzie, and D. W. Olson, *U.S. Geological Survey Open-File Report 2008-1013,* 2008, 9 pp., http://pubs.usgs.gov/of/2008/1013.

Estimating colored stone production is inherently difficult due to the nature of the industry (e.g., lack of government oversight or reporting, significant variations in the quality of rough, and countless small-scale mining operations). These factors also undermine effective regulation, and colored stones—like diamonds—have the potential to fund armed conflict and illegal activities. This paper marks the first attempt by the U.S. Geological Survey (USGS) to establish global production statistics by country for emerald, ruby, sapphire, and tanzanite. A table for each gem shows the inferred production of rough (in kilograms) from 1995 through 2005. The study estimates the carat weight of imports to the U.S. from the top five countries of origin. It also discusses various influences on gem production, such as new and declining gem sources, mining operations and technology, and other market factors such as enhancement processes and political pressures. The authors'

sources include annual USGS Mineral Questionnaires returned from producing countries, export data, company reports, and the trade literature. The paper acknowledges that the monetary value of production is even more difficult to estimate because of complex and rapidly changing market variables. Nevertheless, the authors provide for each gem variety: (1) the systems used to value them, (2) the average per-carat values for rough, and (3) the highly variable price ranges for cut goods. *ERB*

DIAMONDS

A colourless natural diamond showing strong orange and mixed coloured fluorescence images. T. Lu, T. Odaki, K. Yasunaga, and H. Uesugi [info@agt.jp], *Australian Gemmologist*, Vol. 23, No. 4, 2008, pp. 337–340.

A 0.31 ct type Ia colorless brilliant-cut diamond was characterized by standard gemological testing, fluorescence imaging, and UV-Vis-NIR, IR, Raman, and photoluminescence (PL) spectroscopy. The sample displayed strong orange fluorescence to long-wave UV radiation, and it showed mixed-color fluorescence when exposed to the ultra-short-wave radiation of the DiamondView. The UV-Vis-NIR absorption spectrum and PL emissions revealed a weak band at 480 nm and a distinct Ni-related doublet in the PL spectrum at 883 and 885 nm. The authors suggest that for this diamond, which did not have the defects that typically produce the 480 nm band, Ni might be a component in the 480 nm band defect and might also play a role in the orange long-wave fluorescence. *RAH*

The iciest ice. M. Kerawala, *CIM Magazine*, Vol. 3, No. 7, 2008, pp. 70–73.

Canada's Diavik diamond mine (operated by a Rio Tinto subsidiary as a joint venture with Harry Winston Diamond Corp.) is undergoing a $700 million expansion to extend its life to 2020 or beyond. This article offers a glimpse of the mine's history and its plans for the decade ahead.

The Diavik mine is located on East Island in the Northwest Territories. The site's entire infrastructure—including an airstrip, housing, and amenities for workers—had to be built from scratch, starting in 2001. While air travel is used year-round, heavier loads can only be delivered during a two-month span when the winter road is open for truckers. This road services three diamond mines and various exploration projects in the region; over 85% of it traverses lake ice and must be constantly monitored. It takes approximately 15 hours to reach Diavik from Tibbitt (a 373 km trip). Shipments must be carefully planned in advance to ensure that all the year's supplies are delivered during those two months.

Safety and environmental savvy are critical to management of the Diavik mine. To help support the community, two-thirds of Diavik employees are local residents, with half of that group being aboriginals. Due to safety concerns in the frigid temperatures, workers are not required to perform any task they deem to be unsafe. Diavik recycles heat from its power plants for use in its shop, processing plants, and housing.

Diavik has already started augmenting the existing infrastructure to support the transition to underground production, which is expected to be completed by 2012. Further development will also take place at an adjacent pipe, where open-pit mining is just beginning and production is expected in late 2009. Diavik plans to continue drilling at a nearby site to better define an unmined pipe. The company also budgeted $10 million in 2008 for an aggressive exploration program on its claim block around the mine site. *Joshua Sheby*

A Northern Star: Canada's first diamond mine celebrates a milestone. D. Zlotnikov, *CIM Magazine*, Vol. 3, No. 7, 2008, pp. 40–43.

In late 2008, the Ekati mine in Canada's Northwest Territories (NWT) celebrated its 10th anniversary of operation. Under its current plan, the mine can remain active until 2020. However, this could be extended to 2040 as long as operating costs are low enough ($50/tonne ore) to exploit less-accessible diamond-bearing pipes. The key to this is maintaining current efficiencies while developing additional cost-saving steps with minimal impact on the environment. Ekati runs entirely on diesel power, though wind and hydropower are being investigated as energy alternatives. To reduce fuel consumption and greenhouse gas emissions, Ekati has implemented several measures, such as installing motion-sensing light switches in offices, recycling waste heat from generators, and minimizing the idling time of vehicles.

To ensure that northern residents benefit from the diamond wealth being extracted, Ekati has four Impact Benefit Agreements with aboriginal landowners and a Socio-Economic Agreement with the Northwest Territories government. Although Ekati is only contractually obligated to spend 70% of its money within the NWT, it consistently exceeds that amount (e.g., 81% in 2007). In fact, diamond mining and processing now account for 40% of the NWT's gross domestic product. Besides spending money within the community, Ekati hires and trains NWT natives (67% of its workforce, 39% of whom are local aboriginals). The mine also encourages local schoolchildren to complete their education by showing them opportunities awaiting them at the mine after they finish school. As a result, more high school students are graduating and actively seeking higher education. In supporting the environment and the community, Ekati has played a significant role in the Northwest Territories.

Joshua Sheby

The origin of cratonic diamonds—Constraints from mineral inclusions. T. Stachel [tstachel@ualberta.ca] and J. W. Harris, *Ore Geology Reviews*, Vol. 34, 2008, pp. 5–32.

Mineral inclusions in diamonds provide unique information on both (1) the physical and chemical environment deep in the earth's mantle, and (2) the conditions under which diamonds form. This article reviews the geologic origin of diamonds formed in the mantle beneath continental cratons on the basis of geochemical data for nearly 5,000 silicate, oxide, and sulfide mineral inclusions. These different kinds of inclusions are conventionally divided into three categories that represent their principal mantle source rocks. Peridotitic inclusions appear to be related to rocks of peridotite composition that originated by melt extraction in Archean equivalents of mid-ocean ridges or similar shallow, low-pressure environments. Eclogitic inclusions broadly reflect more basaltic source compositions, again in shallow environments along subduction zones. Websteritic inclusions are less well defined, but they appear to originate from pyroxenitic source rocks intermediate in composition between peridotite and eclogite. Geothermometry data suggest that diamonds with all three types of inclusions formed and then were kept under similar thermal conditions in the mantle. Depths of formation are believed to have been <200 km, with the diamonds precipitating from upward-percolating carbonate-bearing melts/fluids. *JES*

GEM LOCALITIES

Ambre mésoaméricain [Mesoamerican amber]. G. L. Cattaneo [ambar@ambarweb.it], *Revue de Gemmologie*, No. 165, 2008, pp. 9–16 [in French].

This article reports on Mesoamerican amber from the Dominican Republic and central Chiapas, Mexico. Dominican and Mexican ambers come from related leguminous *Hymenaea* trees. The estimated ages of these ambers vary from 20 to 17 Ma (Miocene) and 30 to 20 Ma (Oligocene to Miocene) for Dominican amber, and 26 to 22 Ma (Oligocene to Miocene) for Mexican amber. Mesoamerican amber contains no succinic acid and is therefore classified as retinite. Mesoamerican ambers come in many natural colors, mainly different shades of yellow but also some rarer orange-"cognac," "cognac," and "cherry"-red hues. Most Mesoamerican amber has a high degree of transparency and, unlike Baltic amber, does not need to be clarified. However, the presence of organic (and rarely inorganic) inclusions may result in low-quality brownish yellow to brown to blackish brown specimens. Dominican and Mexican ambers can have a beautiful green-blue or blue-violet-green fluorescence, best seen with reflected light (especially sunlight). Rare "blue" amber is mined only at La Cumbre in the Dominican Republic, where the average annual yield does not exceed 25 kg. Its intense fluorescence in reflected light suggests the presence of perylene hydrocarbons.

Since 1996, a rare variety of red amber has been mined almost exclusively in Chiapas, and 2007 production was estimated at no more than 10 kg. The red color is due to an external oxidation layer caused by contamination from percolated water saturated with iron compounds. Some rare green amber from Chiapas (<0.6 kg mined annually) is said to be colored by the effects of colloidal dispersion of organic particles present in the "amber macromolecule."

The majority of Dominican amber is mined from secondary deposits and occurs in layers of lignite or carbonaceous clay interspersed with beds of sandstone. Mexican amber comes from primary deposits and occurs in lenses of lignite interspersed with carbonaceous layers. *FP*

Color-change apatite from Kazakhstan. A. A. Zharinov, V. V. Ponomarenko [mineralvvp@yandex.ru], and I. V. Pekov, *Rocks & Minerals*, Vol. 83, No. 2, 2008, pp. 148–151.

Large crystals of apatite exhibiting a distinct color change have been produced from the Akzhailyau Mountains of Kazakhstan. The area is located in the Semipalatinsk region in the eastern part of the country near the border with China. These mountains consist of three parallel ridges that attain a maximum elevation of ~1500 m. The apatite is found in quartz-feldspar pegmatite bodies that are associated with granites comprising a large exposed pluton. Pegmatites were first found in the area in the mid-1940s, and some 200 sizeable bodies have produced large crystal-filled pockets containing quartz, feldspar, micas, apatite, and several rare minerals. One large pegmatite pocket measured about $4 \times 4 \times 4$ m in volume. The prismatic apatite crystals measure up to 6 cm long, and vary from translucent to transparent. They appear yellowish brown in daylight, pink under incandescent light, and greenish yellow in fluorescent light. Possible inclusion minerals in the apatite are monazite, albite (cleavelandite), muscovite, and dark smoky quartz. Electron microprobe analysis revealed the presence of various rare-earth elements (Ce, Nd, La, Sm, and Pr) in the apatite, which may account for the color-change behavior. Stones up to 15 ct have been faceted from this material. *JES*

Opali di fuoco del Brasile [Fire opals from Brazil]. F. Caucia, C. Ghisoli, and V. Bordoni, *Rivista Gemmologica Italiana*, Vol. 3, No. 3, 2008, pp. 179–188 [in Italian].

While most fire opals come from the well-known Mexican deposits, they are also mined from a number of smaller deposits in Oregon (Opal Butte), Indonesia, and Ethiopia. In the 1970s, fire opals were discovered in Brazil: near Campos Grande (in Rio Grande do Sul State), São Geraldo do Araguaia (Pará State), and Castelo do Piauí (Piauí State). The authors studied a number of yellow-to-red fire opals

from Brazil by standard gemological techniques, powder X-ray diffraction, scanning electron microscopy, and LA-ICP-MS, and the results were compared with data for fire opals from other sources. Measurements of SG and RI alone were not diagnostic of origin, and Fe was confirmed as the cause of the orange bodycolor. *RT*

Ornamental variscite: A new gemstone resource from Western Australia. M. Willing [margotwilling@iinet.net.au], S. Stöcklmayer, and M. Wells, *Journal of Gemmology*, Vol. 31, No. 3/4, 2008, pp. 111–124.

This article provides an in-depth characterization of variscite from Woodlands Station, Western Australia, including its geologic occurrence and mineralogical associations. Data obtained from standard gemological testing and petrographic thin section analysis, as well as SEM-EDS, XRD, EDXRF, and Vis-NIR reflectance spectroscopy, are summarized in numerous figures and tables.

The authors include an overview of variscite occurrences and mining worldwide, which is supplemented by a detailed look at archeological finds from the Neolithic period and the Roman Empire (when it was often referred to as *callais* or *callainite*). Despite the long history of variscite mining, there are few sources of ornamental-quality material, and most of the goods on the market come from stockpiled rough mined in Nevada or Utah. The Woodlands Station deposit represents an important new source of variscite, and its distinctive textural characteristics yield attractive *objets d'art*.

The variscite is hosted in siltstone and occurs in two textures: fibrous and equigranular. Color photos illustrate the wide range of its appearance. Reflectance spectroscopy indicates that while Cr^{3+} is the main chromophore, variscite can also incorporate vanadium in several oxidation states. X-ray diffraction analysis confirms it to be "Meßbach-type" in association with metavariscite, a dimorph of variscite. Inclusions of elemental gold form a rare feature: discrete platelets or granules that are easily visible in dark green variscite. Matrix material was shown to consist of iron oxides, quartz, crandallite, and alunite. *ES*

The Woodlands variscite–gold occurrence in the north Gascoyne region of Western Australia. E. H. Nickel, R. M. Hough, M. R. Verrall, E. Hancock, A. M. Thorne, and D. Vaughan, *Australian Journal of Mineralogy*, Vol. 14, No. 1, 2008, pp. 27–36.

The Woodlands variscite occurrence, near Mt. Egerton, is located in an area of phosphate mineralization within a zone ~0.5 m thick that can be traced for at least 1 km; it consists of several thin seams 10–50 mm thick. Viewed in hand specimen, the variscite is typically bluish green with irregular yellowish brown patches consisting mostly of crandallite, making it attractive gemological material. The color of the variscite varies from white to dark bluish green and appears to depend on grain size. EDXRF and SEM-EDS analyses of the variscite show an appreciable but variable Si content, 1–3 wt.% Fe, up to 0.2 wt.% Cr, and up to 0.4 wt.% V. Gold is observable in some of the variscite from the main vein, with an overall content of 17 ppm Au. The paragenesis is also discussed. *RAH*

Winza rubies identified. A. Peretti [adolf@peretti.ch], F. Peretti, A. Kanpraphai, W. P. Bieri, K. Hametner, and D. Günther, *Contributions to Gemology*, No. 7, 2008.

The authors present the results of a characterization study of gem rubies and sapphires from a relatively new locality near the village of Winza in central Tanzania. Since high-quality rubies were accidentally discovered in this remote region in the fall of 2007, artisanal miners have recovered stones at the surface or in vertical shafts from an area covering several square kilometers.

This report begins with a summary of the region's geology. The rubies occur in association with amphibolites as rhombohedra or as tapered prismatic euhedral and subhedral crystals up to several centimeters long in a garnet-pargasite host rock. Weathering of the host rock near the surface distributed loose corundum crystals in the soil. Most are red to purplish red (occasionally violet or blue). In many instances, the corundum displays internal color zones with banded or irregular areas that are blue, pink, or both. Solid inclusions identified include apatite, chlorite, garnet, pargasite, pyrite, spinel, and talc. Whitish particle clouds and both primary and secondary fluid inclusions are also common, as is crystallographic growth zoning. Especially distinctive in Winza rubies are flat or needle-like inclusions, the latter exhibiting unusual curved or spiral patterns in some cases.

Minor and trace-element data obtained by LA-ICP-MS analysis showed small amounts of Ni (up to ~25 ppm), an unusual trace element in natural corundum. Multiple analyses along the traverses of color-zoned crystals correlated trace-element contents with coloration. Heating experiments on Winza rubies using traditional techniques were not very successful, producing orange coloration and diminishing transparency. Heat treatment appears to be detectable by infrared spectroscopy. *JES*

INSTRUMENTS AND TECHNIQUES

Identification of taaffeite and musgravite using a non-destructive single-crystal X-ray diffraction technique with an EDXRF instrument. A. Abduriyim [ahmadjan@gaaj-zenhokyo.co.jp], T. Kobayashi, and C. Fuduka, *Journal of Gemmology*, Vol. 31, No. 1/2, 2008, pp. 43–54.

Taaffeite ($Mg_3Al_8BeO_{16}$) and musgravite ($Mg_2Al_6BeO_{12}$) are mineral species that belong to the taaffeite mineral group. Both are optically uniaxial and have hexagonal lattices, and they have similar chemical compositions and crystal

structures. Because of these shared characteristics, they cannot be distinguished through standard gemological testing. Taaffeite and musgravite are differentiated only by their symmetries (hexagonal vs. trigonal, respectively) and different lattice-cell constants. Techniques with high resolution and accuracy—such as single-crystal and powder X-ray diffraction, electron microprobe analysis, and Raman spectroscopy—are also effective in distinguishing the minerals. This article describes an EDXRF instrument modified for use as a single-crystal X-ray diffraction apparatus. It operates using a special rotating and tilting stage that nondestructively determines diffraction patterns to distinguish the minerals according to their symmetries, unit-cell dimensions, and space groups. *GL*

Magnetic susceptibility, a better approach to defining garnets. D. B. Hoover [dbhoover@aol.com], C. Williams, B. Williams, and C. Mitchell, *Journal of Gemmology*, Vol. 31, No. 3–4, 2008, pp. 91–103.

Using a new, nondestructive method of gem testing, the authors demonstrate how the major end-member composition of any garnet can be confidently predicted by plotting its RI against measured magnetic susceptibility. On this diagram, eight end-member garnets are plotted so that any unknown sample can be placed in the appropriate ternary area. This method shows how previous methods of identifying garnets (e.g., by their color, RI, and absorption spectrum) are inadequate to correctly identify mineral compositions within the garnet group. Magnetic susceptibility measurements (as opposed to determination of the unit cell dimensions) can be carried out with inexpensive equipment available to most gemologists and mineralogists. *RAH*

Specular reflectance infrared spectroscopy—A review and update of a little exploited method for gem identification. T. Hainschwang [thomas.hainschwang@gemlab.net] and F. Notari, *Journal of Gemmology*, Vol. 31, No. 1/2, 2008, pp. 23–29.

Vibrational spectroscopy, which comprises Raman and infrared spectroscopy, is a very important tool in gemological analysis. However, Raman systems are expensive, and infrared spectroscopy may require destructive sectioning or powdering of the investigated material. This article describes an alternative: specular reflectance infrared spectroscopy. This method detects only those peaks due to major compositional components of a material. Because of this sensitivity to chemical composition and molecular coordination, such a spectrum serves as a fingerprint of a material.

The authors have been building an extensive database of specular reflectance FTIR spectra since 2001. Any material can be rapidly identified if the matching reference spectrum is available. Even in the absence of a reference spectrum, an experienced user can obtain significant clues to a material's identity by relating its major peaks to those of a mineralogical group. The technique is also useful for identifying jewelry-mounted gemstones or very small surface-reaching inclusions. Its speed, precision, and relatively low cost make it an important tool for gemological laboratories. *GL*

JEWELRY HISTORY

The innovative techniques and unusual materials of Art Nouveau jewelry. Y. J. Markowitz and S. Ward, *Antiques*, Vol. 174, No. 1, 2008, pp. 56–63.

During the Art Nouveau movement (roughly, from the 1890s up to the First World War), a small group of avant-garde European artists helped redefine and revolutionize the design and fabrication of what had become a tired and predictable art form. Complex adornments were often fabricated from parts that could be assembled to fit elaborate armatures that allowed the wearer to display the piece in different ways (e.g., as either a brooch or a hair ornament). Metal treatments such as oxidation were also used to achieve different effects and act as a foil for enamels and other materials.

Part of the innate charm of Art Nouveau jewels is their use of unusual and often inexpensive materials in artistic designs produced with consummate technical skill. Horn was first used by René Lalique at the Salon of the Société des Artistes Français in 1896, and was quickly adopted by other Continental jewelers, including Gaillard, Vever, and Aucoc. Lalique and Gaillard were noted for treating some portions of their designs to produce a delicate iridescent "bloom" on the surface of the horn. Other "unusual" materials included glass and enamel, which were sometimes combined masterfully by Lalique. Detailed photos complement the descriptions of fabrication and manufacturing techniques. Each item is analyzed in terms of construction, materials, finish, and design.

The jewelry in this article is from an exhibition titled "Imperishable Beauty: Art Nouveau Jewelry," which was at the Museum of Fine Arts in Boston in 2008 and will be on view at the Cincinnati Art Museum from October 24, 2009, to January 25, 2010. *JEC*

Rocks solid. S. Cooperman, *Forbes*, December 8, 2008.

Art Deco jewelry has always been popular among serious collectors, but it may also have investment possibilities. The cachet of Art Deco has been on the rise since the late 1970s, following a long period when it was out of favor (with some pieces even being disassembled for resale). Despite its increasing popularity, auction houses have repeatedly underestimated the value of the pieces, as evidenced by their sales prices being well above their auction estimates. Demand is expected to stay high, since Art Deco was an era of limited production when jewelry craftsmanship was at its peak.

The introduction of platinum enabled Cartier to start the monochrome or "white-on-white" trend, and Van Cleef adopted it for its innovative "invisible" settings. Baguette-, trapezoid-, and trillion-cut stones were introduced during this period. When color came into vogue, the "fruit-salad" style was created, incorporating contrasting gem materials such as "crystal," turquoise, malachite, lapis lazuli, coral, onyx, and jade; pieces with Cartier's "tutti-frutti" style are still among the most sought-after designs. The discovery of King Tut's tomb in 1922 also had an impact on the period, which saw Van Cleef depicting pharaohs and Cartier using scarabs. Art Deco pieces without colored stones and diamonds also exist, created by independent jeweler-artists whose unconventional designs were entirely outside the realm of the traditional motifs established by the big jewelry houses. Signed Art Deco pieces command a premium at auction, but unsigned work with fine craftsmanship should not be dismissed. Collectors must be patient now that Art Deco jewelry is getting harder to find.

Michele Kelley

Study of the provenance of Belgian Merovingian garnets by PIXE at IPNAS cyclotron. F. Mathis [francois.mathis@ulg.ac.be], O. Vrielynck, K. Laclavetine, G. Chene, and D. Strivay, *Nuclear Instruments and Methods in Physics Research B*, Vol. 266, 2008, pp. 2348–2352.

A 2002 road excavation in the Walloon area of Belgium uncovered a 5th century cemetery containing 436 tombs. Archeological excavations led to the discovery of about 60 jewels inlaid with red garnets. The PIXE technique was used to analyze the garnets, utilizing a 3.1 MeV proton beam at the IPNAS cyclotron of the University of Liege, Belgium. The garnets had a mostly homogeneous composition and thus were probably from a single source. The study confirms that PIXE in external-beam mode is a powerful tool for evaluating the provenance of archeological garnets. *DAZ*

JEWELRY RETAILING

A diamond is forever . . . but the hard-hit jewelry industry is in a state of flux. S. Buxbaum, *The Secured Lender*, November/December 2008, pp. 64–66.

Traditional retail jewelers have been affected more severely than many others by the economic downturn. However, the industry is also witnessing a deep competitive shift toward internet sellers. The author chronicles the success of internet retailer Blue Nile and quotes a prediction by the Jewelers Board of Trade that many mid-market independent stores will probably go out of business during the next five years. Lenders who take jewelry in secured lending transactions must be aware that its value can be subjective, influenced by fashion and workmanship. *RS*

Economic downturn: A challenge or opportunity? *Jewellery News Asia*, No. 293, 2009, pp. 50–52.

Manufacturers of stylish jewelry made from alternative (non-precious) metals have an opportunity to gain sales among hard-pressed middle-income consumers in Asia. In addition, manufacturers of such products may find it easier to keep bank financing while gold hovers at a near-record price. Manufacturers are warned against discounting too deeply, because they may need ample profit margins to survive the economic downturn. *RS*

Romancing the stone. K. Field [kfield@chainstoreage.com], *Chain Store Age*, November 2008, pp. 29–31.

Blue Nile, the internet diamond seller, has seen its sales increase from $14 million in 1999—its first year of operation—to $319 million in 2007. According to CEO Diane Irvine, the company operates on a 22% gross margin, compared to an average of 50% for a typical brick-and-mortar jeweler. While the company acknowledged difficulties as the economy deteriorated in the fall of 2008, Irvine said it could remain profitable and poised for growth. *RS*

SYNTHETICS AND SIMULANTS

Effect of seed sizes on growth of large synthetic diamond crystals. C. Zhang [dndzcy@hpu.edu.cn], R. Li, H. Ma, S. Li, and X. Jia, *Journal of Materials Science and Technology*, Vol. 24, No. 2, 2008, pp. 153–156.

The authors grew synthetic diamond crystals via the temperature-gradient method (high pressure and high temperature) using seed crystals ranging from 0.5 to 2.5 mm. All were grown using the same temperature gradient, at 5.5 GPa and 1550 K, in a cubic anvil apparatus. The carbon source was high-purity graphite, and the catalyst/solvent was a Ni-Mn-Co alloy (ratio of 70:25:5 by weight). The growth surface was the (111) face. The diffusion of carbon in the metal solvent was simulated and analyzed by finite element analysis (FEA).

The authors demonstrated that by increasing the seed size and keeping all other variables constant, the crystals grew at a faster rate. However, larger seeds correlated to a decrease in the quality of crystals produced. With a 1.0 mm seed, the resulting diamond had no metal inclusions. A 1.8 mm seed led to a few small, sheet-like metal inclusions, while a 2.5 mm seed resulted in large, blocky metal inclusions. FEA was used to simulate and report on the carbon diffusion process, since actual diamond growth under these conditions cannot be observed *in situ*. FEA showed that the carbon super-concentration at the seed surface is inhomogeneous—it increases symmetrically about the center of the growth surface, where it is lowest. The slower growth rate at the center of the crystal explains why metal inclusions tend to be concentrated there and not on the edges—the growing crystals simply enwrap the molten metal solvent, which quenches to

form solid inclusions when the experiment is terminated. It also explains why a larger growth surface, with a greater difference in carbon concentration and consequently a greater difference in growth rate from center to rim, leads to larger metal inclusions. *JS-S*

L'ambra: i falsi (Parte V) [Amber: The fakes (Part V)]. G. L. Cattaneo [ambar@ambarweb.it] and F. Talami, *Rivista Gemmologica Italiana*, Vol. 3, No. 3, 2008, pp. 189–195 [in Italian].

A considerable number of materials that imitate genuine amber play an important role in the amber market. With the development of plastics, a series of synthetic polymers have been used, especially celluloid, Bakelite, methacrylate (i.e., acrylic glass, Plexiglas, or Perspex), polystyrene, and polyester. Early examples of imitation resins are found in Victorian and Edwardian jewelry dating back as far as 1870. Specific gravities, refractive indices, and characteristic odors produced by hot point testing are given for these materials. During the 1960s to 1980s, a simulant called Polybern was produced in East Germany, Poland, and Lithuania. It was composed of amber fragments and polyester. Frequently, amber fragments are also processed to form "pressed" amber (reconstructed amber). Last, immature natural resins called copal are used as substitutes for genuine amber. Today, most of this material comes from Colombia and Madagascar, with ages of 80–1,000 years (compared to Baltic amber, at 40–50 million years). Inclusions are not conclusive for separating natural, untreated amber from its many simulants. Although natural inclusions (mostly insects and spiders) are highly prized, these can be artificially introduced into both natural amber and amber substitutes. *RT*

TREATMENTS

Enhanced optical properties of chemical vapor deposited single crystal diamond by low-pressure/high-temperature annealing. Y.-F. Meng, C.-S. Yan, J. Lai, S. Krasnicki, H. Shu, T. Yu, Q. Liang, H.-k. Mao, and R. J. Hemley [hemley@gl.ciw.edu], *Proceedings of the National Academy of Sciences*, Vol. 105, No. 46, 2008, pp. 17620–17625.

Single-crystal chemical vapor deposition (SC-CVD) synthetic diamond was grown at very high growth rates (up to 150 μm/hour) by microwave plasma–assisted techniques. The resulting gem-quality SC-CVD synthetic "plates" had faces up to ~1 cm^2 and ranged from 0.2 to 6.0 mm thick. The addition of a small amount of nitrogen to the synthesis gas (CH_4) produced optically homogeneous, hydrogen-containing type IIa brown crystals with low nitrogen content (<10 ppm) and strong, broad UV-visible absorption. The crystals were annealed in a hydrogen environment at low pressure (<300 torr, less than half of atmospheric pressure) and high temperature (up to 2200°C) for several hours without graphitization.

The low-pressure, high-temperature (LPHT) annealing enhanced the optical properties of the SC-CVD crystals, observed as significant decreases in the intensity of spectral features in the UV, visible, and infrared absorption and photoluminescence spectra. Decreases in sharp spectral features indicate a reduction of nitrogen-vacancy-hydrogen defects during annealing, which the authors ascribe to an increase in the relative concentration of nitrogen-vacancy centers in annealed material. The hydrogen-assisted alteration of defect structures in SC-CVD crystals with LPHT annealing is different from the alteration of natural brown type IIa diamonds during HPHT annealing, where decreases in optical absorption are caused by the removal of defects associated with plastic deformation.

The authors note that LPHT annealing of SC-CVD synthetic diamonds to enhance their optical properties can be performed in CVD growth chambers as a post-growth treatment, and is unconstrained by crystal size. LPHT-annealed SC-CVD synthetics may have technical and scientific applications such as in quantum computing. Of gemological interest are the relatively large, gem-quality specimens produced and their decolorization by LPHT treatment. *Emily V. Dubinsky*

Pre-harvest colour-treated akoya unveiled. *Jewellery News Asia*, No. 284, 2008, pp. 60–62.

Tanabe Pearl Farm of Mie, Japan, announced a new treatment process to produce pink, green, blue, and lavender akoya cultured pearls by injecting a colored liquid into the oysters. The developer of the process, Tomokazu Tanabe, claimed the colors were not dyes but "a combination of man's efforts and nature's power." Thus far, the treated akoyas form only a very small percentage of Tanabe's production, and none have been marketed. A Japanese laboratory, the Gem Science Academy of Tokyo, has provided several techniques for identifying them. Their UV-Vis-NIR reflectance spectra are much different from those of untreated or conventionally dyed akoya cultured pearls. In addition, X-radiographs can detect the metallic compounds that were injected into the oysters. *RS*

Visually distinguishing A-jadeite from B-jadeite. J. Li [geoli@vip.sina.com], X. Liu, Z. Zhang, Y. Luo, Y. Cheng, and H. Liu, *Journal of Gemmology*, Vol. 31, No. 3/4, 2008, pp. 125–131.

After first discussing the distinctions between A-jadeite and B-jadeite in the context of the Chinese gem trade, the authors describe visual skills that can aid in the separation of these two types. A-jadeite is defined as material that has been carved and polished, with minimal wax applied to enhance the luster. Mild acid is considered acceptable as a bleaching agent, provided it does not damage the jadeite's structure; also, iron-containing A-jadeite

may be heated to give it a red color. B-jadeite has been processed with strong acid, and the resulting pores filled with wax or polymer resin. C-jadeite (bleached and dyed) is not addressed.

Visual distinctions are described, illustrated with color photos, and discussed in terms of: (1) surface luster or comparative reflectance differences, (2) distribution of color on the surface, (3) internal inclusion patterns, (4) internal behavior of light resembling the adularescence of moonstone, (5) microfractures and their relationship to color distribution, and (6) item size and quality and the intricacy of the carving. For example, the internal yellow glow found in A-jadeite distinguishes it from B-jadeite, which exhibits a white-blue reflection. The underlying reasons for this effect, as well as other observations listed above, are discussed in detail. Careful attention to these features is required for an accurate determination, though the potential for error still exists and advanced laboratory equipment may be required. *ES*

MISCELLANEOUS

Artisanal diamond cooperatives in Sierra Leone: Success or failure? E. A. Levin [enquiries@ddiglobal.org] and A. B. Turay, *Diamond Development Initiative Policy Brief*, June 2008, 4 pp.

In Sierra Leone, a U.S.-led attempt to establish diamond mining and marketing cooperatives is an apparent failure. Between 1999 and 2005, the five cooperatives funded by the Integrated Diamond Management Program, under the U.S. Agency for International Development (USAID), produced 320 stones weighing a total of 60.37 carats, valued at $4,390. This NGO report alleges that there were many reasons for the failure, including USAID's withdrawal of funding for most of the cooperatives, the working of sites with unproven diamond resources, the lack of mining expertise, delays (the country's civil war had not yet ended when the program began), theft, and weather problems. The report recommends that future projects include surveys to study whether the lands actually contain diamonds, pay more attention to local hierarchies in setting up the cooperatives, give adequate training to the diamond diggers, and provide mechanized mining equipment where needed. *RS*

Diamonds, development and democracy. N. Oppenheimer, *World Policy Journal*, Fall 2008, pp. 211–217.

While diamonds and other commodities have fueled civil war and conflict in a number of African nations, these natural resources can assist with growth and development if governments and their citizens choose that direction. The author, chairman of the De Beers Group, notes successes in Botswana, pointing out that well-managed diamond resources have moved that nation from being one of the world's poorest 40 years ago, to one of the most successful economies in Africa today. Botswana can serve as a roadmap for other African countries to establish functioning, effective democracies; deploy natural resources into public goods; and form innovative 50/50 partnerships between government and large investors. The report stresses that, while the West often views Africa as a single entity, it is a continent of 54 separate nations, each with its own strengths and weaknesses. The author ends with a report on the effectiveness of the Kimberley Process. *RS*

Eco-friendly production: The first step to sustainability. *Jewellery News Asia*, No. 290, 2008, pp. 56–57.

Jewelry manufacturers in Hong Kong are preparing for potential future environmental regulations by building cleaner and more efficient factories. Industry officials say that implementing waste reduction strategies would produce the best results in large-scale plants that process large quantities of precious material. New strategic equipment includes air showers for catching gold dust and laser-welding machines that work at rates of seconds instead of minutes. While eco-friendly production is more costly, saving valuable materials can sometimes pay for the equipment in a matter of months and improve long-term cost effectiveness. *AB*

Jadeite auction results suggest cooling trade, market. *Jewellery News Asia*, No. 243, 2009, pp. 63–64.

The October 2008 Myanma Gems, Jade, and Pearl Emporium saw record low business, with 59.5% of the lots selling, bringing in a total of $163 million. However, some top jade lots did sell for much more than their presale reserve. One was estimated at $101,000 but sold for $868,000. Another, estimated at $25,500, sold for $399,000. In 2008, Myanmar's government sold 12,829 tonnes of jade for a total of $720 million. *RS*

Why China manufacturers are optimistic despite global slowdown. *Jewellery News Asia*, No. 290, 2008, pp. 81–84.

During the global financial crisis, Chinese diamond jewelry manufacturers have turned their attention from exporting to the United States to creating branded jewelry lines for their domestic market. Several polished diamond wholesalers observed that Chinese consumers are broadening their preferences to include diamonds above 0.50 ct and SI clarity, both of which had been a difficult sell there. The manufacturers are also establishing closer ties to local retailers in promoting their branded diamond jewelry pieces, noting the need to pay more attention to fashion trends and changes in the retail environment. *RS*

Because Public Education Happens at the Counter.

GIA launches Retailer Support Kit and website

A $97.00 value, shipping and handling extra.

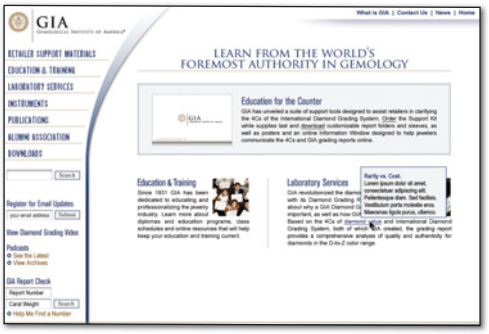

GIA's Retailer Support Kit has been developed to help sales associates educate the public about diamonds, the 4Cs, and thoroughly explain a GIA grading report. Take full advantage of all that GIA has to offer by visiting www.retailer.gia.edu

To order your FREE kit, log on to www.retailer.gia.edu

GIA
Gemological Institute of America®

RTGG09